MOLECULAR RECOGNITION

BY

CYCLODEXTRINS

Susan Elizabeth Brown

Thesis submitted for the degree of

Doctor of Philosophy

in

The University of Adelaide

Department of Chemistry

February 1994

CONTENTS

CONTENTS, continued

ABBREVIATIONS

αCD	alpha-cyclodextrin
βCD	beta-cyclodextrin
γCD	gamma-cyclodextrin
$\alpha CDNH_3^+$	protonated 6^A-amino-6^A-deoxy-alpha-cyclodextrin
$\alpha CDNH_2$	6^A-amino-6^A-deoxy-alpha-cyclodextrin
$\beta CDNH_3^+$	protonated 6^A-amino-6^A-deoxy-beta-cyclodextrin
$\beta CDNH_2$	6^A-amino-6^A-deoxy-beta-cyclodextrin
PMαCD	hexakis(2,3,6-tri-O-methyl)-alpha-cyclodextrin
PMβCD	heptakis(2,3,6-tri-O-methyl)-beta-cyclodextrin
$\beta CDpnH_2^{2+}$	diprotonated 6^A-(3-aminopropylamino)-6^A-deoxy-beta-cyclodextrin
$\beta CDpnH^+$	monoprotonated 6^A-(3-aminopropylamino)-6^A-deoxy-beta-cyclodextrin
βCDpn	6^A-(3-aminopropylamino)-6^A-deoxy-beta-cyclodextrin
DNA	deoxyribose nucleic acid
NAD	nicotinamide adenine dinucleotide
CPK	Corey-Pauling-Koltun
1D, 2D	one dimensional, two dimensional
NMR	Nuclear Magnetic Resonance
NOE	Nuclear Overhauser Effect
NOESY	Nuclear Overhauser Effect SpectroscopY
ROESY	Rotating frame nuclear Overhauser Effect SpectroscopY
HPLC	High Performance Liquid Chromatography
TPS	sodium 3-(trimethylsilyl)-1-propane-sulfonate
GH_2^+	protonated *RS*-α-(4-fluorophenyl)glycine
G^-	deprotonated *RS*-α-(4-fluorophenyl)glycine
A-GH	*RS*-*N*-acetyl-α-(4-fluorophenyl)glycine
$A\text{-}G^-$	deprotonated *RS*-*N*-acetyl-α-(4-fluorophenyl)glycine
VH	*RS*-*N*-(4-fluorobenzoyl)valine
V^-	deprotonated *RS*-*N*-(4-fluorobenzoyl)valine

ABSTRACT

The cyclodextrins are cyclic oligosaccharides capable of forming inclusion complexes in which a guest molecule is held within the cyclodextrin cavity by non-covalent forces alone. The focus of this study is the recognition of a variety of polar molecules by a range of natural and modified cyclodextrins, with a particular interest in the recognition of enantiomers of racemic guests.

Apparent stability constants for the inclusion of carboxylic acids and carboxylates by beta-cyclodextrin and an amino beta-cyclodextrin derivative are determined by potentiometric titrations. Apparent stability constants for the inclusion of fluorinated amino acids by natural, permethylated, and amino cyclodextrins are determined by ^{19}F nuclear magnetic resonance spectroscopy. The inclusion is affected by such factors as the cyclodextrin cavity size and hydrophobicity, the charge and position of the chiral centre of the guest, and the charge on the cyclodextrin. The complexes of anionic guests with a positively charged amino cyclodextrin are up to three times more stable than their complexes with uncharged cyclodextrins.

The chiral recognition of carboxylic or amino acids by the cyclodextrins studied is quite low, with the monosubstituted cyclodextrins generally showing greater recognition than the natural or permethylated cyclodextrins. The cyclodextrins studied generally show greater chiral recognition for anionic guests.

The formation of metallocyclodextrins, in which a metal ion is coordinated to a diamino beta-cyclodextrin derivative, is monitored by potentiometric titrations. The presence of Co^{2+}, Ni^{2+}, Cu^{2+} or Zn^{2+} is found to substantially increase the stability of the cyclodextrin complexes of amino acids, relative to the stability of their beta-cyclodextrin complexes. The metal ion also substantially increases the observed chiral recognition. The highest chiral recognition observed is for the complexation of *RS*-tryptophan by the Ni^{2+} complex of the diamino beta-cyclodextrin derivative, where the apparent stability constant for the *S* enantiomer is ten times larger than that for the *R* enantiomer. The conditions necessary for high chiral recognition are the simultaneous presence of the cyclodextrin and the metal ion, and

geometric constraints on the metal ion from ligand field effects. The magnitude of the observed chiral recognition is substantially dependent on the identity of the metal ion.

DECLARATION

This work contains no material which has been accepted for the award of any other degree or diploma in any university or other tertiary institution and, to the best of my knowledge and belief, contains no material previously published or written by another person, except where due reference has been made in the text.

I give consent to this copy of my thesis, when deposited in the University Library, being available for loan and photocopying.

SIGNED : DATE : 23/2/94

ACKNOWLEDGEMENTS

I would like to thank my supervisors, Steve Lincoln and John Coates, who have encouraged and guided me throughout this research. I am also grateful to Tom Kurucsev for computational and mathematical advice.

Many thanks to various organic chemists who have helped me over the years, especially Chris Easton, Dan Coghlan, Bruce May and Mike Williams. I am also grateful for the NMR expertise provided by Phil Clements and Andrea Hounslow. Thanks also to the general staff of our Department, who have helped me in so many ways over the years.

I am grateful to the Australian government for the financial support provided during my studies.

Many thanks to my colleagues, especially Carolyn, Jo, and Ashley, who have answered my questions, listened to my complaints and kept me laughing.

Finally, I would like to thank John, who has been a special friend for so long.

CHAPTER ONE

INTRODUCTION

1.1 General

The concept of molecular recognition is very important in many areas of science, including such diverse fields as chemistry, pharmacy, medicine, genetics, biochemistry and materials science. Molecular recognition can be thought of as a method of information transfer between molecules, and is often particularly dependent on non-covalent interactions such as hydrophobic, electrostatic and hydrogen bonding interactions. Non-covalent interactions are vital in biological systems, controlling functions such as DNA duplication, membrane transport, and the interaction of substrates and enzymes, drugs and receptors, and antigens and antibodies. A systematic and general understanding of the underlying intermolecular forces operating in biological systems is still in its infancy, and is a desirable goal for synthetic chemists hoping to mimic the amazing efficiency and versatility of biological systems. The functions of biological systems worth mimicking include selective recognition, fast and reversible information transfer, high catalytic activity, and chemical conversions under mild conditions. The improved understanding of non-covalent interactions in biological systems leads to new industrial and research applications.

A chemical species consisting of two or more molecules associated by non-covalent interactions may be called a 'complex'. For moderate to large sized molecules it is often found that a 'host' molecule contains a cavity into which a 'guest' molecule can bind, forming what is commonly termed a 'host-guest' or 'inclusion' complex. The integrity of the complex is maintained by weak non-covalent interactions. All effective biological hosts, such as enzyme active sites and transport proteins, can be considered to be orderly arrays of functional groups. The distances and angles between the functional groups are critical, and allow the biological host to recognize a specific substrate by non-covalent interactions.[1]

No particular molecular structure has been identified as common or essential to a good host, and thus there are many varied types of hosts.[1] Generally a good host must have steric and electronic features suitable for the guest being bound, and an appropriate balance between flexibility and rigidity. There are many examples of natural and synthetic hosts which are capable of forming inclusion complexes. Commonly used hosts are organic molecules such as cyclodextrins, calixarenes, cyclophanes, cryptands, spherands, cavitands and cryptophanes. Several of these hosts, including crown ethers, cryptands and calixarenes, are used to bind metal cations selectively, and thus have uses in molecular transport and separation.[1,2] Carbohydrate hosts such as amylose are conformationally flexible and can form helical complexes with long chain molecules. The structure of the helices is maintained by hydrogen bonds, and such complexes are believed to be important for recognition and regulation among cells.[1] Hosts such as zeolites rely on an extended molecular lattice to trap a molecular species. Zeolites have a silicate framework containing channels and cavities which can trap guests and cations, and are thus useful as cation exchangers, molecular sieves, shape selective catalysts and storage media.[2] There are many possible applications for natural and synthetic hosts, including sensor technologies, controlled release of drugs, transmission of information, catalysis, separation technologies, and transport systems.[1]

As biological systems are often too complex to study directly, chemists have made invaluable contributions to understanding such systems through the use of practical models, called 'biomimetic models', which emphasize certain features of biological systems. A biological process often mimicked is photosynthesis, where electron transfer has been modelled using synthetic molecular assemblies with photoactive units.[1] Another area of growth is the design of self-assembling supramolecular structures, where syntheses rely on non-covalent interactions to control reactions and result in a host which has desired structures and properties. New structures that have been synthesized include double and triple helices, catenanes, rotaxanes and cages.[3] The design of new hosts and the development of new applications requires a good understanding of the fundamental non-covalent interactions governing the underlying molecular recognition.

Cyclodextrins provide an excellent basis for the study of inclusion chemistry, quite apart from their intrinsic interest. This is demonstrated in this thesis, in which natural and modified cyclodextrins are used as hosts for the inclusion of a range of polar guests.

1.2 Structural Properties of Cyclodextrins

Cyclodextrins, also known as cyclomaltopolyoses, are cyclic 1,4-linked oligomers of α-*D*-glucopyranose, as shown in Figure 1.1. They are produced through the degradation of starch by the enzyme cyclodextrin transglycosylase which is obtained from *Bacillus macerans* and related bacteria.[4] Cyclodextrins are general purpose hosts, forming complexes with a very wide range of guests, including noble gases, salts, aliphatic molecules, and aromatic molecules.[5] They had a special role in the development of host-guest chemistry because they provided a sure example of inclusion of a guest molecule by a single host molecule. Another advantage of cyclodextrin complexes is that they form in solution, whereas many other types of complex, such as clathrates and intercalates, require the crystal lattice of the host to maintain the complex.[6] The cyclodextrins are also distinguished from most other hosts by their inherent chirality which may result in the preferential inclusion of chiral guests.

Cyclodextrins are named according to their number of glucopyranose units, with the natural cyclodextrins being alpha-, beta- and gamma-cyclodextrin, which consist of six, seven and eight glucopyranose units, respectively. Higher homologs do exist,[7] but are difficult to purify and their complexing ability is poor;[6] lower homologs are unknown, probably as a consequence of steric constraints.[6] A space-filled molecular representation of αCD is shown in Figure 1.2. The physical properties and dimensions of αCD, βCD and γCD are listed in Table 1.1. The circular arrangement of the glucopyranose units results in a structure with a cavity in which guest molecules can be accommodated. Cyclodextrins have a non-cylindrical conical shape which results from each glucopyranose unit being in the $^4C_1$ chair conformation and the lack of free rotation about the glycosidic bonds. This causes the primary hydroxyls to be grouped at one end of the molecule to form a narrow primary end, and the secondary hydroxyls to be grouped at the other end of the molecule to form a wider secondary end.

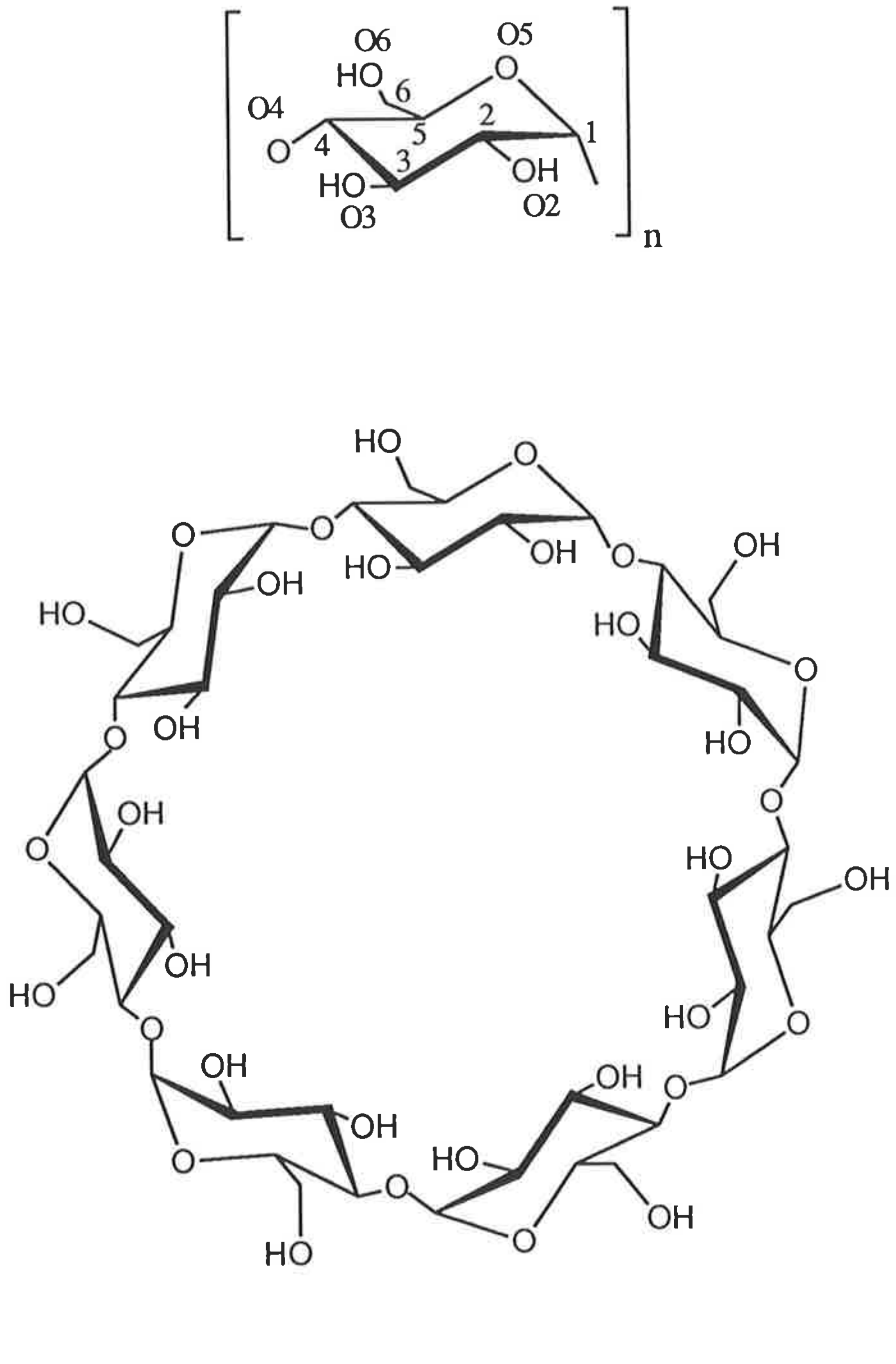

Figure 1.1 General structure of a cyclodextrin, showing the numbering system for the α-*D*-glucopyranose units, and how they link together to form beta-cyclodextrin (n=7).

As a consequence of their conical shape, the cyclodextrins are often represented as truncated cones, as shown in Figure 1.3, with the inside of the cone representing the cyclodextrin cavity. The shape of a cyclodextrin is maintained in both the solution and solid states by a ring of hydrogen bonds between the secondary hydroxyl groups on adjacent glucopyranose residues. The strength of the hydrogen bonds increases from αCD to γCD. The cavity is relatively apolar, as it is lined with the H5 ring of hydrogen atoms bonded to C5, the O4 ring of ether-like oxygens, and the H3 ring of hydrogen atoms bonded to C3. The presence of the hydroxyl groups allows the hydrophobic molecule to be soluble in aqueous solution. The structure of αCD is distorted and asymmetric due to the partial rotation of one of the glucopyranose units relative to the others, whereas the structures of βCD and γCD are quite symmetrical.[5,6]

Table 1.1 General physical properties of the cyclodextrins.[5,8]

Physical Property	αCD	βCD	γCD
Number of α-*D*-glucopyranose residues	6	7	8
Molecular weight	973	1135	1297
Solubility in H_2O (g/100 cm^{-3}, 298 K)	14.5	1.85	23.2
Internal diameter (pm) [a]	470 - 520	600 - 650	750 - 850
External diameter (pm) [a]	1370 - 1460	1530 -1540	1690 - 1750
Height (pm)	790 - 800	790 - 800	790 - 800
Volume of cavity (nm^3)	0.176	0.346	0.510

[a]The smaller value refers to the diameter at the primary end and the larger value refers to the diameter at the secondary end of the cyclodextrin.

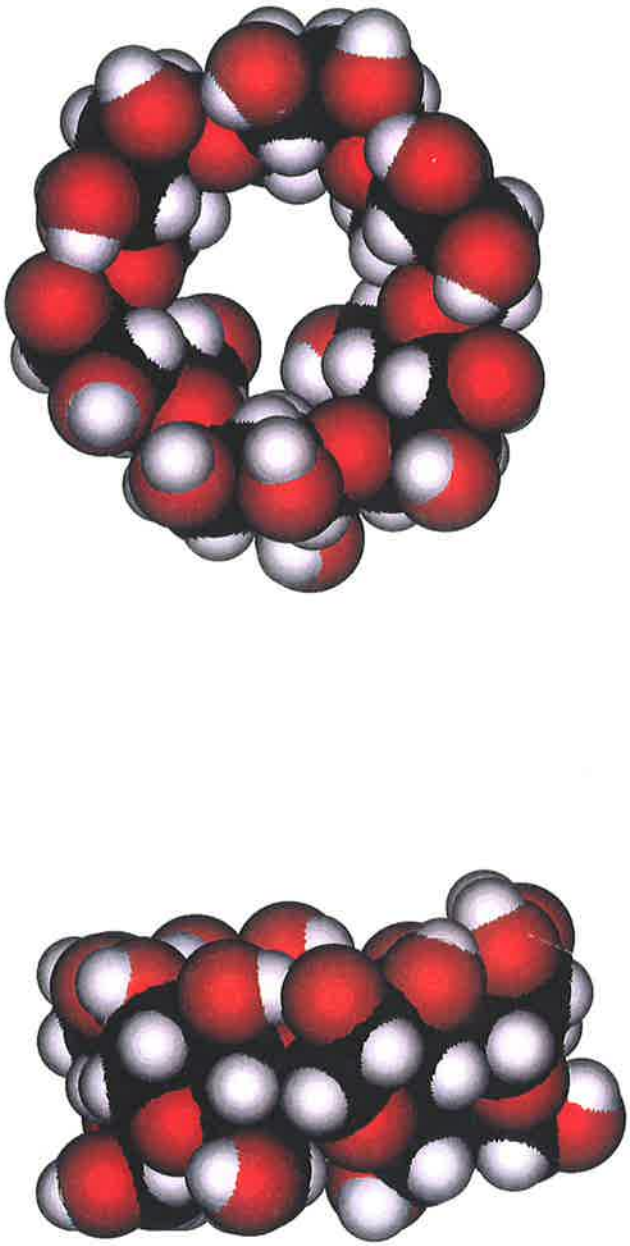

Figure 1.2 View of αCD from the secondary end of the molecule, and from the side of the molecule, where the colours representing the atoms are black for carbon, red for oxygen and white for hydrogen. This space-filled molecular representation was constructed using the software PROPHET[9] and crystallographic data[10] obtained from the Cambridge Crystallographic Database. Water molecules associated with the cyclodextrin have been omitted.

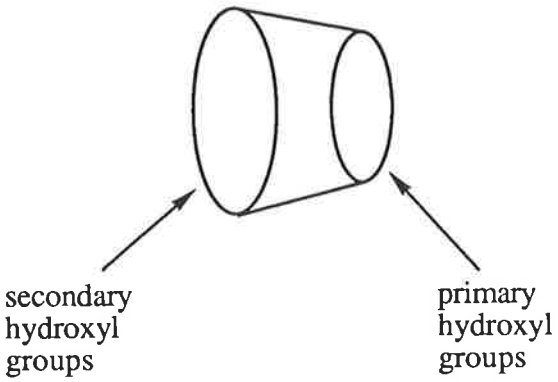

Figure 1.3 Truncated cone representation of a cyclodextrin showing the primary and secondary ends of the molecule.

Molecular orbital calculations, based on crystallographic data, reveal that cyclodextrins possess a dipole moment directed from the secondary hydroxyls to the primary hydroxyls approximately through the centre of the cavity,[11] as shown in Figure 1.4. Each glucopyranose unit has a dipole moment, and because all glucopyranose units are in the same conformation the individual dipole moments do not cancel, but add to give an overall molecular dipole moment of around 10 - 20 Debye (1 Debye = 3.33564×10^{-3} Cm).[11] Thus, the magnitude of the dipole moment increases on moving from αCD to γCD as the number of glucopyranose units increase. The electrostatic properties of the cavity can vary considerably with the conformation of the cyclodextrin.[12] This is seen in the reduced dipole moment of αCD, as compared with the dipole moment that would result if αCD was symmetrical, which results from the partial rotation of one of the glucopyranose units of αCD.[12]

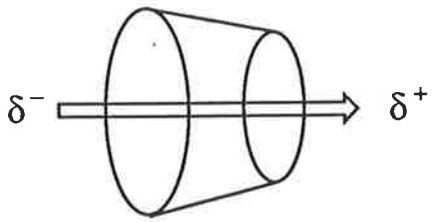

Figure 1.4 Schematic diagram showing the dipole moment of a cyclodextrin.

1.3 Cyclodextrin Inclusion Complexes

It is generally agreed that a cyclodextrin complex usually has a guest molecule situated in the cyclodextrin cavity. Although there is much indirect evidence that this is the case, the only direct evidence for such inclusion comes from X-ray crystallographic and NMR studies. Many X-ray structures show that in the solid state guests are situated in the cyclodextrin cavity. Such structures cannot necessarily be assumed to exist in solution. The strongest evidence for inclusion in the cavity in solution comes from 2D NMR spectroscopy. Although 1D ^{1}H and ^{13}C NMR studies of many cyclodextrin complexes provide very convincing evidence that guests are situated in the cavity, the first conclusive evidence for inclusion within the cavity in solution came from a 2D NMR NOESY study on the complex formed between 4-nitrophenolate and αCD.[13]

It should be noted that cyclodextrins have also been known to form complexes in which the guest is not included within the cavity. The complex formed between bilirubin and βCD is believed to be an 'outside' complex where the guest is hydrogen bonded to the secondary hydroxyl groups of the cyclodextrin and there is no actual contact of the guest with the inside of the cavity.[14] Similarly, the complexes formed between αCD and ribonucleosides are believed to be 'outside' complexes.[14] The separation of some compounds on cyclodextrin

chromatographic columns has been demonstrated to be due to an external interaction between the guest and the hydroxyl groups of the immobilized cyclodextrin derivative, and not due to inclusion within the cavity.[15-17]

The most common guests are aromatic molecules, and it is generally found that the aromatic portion of a molecule is included within the apolar cyclodextrin cavity. The change in environment of the guest upon inclusion, from the solvent to the hydrophobic cavity, induces changes in the physical and chemical properties of a guest.[6,18] Such changes facilitate detection and monitoring of complex formation in solution. Perturbation of the electronic energy levels of a guest, either by a direct interaction with the cyclodextrin or by the exclusion of solvating water molecules, often causes changes in the electronic spectrum of a guest. Inclusion in a cyclodextrin cavity may protect a guest from collisional quenching of an excited state by oxygen or the solvent, and may result in enhancement of the fluorescence spectrum of the guest. Changes in the environment of nuclei of the guest and host due to such factors as anisotropic shielding, conformational and solvation changes, or direct contact between the host and guest, often cause changes in the NMR spectrum of both the cyclodextrin and the guest. The circular dichroism spectrum of a chiral guest may be changed by interaction with the chiral cyclodextrin, and an achiral guest may exhibit an induced circular dichroism spectrum due to inclusion within the chiral cyclodextrin cavity. Inclusion may also alter the pK_a values of acidic and basic guests, allowing complex formation to be monitored by potentiometric titrations. In principle, any property of the cyclodextrin or guest that is significantly modified by complexation may be used to follow the complexation process.

The modification of the chemical and physical properties of a guest upon inclusion by a cyclodextrin results in many interesting applications for cyclodextrins.[4,5] Cyclodextrins are used to improve the handling of active ingredients such as insecticides, flavours, fragrances, drugs, poisons and explosives, as encapsulation of molecules within the cavity may reduce volatility, oxidation, decomposition and hydrolysis. They are widely used in the pharmaceutical industry, to enhance the bioavailability of drugs via increased solubility or improved drug delivery, to suppress unpleasant tastes, and to reduce side effects such as ulceration. Cyclodextrins are also used in analytical chemistry,[19] to enhance the detection of

chemical species by various spectroscopic methods, as chiral shift reagents in NMR spectroscopy, in electroanalytical methods such as polarography and voltammetry, and to separate a wide range of molecules by chromatography.

The stoichiometry of cyclodextrin complexes is determined largely by the size of the guest relative to the size of the cyclodextrin cavity. The most common stoichiometry in solution is one to one. For guests which cannot be totally included in the cavity another cyclodextrin may complex the protruding portion of the guest, as in the two host to one guest complex formed by βCD and pyrene.[20] Alternatively, two guest molecules may be simultaneously included in the cyclodextrin cavity, as in the two guest to one host complex formed by Tropaeolin 000 No. 2 and βCD.[21] Complexes have also been found where a cyclodextrin simultaneously encapsulates different guests, as in the complexes formed between βCD, pyrene and alcohols.[22] The formation of a complex can be characterized by an equilibrium constant, called a 'stability' constant, which is a measure of the extent a guest is complexed by a cyclodextrin. The determination of complex stoichiometry and stability provides information about the nature of the complex, and allows direct comparison between complexes of different guests and cyclodextrins.

In attempting to understand further the factors affecting cyclodextrin complexation it is important to have as much information as possible about the position of a guest in the cavity. Although the only conclusive evidence for complex geometry in solution comes from 2D NMR studies, clues to the complex structure may be found through a variety of physical methods. Several general trends have been found for the complexation of simple aromatic guests by αCD, βCD and γCD. The depth of insertion of an aromatic guest into the cyclodextrin cavity can generally be correlated with the stability of the complex, where a shallow inclusion results in a complex of low stability and a deep inclusion results in a complex of high stability. This is clearly shown by the generally low stability constants of αCD complexes, where NMR and molecular modelling studies show that a phenyl ring can only be partially inserted into the cyclodextrin cavity.[23] Studies of the induced circular dichroism spectra of mono- and di-substituted aromatic guests included in βCD indicate that the inclusion of the phenyl ring tends to be axial, with the long axis of the aromatic guest

aligned approximately parallel to the axis through the centre of the βCD cavity.[24,25] For cyclodextrins such as γCD where an aromatic guest is often smaller than the diameter of the cavity, crystallographic studies show that a guest is not constrained in one position, but is usually disordered and occupies several positions.[5]

Although the natural cyclodextrins complex many guests, often the stability of the complexes is quite low, and the selectivity for different guests is small. A growing field in cyclodextrin chemistry is the synthetic modification of the basic cyclodextrin unit to create new cyclodextrins which form more stable and selective complexes. The main sites for modification are the primary and secondary hydroxyl groups, and modifications range from introducing a single functional group, to introducing several functional groups, to dimeric and even polymeric cyclodextrins. One interesting example is the synthesis of dimeric cyclodextrins in which two cyclodextrin units are joined by either one or two linking groups. These cyclodextrins complex suitable guests very strongly, and the stability of the complexes approaches that of very strong antibodies and antigens.[26]

1.4 Driving Forces for Cyclodextrin Complex Formation

The thermodynamics of cyclodextrin complex formation are very dependent on the particular system being studied. However, it is generally found that ΔH^0 and ΔS^0 are compensating, indicating a common mechanism for the interaction of different cyclodextrins with different guests.[6] ΔH^0 is usually favourable for complex formation, but ΔS^0 can vary considerably,[6] so it is not possible to make predictions about thermodynamic parameters for cyclodextrin complex formation. Although most researchers agree on the general nature of the forces contributing to cyclodextrin complex formation, there is continued debate about the relative importance of the various driving forces. It is interesting to note that the enthalpy-entropy compensation effect may be used to discuss the thermodynamic behaviour of a variety of different hosts, including cyclodextrins, podands, crown ethers and cryptands.[27] This confirms the general nature of the weak interactions governing the host-guest complexation, despite the great differences in the hosts.

For an inclusion complex to form it must be possible for the guest, or a portion of the guest, to fit within the cyclodextrin cavity, and some contact must occur between the host and guest. London dispersion forces have been shown to be important in the solid state as distances found in crystal structures are consistent with such interactions,[28] and in solution by the observation of a relationship between strength of complexation and the polarizability of a guest.[6,29] The importance of hydrophobic interactions is shown by the observation that only weak complex formation, by comparison with that in water, occurs in solvents such as dimethyl sulfoxide[30] and chloroform,[31] and that the spectroscopic changes experienced by a guest upon complexation parallel those a guest would experience on being transferred from water to a relatively apolar solvent.[11] Solvation changes must be involved, as the cyclodextrin cavity contains water molecules which have to be expelled or moved to allow complex formation. This is confirmed by surface tension studies,[32] and the observation that inorganic salts affect measured stability constants.[33] Steric factors, London dispersion forces, hydrophobic interactions and solvation changes are believed to be important for the formation of all cyclodextrin complexes. The fact that inclusion complex formation relies on these relatively weak interactions is confirmed by solid state NMR, which shows that even in the solid state the guest retains some degree of motion within the cavity.[34]

Other factors possibly contributing to complexation include hydrogen bonds, conformational changes and electrostatic interactions, and the importance of these factors depends on the particular cyclodextrin and guest being studied. Hydrogen bonding interactions between a guest and the cyclodextrin hydroxyl groups require appropriate functional groups on the guest. The formation of hydrogen bonds has been unequivocally demonstrated in the solid state by crystallographic studies, such as in the complex of propranolol with βCD.[35] There is no conclusive evidence for hydrogen bonding interactions in solution, although the results of many NMR, fluorescence and molecular modelling studies strongly suggest the formation of hydrogen bonds.[36-39] Conformational changes in the cyclodextrin structure are believed to be particularly important for αCD, as complex formation can relieve the ring strain of the distorted macrocyclic ring.[5] Conformational changes may also occur upon complexation for other cyclodextrins, as in the complexation of adamantane and derivatives by βCD,[40] but are less common. Electrostatic interactions, such as dipole-

dipole, dipole-charge, and charge-charge interactions, seem to be important in the inclusion of polar and charged guests by cyclodextrins, particularly for modified cyclodextrins which can become charged. However, as there is no agreement on the general importance of electrostatic interactions in cyclodextrin complex formation, it is of interest to continue to investigate such interactions.

In complexes formed with the natural cyclodextrins there is considerable evidence for significant electrostatic interactions such as dipole-dipole and charge-dipole interactions. Dipole-dipole interactions are believed to explain the complex stability and the orientation of the guests for the inclusion of polar substituted benzene derivatives in αCD. In these complexes the guest is situated so that its dipole moment is aligned antiparallel with the cyclodextrin dipole moment.[11] Experimental evidence and molecular modelling studies indicate that electrostatic interactions are crucial in providing a driving force for the cyclodextrin inclusion of the phenylcyanoacetate anion, and the subsequent catalysis of the decarboxylation of this guest.[23] Charged species may be included more strongly than the corresponding neutral species, as found for the inclusion of phenols and phenolates by αCD,[41] and dicyanobenzenes and their anion radicals by the natural cyclodextrins.[42] Calculations based on crystallographic studies of αCD complexes show that polar guests induce a large electrostatic potential along the cyclodextrin cavity axis.[12] The electrostatic interactions are strong enough to distort the cavity and cause a large variation in the cyclodextrin dipole moment.[11] Calculations also show that the complexation of 4-nitrophenol by αCD induces a conformation in the cyclodextrin that optimizes the electrostatic interactions between the host and guest.[12] The importance of such polar interactions is not agreed upon, however, as calculations have also shown that polar interactions are insignificant in the complexation of 4-nitrophenol by αCD.[43]

Electrostatic interactions may be even more important in the complexation of guests by modified cyclodextrins, as suitably modified hosts may allow a direct charge-charge interaction between an oppositely charged host and guest. Force field calculations on the inclusion of tryptophan by a charged modified cyclodextrin show that the direct Coulombic interaction between oppositely charged groups on the host and guest is one of the most

important factors contributing to the inclusion.[43] Studies on the inclusion of 1,2-dihydroxy-benzene anions in amino βCD derivatives indicate that the anions are complexed two to three times more strongly when the host is positively charged.[44] Positively charged modified βCD derivatives complex anionic drugs two to three times more strongly than βCD, but complex neutral and cationic drugs three to four times less strongly than βCD.[45] Similarly, a negatively charged modified βCD derivative complexes propranolol, a cationic drug, twice as strongly as βCD, but complexes neutral and anionic drugs one to four times more weakly than βCD.[45] Similar results have been reported for the interaction of anionic, cationic and neutral dyes with sulfonato and pyridino βCD derivatives.[46] There is clear evidence in these systems that the direct charge interaction between an oppositely charged host and guest results in complexes of higher stability than for those systems in which the electrostatic interaction cannot occur. Such experimental evidence for electrostatic interactions for a variety of guests and cyclodextrins suggests that electrostatic interactions may be very important in cyclodextrin systems, particularly for ionic guests interacting with charged cyclodextrins.

A study of the complexation free energies of a variety of host-guest complexes indicates that a direct electrostatic interaction between an ion pair in a complex has an estimated mean free energy of around 5 kJ mol^{-1}.[47,48] This value is calculated from a variety of host-guest systems, including complexes held together exclusively by electrostatic forces, and complexes in which electrostatic interactions dominate so that contributions from other forces can either be ignored or easily subtracted from the overall interaction. Such a favourable ion pair interaction would result in a ten fold increase in the stability constant for a complex, relative to that of a system where the charge interaction cannot occur. If an observed effect is smaller than this, the ion pair distances are probably too great for an optimal interaction. Many of the cyclodextrin examples listed above have a stability enhancement of only a factor of two to three, indicating that the ion pair interaction is not maximized by the geometry of the cyclodextrin complexes.

The study of the importance of electrostatic interactions, particularly between charged cyclodextrins and guests, has tended to be carried out on complex systems, with a multiply substituted cyclodextrin and a particular drug or dye molecule. Such systems have many steric

factors to consider as well as electrostatic factors, so it is of interest to investigate electrostatic interactions in simpler systems not complicated by steric factors. Thus, I have studied the complexation of simple aromatic carboxylic acids by βCD and an amino βCD derivative (see Chapter 2). Results obtained from the study of these cyclodextrin systems may help understand biological interactions such as the binding of ionic substrates to enzymes.

1.5 Chiral Discrimination by Cyclodextrins

The cyclodextrins exist only as the *D* enantiomer, so it is possible that they will show chiral discrimination by preferentially complexing one enantiomer of a racemic guest to form diastereomeric complexes which have different physical and chemical properties. The chiral discrimination may be significant enough to allow measurement of different stability constants for the complexes of the enantiomers (thermodynamic discrimination). If thermodynamic discrimination is occurring but is not large enough to be measured accurately, it is possible that the small energy differences between the complexes of the enantiomers may still be detected spectroscopically. For example, if enantiomers have slightly different magnetic environments in a cyclodextrin complex (magnetic discrimination), separate NMR signals may be detected for the diastereomeric complexes even though separate stability constants cannot be measured.

The model generally accepted for chiral discrimination by cyclodextrins is an adaptation of the 'three-point interaction model'.[35] Firstly, an inclusion complex must form, such that there is a relatively tight fit between the host and guest. There must also be at least two other chiral contacts between the chiral centre of the guest and the cyclodextrin, although it has been speculated that an aromatic ring may constitute a multiple interaction point.[49] Hydrogen bonding and electrostatic interactions are believed to be very important, though not essential, for chiral discrimination to occur, as these forces are very direction dependent. Conversely, London dispersion forces and hydrophobic interactions are not expected to contribute much to any observed chiral discrimination, as they depend largely on contact distances. Hydrogen bonding interactions are believed to be important in chiral discrimination as molecular modelling studies consistently find guests that are situated at hydrogen bonding distance from the cyclodextrin hydroxyl groups, and the difference between diastereomeric

structures is often reflected in the guest to cyclodextrin hydrogen bond distances.[35,39,50] Computer modelling and X-ray crystallographic studies of the complex of propranolol with βCD shows that the naphthol moiety is in the same position in the cavity for both the *D* and *L* enantiomers.[35] The closer cavity contact of the secondary amine group of *D*-propranolol, as compared with *L*-propranolol, allows stronger hydrogen bonding with the cyclodextrin, resulting in the favoured inclusion of the *D* enantiomer. The asymmetry arising through such hydrogen bonding or electrostatic interactions is enough to overcome the inherent symmetry of the cyclodextrin so that discrimination can occur.

The chiral discrimination shown for racemic guests by the natural cyclodextrins is often quite low, because of the inherent symmetry of the natural cyclodextrins. Synthetic modifications, such as mono- and di-substitutions, increase the asymmetry of the cyclodextrin unit and can thus lead to increased chiral discrimination. This is found for the complexation of nucleotides by amino cyclodextrins, where mono- and di-substituted amino cyclodextrins show greater discrimination than a fully substituted amino cyclodextrin.[51]

The enantiomer recognition ability of cyclodextrins leads to some specific applications, such as the separation of racemates. Cyclodextrin complexed enantiomers may have different solubilities, which allows separation by preferential precipitation. Separation of racemic isopropyl methylphosphinates and their ethyl analogues is achieved by this method in up to 66% enantiomeric purity using αCD and βCD.[52] Generally, however, selectivity by preferential precipitation is low, giving optical purities of less than 15%,[52,53] so that effective enantiomer separation requires several successive crystallizations. Better separation of enantiomers is obtained through the use of cyclodextrins in a variety of chromatographic methods, including thin layer, liquid, gas, and electrokinetic chromatographies. A variety of natural and modified cyclodextrins have been used to separate enantiomers by chromatography, such as the separation of racemic amino acids on a HPLC column which has βCD bonded to a silica gel.[54] Cyclodextrins have also been used to separate a range of other isomers by chromatography, including structural isomers, geometric isomers, diastereomers and steroid epimers.[55]

The chiral discriminating ability of cyclodextrins can also be seen in reactions, where it is possible for a cyclodextrin either to promote preferential reaction with a particular enantiomer or to produce one enantiomer preferentially. Cyclodextrins preferentially catalyse the hydrolysis of the *D* enantiomer of amino acid nitrophenyl esters at basic pH.[56] The $NaBH_4$ reduction of achiral benzoyl formic acid by a modified βCD preferentially produces the *L* enantiomer of mandelic acid in the pH range 4 - 10.[57,58] Deacylation of a racemic βCD-ibuprofen prodrug at pH 11.5 occurs ten times faster for the *R* enantiomer than for the *S* enantiomer, allowing separation of the enantiomers by preferential hydrolysis.[59] Other asymmetric syntheses performed using cyclodextrins include epoxidation, halogenation and hydrogenation of olefins, and reduction of ketones.[60]

The best method for characterizing the extent of the chiral discrimination is to measure stability constants for the cyclodextrin diastereomers. If a difference in stability constants is found, then a mean free energy difference between the diastereomers, a $\Delta\Delta G$ value, can also be calculated. $\Delta\Delta G$ values determined for a range of enantiomers separated by gas chromatography are in the order of 0.3 - 1.8 kJ mol^{-1}.[61] Such energy differences, of the order of a few kJ, are typical for the formation of a range of cyclodextrin diastereomers, including the complexes of phenprocoumon with βCD,[62] and amino acids with βCD and modified βCD derivatives.[63-65] The magnitude of the free energy difference between the diastereomers may give some clues as to the differences in bonding for the enantiomers. $\Delta\Delta G$ values of a few kJ may indicate differences in hydrogen bonding interactions, as the energy of a hydrogen bond in water is calculated as being around 4 - 8 kJ mol^{-1}.[66] A difference in electrostatic interactions is also expected to be of the order of a few kJ (see Section 1.4). However, finding a $\Delta\Delta G$ value less than this magnitude does not conclusively indicate that hydrogen bonding or electrostatic interactions are not responsible for the differences between the diastereomers. This is because atoms may be able to form hydrogen bonds or ion pair interactions that are not at an optimal distance, resulting in interactions of lower energy. It is also possible that the enantiomers form several complexes of different geometries, as suggested by time-resolved fluorescence studies,[67] and that only a few of these conformations are responsible for the chiral discrimination.[68] The averaging of the energy differences over the possible complex conformers would lower the energy difference between the complexes.

Despite the many applications of the enantiomer recognition property of cyclodextrins, it is still not possible to make predictions about whether or not discrimination will occur for a specific guest and cyclodextrin, and if it does occur what the magnitude of the discrimination will be. This is basically because of the incomplete understanding of the chiral discrimination process. As cases of large chiral discrimination have tended to be for very specific interactions between specifically shaped guests and highly modified cyclodextrins, it is of interest to investigate chiral recognition in simpler systems. Thus, I have studied the complexation of racemic amino acids by a range of simple cyclodextrins, testing how factors such as the size, shape and charge of the chiral centre affect the chiral discrimination (see Chapter 4). Results obtained from the study of these cyclodextrin systems may help understand biological interactions such as the high enantiomer selectivity of enzymes.

1.6 Cyclodextrins As Biomimetic Models

Cyclodextrins have been used as models for a broad range of biological functions. They are useful as photoactive supramolecular assemblies, as they can perform such functions as selectively complexing an electron acceptor or donor, shielding active intermediates from the external environment, eliminating back reactions, and controlling stereospecific and stereoselective phototransformations.[1] A modified cyclodextrin, which has two cyclodextrin units connected by a porphyrin ring, complexes quinones and acts as a model for the initial process of electron transfer in photosynthetic systems.[69] βCD derivatives with seven 2-naphthoyloxy chromophores on either the primary or secondary face allow the study of excitation energy migration, acting as a model for the antenna effect in photosynthetic systems and in photochemical molecular devices.[70] Cyclodextrins have also been used to model transport phenomena, with modified cyclodextrins capable of binding iron acting as synthetic siderophores, molecules that are important in the transport of iron in microorganisms.[71,72] In the rapidly growing field of self-assembling molecular structures, cyclodextrins have been used to construct rotaxanes,[73,74] and polyrotaxanes[75] where crosslinking between rotaxanes results in molecular tube structures similar to carbon nanotubes.

One extensive use of cyclodextrins as biomimetic models is in the field of enzymatic catalysis. The cyclodextrin represents the active site of an enzyme, and the included guest represents a bound substrate. The cyclodextrins are suitable models because they have a cavity capable of binding a substrate in a well defined host-guest relationship, and the hydroxyl groups can play an important role in catalysis and selectivity, including enantioselectivity. Cyclodextrins and modified cyclodextrins have been used to mimic enzymes such as α-chymotrypsin, carbonic anhydrase, ribonuclease[8] and cytochrome P-450,[76] and also co-enzymes such as NAD.[77]

Reactions catalysed by cyclodextrins can generally be classified as either covalent catalysis or microsolvent catalysis. In covalent catalysis the cyclodextrin reacts with the included guest molecule to form a new covalent intermediate. This is found in the hydrolysis of phenyl esters, where the nucleophilic attack of a secondary hydroxyl group of the cyclodextrin on the complexed ester accelerates hydrolysis by a factor of up to three hundred, and is analogous to ester cleavage by the enzyme α-chymotrypsin.[29] In microsolvent catalysis the cyclodextrin provides a reaction environment, but does not actually take part in the reaction. Thus, the cyclodextrin cavity may act in several ways, to constrain the guest geometrically, to stabilize conformations that are less favoured, to direct reaction towards a certain part of the complexed species, or to provide a hydrophobic environment. An example of microsolvent catalysis is the increased Diels Alder reaction rate of cyclopentadiene and butenone, which results from the close proximity of the two reactants upon simultaneous encapsulation by βCD.[78]

The natural cyclodextrins are fairly limited in their application as enzyme models, as enzymes usually require the cooperation of several catalytic groups, such as acidic and basic side chains, metal ions and bound co-enzymes. The use of cyclodextrins as enzyme models may be improved by appropriate modifications of the cyclodextrin unit which increase the number of recognition sites. Suitable modifications include linking cyclodextrins together, substituting catalytic groups on the cavity rim, binding metal ions to the cyclodextrin, and capping the cavity with functional groups that improve the hydrophobicity of the cavity. Metallocyclodextrins, cyclodextrins with a metal ion coordinated either directly to the

cyclodextrin hydroxyl groups,[79,80] or to a functional group substituted on a modified cyclodextrin,[81,82] have been particularly useful enzyme models. Metals in cyclodextrin systems can act analogously to metals in enzymatic systems, promoting strong substrate binding, and activating the complexed guest for subsequent reaction. Metallocyclodextrins have been used to catalyse a range of reactions including carbon dioxide hydration, phosphotriester hydrolysis, ester hydrolysis, furoin oxidation, and decarboxylation.[81] The zinc complex of a βCD derivative with two histamine groups acts as a mimic for some functions of the enzyme carbonic anhydrase.[82] The cobalt complex of a cyclen substituted βCD derivative simulates some of the properties of acyl and phosphoryl transfer enzymes.[81]

As outlined in Section 1.5, a main reason for investigating the inclusion of enantiomeric guests by cyclodextrins is to gain a greater understanding of factors affecting chiral discrimination. An extension of this is to introduce metal ions to the cyclodextrin system and examine how this new factor affects the chiral discrimination. Thus, I have studied the complexation of racemic amino acids by a modified cyclodextrin capable of binding a metal ion (see Chapter 3). Of particular interest is the effect of the nature of the metal ion on the extent of the chiral discrimination. Results obtained from the study of these cyclodextrin systems may help understand biological interactions such as the role of metal ions in biological enantiomer selectivity.

BIBLIOGRAPHY

(1) *Frontiers in Supramolecular Organic Chemistry and Photochemistry*; Schneider, H.-J., Dürr, H., Eds; VCH Publishers: New York, **1991.**

(2) *Inclusion Phenomena and Molecular Recognition*; Atwood, J. L., Ed; Plenum Press: New York, **1990.**

(3) Lehn, J.-M. *Science* **1993**, *260*, 1762.

(4) Saenger, W. *Angew. Chem., Int. Ed. Engl.* **1980**, *19*, 344.

(5) Saenger, W. *Inclusion Compounds*; Atwood, J. L., Davies, J. E., MacNicol, D. D., Eds; Academic Press: London, **1984**, Vol. 2, pp 231-257.

(6) Clarke, R. J.; Coates, J. H.; Lincoln, S. F. *Adv. Carbohydr. Chem. and Biochem.* **1988**, *46*, 205.

(7) Fujiwara, T.; Tanaka, N.; Kobayashi, S. *Chem. Lett.* **1990**, 739.

(8) Schurig, V.; Nowotny, H.-P. *Angew. Chem., Int. Ed. Engl.* **1990**, *29*, 939.

(9) PROPHET, BBN Systems and Technologies Corporation, Cambridge, MA, USA.

(10) Saenger, W. *Nature* **1979**, *279*, 343.

(11) Sakurai, M.; Kitagawa, M.; Hoshi, H.; Inoue, Y.; Chûjô, R. *Carbohydr. Res.* **1990**, *198*, 181.

(12) Sakurai, M.; Kitagawa, M.; Hoshi, H.; Inoue, Y.; Chûjô, R. *Chem. Lett.* **1988**, 895.

(13) Yamamoto, Y.; Ondo, M.; Kitagawa, M.; Inoue, Y.; Chûjô, R. *Carbohydr. Res.* **1987**, *167*, c11.

(14) Kano, K.; Yoshiyasu, K.; Yasuoka, H.; Hata, S.; Hashimoto, S. *J. Chem. Soc., Perkin Trans. 2* **1992**, 1265.

(15) West, R. R.; Cardellina, J. H. *J. Chromatogr.* **1991**, *539*, 15.

(16) Armstrong, D. W.; Stalcup, A. M.; Hilton, M. L.; Duncan, J. D.; Faulkner, J. R.; Chang, S.-C. *Anal. Chem.* **1990**, *62*, 1610.

(17) Hooper, A. J.; Heindl, J.; Wright, P.; Eastman, M. P.; Kooser, R. G. *J. Phys. Chem.* **1992**, *96*, 5495.

(18) Szejtli, J. *Cyclodextrins and Their Inclusion Complexes*; Akadémiai Kiadó: Budapest, **1982.**

(19) Li, S.; Purdy, W. C. *Chem. Rev.* **1992**, *92*, 1457.

(20) Muñoz de la Peña, A.; Ndou, T.; Zung, J. B.; Warner, I. M. *J. Am. Chem. Soc.* **1991**, *95*, 3330.

(21) Clarke, R. J.; Coates, J. H.; Lincoln, S. F. *J. Chem. Soc., Faraday Trans. 1* **1984**, *80*, 3119.

(22) Muñoz de la Peña, A.; Ndou, T. T.; Zung, J. B.; Greene, K. L.; Live, D. H.; Warner, I. M. *J. Am. Chem. Soc.* **1991**, *113*, 1572.

(23) Furuki, T.; Hosokawa, F.; Sakurai, M.; Inoue, Y.; Chûjô, R. *J. Am. Chem. Soc.*

1993, *115*, 2903.

(24) Shimizu, H.; Kaito, A.; Hatano, M. *Bull. Chem. Soc. Jpn.* **1981**, *54*, 513.

(25) Kamiya, M.; Mitsuhashi, S.; Makino, M.; Yoshioka, H. *J. Phys. Chem.* **1992**, *96*, 95.

(26) Breslow, R. *Isr. J. Chem.* **1992**, *32*, 23.

(27) Inoue, Y.; Hakushi, T.; Liu, Y.; Tong, L.-H.; Shen, B.-J.; Jin, D.-S. *J. Am. Chem. Soc.* **1993**, *115*, 475.

(28) Saenger, W. *Proc. Int. Symp. Cyclodextrins, 1st (Budapest)* ; Szejtli, J. Ed; Akadémiai Kiadó: Budapest, **1981**, p141.

(29) van Etten, R. L.; Sebastian, J. F.; Clowes, G. A.; Bender, M. L. *J. Am. Chem. Soc.* **1967**, *89*, 3242.

(30) Gerasimowicz, W. V.; Wojcik, J. F. *Bioorg. Chem.* **1982**, *11*, 420.

(31) Danil de Namor, A. F.; Pacheco Tanaka, D. A.; Reguira, L. N.; Orellana, I. G. *J. Chem. Soc., Faraday Trans.* **1992**, *88*, 1665.

(32) Örstan, A.; Ross, J. B. A. *J. Phys. Chem.* **1987**, *91*, 2739.

(33) Buvári, Á.; Barcza, L. *J. Inclusion Phenom. Mol. Recognit. Chem.* **1989**, *7*, 379.

(34) Inoue, Y.; Kuan, F.-H.; Chûjô, R. *Carbohydr. Res.* **1987**, *159*, 1.

(35) Armstrong, D. W.; Ward, T. J.; Armstrong, R. D.; Beesley, T. E. *Science* **1986**, *232*, 1132.

(36) Hamai, S. *Bull. Chem. Soc. Jpn.* **1992**, *65*, 2323.

(37) Soujanya, T.; Krishna, T. S. R.; Samanta, A. *J. Phys. Chem.* **1992**, *96*, 8544.

(38) Takahashi, K. *Bull. Chem. Soc. Jpn.* **1993**, *66*, 550.

(39) Amato, M. E.; Pappalardo, G. C.; Perly, B. *Magn. Reson. Chem.* **1993**, *31*, 455.

(40) Jaime, C.; Redondo, J.; Sánchez-Ferrando, F.; Virgili, A. *J. Mol. Struct.* **1991**, *248*, 317.

(41) Connors, K. A.; Lin, S.-F., *J. Pharm. Sci.* **1983**, *72*, 1333.

(42) Kano, K.; Mori, K.; Uno, B.; Goto, M.; Kubota, T. *J. Am. Chem. Soc.* **1990**, *112*, 8645.

(43) Tabushi, I.; Mizutani, T. *Tetrahedron* **1987**, *43*, 1439.

(44) Yatsimirsky, A. K.; Eliseev, A. V. *J. Chem. Soc., Perkin Trans. 2* **1991**, 1769.

(45) Thuaud, N.; Sebille, B.; Deratani, A.; Lelievre, G. *J. Chromatogr.* **1990**, *503*, 453.

(46) Matsui, Y.; Ogawa, K.; Mikami, S.; Yoshimoto, M.; Mochida, K. *Bull. Chem. Soc. Jpn.* **1987**, *60*, 1219.

(47) Schneider, H.-J.; Theis, I. *Angew. Chem., Int. Ed. Engl.* **1989**, *28*, 753.

(48) Schneider, H.-J. *Angew. Chem., Int. Ed. Engl.* **1991**, *30*, 1417.

(49) Camilleri, P.; Edwards, A. J.; Rzepa, H. S.; Green, S. M. *J. Chem. Soc., Chem. Commun.* **1992**, 1122.

(50) Amato, M. E.; Djedaïni-Pilard, F.; Perly, B.; Scarlata, G. *J. Chem. Soc., Perkin Trans. 2.* **1992**, 1065.

(51) Eliseev, A. V.; Schneider, H.-J. *Angew. Chem., Int. Ed. Engl.* **1993**, *32*, 1331.

(52) Benschop, H. P.; Van den Berg, G. R. *Chem. Commun.* **1970**, 1431.
(53) Mikolajczyk, M.; Drabowicz, J. *J. Am. Chem. Soc.* **1978**, *100*, 2510.
(54) Hinze, W. L.; Riehl, T. E.; Armstrong, D. W.; DeMond, W.; Alak, A.; Ward, T. *Anal. Chem.* **1985**, *57*, 237.
(55) Armstrong, D. W.; DeMond, W.; Alak, A.; Hinze, W. L.; Riehl, T. E.; Bui, K. H. *Anal. Chem.* **1985**, *57*, 234.
(56) Ihara, Y.; Nakanishi, E.; Nango, M.; Koga, J. *Bull. Chem. Soc. Jpn.* **1986**, *59*, 1901.
(57) Hattori, K.; Takahashi, K.; Uematsu, M.; Sakai, N. *Chem. Lett.* **1990**, 1463.
(58) Hattori, K.; Takahashi, K.; Sakai, N. *Bull. Chem. Soc. Jpn.* **1992**, *65*, 2690.
(59) Coates, J. H.; Easton, C. J.; van Eyk, S. J.; May, B. L.; Singh, P.; Lincoln, S. F. *J. Chem. Soc., Chem. Commun.* **1991**, 759.
(60) Guy, A.; Doussot, J.; Garreau, R.; Godefroy-Falguieres, A. *Tetrahedron: Asymmetry* **1992**, *3*, 247.
(61) Jung, M.; Schmalzing, D.; Schurig, V. *J. Chromatogr.* **1991**, *552*, 43.
(62) Karnik, N. A.; Prankerd, R. J.; Perrin, J. H. *Chirality* **1991**, *3*, 124.
(63) Tabushi, I. *Pure Appl. Chem.* **1986**, *58*, 1529.
(64) Takahashi, K.; Ohtsuka, Y.; Hattori, K. *Chem. Lett.* **1990**, 2227.
(65) Takahashi, K. *Bull. Chem. Soc. Jpn.* **1993**, *66*, 550.
(66) Kano, K.; Tamiya, Y.; Hashimoto, S. *J. Inclusion Phenom. Mol. Recognit. Chem.* **1992**, *13*, 287.
(67) Bright, F. V.; Catena, G. C.; Huang, J. *J. Am. Chem. Soc.* **1990**, *112*, 1343.
(68) Arad-Yellin, R.; Green, B. S.; Knossow, M.; Tsoucaris, G. *Inclusion Compounds*; Atwood, J. L., Davies, J. E., MacNicol, D. D.,Eds; Academic Press: London, **1984**, Vol. 3, pp 265-272.
(69) Kuroda, Y.; Ito, M.; Sera, T.; Ogoshi, H. *J. Am. Chem. Soc.* **1993**, *115*, 7003.
(70) Berberan-Santos, M. N.; Canceill, J.; Brochon, J.-C.; Jullien, L.; Lehn, J.-M.; Pouget, J.; Tauc, P.; Valeur, B. *J. Am. Chem. Soc.* **1992**, *114*, 6427.
(71) Akiyama, M.; Katoh, A.; Kato, J.; Takahashi, K.; Hattori, K. *Chem. Lett.* **1991**, 1189.
(72) Coleman, A. W.; Ling, C.-C.; Miocque, M. *Angew. Chem., Int. Ed. Engl.* **1992**, *31*, 1381.
(73) Isnin, R.; Kaifer, A. E. *J. Am. Chem. Soc.* **1991**, *113*, 8188.
(74) Wylie, R. S.; Macartney, D. H. *J. Am. Chem. Soc.* **1992**, *114*, 3136.
(75) Harada, A.; Li, J.; Kamachi, M. *Nature* **1993**, *364*, 516.
(76) Tabushi, I. *Coord. Chem. Rev.* **1988**, *86*, 1.
(77) Yoon, C.-J.; Ikeda, H.; Kojin, R.; Ikeda, T.; Toda, F. *J. Chem. Soc., Chem. Commun.* **1986**, 1080.
(78) Rideout, D. C.; Breslow, R. *J. Am. Chem. Soc.* **1980**, *102*, 7817.
(79) McNamara, M.; Russell, N. R. *J. Inclusion Phenom. Mol. Recognit. Chem.* **1992**,

13, 145.

(80) Fuchs, R.; Habermann, N.; Klüfers, P. *Angew. Chem., Int. Ed. Engl.* **1993**, *32*, 852.

(81) Akkaya, E. U.; Czarnik, A. W. *J. Phys. Org. Chem.* **1992**, *5*, 540.

(82) Tabushi, I.; Kuroda, Y. *J. Am. Chem. Soc.* **1984**, *106*, 4580.

CHAPTER TWO

THE COMPLEXATION OF CARBOXYLIC ACIDS BY BETA-CYCLODEXTRIN AND AN AMINO BETA-CYCLODEXTRIN DERIVATIVE

2.1 Introduction

The role of electrostatic interactions in the formation of cyclodextrin complexes is still not well understood, and so it is of interest to investigate the complexation of polar guests by cyclodextrins. The complexation of either an acidic or basic guest by a host such as a cyclodextrin usually leads to a change in the acid-base equilibria in solution. The resulting change in pH can easily be monitored to yield stability constants, making potentiometric titration a suitable method for studying the complexation of polar guests by cyclodextrins. Potentiometric titration is a desirable technique as it is very efficient and convenient, it can be used to measure a wide range of stability constants, and it can be used at quite low concentrations of guests. The method is widely applicable simply because guests are often acidic or basic.

The monosubstituted amino cyclodextrin, $\beta CDNH_2$, was chosen to investigate the effect of substitution and charge on the complexation and chiral discrimination characteristics of the βCD annulus. The replacement of a primary hydroxyl group of βCD by an amino group is particularly attractive, as at an appropriate pH the cyclodextrin can become positively charged, and apart from a slightly greater asymmetry it is likely that the basic cyclodextrin unit remains unperturbed. Results obtained from crystallographic studies indicate that O6 monosubstituted βCD derivatives have essentially the same macrocyclic conformation as βCD.[1] Benzoic acid, 4-methylbenzoic acid and *R*- and *S*-2-phenylpropanoic acid and their conjugate bases were chosen as guests that were likely to form complexes characterized by reasonable apparent stability constants with βCD and related hosts as a consequence of their

size and aromatic character. The simplicity of their structure makes it unlikely that their inclusion will be dominated by steric effects, making them suitable guests for investigating electrostatic interactions. The structures of the carboxylic acids and βCDNH$_2$ are shown in Figure 2.1.

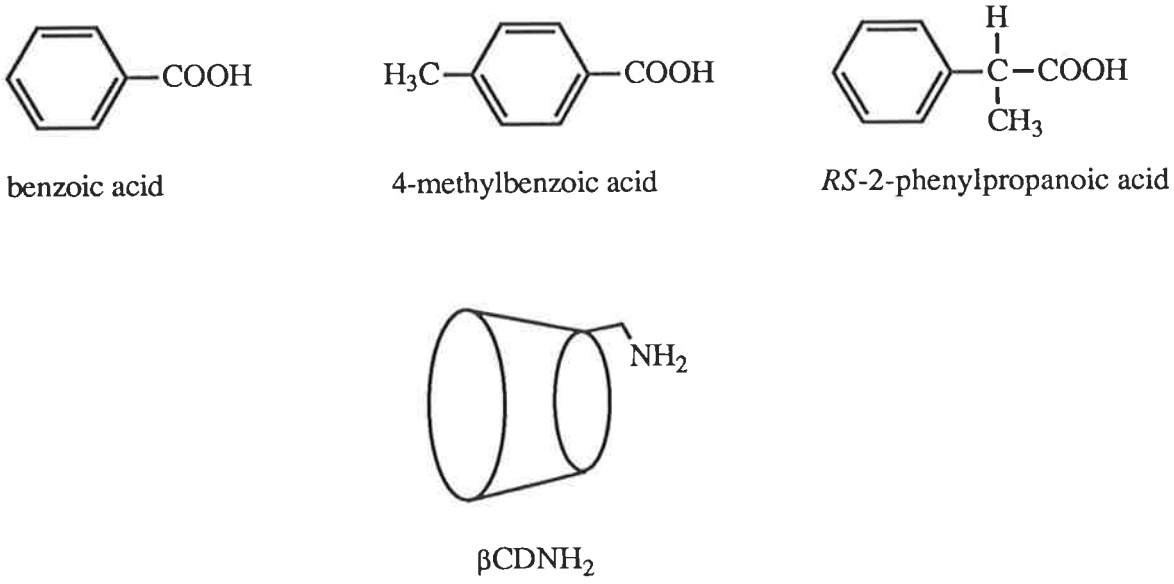

benzoic acid

4-methylbenzoic acid

RS-2-phenylpropanoic acid

βCDNH$_2$

Figure 2.1 Chemical structures of the carboxylic acid guests and the modified cyclodextrin studied.

Consider the complexation of a carboxylic acid, HA, and its conjugate base, A$^-$, by βCD, which may be expressed as in Scheme 2.1.

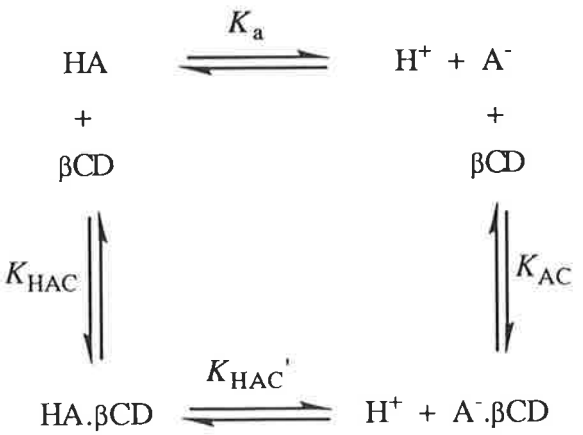

(2.1)

The subscripts used to define the apparent stability constants, K, are C for βCD, Ca for $\beta CDNH_2$, and A for the carboxylate guest, with protonations as indicated. In Scheme 2.1, K_a is the acid dissociation constant of the carboxylic acid, K_{HAC} and K_{AC} are the apparent stability constants for the complexation of HA and A^- by βCD, respectively, and K_{HAC}' is the acid dissociation constant of HA in the HA.βCD complex. Provided that K_{HAC} and K_{AC} are different (or equivalently, that K_a and K_{HAC}' are different), the addition of βCD to a solution containing a mixture of HA and A^- causes a shift in the measured pH of the solution, allowing K_{HAC} and K_{AC} to be determined. The value of K_a can be independently measured and used as a fixed parameter in the fitting process; the value of K_{HAC}' can be calculated from the values of K_{HAC}, K_{AC} and K_a.

In similar systems involving modified cyclodextrins such as $\beta CDNH_2$, the protonation state of the cyclodextrin must also be considered. At low pHs, the complexation of HA and A^- by $\beta CDNH_3^+$ may be expressed as in Scheme 2.2,

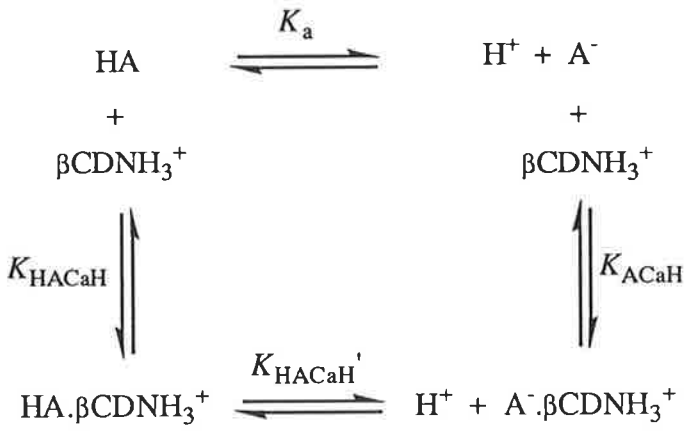

(2.2)

where K_a, K_{HACaH}, K_{ACaH} and K_{HACaH}' are constants characterizing the equilibria as shown, directly analogous to the complexation of HA and A^- by βCD. An appropriate choice of pH range, as determined by the pK_a values of HA and $\beta CDNH_3^+$, renders the species $A^-.\beta CDNH_2$ unimportant in the pH region chosen. Provided K_{HACaH} and K_{ACaH} are different, the addition of $\beta CDNH_3^+$ to a solution containing a mixture of HA and A^- causes a shift in the measured pH of the solution, allowing K_{HACaH} and K_{ACaH} to be determined. Similarly, at high pHs the complexation of A^- by $\beta CDNH_3^+$ and $\beta CDNH_2$ may be expressed as in Scheme 2.3,

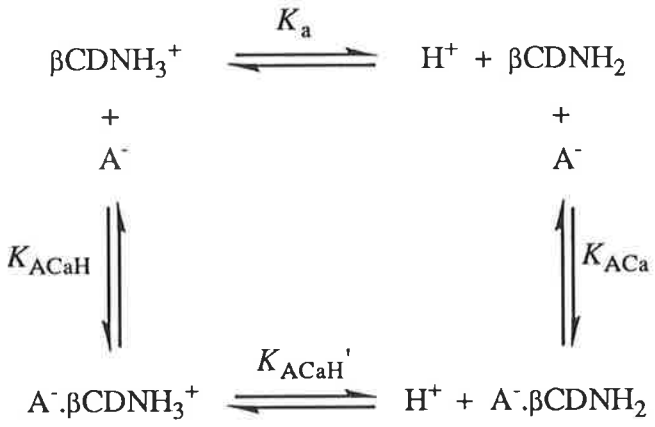

(2.3)

where K_a, K_{ACaH}, K_{ACa} and K_{ACaH}' are constants characterizing the equilibria as shown. An appropriate choice of pH range, as determined by the pK_a values of HA and $\beta CDNH_3^+$, renders the species HA.$\beta CDNH_3^+$ unimportant in the pH region chosen. Provided K_{ACaH} and K_{ACa} are different, the addition of A^- to a solution containing a mixture of $\beta CDNH_3^+$ and $\beta CDNH_2$ causes a shift in the measured pH of the solution, allowing K_{ACaH} and K_{ACa} to be determined. A combination of the experiments outlined in Schemes 2.2 and 2.3 allows separate determinations of K_{ACaH} which may then be compared.

In summary, for appropriate host-guest systems, monitoring the pH changes in solutions of guest or cyclodextrin as cyclodextrin or guest is added allows determination of apparent stability constants.

2.2 Results and Discussion

The apparent stability constants derived from the best fit of the experimental data (see Section 6.1.2) to Schemes 2.1, 2.2 and 2.3 for the complexation of benzoic acid, 4-methyl-benzoic acid and *R*- and *S*-2-phenylpropanoic acid and their conjugate bases by βCD, $\beta CDNH_3^+$ and $\beta CDNH_2$ are listed in Tables 2.1 and 2.2. The acid dissociation constants for HA and $\beta CDNH_3^+$, and the derived acid dissociation constants for HA complexed by βCD and $\beta CDNH_3^+$, and $\beta CDNH_3^+$ complexed by A^-, are listed in Table 2.3. The apparent stability constants for *R*- and *S*-2-phenylpropanoic acid are determined by independent titrations of the resolved enantiomers. Typical experimental data and best fit curves are shown in Figures 2.2, 2.3 and 2.4, for the interaction of *R*- and *S*-2-phenylpropanoic acid/phenylpropanoate with βCD, $\beta CDNH_3^+$ and $\beta CDNH_2$.

Table 2.1 Apparent stability constants for the complexes of βCD with benzoic acid, 4-methylbenzoic acid and *R*- and *S*-2-phenylpropanoic acid and their conjugate bases at $I = 0.10$ (KCl) and 298.2 K.

Guest	K_{HAC} $dm^3\ mol^{-1}$	K_{AC} $dm^3\ mol^{-1}$
benzoic acid	590 ± 60	
benzoate		60 ± 10
4-methylbenzoic acid	1680 ± 90	
4-methylbenzoate		110 ± 1
R-2-phenylpropanoic acid	1090 ± 30	
R-2-phenylpropanoate		63 ± 8
S-2-phenylpropanoic acid	1010 ± 40	
S-2-phenylpropanoate		52 ± 5

Table 2.2 Apparent stability constants for the complexes of $\beta CDNH_2$ and $\beta CDNH_3^+$ with benzoic acid, 4-methylbenzoic acid and *R*- and *S*-2-phenylpropanoic acid and their conjugate bases at $I = 0.10$ (KCl) and 298.2 K.

Guest	K_{HACaH} $dm^3\ mol^{-1}$	K_{ACaH} $dm^3\ mol^{-1}$	K_{ACa} $dm^3\ mol^{-1}$
benzoic acid	340 ± 30		
benzoate		120 ± 20	50 ± 20
4-methylbenzoic acid	910 ± 20		
4-methylbenzoate		330 ± 20	100 ± 20
R-2-phenylpropanoic acid	580 ± 20		
R-2-phenylpropanoate		150 ± 8	36 ± 6
S-2-phenylpropanoic acid	480 ± 10		
S-2-phenylpropanoate		110 ± 10	13 ± 7

Table 2.3 Acid dissociation constants for free and complexed βCDNH$_3^+$, benzoic acid, 4-methylbenzoic acid and *R*- and *S*-2-phenylpropanoic acid at I = 0.10 (KCl) and 298.2 K.

Guest	pK_a	p$K_{HAC'}$	p$K_{HACaH'}$	p$K_{ACaH'}$ [a]
benzoic acid	4.06 ± 0.04	5.1 ± 0.1	4.5 ± 0.1	
benzoate				8.9 ± 0.2
4-methylbenzoic acid	4.20 ± 0.08	5.39 ± 0.09	4.6 ± 0.1	
4-methylbenzoate				9.0 ± 0.1
R-2-phenylpropanoic acid	4.23 ± 0.05	5.47 ± 0.08	4.82 ± 0.06	
R-2-phenylpropanoate				9.11 ± 0.08
S-2-phenylpropanoic acid	4.23 ± 0.05	5.52 ± 0.07	4.87 ± 0.07	
S-2-phenylpropanoate				9.4 ± 0.4

[a]The pK_a of βCDNH$_3^+$ at I = 0.10 (KCl) and 298.2 K is 8.49 ± 0.01.

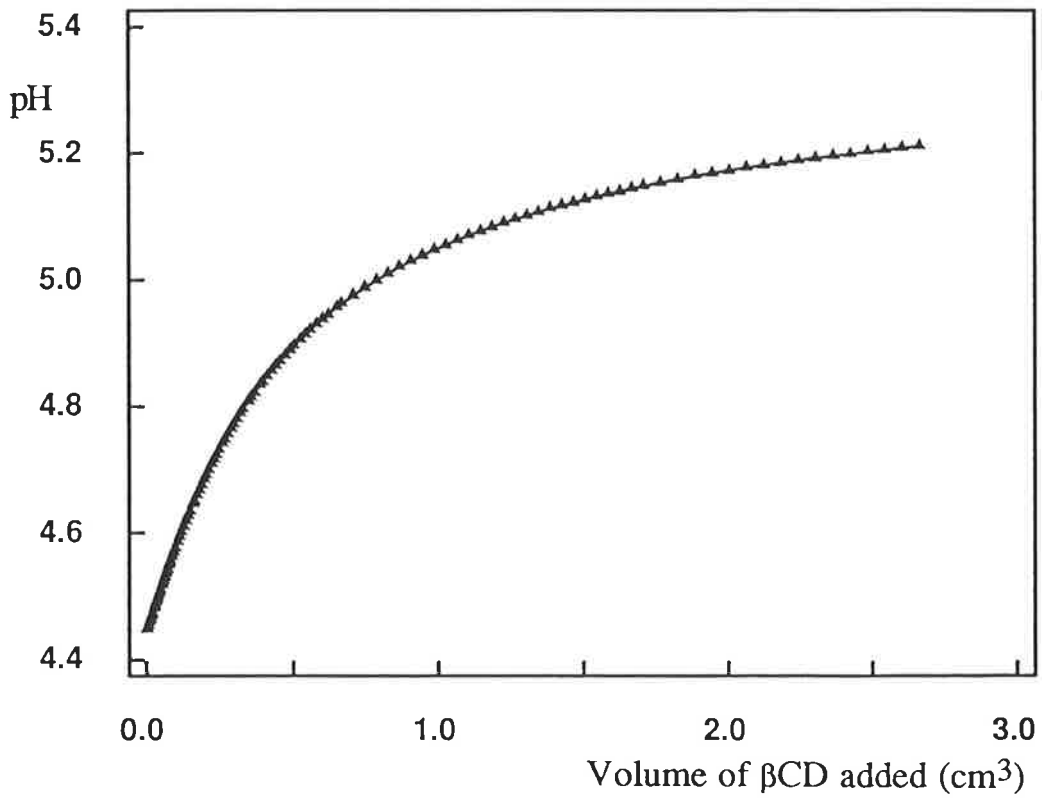

Figure 2.2 Variation of the pH of a 2.0 cm^3 solution of *R*-2-phenylpropanoic acid/phenylpropanoate (2.28 x 10^{-3} mol dm^{-3}) with volume of added βCD (1.51 x 10^{-2} mol dm^{-3}) at $I = 0.10$ (KCl) and 298.2 K. The curve through the data points represents the best fit of the data to Scheme 2.1 using SUPERQUAD (see Section 6.1.2). The data for *S*-2-phenylpropanoic acid at a similar concentration is coincident with this curve.

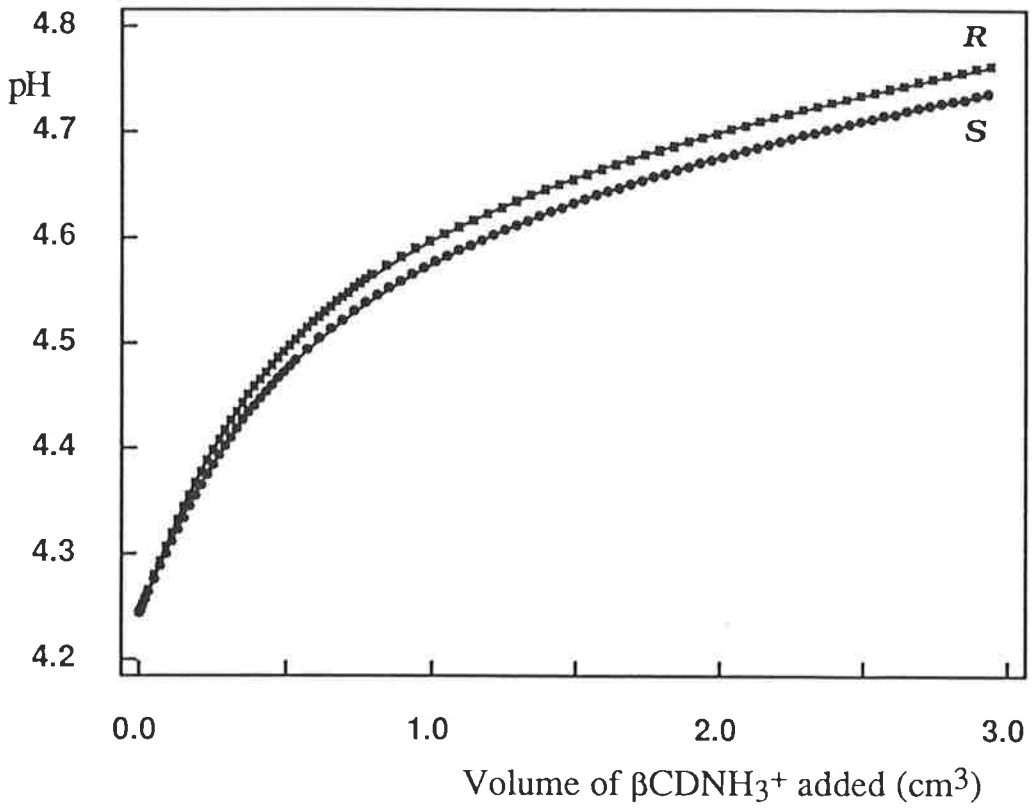

Figure 2.3 Variation of the pH of a 2.0 cm^3 solution of *R*- and *S*-2-phenylpropanoic acid/phenylpropanoate (2.28 x 10^{-3} and 2.10 x 10^{-3} mol dm^{-3}, respectively) with volume of added $\beta CDNH_3^+$ (1.58 x 10^{-2} mol dm^{-3}) at I = 0.10 (KCl) and 298.2 K. The upper and lower data sets refer to *R*- and *S*-2-phenylpropanoic acid/phenylpropanoate, respectively. The curves through the data points represent the best fit of the data to Scheme 2.2 using SUPERQUAD (see Section 6.1.2).

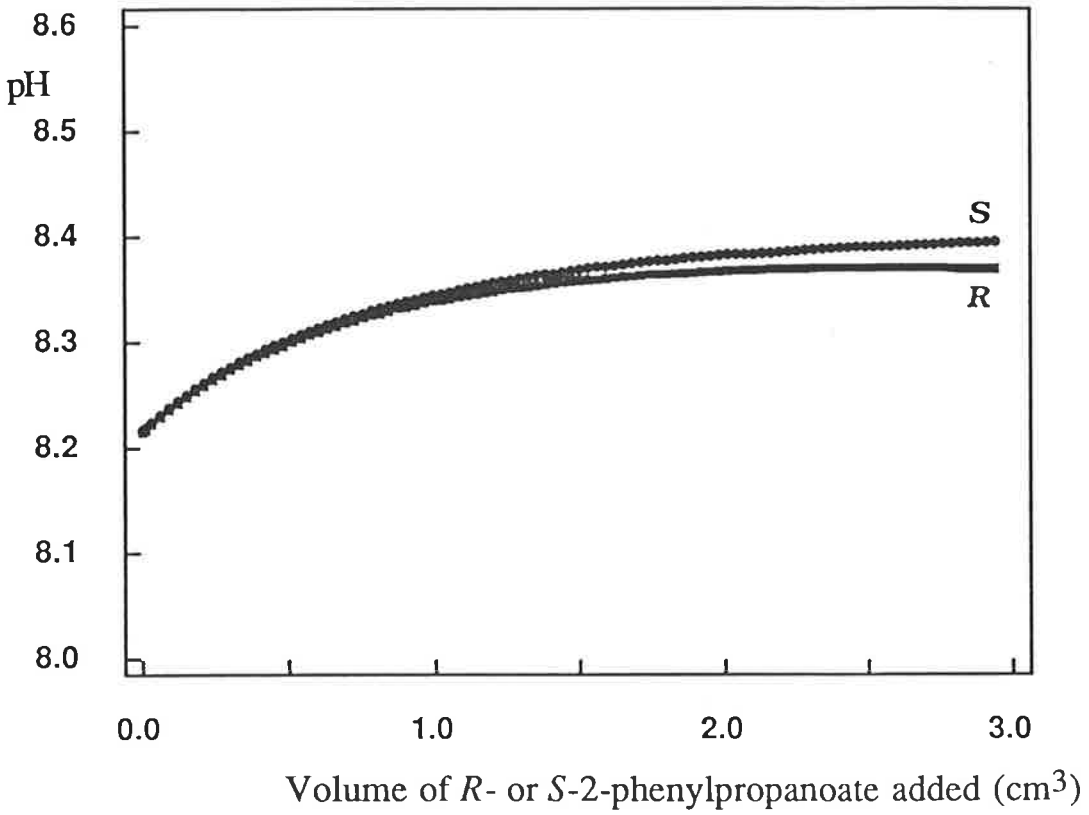

Figure 2.4 Variation of the pH of a 2.0 cm^3 solution of $\beta CDNH_3^+/\beta CDNH_2$ (2.21 x 10^{-3} mol dm^{-3}) with volume of added *R*- and *S*-2-phenylpropanoate (1.40 x 10^{-2} and 1.50 x 10^{-2} mol dm^{-3}, respectively) at $I = 0.10$ (KCl) and 298.2 K. The upper and lower data sets refer to *S*- and *R*-2-phenylpropanoate, respectively. The curves through the data points represent the best fit of the data to Scheme 2.3 using SUPERQUAD (see Section 6.1.2).

The experimentally determined pK_a values of the carboxylic acids listed in Table 2.3 compare reasonably well with literature values.[2] The pK_a value of $\beta CDNH_3^+$ is 8.49 ± 0.01 at I = 0.10 and 298.2 K, and this value may be compared with 10.66 for 1-aminoethane at I = 0.5 and 298 K, 9.52 for 2-hydroxyaminoethane at I = 0.1 and 298 K, and 9.30 for 2-methoxyaminoethane at I = 0.5 and 298 K.[2] The particularly low pK_a value of $\beta CDNH_3^+$, as compared with other primary amines, is attributed to intramolecular interactions between the NH_3^+ substituent and the adjacent hydroxyl residues and ether linkages of the cyclodextrin annulus.[3,4] This is consistent with the pK_a values of 5.81 and 8.01 reported for 6^A-[2-(4-imidazolyl)ethylamino]-6^A-deoxy-β-cyclodextrin, as compared with the pK_a values of 6.08 and 9.8 for 2-(4-imidazolyl)ethylamine.[5] 1D ^1H and ^{13}C NMR evidence indicates that an intramolecular hydrogen bond between the amine and the imidazole *N*-1 needs to be broken before deprotonation can occur, causing an increase in the acidity of the amine adjacent to the cyclodextrin.

Apparent stability constants of 546 ± 2 and 36.2 ± 0.4 are reported for the complexation of benzoic acid and benzoate, respectively, by βCD, at 298 K and an unspecified ionic strength, as determined by potentiometric titration.[6] An apparent stability constant of 604 is reported for the complexation of benzoic acid by βCD at room temperature in 0.1 mol dm^{-3} HCl, as determined by circular dichroism.[7] An apparent dissociation constant of 4.95 is reported for benzoic acid in the benzoic acid.βCD complex at 298 K and an unspecified ionic strength, as determined by potentiometric titration.[8] These values compare quite well to those determined in this study. No literature values can be found for the other complexes investigated.

2.2.1 Orientation of the Guests in the Cyclodextrin Cavity

To interpret the apparent stability constants it is important to gain as much information as possible about the orientation of the guests in the cyclodextrin cavity. The only definitive way of gaining this information in solution is by 2D NMR techniques such as ROESY (see Section 6.2.3). Of the host-guest combinations investigated, only the 4-methyl-benzoate.$\beta CDNH_3^+$ complex is suitable for detailed study by ROESY. It should be noted,

however, that the ROESY spectrum of *RS*-2-phenylpropanoic acid with $\beta CDNH_3^+$ shows strong crosspeaks between the aromatic signals of the guest and the internal protons of the cyclodextrin cavity, indicating that an intermolecular complex is forming, but that no information about the direction of inclusion can be obtained from the spectrum.

The ROESY spectrum of 4-methylbenzoate with $\beta CDNH_3^+$ is shown in Figure 2.5, with the complete 1D ^1H spectrum for this system shown on the left hand side of the diagram, including assignment of the significant peaks. The three signals from the 4-methylbenzoate protons are the singlet at 2.4 ppm for the methyl group, and the two pseudo-doublets for the aromatic protons at 7.3 ppm for the meta protons (adjacent to the methyl group), and 7.8 ppm for the ortho protons (adjacent to the carboxylate group). Comparison of the chemical shifts of $\beta CDNH_3^+$ complexed 4-methylbenzoate with free 4-methylbenzoate shows that the shift experienced by the guest protons upon complexation is greatest for the ortho protons, with the meta and methyl protons experiencing smaller shift changes of a similar magnitude. The cyclodextrin signals are assigned by comparison of the chemical shifts and peak multiplicities with the literature,[9] and confirmed using standard COSY and ^1H decoupling experiments (see Section 6.2.3). The basic symmetry of the cyclodextrin molecule is retained for the modified cyclodextrin $\beta CDNH_3^+$, so signals are easily identified. Starting with the signals that appear the furthest downfield, H1 appears at around 5 ppm, H3 at 3.9 ppm, H5 and H6 as the strong broad unresolved peak at around 3.75 ppm, H2 at 3.55 ppm, and H4 at 3.47 ppm. Smaller signals from the modified glucose unit are visible around 3.2 ppm and 4.05 ppm, but attempts to assign these signals by COSY and ^1H decoupling spectroscopy are inconclusive. However, experimental and literature evidence suggests that the signal at 4.05 ppm is most likely to arise from the H5 protons on the modified glucose unit.[4] The H3, H5 and H6 protons are located on the inside of the cavity, with the H3 protons situated at the wider secondary end of the cavity, and the H5 and H6 protons located near the narrower primary end of the cavity. The H3 and H5/H6 protons of $\beta CDNH_3^+$ in the 4-methylbenzoate.$\beta CDNH_3^+$ complex experience greater shift changes than the H1, H2 and H4 protons, indicative of the formation of an intermolecular inclusion complex.

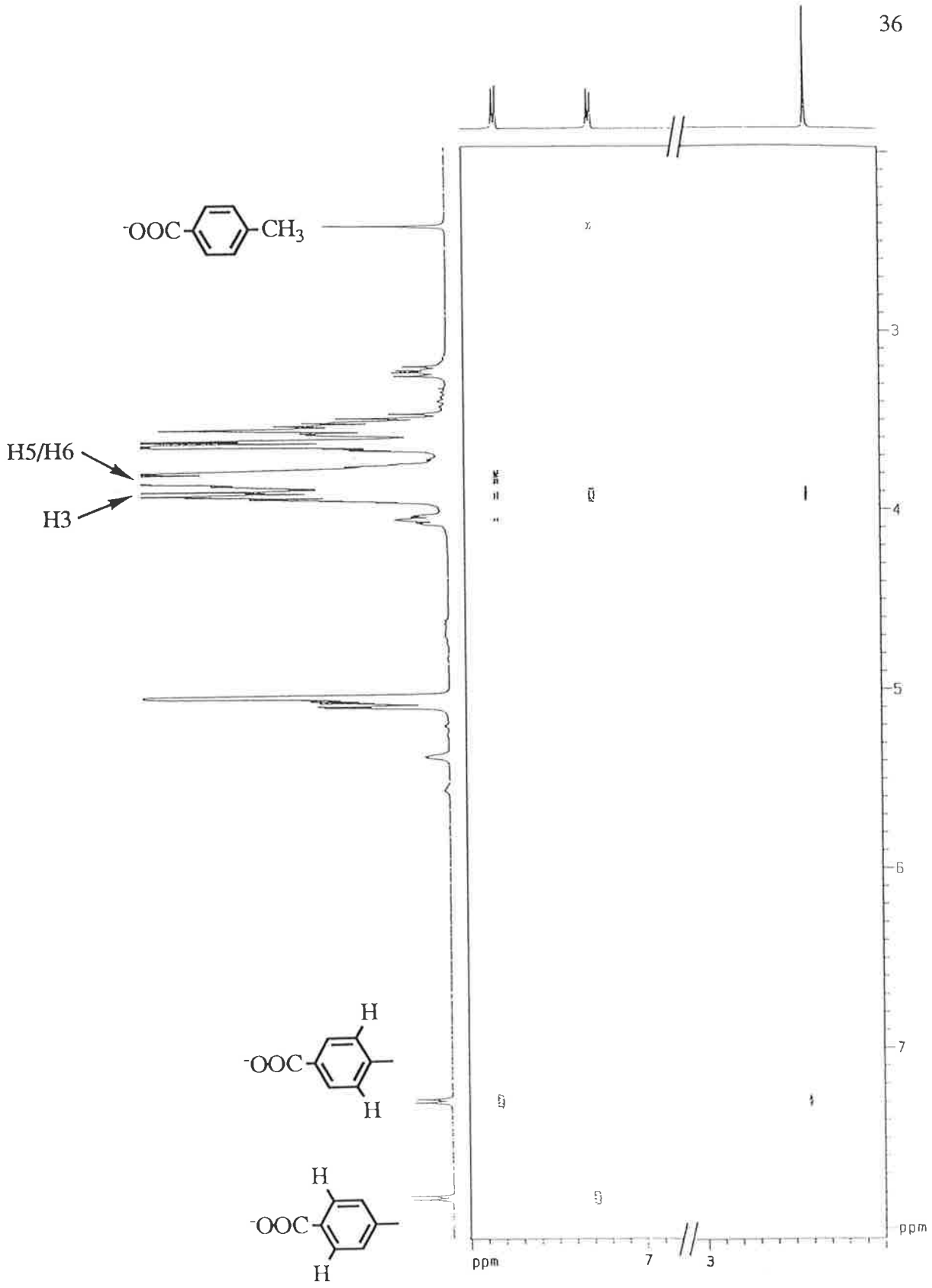

Figure 2.5 Partial contour plot of the negative levels of the ROESY spectrum (400 MHz) of 4-methylbenzoate (0.005 mol dm^{-3}) and $\beta CDNH_3^+$ (0.03 mol dm^{-3}) at pH 6.4 and 0.2 mol dm^{-3} (phosphate buffer in D_2O). Peak assignments are shown for the aromatic and methyl protons of the guest, and the H3 and H5/H6 protons of the cyclodextrin. Crosspeaks indicate protons that are close in space. The spectrum was run by Peter Barron of Bruker (Australia) on a Bruker AMX 400 spectrometer in Melbourne, Australia.

Crosspeaks in a ROESY spectrum are inverted relative to the diagonal peaks, and indicate protons that are close in space, typically less than 300 - 400 pm (3 - 4 Å).[10] Figure 2.5 shows crosspeaks between the ortho protons of the guest and the H5/H6 and H3 internal cavity protons of the cyclodextrin. This provides definitive evidence for the formation of the inclusion complex. It also indicates that the ortho protons are in a position in the cavity to interact with both the primary and secondary ends of the cyclodextrin molecule. The methyl and meta protons of the guest show crosspeaks with the H3 cyclodextrin cavity protons, but no interaction with the H5/H6 cyclodextrin cavity protons. The ortho protons also show a crosspeak with the signal at 4.05 ppm, indicating that the ortho protons of the guest are interacting strongly with the modified glucose unit of the cyclodextrin, probably with the H5 protons.

All of this evidence indicates that 4-methylbenzoate is orientated in the $\beta CDNH_3^+$ cavity with the carboxylate group near the primary end and the methyl group near the secondary end, as shown in Figure 2.6. This allows a specific electrostatic interaction between the oppositely charged functional groups on the host and guest, and is consistent with an antiparallel alignment of the dipoles of the host and guest (see Section 1.4). The similarity in the behaviour of benzoate and *RS*-2-phenylpropanoate with $\beta CDNH_3^+$, as reflected in their apparent stability constants, to that of 4-methylbenzoate with $\beta CDNH_3^+$, makes it probable that these guests are aligned in the cavity in a similar fashion.

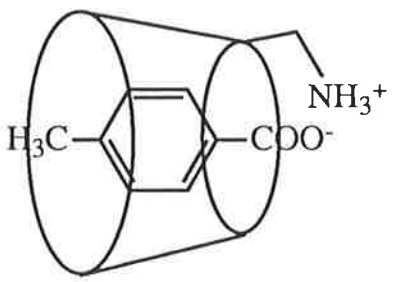

Figure 2.6 Structure of the complex formed between 4-methylbenzoate and $\beta CDNH_3^+$, as determined by ROESY spectra.

It is interesting to compare this result with other studies performed to determine the orientation of polar and charged guests in a cyclodextrin cavity. Most other studies rely on either the interpretation of 1D ^{1}H and ^{13}C NMR spectra, or the extrapolation of structures determined crystallographically to the solution state. Although less definitive than 2D NMR spectroscopy, these studies still provide some interesting information. Most detailed studies of cyclodextrin systems have concentrated on αCD, and the range of information on βCD complexes is considerably smaller and less systematic. There is, however, useful information to be gained from a discussion of the inclusion of carboxylic acid guests by αCD, despite the inherent difficulties in applying results determined for αCD to systems involving βCD.

For the complexation of benzoic acid by αCD, 1D ^{1}H, ^{13}C and intermolecular NOE NMR studies show that the carboxylic acid group is situated in the vicinity of the primary hydroxyl groups of αCD.[11,12] This orientation is consistent with an antiparallel alignment of the αCD and benzoic acid dipole moments. The crystal structure of the αCD complex of 4-hydroxybenzoic acid shows that the carboxylic acid group is so deeply inserted in the cavity that it is adjacent to the primary hydroxyl groups.[13] The apparent stability constants for the complexation of a range of 4-substituted benzoic acids by αCD decrease as the electron withdrawing nature of the 4- substituent increases. This is interpreted as indicating that the carboxylic acid group is situated in the cavity.[14] All of this evidence indicates that the carboxylic acid group is usually situated in the cavity when simple carboxylic acid derivatives are complexed by αCD.

The orientation of benzoate and other carboxylate guests in the αCD cavity is less certain, as the low apparent stability constants of such complexes hinder comprehensive studies. The 1D ^{1}H NMR spectrum of the benzoate.αCD complex is interpreted as indicating that the carboxylate group is situated in the cavity,[11] yet 1D ^{13}C NMR evidence for the same complex is interpreted as indicating that the phenyl group is situated in the cavity.[12,15] Such differences in interpretation highlight the difficulty in making definitive statements about the orientation of guests in the cyclodextrin cavity in solution without direct evidence from 2D NMR studies. A 1D ^{13}C NMR study on the complex of αCD with 4-methylcinnamate indicates that the carboxylate group is situated in the cavity.[16] Another 1D ^{13}C NMR study

shows that the complex formed by 4-biphenylcarboxylate and two αCD molecules is so stable that the binary complex cannot be detected.[17] This indicates that complexation of both ends of the guest, including the carboxylate group, is very strong. The stability of the complexes of 4-substituted benzoates with αCD increases as the electron withdrawing nature of the 4- substituent increases, a trend opposite to that observed for the complexation of similar 4-substituted benzoic acids by αCD. This trend is interpreted as indicating that the 4- substituent of the benzoate guest is bound in the cavity while the carboxylate group projects into the solvent.[14] All of this evidence shows that it is not possible to conclude that carboxylate guests are usually orientated in the cavity in a certain direction, but that there are circumstances where carboxylate guests are very strongly included with the carboxylate group inside the cyclodextrin cavity.

For the larger βCD host, circular dichroism studies show that simple mono- and di-substituted aromatic guests are included with their long axis parallel to the axis through the centre of the βCD cavity (see Section 1.3). Such axial inclusion makes it still possible to say, especially for mono- and 1,4-substituted aromatic guests, that a certain functional group of the guest is located in the βCD cavity while another part of the guest is in the solvent. These βCD complexes are then comparable with similar αCD complexes, and this allows conclusions about the orientation of carboxylic acid and carboxylate guests in the αCD cavity to be applied to βCD complexes. It is thus reasonable to assume that the carboxylic acid group is situated in the cavity in the βCD complexation of the acid form of the guests studied. This corresponds to an antiparallel alignment of the dipoles of the host and guest.

Again, the situation is less clear for the complexation of carboxylates by βCD. Although the ROESY spectrum shows that the carboxylate group is situated in the cavity for the complex of 4-methylbenzoate with $\beta CDNH_3^+$, the carboxylate guests in their complexes with βCD and $\beta CDNH_2$ may position with either the carboxylate or the phenyl group in the cavity. The former is the favoured arrangement, as it corresponds to an antiparallel alignment of the host and guest dipole moments. The increase in complex stability when the cyclodextrin host becomes positively charged may then be attributed to a deeper insertion of the guest due to the attraction between the opposite charges.

2.2.2 Trends in Apparent Stability Constants

In discussing the apparent stability constants for the complexation of the three carboxylic acid guests by the cyclodextrins, it is useful to think in terms of the competition between the water to solvate the guest and the cyclodextrin to complex the guest. From Tables 2.1 and 2.2 it is apparent that the carboxylic acid complexes are of higher stability than the analogous carboxylate complexes for both βCD and $\beta CDNH_3^+$, indicating that these cyclodextrins compete most strongly for the uncharged carboxylic acids.

The stability of the carboxylate complexes with βCD, $\beta CDNH_2$ and $\beta CDNH_3^+$ increases in the sequence $A^-.\beta CDNH_2 \leq A^-.\beta CD < A^-.\beta CDNH_3^+$, as shown in Tables 2.1 and 2.2. For all three guests the stability of the carboxylate complex with $\beta CDNH_3^+$ is increased by a factor of 2 - 3 relative to its stability with either uncharged βCD or $\beta CDNH_2$. The increased stability results in the complexation of 60 - 80% of the carboxylate by $\beta CDNH_3^+$, compared with 40 - 60% by βCD, for 0.001 mol dm^{-3} carboxylate and 0.015 mol dm^{-3} cyclodextrin at pH 7. The enhanced stability is due specifically to the positive charge on $\beta CDNH_3^+$ and not just the presence of the amine functional group, as the stability of the carboxylate complexes with $\beta CDNH_2$ and βCD are similar. This is consistent with ROESY results that suggest a direct interaction between the positive and negative charges of the host and guest. The stability of the carboxylic acid complexes with $\beta CDNH_3^+$ decreases by a factor of 1.5 - 2 relative to βCD, suggesting that the positive charge on the cyclodextrin reduces the overall hydrophobic interaction (see Section 1.4), causing a decrease in the apparent stability constants.

Similar overall stability enhancements, of the order of a factor of 2 - 3, have been observed in several other cyclodextrin systems which have the possibility of a direct interaction between positive and negative charges (see Section 1.4). The similar magnitude of this stability enhancement for a variety of singly charged guests with singly charged cyclodextrins indicates that it is a general effect. A single ion pair contact is expected to result in a ten-fold increase in the apparent stability constant, relative to a system where the electrostatic interaction cannot occur (see Section 1.4). The observation that the effect is generally smaller than this in cyclodextrin systems indicates either that the ion pair distances

are too great for the maximum possible interaction, or that the charged group(s) have decreased other interactions in the system, such as reducing the hydrophobic interaction or introducing unfavourable steric constraints.

The favourable effects of ionic interactions are evident in the $NaBH_4$ reduction of benzoyl formic acid to mandelic acid in the presence of $\beta CDNH_3^+$.[18,19] Asymmetric selectivity producing a 13% excess of *R*-mandelic acid is maximized in the pH range where the cyclodextrin and guest are oppositely charged, and selectivity is not observed for esters of benzoyl formic acid which have no possibility of an ionic interaction with the positively charged host. The greater selectivity of $\beta CDNH_3^+$, relative to βCD and for ionic guests, is attributed to the higher stability of the complex and the possibility of a direct ionic interaction between the positively charged amine group of $\beta CDNH_3^+$ and the negatively charged carboxylate group of the guest.[18,19]

From Tables 2.1 and 2.2, the stability of the carboxylic acid complexes with βCD, $\beta CDNH_2$ and $\beta CDNH_3^+$ increases in the sequence benzoic acid < *RS*-2-phenylpropanoic acid < 4-methylbenzoic acid. Three different factors are possibly important in determining this sequence. Firstly, the hydrophobic surface areas of *RS*-2-phenylpropanoic acid and 4-methylbenzoic acid are greater than that of benzoic acid, allowing these guests to have more extensive van der Waals interactions with the cyclodextrin cavity. Secondly, the solvated part of the molecule is proportionally larger for benzoic acid than for the other guests and this is likely to reduce the hydrophobic interaction for benzoic acid. Thirdly, an inspection of CPK models shows that it is probable that the fit of the guest species to the cyclodextrin cavity improves in the sequence benzoic acid < *RS*-2-phenylpropanoic acid < 4-methylbenzoic acid. Similarly, the stability of the carboxylate complexes in this study increases in the sequence *RS*-2-phenylpropanoate ≤ benzoate < 4-methylbenzoate. Although the three factors outlined above are also likely to be important in the complexation of the carboxylates, it seems as though the increase in solvation arising from the negative carboxylate charge has made the solvation factor more significant. Specifically, the extra solvation of the already bulky propanoate group has resulted in the stabilities of the benzoate and *RS*-2-phenylpropanoate complexes becoming comparable.

The results in Table 2.3 show that the derived acid dissociation constants for the complexed species are higher than the acid dissociation constants for the corresponding uncomplexed species. This indicates that in comparison with the uncomplexed state the acidity of the carboxylic acid guest and the protonated cyclodextrin is weakened by complexation, consistent with the conjugate bases of the complexes being destabilized relative to their conjugate acids. For the guest species, the negative charge of the carboxylate will cause it to be more strongly solvated than the carboxylic acid. The decreased solvation which must result from inclusion in the cyclodextrin appears to have a greater effect on the carboxylate, with the consequence that it is destabilized by comparison with the included carboxylic acid. This has the overall effect of decreasing the acidity of the complexed carboxylic acid. The relative stabilization of the anionic conjugate base by the positively charged cyclodextrin is clearly reflected in the greater acidity of HA in the HA.βCDNH$_3^+$ complex relative to HA in the HA.βCD complex. For βCDNH$_3^+$, the inclusion of the carboxylate may disrupt the intramolecular interactions between the NH$_3^+$ substituent and the adjacent hydroxyl residues and ether linkages of the cyclodextrin (see Section 2.2), resulting in a decrease in acidity.

2.2.3 Chiral Discrimination in the Complexation of *RS*-2-Phenylpropanoic acid/phenylpropanoate

The results in Tables 2.1 and 2.2 show that the *R* enantiomer of 2-phenylpropanoic acid is preferentially complexed by βCD and βCDNH$_3^+$. Similarly, the *R* enantiomer of 2-phenylpropanoate is preferentially complexed by βCDNH$_3^+$ and βCDNH$_2$, but within experimental error, no preferential complexation is observed when *RS*-2-phenylpropanoate is complexed by βCD. This indicates that thermodynamic discrimination (see Section 1.5) is occurring for all of the complexes studied, except for the complex of *RS*-2-phenylpropanoate and βCD. The replacement of a primary hydroxyl group by either NH$_3^+$ or NH$_2$ increases the asymmetry of the cyclodextrin annulus and accordingly βCDNH$_3^+$ and βCDNH$_2$ are more likely to discriminate between guest enantiomers than βCD (see Section 1.5). The differing extents of the complexation of the *R* and *S* enantiomers by βCDNH$_3^+$ and βCDNH$_2$ are shown in the species plot in Figure 2.7.

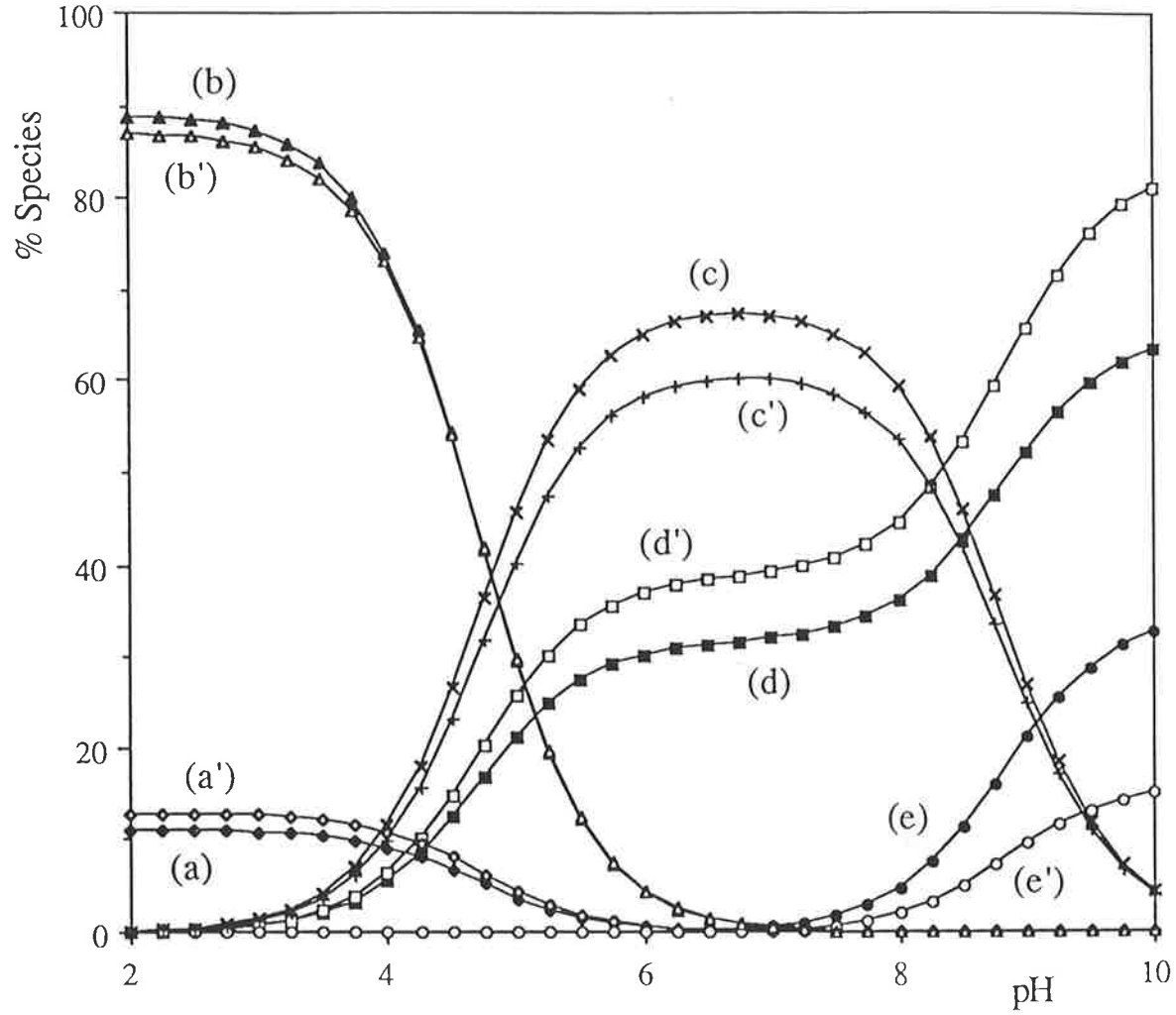

Figure 2.7 Species plot for the *RS*-2-phenylpropanoic acid/phenylpropanoate and $\beta CDNH_3^+/\beta CDNH_2$ system, as calculated from appropriate values in Table 2.2. The total concentration of either *R*- or *S*-2-phenylpropanoic acid/phenylpropanoate is 0.001 mol dm^{-3} and is defined as 100%. The total concentration of $\beta CDNH_3^+/\beta CDNH_2$ is 0.015 mol dm^{-3}, and free cyclodextrin species are not shown. *R*-2-phenylpropanoic acid/phenylpropanoate species are indicated by the filled shapes and unprimed letters; *S*-2-phenylpropanoic acid/phenylpropanoate species are represented by the open shapes and primed letters. The curves represent: (a) *R*-2-phenylpropanoic acid; (a') *S*-2-phenylpropanoic acid; (b) *R*-2-phenylpropanoic acid.$\beta CDNH_3^+$; (b') *S*-2-phenylpropanoic acid.$\beta CDNH_3^+$; (c) *R*-2-phenylpropanoate.$\beta CDNH_3^+$; (c') *S*-2-phenylpropanoate.$\beta CDNH_3^+$; (d) *R*-2-phenylpropanoate; (d') *S*-2-phenylpropanoate; (e) *R*-2-phenylpropanoate.$\beta CDNH_2$ and (e') *S*-2-phenylpropanoate.$\beta CDNH_2$.

The upfield regions of the 1D ^{1}H NMR spectra of *RS*-2-phenylpropanoic acid with βCD and βCDNH$_3^+$, and *RS*-2-phenylpropanoate with βCDNH$_3^+$, are shown in Fig 2.8. In the 1D ^{1}H NMR spectrum of *RS*-2-phenylpropanoic acid in D_2O/DCl at pH 1, the methyl proton resonances appear as a doublet at 1.289 ppm with $J_{H\text{-}H}$ = 7.2 Hz. In the presence of βCD this methyl resonance appears as two doublets, with the *R* enantiomer at 1.409 ppm with $J_{H\text{-}H}$ = 6.6 Hz and the *S* enantiomer at 1.421 ppm with $J_{H\text{-}H}$ = 6.9 Hz. In the presence of βCDNH$_3^+$ the methyl resonance appears as two doublets, with the *R* enantiomer at 1.428 ppm with $J_{H\text{-}H}$ = 6.9 Hz and the *S* enantiomer at 1.440 ppm with $J_{H\text{-}H}$ = 6.9 Hz. In the spectrum of *RS*-2-phenylpropanoate in phosphate buffer/D_2O at pH 6.4, the methyl proton resonances appear as a doublet at 1.357 ppm with $J_{H\text{-}H}$ = 7.2 Hz. In the presence of βCDNH$_3^+$ their methyl resonance appears as a doublet at 1.315 ppm with $J_{H\text{-}H}$ = 6.9 Hz. The broader ^{1}H resonances observed in the *RS*-2-phenylpropanoate spectra may result from an increased solution viscosity, due to the high concentration of the guest, cyclodextrin and phosphate buffer. It is not possible to carry out similar experiments with *RS*-2-phenylpropanoate in the presence of either βCD or βCDNH$_2$ as K_{AC} and K_{ACa} are too small to give sufficient concentrations of the inclusion complexes within the solubility limits of the systems (see Section 6.2.3).

The observation of separate *R* and *S* resonances for the methyl group of *RS*-2-phenylpropanoic acid in the presence of βCD and βCDNH$_3^+$ indicates that the magnetic environments of the methyl protons in the diastereomeric complexes are different. Thus, a magnetic discrimination (see Section 1.5) occurs when *RS*-2-phenylpropanoic acid is complexed by either βCD or βCDNH$_3^+$, but not when *RS*-2-phenylpropanoate is complexed by βCDNH$_3^+$. In contrast, significant thermodynamic discrimination occurs when either *RS*-2-phenylpropanoic acid or *RS*-2-phenylpropanoate is complexed by any of the cyclodextrins in this study, except when *RS*-2-phenylpropanoate is complexed by βCD. The lack of magnetic discrimination in the complexation of *RS*-2-phenylpropanoate by βCDNH$_3^+$, despite the observed thermodynamic discrimination for this complex, indicates that the methyl groups of *R*- and *S*-2-phenylpropanoate must either be in the same position or have very similar magnetic environments in this complex. This indicates that the existence of significant

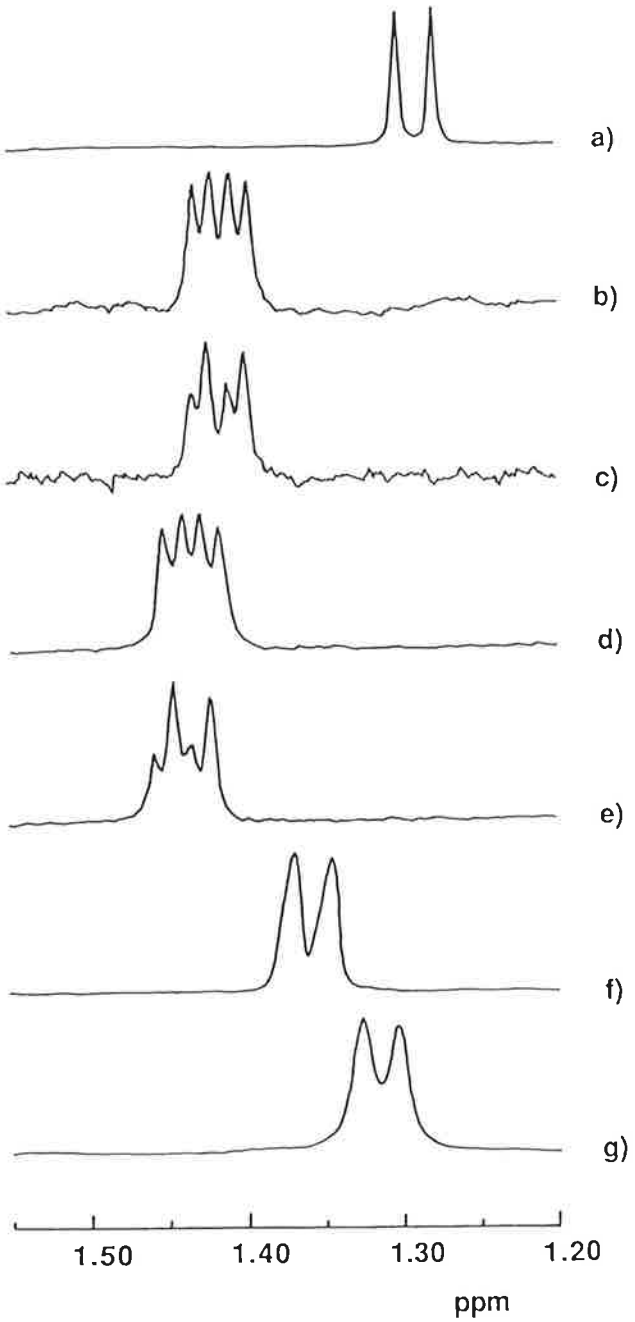

Figure 2.8 1D ^{1}H NMR (300 MHz) spectra of the methyl groups of: (a) *RS*-2-phenylpropanoic acid (0.005 mol dm^{-3}) at pH 1; (b) *RS*-2-phenylpropanoic acid (0.003 mol dm^{-3}) in the presence of βCD (0.011 mol dm^{-3}) at pH 1; (c) *RS*-2-phenylpropanoic acid (0.001 mol dm^{-3}) with added *R*-2-phenylpropanoic acid (0.0003 mol dm^{-3}) in the presence of βCD (0.011 mol dm^{-3}) at pH 1; (d) *RS*-2-phenylpropanoic acid (0.005 mol dm^{-3}) in the presence of $\beta CDNH_3^+$ (0.03 mol dm^{-3}) at pH 1; (e) *RS*-2-phenylpropanoic acid (0.002 mol dm^{-3}) with added *R*-2-phenylpropanoic acid (0.002 mol dm^{-3}) in the presence of $\beta CDNH_3^+$ (0.03 mol dm^{-3}) at pH 1; (f) *RS*-2-phenylpropanoate (0.01 mol dm^{-3}) at pH 6.4 and (g) *RS*-2-phenylpropanoate (0.01 mol dm^{-3}) in the presence of $\beta CDNH_3^+$ (0.09 mol dm^{-3}) at pH 6.4. The chemical shifts are downfield from TPS.

thermodynamic chiral discrimination does not necessarily induce sufficient magnetic inequivalence in the diastereomeric complexes to be detectable by 1D ^{1}H NMR spectroscopy. It should also be noted that the complexation induced shift changes are greater for the methyl group of the *S* enantiomer, despite the fact that the *R* enantiomer has the larger apparent stability constant. This highlights the fact that the magnitude of the complexation induced shift changes cannot be directly related to the magnitude of the apparent stability constants.

Chiral discrimination by a cyclodextrin, even on this small scale, may result in differences in complex structure and solution speciation that have significant effects on a particular system. The *R* enantiomer of *RS*-2-phenylpropanoic acid chloride preferentially reacts with βCD at pH 6.0, resulting in a product ratio of 1.3 : 1 for the *R* and *S* diastereomers. These diastereomeric 2-arylpropanoic acid esters of βCD also show different hydrolysis rates at pH 11.5, with the *R* enantiomer being hydrolysed twice as quickly as the *S* enantiomer.[20] The *R* selectivity in these deacylation and acylation reactions is probably the result of inclusion complex formation, with chiral interactions occurring as in the related complexation of *RS*-2-phenylpropanoic acid/phenylpropanoate by βCD and derivatives. Thus, the observed enantioselectivity can be attributed to such factors as the slightly different orientation of the enantiomers in the complex, and the higher stability of the βCD complex of the *R* enantiomer.

BIBLIOGRAPHY

(1) Harata, K. *Inclusion Compounds*; Atwood, J. L., Davies, J. E., MacNicol, D. D., Eds; Oxford University Press: Oxford, **1991**, Vol. 5, pp 311-344.

(2) *Critical Stability Constants*; Smith, R. M., Martell, A. E., Eds; Plenum Press: New York, **1975**, Vols 2, 3.

(3) Brown, S. E.; Coates, J. H.; Coghlan, D. R.; Easton, C. J.; van Eyk, S. J.; Janowski, W.; Lepore, A.; Lincoln, S. F.; Luo, Y.; May, B. L.; Schiesser, D. S.; Wang P.; Williams, M. L. *Aust. J. Chem.* **1993**, *46*, 953.

(4) Bonoma, R. P.; Cucinotta, V.; D'Alessandro, F.; Impellizzeri, G.; Maccarrone, G.; Rizzarelli E.; Vecchio, G. *J. Inclusion Phenom. Mol. Recognit. Chem.* **1993**, *15*, 167.

(5) Bonoma, R. P.; Cucinotta, V.; D'Alessandro, F.; Impellizzeri, G.; Maccarrone, G.; Vecchio, G.; Rizzarelli E. *Inorg. Chem.* **1991**, *30*, 2708.

(6) Gelb, R. I.; Schwartz, L. M. *J. Inclusion Phenom. Mol. Recognit. Chem.* **1989**, *7*, 465.

(7) Shimizu, H.; Kaito, A.; Hatano, M. *Bull. Chem. Soc. Jpn.* **1979**, *52*, 2678.

(8) Connors, K. A.; Lipari, J. M. *J. Pharm. Sci.* **1976**, *65*, 379.

(9) Schuette, J. M.; Ndou, T.; de la Peña, A. M.; Greene, K. L.; Williamson, C. K.; Warner, I. M. *J. Phys. Chem.* **1991**, *95*, 4897.

(10) Djedaïni, F.; Perly, B. *Cyclodextrins and Their Industrial Uses*; Duchêne, D., Ed; Editions de Santé: Paris, **1987**, pp 215-246.

(11) Bergeron, R. J.; Channing, M. A.; McGovern, K. A. *J. Am. Chem. Soc.* **1978**, *100*, 2878.

(12) Gelb, R. I.; Schwartz, L. M.; Johnson, R. F.; Laufer, D. A. *J. Am. Chem. Soc.* **1979**, *101*, 1869.

(13) Harata, K. *Bull. Chem. Soc. Jpn.* **1977**, *50*, 1416.

(14) Connors, K. A.; Lin, S.-F.; Wong, A. B. *J. Pharm. Sci.* **1982**, *71*, 217.

(15) Gelb, R. I.; Schwartz, L. M.; Cardelino, B.; Fuhrman, H. S.; Johnson, R. F.; Laufer, D. A. *J. Am. Chem. Soc.* **1981**, *103*, 1750.

(16) Gelb, R. I.; Schwartz, L. M.; Laufer, D. A. *J. Am. Chem. Soc.* **1978**, *100*, 5875.

(17) Gelb, R. I.; Schwartz, L. M.; Murray, C. T.; Laufer, D. A. *J. Am. Chem. Soc.* **1978**, *100*, 3553.

(18) Hattori, K.; Takahashi, K.; Uematsu, M.; Sakai, N. *Chem. Lett.* **1990**, 1463.

(19) Hattori, K.; Takahashi, K.; Sakai, N. *Bull. Chem. Soc. Jpn.* **1992**, *65*, 2690.

(20) Coates, J. H.; Easton, C. J.; Fryer, N. L.; Lincoln, S. F., in press.

CHAPTER THREE

THE COMPLEXATION OF AMINO ACIDS BY BETA-CYCLODEXTRIN, A DIAMINO BETA-CYCLODEXTRIN DERIVATIVE AND ITS Co^{2+}, Ni^{2+}, Cu^{2+} AND Zn^{2+} COMPLEXES

3.1 Introduction

Modified cyclodextrins with suitable substituents may be able to coordinate a metal ion to form a metal-cyclodextrin complex, and this metallocyclodextrin may be able to include a guest to form a ternary metal-cyclodextrin-guest complex. Such a metallocyclodextrin host has a high possibility of exhibiting significant chiral discrimination for an enantiomeric guest, as the metal ion may provide an extra recognition point for the complexed molecule which is situated in the cyclodextrin annulus. Potentiometric titration, commonly used to investigate the binding of metal ions to ligands in solution, can be used to study metallocyclodextrins.

The monosubstituted amino cyclodextrin, βCDpn, was chosen to investigate the effect of metal ion coordination on the complexation and chiral discrimination characteristics of the βCD annulus. The replacement of a primary hydroxyl group of βCD with a 3-aminopropyl-amine group allows coordination of a metal ion near the primary rim of the cyclodextrin. The amino acids *RS*-phenylalanine and *RS*-tryptophan were chosen as guests that were likely to form complexes characterized by reasonably large apparent stability constants with βCD and related hosts as a consequence of their size and aromatic character, and their ability to coordinate to a metal ion via two binding sites. These amino acids have the same chiral centre but different aromatic entities. The divalent metal ions Co^{2+}, Ni^{2+}, Cu^{2+} and Zn^{2+} were chosen because they were known to form complexes characterized by reasonably large apparent stability constants with amine and amino acid ligands. These metal ions also allow investigation of the effects of the metal ion size and *d* electron configuration on the stability

and chiral discrimination of the cyclodextrin systems. The structures of βCDpn, and the anions of *RS*-phenylalanine and *RS*-tryptophan, are shown in Figure 3.1.

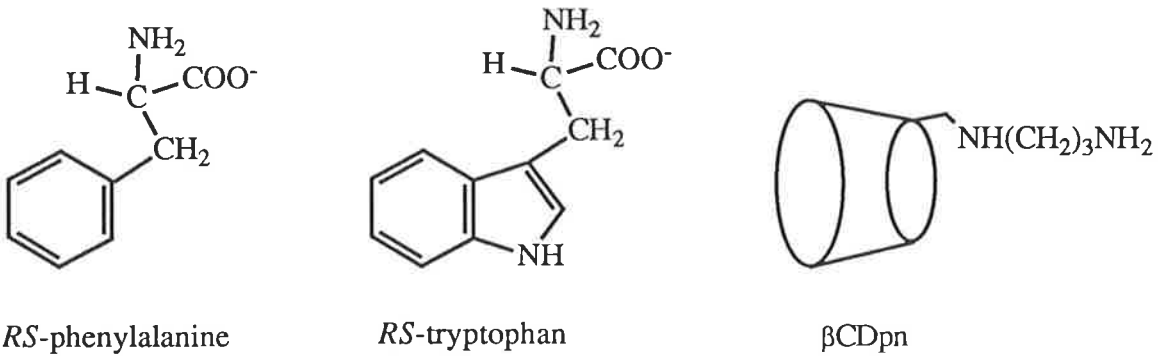

RS-phenylalanine *RS*-tryptophan βCDpn

Figure 3.1 Chemical structures of the amino acid guests and the modified cyclodextrin studied.

The use of potentiometric titrations for metal-ligand systems is based on the formation of > 5% of a metal-ligand species causing deviation of the metal-ligand titration curve from the titration curve of the ligand alone. Apparent stability constants can be determined from the difference between these two titration curves. The convenience of titrimetric methods is described in Section 2.1. Many species form in solutions of metal, cyclodextrin and guest, so it is necessary to independently determine as many apparent stability constants as possible. These values can then be fixed as constants when fitting the ternary system. The acid dissociation constants of the cyclodextrin and guest are measured first, and used to determine the apparent stability constants for the metal-cyclodextrin, cyclodextrin-guest and metal-guest systems. Finally, with these previously determined values as fixed constants, the apparent stability constants for the ternary metal-cyclodextrin-guest system can be determined.

In summary, for appropriate guests, cyclodextrins and metal ions, monitoring the pH changes of solutions of metal, cyclodextrin and guest as base is added allows determination of apparent stability constants for the ternary metal-cyclodextrin-guest complexes.

3.2 Results and Discussion

3.2.1 General

The equilibria discussed below completely characterize the systems studied, although not all species form for each metal ion and guest studied. The subscripts used to define the apparent stability constants, K, are C for βCD, Cp for βCDpn, M for the metal ion M^{2+}, and A, *R*-A and *S*-A as appropriate for the amino acid *RS*-A, with protonations as indicated. The apparent stability constants for the *R* and *S* enantiomers are determined by independent titrations of the resolved enantiomers, and if possible the experimental data for the enantiomers of a racemic pair are fitted over similar mV ranges. A chemical model for the solution equilibria is chosen by using the minimum number of species required for a good fit, where any species forming to less than 5% of the total cyclodextrin or amino acid concentration is dismissed as insignificant.

3.2.2 Acid Dissociations

Successive acid dissociations of the diprotonated amino acid AH_2^+ result in the formation of a monoprotonated zwitterion and a fully deprotonated anion, as shown in Equations 3.1 - 3.2.

$$AH_2^+ \overset{K_{a1}}{\rightleftharpoons} AH + H^+ \qquad (3.1)$$

$$AH \overset{K_{a2}}{\rightleftharpoons} A^- + H^+ \qquad (3.2)$$

The pK_a values determined are $pK_{a1} = 2.3 \pm 0.2$ and $pK_{a2} = 9.08 \pm 0.08$ for *RS*-phenylalanine, and $pK_{a1} = 2.40 \pm 0.02$ and $pK_{a2} = 9.28 \pm 0.01$ for *RS*-tryptophan. These values compare reasonably well with literature values.[1] The high error for the pK_{a1} value of *RS*-phenylalanine is thought to result from the decreased electrode sensitivity at low pH which makes it difficult to determine such low pK_a values.

The diprotonated 3-aminopropylamine substituent of βCDpn can be deprotonated as shown in Equations 3.3 - 3.4.

$$\beta CDpnH_2^{2+} \overset{K_{a1}}{\rightleftharpoons} \beta CDpnH^+ + H^+ \qquad (3.3)$$

$$\beta CDpnH^+ \overset{K_{a2}}{\rightleftharpoons} \beta CDpn + H^+ \qquad (3.4)$$

The pK_a values determined for $\beta CDpnH_2^{2+}$ are $pK_{a1} = 7.39 \pm 0.04$ and $pK_{a2} = 9.9 \pm 0.1$, where the first pK_a corresponds to the loss of a proton from the secondary amine adjacent to the cyclodextrin unit, and the second pK_a corresponds to the loss of a proton from the primary amine. These pK_a values may be compared with the values of 8.74 and 10.52, respectively, reported for 3-aminopropylamine at $I = 0.1$ and 298 K.[1] The low pK_a values of the modified cyclodextrin are attributed to intramolecular hydrogen bonding involving the 3-aminopropylamine substituent (see Section 2.2).

3.2.3 Complexation of Amino Acids by Beta-Cyclodextrin and a Diamino Beta-Cyclodextrin Derivative

The complexation of the enantiomeric amino acid anions by βCD and βCDpn occurs as shown in Equations 3.5 - 3.8.

$$\beta CD + R\text{-}A^- \overset{K_{CRA}}{\rightleftharpoons} \beta CD.R\text{-}A^- \qquad (3.5)$$

$$\beta CD + S\text{-}A^- \overset{K_{CSA}}{\rightleftharpoons} \beta CD.S\text{-}A^- \qquad (3.6)$$

$$\beta CDpn + R\text{-}A^- \overset{K_{CpRA}}{\rightleftharpoons} \beta CDpn.R\text{-}A^- \qquad (3.7)$$

$$\beta CDpn + S\text{-}A^- \overset{K_{CpSA}}{\rightleftharpoons} \beta CDpn.S\text{-}A^- \qquad (3.8)$$

The log values of the apparent stability constants derived from the best fit of the experimental data (see Section 6.1.2) to Equations 3.5 - 3.8 for the complexation of the *R*- and *S*-phenylalanine and *R*- and *S*-tryptophan anions by βCD and βCDpn are listed in Table 3.1. No protonated species are detected, indicating that no significant inclusion of either the zwitterion or the cation is occurring, especially in the fitting region finally used (pH 8.0 - 10.0 for βCD, and pH 8.5 - 11.5 for βCDpn). The absence of protonated species is consistent with literature reports which indicate that amino acid zwitterions are complexed weakly by βCD, as shown by the apparent stability constants of around 10 $dm^3\ mol^{-1}$ reported for the complexation of *R*- and *S*-tryptophan by βCD at pH 8.9.[2,3]

Table 3.1 Apparent stability constants[a,b] for the complexes of βCD and βCDpn with *R*- and *S*-phenylalanine and *R*- and *S*-tryptophan at $I = 0.10$ ($NaClO_4$) and 298.2 K.

Guest	log K_{CRA}	log K_{CSA}
RS-phenylalanine	2.91 ± 0.08 (0.1)	2.83 ± 0.06 (0.1)
RS-tryptophan	2.33 ± 0.2 (0.06)	2.33 ± 0.2 (0.08)
Guest	**log K_{CpRA}**	**log K_{CpSA}**
RS-phenylalanine	2.51 ± 0.07 (0.2)	2.74 ± 0.05 (0.1)
RS-tryptophan	3.41 ± 0.02 (0.05)	3.40 ± 0.07 (0.1)

[a]The units of K_{CRA}, K_{CSA}, K_{CpRA} and K_{CpSA} are $dm^3\ mol^{-1}$.
[b]The first and second errors quoted for the diastereomers are calculated assuming 100% and 99% enantiomeric purity of the amino acid, respectively (see Section 6.3.1).

No information about the geometry of the βCD and *RS*-tryptophan complex can be found in the literature. However, an apparent stability constant of 184 ± 11, equivalent to a log (K/dm^3 mol^{-1}) value of 2.26, is reported for the inclusion of indole by βCD at 298 K.[4] It is proposed that the dimensions of indole allow it to be encapsulated lengthwise in the βCD cavity, with the possibility of a hydrogen bond between the *N*-1 hydrogen of indole and either a primary or secondary hydroxyl group of the cyclodextrin. The similar magnitude of the apparent stability constants for the complexation of indole and *RS*-tryptophan by βCD implies a similar lengthwise inclusion for the indole moiety of *RS*-tryptophan, with the amine and carboxylate groups of *RS*-tryptophan being able to interact with either the primary or secondary hydroxyl groups of the cyclodextrin.

Results in Table 3.1 show that *RS*-tryptophan is complexed nearly twelve times more strongly by βCDpn than by βCD. This results in 54% of the βCDpn complex being formed in solution at pH 12 at total βCDpn and *RS*-tryptophan concentrations of 0.001 mol dm^{-3}. This compares with 15% of the βCD complex being formed under similar conditions. This stability increase is consistent with favourable hydrogen bonding between the 3-aminopropylamine substituent of βCDpn and the amino acid group of *RS*-tryptophan, indicating that the amino acid group is most likely to be positioned in the cavity near the primary hydroxyl groups of the cyclodextrin.

The complex of *RS*-phenylalanine with βCD is most likely to have the phenyl ring situated in the cavity, as reported in a study of the 1D ^{13}C NMR relaxation times of this system.[5] Results in Table 3.1 show that the enhanced interaction observed for *RS*-tryptophan and βCDpn is not observed for *RS*-phenylalanine and βCDpn, as *S*-phenylalanine has similar apparent stability constants with βCDpn and βCD, and *R*-phenylalanine is complexed 2 - 3 times more weakly by βCDpn than by βCD. The presence of the polar 3-aminopropylamine substituent appears to decrease the overall interaction between the host and guest, particularly for *R*-phenylalanine.

Results in Table 3.1 show that within experimental error, βCD does not thermodynamically discriminate between the *R* and *S* enantiomers for either *RS*-phenylalanine

or *RS*-tryptophan. βCDpn shows no chiral discrimination for *RS*-tryptophan, but shows chiral discrimination in favour of the *S* enantiomer for *RS*-phenylalanine. A literature report indicates that the *S* enantiomer is eluted first when *RS*-phenylalanine and *RS*-tryptophan are separated by liquid chromatography on an αCD bonded phase, but neither amino acid is separated on a similar βCD bonded phase.[6] Chiral discrimination for *RS*-phenylalanine and *RS*-tryptophan by αCD is also reported from 1D ^{1}H NMR and molecular mechanics studies.[7] Although these studies indicate that chiral discrimination is occurring in the complexation of *RS*-phenylalanine and *RS*-tryptophan by αCD, there is no literature evidence for chiral discrimination in the analogous βCD systems, consistent with the observations made in this study. The chiral discrimination observed in this study for the complexation of *RS*-phenylalanine by βCDpn, despite the lack of chiral discrimination observed for the complexation of this guest by βCD, is likely to be due to a change in orientation of the guest in the cyclodextrin cavity due to the presence of the 3-aminopropylamine group.

3.2.4 Complexation of Co^{2+}, Ni^{2+}, Cu^{2+} and Zn^{2+} by a Diamino Beta-Cyclodextrin Derivative

The complexation of metal ions by βCDpn occurs as shown in Equations 3.9 - 3.10.

$$\beta\text{CDpn} + M^{2+} \overset{K_{MCp}}{\rightleftharpoons} [M(\beta\text{CDpn})]^{2+} \qquad (3.9)$$

$$\beta\text{CDpnH}^{+} + M^{2+} \overset{K_{MCpH}}{\rightleftharpoons} [M(\beta\text{CDpnH})]^{3+} \qquad (3.10)$$

The log values of the apparent stability constants derived from the best fit of the experimental data (see Section 6.1.2) to Equations 3.9 - 3.10 for the metal species of βCDpn are listed in Table 3.2. No bis complexes are detected, but a hydroxy species is detected for Ni^{2+} and Cu^{2+}. No hydroxy species are detected for Co^{2+} and Zn^{2+}, probably because the precipitation of a metal hydroxide species above pH 8.5 and 7.5, respectively, interferes with the titrations. The apparent stability constants are derived from data in the approximate pH ranges 6.0 - 8.5, 5.5 - 8.5, 5.5 - 9.0 and 5.5 - 7.5 for Co^{2+}, Ni^{2+}, Cu^{2+} and Zn^{2+}, respectively.

Table 3.2 Apparent stability constants[a] for the complexes of βCDpn with Co^{2+}, Ni^{2+}, Cu^{2+} and Zn^{2+} in aqueous solution at $I = 0.10$ ($NaClO_4$) and 298.2 K.

Metal Ion	log K_{MCp}	log K_{MCpH}
Co^{2+}	4.22 ± 0.02	2.5 ± 0.2
Ni^{2+}	5.2 ± 0.1	3.1 ± 0.1
Cu^{2+}	7.35 ± 0.04	3.09 ± 0.04
Zn^{2+}	7.96 ± 0.08	3.0 ± 0.1

[a]The units of K_{MCp} and K_{MCpH} are $dm^3\ mol^{-1}$.

The stability of $[M(\beta CDpn)]^{2+}$ varies with the nature of the metal ion as shown in Table 3.2 by the variation of log ($K_{MCp}/dm^3\ mol^{-1}$) in the sequence $Co^{2+} < Ni^{2+} < Cu^{2+} > Zn^{2+}$. This is as expected from the Irving-Williams series.[8] To explain the trends observed for the binding of the metal ions to βCDpn it is necessary to compare their apparent stability constants with values reported in the literature for a range of related metal complexes.

Literature log ($K/dm^3\ mol^{-1}$) values reported for the binding of Cu^{2+} to 3-amino-propylamine are 9.75 ± 0.07 for the mono complex and 7.15 ± 0.2 for the bis complex at $I = 0.1$ and 298 K.[1] Literature log ($K/dm^3\ mol^{-1}$) values reported for the binding of Ni^{2+} to 3-aminopropylamine are 6.31 ± 0.1 for the mono complex and 3.29 ± 0.2 for the bis complex at $I = 0.1$ and 298 K.[1] Hydroxy species are reported for Cu^{2+} but not for Ni^{2+}, and no protonated species are reported for either metal ion. A comparison of these values to those in Table 3.2 indicates that the binding of the metal ions to βCDpn, a cyclodextrin substituted 3-aminopropylamine, is several orders of magnitude lower than their binding to 3-aminopropylamine, and a different range of species is formed.

Literature log (K/dm^3 mol^{-1}) values reported for the binding of Ni^{2+}, Cu^{2+} and Zn^{2+} to *N*-methyl-2-aminoethylamine and *N*-(hydroxyethyl)-2-aminoethylamine, as compared with 2-aminoethylamine, are up to 0.5 log units lower for the mono complex and up to 2 log units lower for the bis complex.[1] Hydroxy species are reported to form for the substituted amines, but not for 2-aminoethylamine. This indicates that substitution of either alkyl or hydroxyalkyl groups at a primary amine site lowers the stability of the metal complex, particularly the bis complex, and allows formation of different species, particularly hydroxy species. Thus, the lower stability and different speciation observed for the metal complexes of βCDpn, as compared with 3-aminopropylamine, can be attributed partly to substitution at one of the primary amine sites.

This study is also consistent with other investigations of the binding of metal ions to modified cyclodextrins. A log (K/dm^3 mol^{-1}) value of 17.9 is reported for the binding of Cu^{2+} to 6^A-[2,2'-diaminodiethylamino]-6^A-deoxy-βCD, lower than the value of 18.8 reported for the binding of Cu^{2+} to 2,2'-diaminodiethylamine.[9] Literature log (K/dm^3 mol^{-1}) values reported for the binding of Cu^{2+} to 6^A-[1-(2-amino)ethylamino]-6^A-deoxy-βCD are 7.81 and 6.17 for the mono and bis complexes, respectively, lower than the values of 10.46 and 9.01, respectively, for the binding of Cu^{2+} to 1-(2-amino)ethylamine.[10] Literature log (K/dm^3 mol^{-1}) values reported for the binding of Cu^{2+} to 6^A-[2-(4-imidazolyl)ethyl-amino]-6^A-deoxy-βCD are 7.26 for the mono complex and 2.94 for the protonated complex, lower than the values of 9.57 and 3.07, respectively, for the binding of Cu^{2+} to 2-(4-imidazolyl)ethylamine.[11] In the latter system, a hydroxy species is reported as probably existing but not being necessary for a good fit of the titrimetric data, and a bis complex is detected by electron spin resonance spectroscopy, but only at higher ligand to metal ratios than those used in the titration study. In cyclodextrin and metal systems where bis complexes have been reported, the bis complex is of low stability, as for the $[Cu\{6^A$-(2-aminoethylamino)-6^A-deoxy-βCD$\}_2]^{2+}$ complex, which is at least three orders of magnitude less stable than the $[Cu(2\text{-aminoethylamine})_2]^{2+}$ complex at 298 K.[10,12,13] The stability of the metallocyclodextrins, particularly the bis complexes, is lowered by the unfavourable steric interactions which occur when a bulky cyclodextrin unit is attached to a coordinating functional group of a ligand.

In summary, the metal ions are complexed more weakly by βCDpn than by 3-aminopropylamine, and a different range of species occurs with βCDpn. These trends can be attributed to steric factors, and substitution at the primary amine group of 3-aminopropylamine.

Although there is no information about the structure of the metal complexes in this study, it is most likely that the metal ion has either an octahedral or pseudo-octahedral geometry. Electron spin resonance measurements reported for the [Cu(6^{A}-{2-(4-imidazolyl)-ethylamino}-6^{A}-deoxy-βCD)]$^{2+}$ complex indicate that it has a similar structure to the [Cu{2-(4-imidazolyl)ethylamine}]$^{2+}$ complex, although the cyclodextrin complex does exhibit a slightly greater apical distortion. The apical distortion of the cyclodextrin complex is thought to result from the interaction of one of the two bound apical water molecules with the cyclodextrin cavity. This interaction either forces the water molecule to be at a shorter or longer distance than in the [Cu{2-(4-imidazolyl)ethylamine}]$^{2+}$ complex, or it is replaced by one of the cavity hydroxymethyl oxygens which is more firmly bound to copper.[11,14] Conversely, the [Cu(6^{A}-{4-(2-aminoethyl)imidazolyl}-6^{A}-deoxy-βCD)]$^{2+}$ complex has nearly identical magnetic parameters to the [Cu{2-(4-imidazolyl)ethylamine}]$^{2+}$ complex, indicating that these complexes have similar elongated octahedral geometries.[14] Generally, the coordination geometry of a metal ion bound to a ligand attached to a cyclodextrin appears to be similar to the geometry of the metal ion bound to the ligand alone.

The protonated species [M(βCDpnH)]$^{3+}$ identified in this study results from the binding of a metal ion to monoprotonated βCDpn. A 1D ^{13}C NMR study of [Zn(βCDpnH)]$^{3+}$ at pH 7.5 indicates that it is most likely that the primary amine is protonated and the secondary amine adjacent to the cyclodextrin is coordinated to the metal ion. It is not possible, however, to make a definitive statement about the location of this proton. The log (K_{MCpH}/dm^3 mol^{-1}) values for the formation of [M(βCDpnH)]$^{3+}$ are 1.5 - 4 orders of magnitude lower than the log (K_{MCp}/dm^3 mol^{-1}) values for [M(βCDpn)]$^{2+}$, reflecting the lower binding capacity of the monoprotonated cyclodextrin. This is as expected from the charge repulsion between the positively charged cyclodextrin and metal ion, and the monodentate nature of the protonated cyclodextrin. The monoprotonated species [M(βCDpnH)]$^{3+}$ is, however, more important in

the βCDpn systems than the 3-aminopropylamine systems. This is probably because the low stability of the mono complex $[M(\beta CDpn)]^{2+}$ prevents it from forming until around pH 6, allowing the protonated species to form in the low pH region. The species $[Cu(\beta CDpnH)]^{3+}$ has a log (K/dm^3 mol^{-1}) value of only 3.09 and only forms to a maximum of 5 - 10% of the total cyclodextrin concentration. This minor complex is included as a valid species because it does result in a better fit for the Cu^{2+} system, but it must be noted that it is not a particularly significant complex. The K_{MCpH} values may also be expressed as pK_a values corresponding to the deprotonation of the species $[M(\beta CDpnH)]^{3+}$. These pK_a values are 8.3 ± 0.1, 7.83 ± 0.02, 5.74 ± 0.05 and 8.1 ± 0.1 for Co^{2+}, Ni^{2+}, Cu^{2+} and Zn^{2+}, respectively.

The hydroxy species $[M(\beta CDpn)OH]^+$ detected in this study for Ni^{2+} and Cu^{2+} is likely to result from deprotonation of an aqua ligand bound to the metal ion in the $[M(\beta CDpn)]^{2+}$ complex. The pK_a values determined for the deprotonation of $[M(\beta CDpn)]^{2+}$ are 9.20 ± 0.04 and 7.84 ± 0.03 for Ni^{2+} and Cu^{2+}, respectively. Similar hydroxy species have been reported in other systems involving cyclodextrins and metal ions, such as the Cu^{2+} and 6^A-[2-(4-imidazolyl)ethylamino]-6^A-deoxy-βCD system.[11] A metal hydroxide species is also reported to be important in the Cu^{2+} catalysis of the hydrolysis of nitrophenyl esters by a βCD dimer with two pyridine linking groups.[15] The Cu^{2+} is bound to the pyridine linking groups, and the metal hydroxide species results from the deprotonation of a bound water molecule with a pK_a of around 7.15. The catalysis is believed to result from the attack of this metal hydroxide on the included ester.

3.2.5 Complexation of Co^{2+}, Ni^{2+}, Cu^{2+} and Zn^{2+} by Amino Acids

The complexation of metal ions by *RS*-phenylalanine and *RS*-tryptophan occurs as shown in Equations 3.11 - 3.12.

$$M^{2+} + RS\text{-}A^- \overset{K_{MA}}{\rightleftharpoons} [M(RS\text{-}A)]^+ \qquad (3.11)$$

$$[M(RS\text{-}A)]^+ + RS\text{-}A^- \overset{K_{MA_2}}{\rightleftharpoons} [M(RS\text{-}A)_2] \qquad (3.12)$$

The log values of the apparent stability constants derived from the best fit of the experimental data (see Section 6.1.2) to Equations 3.11 - 3.12 for the metal species of *RS*-phenylalanine and *RS*-tryptophan are listed in Table 3.3. These values differ by no more than 0.6 log units from the literature values, a difference which is reasonable if allowances are made for different ionic strengths.[1] The apparent stability constants for *RS*-phenylalanine are derived from data in the approximate pH ranges 6.5 - 8.5, 5.5 - 8.0, 4.0 - 7.0 and 5.5 - 7.5 for Co^{2+}, Ni^{2+}, Cu^{2+} and Zn^{2+}, respectively. The apparent stability constants for *RS*-tryptophan are derived from data in the approximate pH ranges 6.5 - 8.5, 5.0 - 9.0, 3.0 - 6.5 and 5.5 - 7.0 for Co^{2+}, Ni^{2+}, Cu^{2+} and Zn^{2+}, respectively.

Table 3.3 Apparent stability constants[a] for the complexes of *RS*-phenylalanine and *RS*-tryptophan with Co^{2+}, Ni^{2+}, Cu^{2+} and Zn^{2+} in aqueous solution at $I = 0.10$ ($NaClO_4$) and 298.2 K.

Guest	Metal Ion	log K_{MA}	logK_{MA_2}
RS-phenylalanine	Co^{2+}	4.19 ± 0.03	3.38 ± 0.07
	Ni^{2+}	5.09 ± 0.05	4.3 ± 0.1
	Cu^{2+}	7.8 ± 0.1	6.9 ± 0.1
	Zn^{2+}	4.59 ± 0.04	
RS-tryptophan	Co^{2+}	4.41 ± 0.05	4.01 ± 0.08
	Ni^{2+}	5.42 ± 0.03	4.67 ± 0.03
	Cu^{2+}	8.11 ± 0.03	7.20 ± 0.07
	Zn^{2+}	4.90 ± 0.04	

[a]The units of K_{MA} and K_{MA_2} are $dm^3\ mol^{-1}$.

For a particular amino acid, the stabilities of $[M(RS\text{-}A)]^+$ and $[M(RS\text{-}A)_2]$ vary with the nature of the metal ion as shown in Table 3.3 by the variation of log (K_{MA}/dm^3 mol^{-1}) and log (K_{MA_2}/dm^3 mol^{-1}) in the sequence $Co^{2+} < Ni^{2+} < Cu^{2+} > Zn^{2+}$. This is as expected from the Irving-Williams series.[8] The apparent stability constants of the *RS*-phenylalanine metal complexes are 0.2 - 0.6 log units lower than the corresponding values for the *RS*-tryptophan complexes.

A hydroxy species is necessary to obtain a satisfactory fit in the *RS*-phenylalanine and Cu^{2+} system, and the *RS*-tryptophan and Ni^{2+} and Cu^{2+} systems. This species is not detected in the Co^{2+} and Zn^{2+} systems, probably because the precipitation of a metal hydroxide species above pH 8.5 and 7.5, respectively, interferes with the titrations. The [M(*RS*-A)OH] complexes are likely to result from deprotonation of an aqua ligand bound to the metal ion in the $[M(RS\text{-}A)]^+$ complex. The pK_a values determined for these deprotonations are 7.46 ± 0.05 for Cu^{2+} and *RS*-phenylalanine, 9.1 ± 0.1 for Ni^{2+} and *RS*-tryptophan, and 7.28 ± 0.07 for Cu^{2+} and *RS*-tryptophan.

3.2.6 Complexation of Amino Acids by the Co^{2+}, Ni^{2+}, Cu^{2+} and Zn^{2+} Complexes of a Diamino Beta-Cyclodextrin Derivative

The complexation of *R*- and *S*-phenylalanine and *R*- and *S*-tryptophan by the metallo-cyclodextrins occurs as shown in Equations 3.13 - 3.16.

$$[M(\beta CDpn)]^{2+} + R\text{-}A^- \underset{}{\overset{K_{MCpRA}}{\rightleftharpoons}} [M(\beta CDpn)(R\text{-}A)]^+ \qquad (3.13)$$

$$[M(\beta CDpn)]^{2+} + S\text{-}A^- \underset{}{\overset{K_{MCpSA}}{\rightleftharpoons}} [M(\beta CDpn)(S\text{-}A)]^+ \qquad (3.14)$$

$$[M(\beta CDpn)]^{2+} + R\text{-}AH \underset{}{\overset{K_{MCpRAH}}{\rightleftharpoons}} [M(\beta CDpn)(R\text{-}AH)]^{2+} \qquad (3.15)$$

$$[M(\beta CDpn)]^{2+} + S\text{-}AH \underset{}{\overset{K_{MCpSAH}}{\rightleftharpoons}} [M(\beta CDpn)(S\text{-}AH)]^{2+} \qquad (3.16)$$

The log values of the apparent stability constants derived from the best fit of the experimental data (see Section 6.1.2) to Equations 3.13 - 3.16 for the complexes of *R*- and *S*-phenylalanine and *R*- and *S*-tryptophan with the metal ions and βCDpn are listed in Table 3.4. Figure 3.2 shows typical experimental data for the addition of base to solutions of βCDpn and *R*-tryptophan, and βCDpn, *R*-tryptophan and Cu^{2+}. Species plots for the Cu^{2+}, βCDpn and *S*-tryptophan system are shown in Figures 3.3 and 3.4. The protonated complexes of Equations 3.15 - 3.16 are only detected in the *RS*-tryptophan, βCDpn and Cu^{2+} system, and have apparent stability constants log (K_{MCpRAH}/dm^3 mol^{-1}) = 5.29 ± 0.05 (0.1) and log (K_{MCpSAH}/dm^3 mol^{-1}) = 5.4 ± 0.1 (0.2). A hydroxy species is detected in the Cu^{2+} systems of both *RS*-phenylalanine and *RS*-tryptophan. This hydroxy species is not detected in the Co^{2+}, Ni^{2+} and Zn^{2+} systems, probably because the precipitation of a metal hydroxide species above pH 8.5, 9.0 and 7.5, respectively, interferes with the titrations. For the Co^{2+} and Zn^{2+} systems the ternary complex only forms to a maximum of 5 - 10% of the total cyclodextrin or amino acid concentration, indicating that the ternary complex is only a minor species in these systems. However, the ternary complex is included as a valid species because it does result in slightly better fits for these systems. The apparent stability constants for *RS*-phenylalanine are derived from data in the approximate pH ranges 7.5 - 8.5, 7.5 - 9.5, 6.0 - 10.0 and 6.5 - 7.5 for Co^{2+}, Ni^{2+}, Cu^{2+} and Zn^{2+}, respectively. The apparent stability constants for *RS*-tryptophan are derived from data in the approximate pH ranges 7.5 - 8.5, 7.0 - 9.0, 4.5 - 9.5 and 6.5 - 8.0 for Co^{2+}, Ni^{2+}, Cu^{2+} and Zn^{2+}, respectively.

Table 3.4 Apparent stability constants[a,b] for the complexes of *R*- and *S*-phenylalanine and *R*- and *S*-tryptophan with the Co^{2+}, Ni^{2+}, Cu^{2+} and Zn^{2+} complexes of βCDpn in aqueous solution at $I = 0.10$ ($NaClO_4$) and 298.2 K.

Guest	Metal Ion	log K_{MCpRA}	log K_{MCpSA}
RS-phenylalanine	Co^{2+}	3.6 ± 0.2 (0.2)	3.69 ± 0.06 (0.1)
	Ni^{2+}	< 3.6[c]	4.4 ± 0.1 (0.1)
	Cu^{2+}	7.2 ± 0.1 (0.1)	6.9 ± 0.1 (0.1)
	Zn^{2+}	4.7 ± 0.1 (0.1)	4.7 ± 0.2 (0.2)
RS-tryptophan	Co^{2+}	4.04 ± 0.03 (0.1)	4.32 ± 0.05 (0.09)
	Ni^{2+}	4.1 ± 0.2 (0.2)	5.1 ± 0.2 (0.2)
	Cu^{2+}	7.85 ± 0.07 (0.07)	8.09 ± 0.05 (0.06)
	Zn^{2+}	5.3 ± 0.1 (0.1)	5.3 ± 0.1 (0.1)

[a]The units of K_{MCpRA} and K_{MCpSA} are $dm^3\ mol^{-1}$.

[b]The first and second errors quoted for the diastereomers are calculated assuming 100% and 99% enantiomeric purity of the amino acid, respectively (see Section 6.3.1).

[c]The limit on K_{MCpRA} corresponds to the apparent stability constant that results in the formation of 5 - 10% of the ternary species $[Ni(\beta CDpn)(R\text{-}A)]^+$. As this ternary species is not detected at a significant concentration, K_{MCpRA} must be less than this value, allowing an upper limit to be placed on the value of K_{MCpRA}.

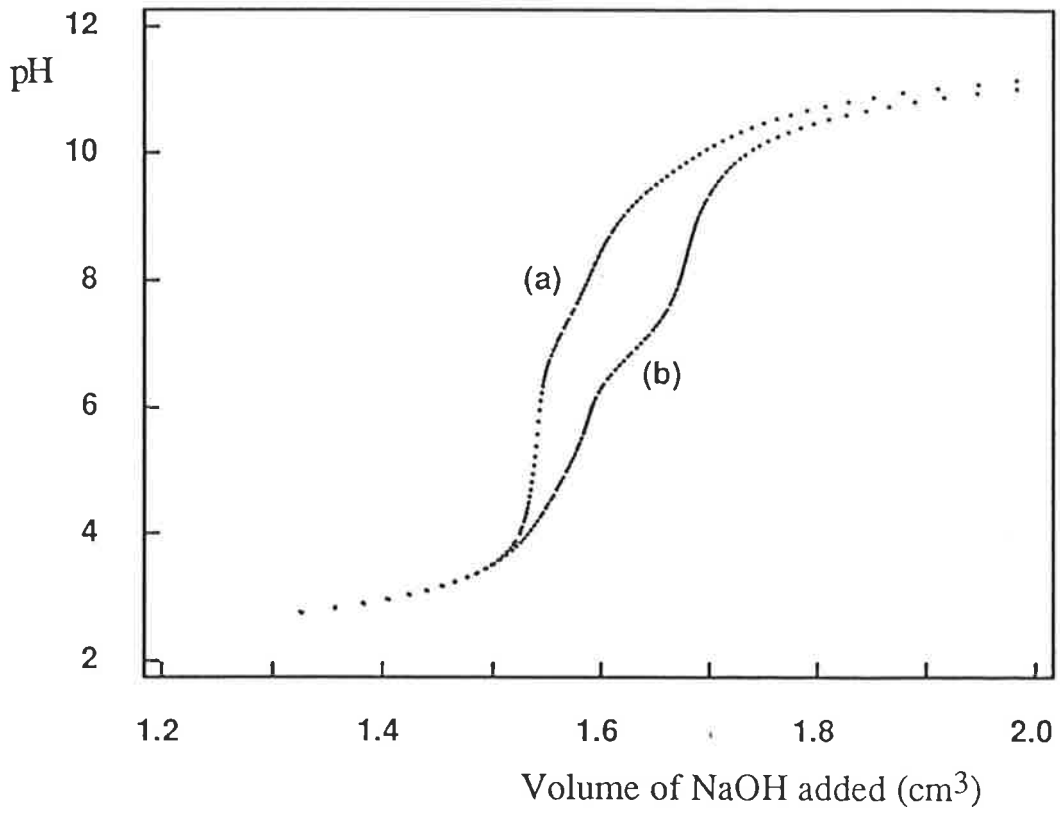

Figure 3.2 Experimental titration profiles of: (a) βCDpn (5.04×10^{-4} mol dm^{-3}) and *R*-tryptophan (5.08×10^{-4} mol dm^{-3}) and (b) βCDpn (5.02×10^{-4} mol dm^{-3}), *R*-tryptophan (5.05×10^{-4} mol dm^{-3}) and Cu^{2+} (4.50×10^{-4} mol dm^{-3}), against 0.101 mol dm^{-3} NaOH, in aqueous 0.010 mol dm^{-3} $HClO_4$ and 0.090 mol dm^{-3} $NaClO_4$ at 298.2 K. The curves representing the best fit of the data (see Section 6.1.2) run directly through the experimental points in the pH range used for fitting.

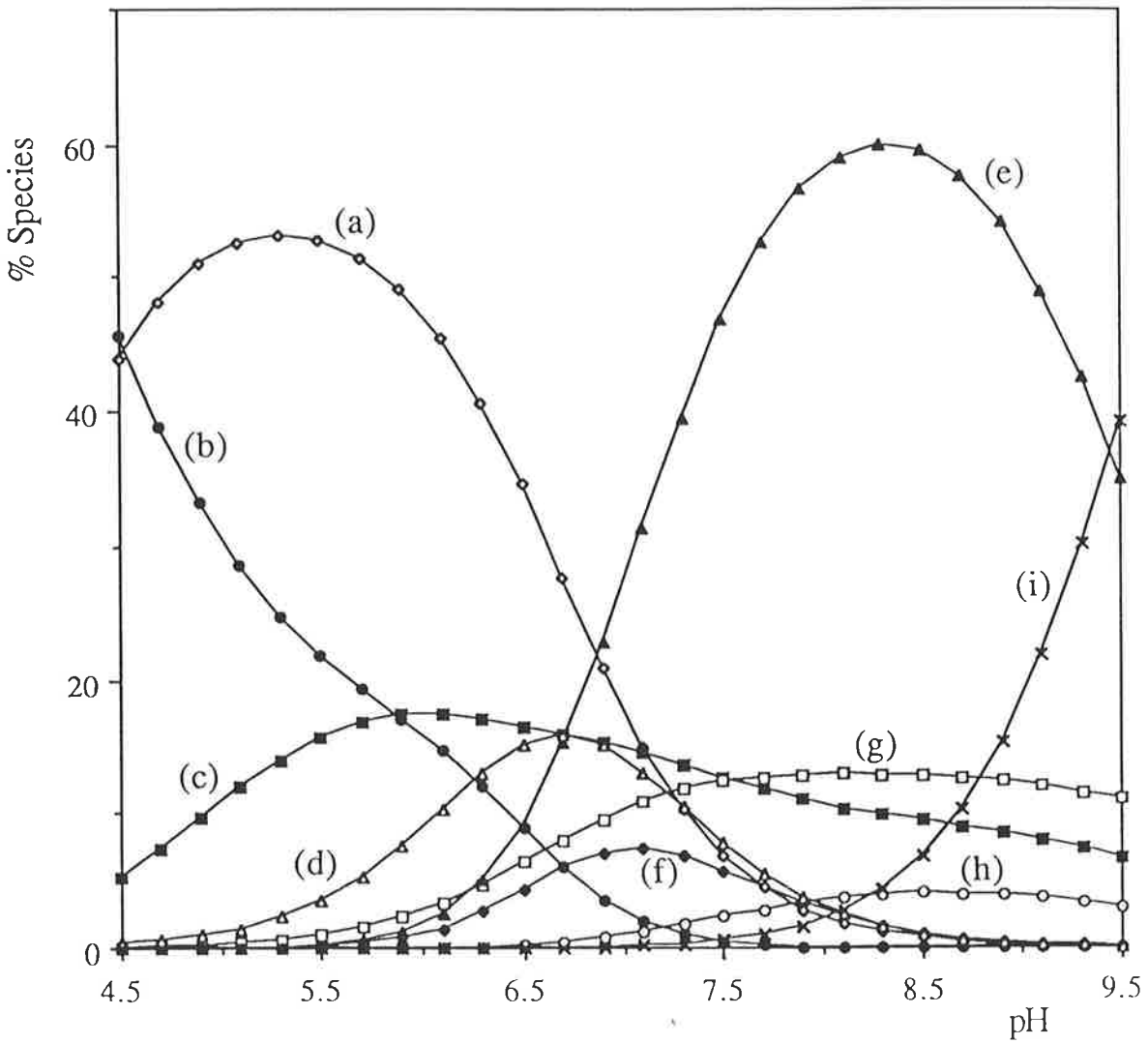

Figure 3.3 Plot of the Cu^{2+} species for the Cu^{2+}, βCDpn and *S*-tryptophan system, as calculated from appropriate values in Tables 3.1 - 3.4. The total concentrations of *S*-tryptophan and βCDpn are 0.001 mol dm^{-3} and are defined as 100%; the total concentration of Cu^{2+} is 0.00095 mol dm^{-3}. The curves represent: (a) $[Cu(S\text{-}A)]^{+}$; (b) Cu^{2+}; (c) $[Cu(S\text{-}A)_2]$; (d) $[Cu(\beta CDpn)(S\text{-}AH)]^{2+}$; (e) $[Cu(\beta CDpn)(S\text{-}A)]^{+}$; (f) $[Cu(\beta CDpn)]^{2+}$; (g) [Cu(*S*-A)OH]; (h) $[Cu(\beta CDpn)OH]^{+}$ and (i) [Cu(βCDpn)(*S*-A)OH].

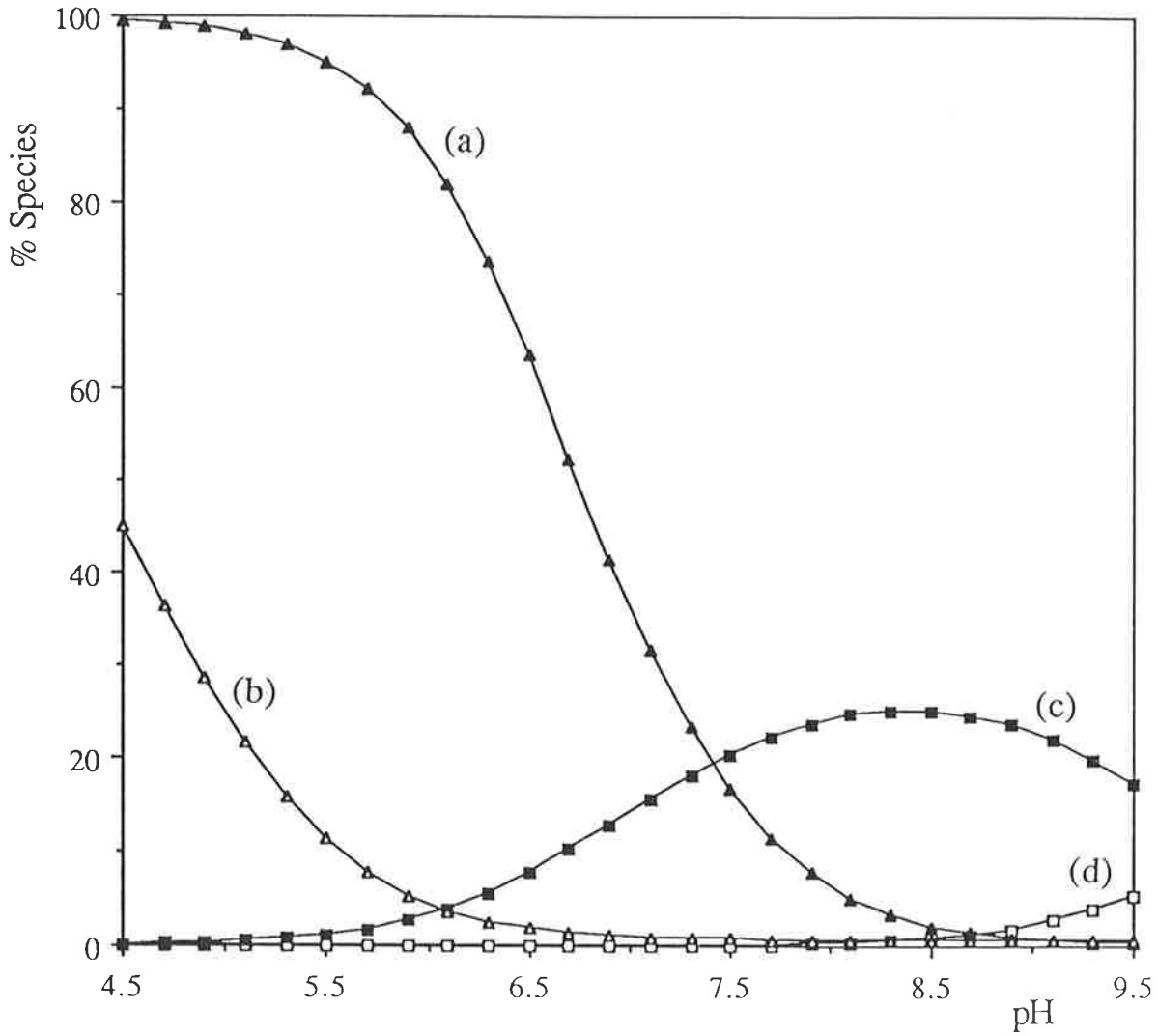

Figure 3.4 Plot of the non-Cu^{2+} species for the Cu^{2+}, βCDpn and *S*-tryptophan system, as calculated from appropriate values in Tables 3.1 - 3.4. The total concentrations of *S*-tryptophan and βCDpn are 0.001 mol dm^{-3} and are defined as 100%; the total concentration of Cu^{2+} is 0.00095 mol dm^{-3}. The curves represent: (a) $\beta CDpnH_2^{2+}$; (b) *S*-AH; (c) $\beta CDpnH^+$ and (d) βCDpn.

For a particular amino acid, the stabilities of the $[M(\beta CDpn)(R\text{-}A)]^+$ and $[M(\beta CDpn)(S\text{-}A)]^+$ complexes vary with the nature of the metal ion as shown in Table 3.4 by the variation of log (K_{MCpRA}/dm^3 mol^{-1}) in the sequence Co^{2+}, $Ni^{2+} < Cu^{2+} > Zn^{2+}$, and log ($K_{MCpSA}$/dm^3 mol^{-1}) in the sequence $Co^{2+} < Ni^{2+} < Cu^{2+} > Zn^{2+}$. This is basically as expected from the Irving-Williams series.[8] The structure envisaged for the ternary complex has the aromatic moiety of the amino acid inside the cyclodextrin annulus with the chiral centre in the vicinity of the primary hydroxyl groups of the cyclodextrin, and the amine and carboxylate groups coordinated to the six-coordinate metal ion. This structure is confirmed as possible using CPK models, and is shown in Figure 3.5 for the complex formed between *RS*-tryptophan, βCDpn and the metal ion. It has been argued that the complexation of *RS*-tryptophan by the Cu^{2+} complexes of 6^A-[4-(2-aminoethyl)imidazolyl]-6^A-deoxy-βCD and 6^A-[2-(4-imidazolyl)ethylamino]-6^A-deoxy-βCD, which preferentially complex *S*-tryptophan and *R*-tryptophan, respectively, have the indole moiety inside the cyclodextrin cavity only for the diastereomer with the higher stability.[14,16] There is no evidence for such major structural differences in the complexes discussed here.

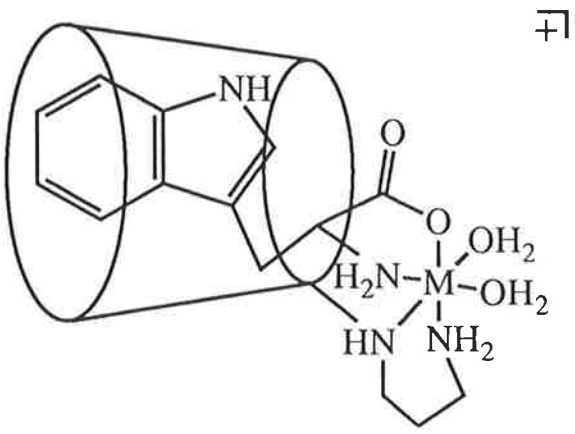

Figure 3.5 Possible structure for the complex formed between *RS*-tryptophan, βCDpn and a metal ion. An analogous structure is envisaged for the ternary complexes of *RS*-phenyl-alanine.

For the complexes studied, the greater magnitudes of K_{MCpRA} and K_{MCpSA} compared with K_{CpRA} and K_{CpSA}, demonstrate that the presence of the metal ion strengthens the complexation of the amino acid. The complexation of *RS*-phenylalanine by the metallocyclodextrin is strengthened by a factor of 5 - 20000 relative to βCD and 9 - 49000 relative to βCDpn. Similarly, the complexation of *RS*-tryptophan by the metallocyclodextrin is strengthened by a factor of 50 - 57000 relative to βCD and 4 - 49000 relative to βCDpn. In comparison, the complexation of a variety of guests by [Zn{6^A-(2,2'-diaminodiethylamino)-6^A-deoxy-βCD}]$^{2+}$ at basic pH is enhanced by a factor of 1 - 330 relative to βCD,[9] and the complexation of cyclohexane guests by [Zn(A,C-6,6'-bisimidazolyl-βCD)]$^{2+}$ at neutral pH is enhanced by a factor of 3 - 8 relative to βCD.[17] The stability enhancements in this study are significantly greater than those reported for other systems where a guest is simultaneously included and bound to a metal ion attached to a cyclodextrin. However, for Co^{2+}, Ni^{2+} and Cu^{2+}, the K_{MCpRA} and K_{MCpSA} values are less than the corresponding K_{MA} values, so it appears that the factors stabilizing complexation of the amino acid by βCDpn and the metal ion are not mutually reinforcing in the ternary complex. In contrast, for Zn^{2+} the K_{MCpRA} and K_{MCpSA} values are greater than the corresponding K_{MA} values, so some mutual reinforcement of the complexation of the amino acid by βCDpn and Zn^{2+} is occurring in the ternary complex.

From Table 3.4, the apparent stability constants for [M(βCDpn)(*R*-A)]$^+$ and [M(βCDpn)(*S*-A)]$^+$ reveal a substantial chiral discrimination in favour of the *S* enantiomer for the interaction of both *RS*-phenylalanine and *RS*-tryptophan with Ni^{2+} and βCDpn. This discrimination appears to be the highest reported thus far in the literature for a metallocyclodextrin. Figure 3.6 shows a plot of the species significantly affected by the chiral discrimination in the Ni^{2+}, βCDpn and *RS*-tryptophan system. For Cu^{2+} and βCDpn there is a moderate chiral discrimination, favouring the *R* enantiomer for *RS*-phenylalanine, and the *S* enantiomer for *RS*-tryptophan. The magnitude of the chiral discrimination observed in the Cu^{2+} ternary system is similar to that reported for the complexation of *RS*-tryptophan by [Cu(6^A-{2-(4-imidazaloyl)ethylamino}-6^A-deoxy-βCD)]$^{2+}$.[16] For Co^{2+} and βCDpn there is moderate discrimination in favour of the *S* enantiomer with *RS*-tryptophan, and no

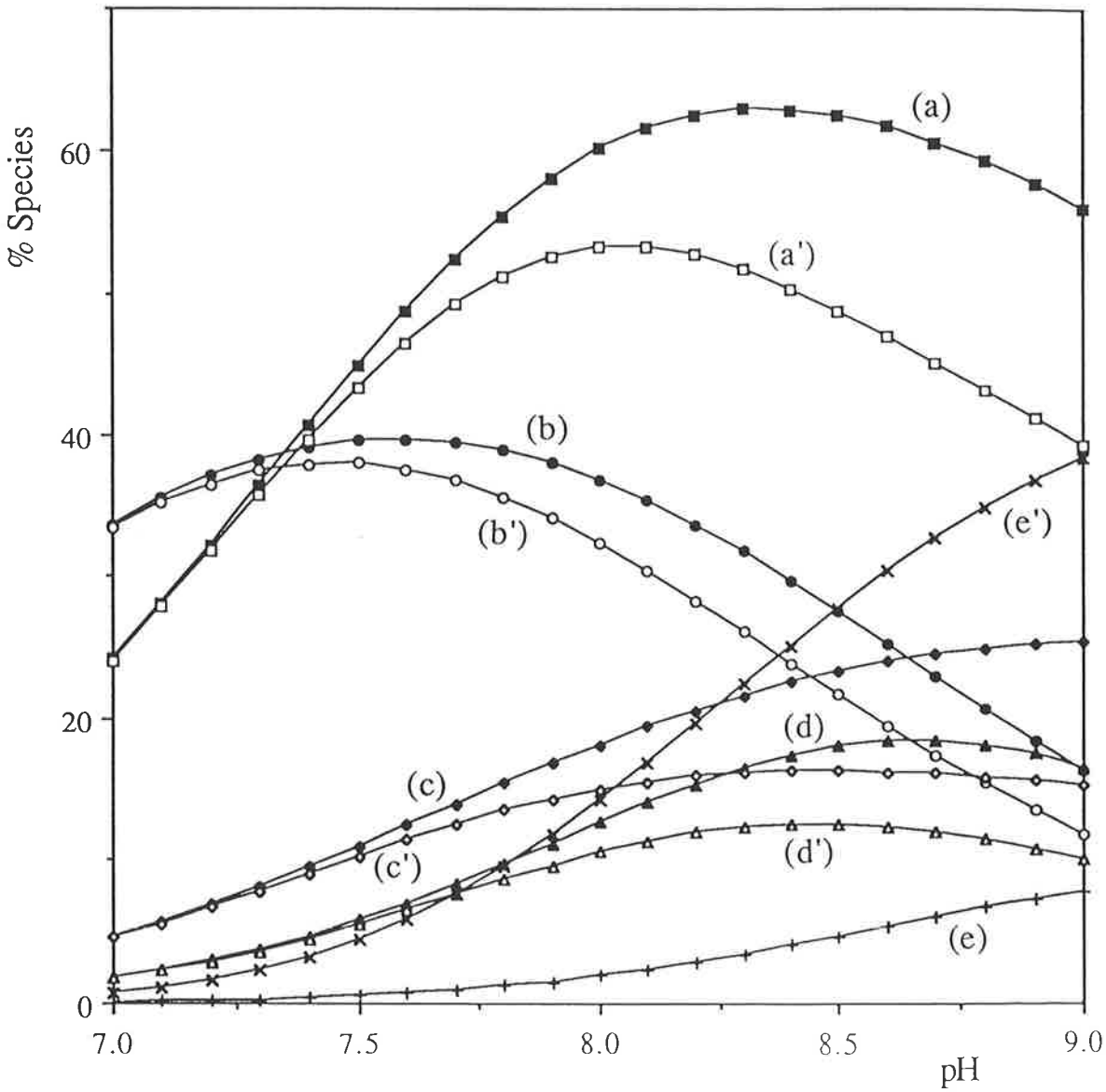

Figure 3.6 Plot of the species experiencing significant discrimination in the Ni^{2+}, βCDpn and *RS*-tryptophan system, as calculated from appropriate values in Tables 3.1 - 3.4. The total concentrations of *RS*-tryptophan and βCDpn are 0.001 mol dm^{-3} and are defined as 100%; the total concentration of Ni^{2+} is 0.00095 mol dm^{-3}. *R*-tryptophan species are represented by the filled shapes and the unprimed letters; *S*-tryptophan species are represented by the open shapes and the primed letters. The curves represent: (a) $\beta CDpnH^+$; (a') $\beta CDpnH^+$; (b) $[Ni(R\text{-}A)]^+$; (b') $[Ni(S\text{-}A)]^+$; (c) $[Ni(R\text{-}A)_2]$; (c') $[Ni(S\text{-}A)_2]$; (d) $[Ni(\beta CDpn)]^{2+}$; (d') $[Ni(\beta CDpn)]^{2+}$; (e) $[Ni(\beta CDpn)(R\text{-}A)]^+$ and (e') $[Ni(\beta CDpn)(S\text{-}A)]^+$.

discrimination within experimental error for *RS*-phenylalanine. For Zn^{2+} and βCDpn no chiral discrimination is observed for either *RS*-phenylalanine or *RS*-tryptophan.

For chiral discrimination to occur in cyclodextrin systems it is generally agreed that a guest must be firmly fixed in a particular position in the cyclodextrin cavity (see Section 1.5). The interaction of the aromatic moiety of the amino acid guest with the cyclodextrin cavity is thus crucial in the chiral recognition process. This is shown by the report that [Cu(6^{A}-{2-(4-imidazaloyl)ethylamino}-6^{A}-deoxy-βCD)]$^{2+}$ shows chiral discrimination for *RS*-tryptophan but not for *RS*-alanine.[16] The absence of chiral discrimination for *RS*-alanine is attributed to the lack of an aromatic unit to interact with the cyclodextrin cavity. In this study, the chiral discrimination observed for *RS*-phenylalanine is lower than the chiral discrimination observed for *RS*-tryptophan. In comparison with *RS*-tryptophan, *RS*-phenylalanine binds more weakly to the metal ion, and is also likely to fit less tightly in the cyclodextrin cavity because of the smaller size of the phenyl ring relative to the indole entity. These factors may prevent *RS*-phenylalanine from being firmly fixed in a position in the cyclodextrin cavity, lowering the chiral discrimination that is occurring.

The importance of the metal ion in the chiral recognition process is highlighted by the fact that only small chiral discrimination, if any, is observed in the complexation of *RS*-phenylalanine and *RS*-tryptophan by βCDpn. The discrimination observed for the ternary metal complexes reflects the variation in the ionic radii of six-coordinate Co^{2+}, Ni^{2+}, Cu^{2+} and Zn^{2+}, which are 74.5, 69, 73 and 74 pm,[18] respectively, and the geometric constraints arising from ligand field effects in Co^{2+}, $Ni^{2+}$and Cu^{2+}.[19] The observation that the Zn^{2+} diastereomers are of the same stability suggests that the absence of ligand field generated geometric constraints on d^{10} Zn^{2+} allows significant flexibility in the complex structures so that no chiral discrimination occurs. In contrast, the d^{9} electron configuration for similar sized Cu^{2+} results in a tetragonally distorted octahedral geometry, which may place greater constraints on the interaction of the chiral centre of the guest with the cyclodextrin, leading to chiral discrimination in the ternary complex. Similar arguments may be applied in the cases of d^{7} Co^{2+} and d^{8} Ni^{2+} whose six coordinate geometries are also distorted from regular octahedrons. The greater chiral discrimination caused by Ni^{2+} indicates that the size of the

metal centre is important, and that a difference of 4 pm may substantially change the degree of chiral discrimination. It appears as though the smaller size of Ni^{2+} allows the most favourable geometry around the metal ion for chiral discrimination to occur. Although chiral discrimination is observed for the ternary complex of *RS*-tryptophan with $[Co(\beta CDpn)]^{2+}$, no significant chiral discrimination is observed for the ternary complex of *RS*-phenylalanine with $[Co(\beta CDpn)]^{2+}$. Again, this lack of chiral discrimination is likely to result from the weaker binding of *RS*-phenylalanine to the metal centre, and the looser fit of the phenyl ring in the cyclodextrin cavity.

In this study, a protonated species is detected in the Cu^{2+}, *RS*-tryptophan and βCDpn system. It is not possible to make an unambiguous assignment for the location of the proton in this complex, as it may be attached to either βCDpn or *RS*-tryptophan. For convenience, the apparent stability constants have been expressed as shown in Equations 3.15 - 3.16, corresponding to the complexation of the zwitterion by the metallocyclodextrin $[M(\beta CDpn)]^{2+}$. Protonated species have been reported in other cyclodextrin and metal systems, such as the singly and doubly protonated complexes of [Cu(6^{A}-{2-(4-imidazolyl)ethylamino}-6^{A}-deoxy-βCD)(*RS*-tryptophan)]$^{+}$.[16] The K_{MCpRAH} and K_{MCpSAH} values determined in this study for the interaction of the *RS*-tryptophan zwitterion with $[Cu(\beta CDpn)]^{2+}$ are lower than the corresponding K_{MCpRA} and K_{MCpSA} values. This is as expected from the monodentate nature of the protonated *RS*-tryptophan, and the repulsion between the positively charged metal ion and zwitterionic *RS*-tryptophan. Within experimental error, no chiral discrimination is observed for the protonated species, probably because *RS*-tryptophan is acting as a monodentate ligand, making it less sterically constrained than when bidentate coordination is possible. The K_{MCpRAH} and K_{MCpSAH} values for *RS*-tryptophan may also be expressed as pK_a values corresponding to the deprotonation of the species $[Cu(\beta CDpn)(R\text{-AH})]^{2+}$ and $[Cu(\beta CDpn)(S\text{-AH})]^{2+}$, respectively. These p$K_a$ values are 6.72 ± 0.08 (0.1) and 6.6 ± 0.1 (0.2) for *R*- and *S*-tryptophan, respectively.

The hydroxy species [Cu(βCDpn)(*R*-A)OH] and [Cu(βCDpn)(*S*-A)OH] detected in this study for both *RS*-phenylalanine and *RS*-tryptophan are likely to result from deprotonation of aqua ligands bound to the metal ion in $[Cu(\beta CDpn)(R\text{-A})]^{+}$ and

$[Cu(\beta CDpn)(S\text{-}A)]^+$. The pK_a values determined for these deprotonations are 9.56 ± 0.04 (0.05) and 9.6 ± 0.1 (0.2) for *R*- and *S*-phenylalanine, respectively, and 9.48 ± 0.07 (0.09) and 9.37 ± 0.04 (0.05) for *R*- and *S*-tryptophan, respectively. As expected, no discrimination is observed for this deprotonation.

For the systems studied, the simultaneous presence of both the cyclodextrin and the metal ion is necessary for large chiral discrimination to occur. This is consistent with the general belief that for chiral discrimination to occur in cyclodextrin systems a strong interaction is required between the guest and the cyclodextrin cavity, so that the enantiomers are held firmly in different positions. The addition of a metal ion to the cyclodextrin system provides an extra recognition point for the guest, and the required geometric arrangement around this metal centre may force the guests to occupy particular positions in the cavity, resulting in an increase in the observed chiral discrimination.

BIBLIOGRAPHY

(1) *Critical Stability Constants*; Smith, R. M., Martell, A. E., Eds; Plenum Press: New York, **1975,** Vol. 1.

(2) Tabushi, I.; Kuroda, Y.; Mizutani, T. *J. Am. Chem. Soc.* **1986**, *108*, 4514.

(3) Tabushi, I.; Kuroda, Y.; Yamada, M.; Sera, T. *J. Inclusion Phenom.* **1988**, *6*, 599.

(4) Örstan, A.; Ross, J. B. A. *J. Phys. Chem.* **1987**, *91*, 2739.

(5) Inoue, Y.; Miyata, Y. *Bull. Chem. Soc. Jpn.* **1981**, *54*, 809.

(6) Armstrong, D. W.; Yang, X.; Han, S. M.; Menges, R. A. *Anal. Chem.* **1987**, *59*, 2594.

(7) Lipkowitz, K. B.; Raghothama, S.; Yang, J. *J. Am. Chem. Soc.* **1992**, *114*, 1554.

(8) Irving, H.; Williams, R. J. P. *J. Chem. Soc.* **1953**, 3192.

(9) Tabushi, I.; Shimizu, N.; Sugimoto, T.; Shiozuka, M.; Yamamura, K. *J. Am. Chem. Soc.* **1977**, *99*, 7100.

(10) Bonoma, R. P.; Cucinotta, V.; D'Alessandro, F.; Impellizzeri, G.; Maccarrone, G.; Rizzarelli E.; Vecchio, G. *J. Inclusion Phenom. Mol. Recognit. Chem.* **1993**, *15*, 167.

(11) Bonoma, R. P.; Cucinotta, V.; D'Alessandro, F.; Impellizzeri, G.; Maccarrone, G.; Vecchio, G.; Rizzarelli E. *Inorg. Chem.* **1991**, *30*, 2708.

(12) Schneider, H.-J.; Xiao, F. *J. Chem. Soc., Perkin Trans. 2* **1992**, 387.

(13) Matsui, Y.; Yokoi, T.; Mochida, K. *Chem. Lett.* **1976**, 1037.

(14) Cucinotta, V.; D'Alessandro, F.; Impellizzeri, G.; Vecchio, G. *J. Chem. Soc., Chem. Commun.* **1992**, 1743.

(15) Breslow, R.; Zhang, B. *J. Am. Chem. Soc.* **1992**, *114*, 5882.

(16) Impellizzeri, G.; Maccarrone, G.; Rizzarelli, E.; Vecchio, G.; Corradini, R.; Marchelli, R. *Angew. Chem., Int. Ed. Engl.* **1991**, *30*, 1348.

(17) Tabushi, I.; Kuroda, Y.; Mizutani, T. *Tetrahedron* **1984**, *40*, 545.

(18) Shannon, R. D. *Acta Crystallogr., Sect. A: Cryst. Phys. Diffr., Theor. Gen. Crystallog.* **1976**, *A32*, 751.

(19) *Advanced Inorganic Chemistry*; Cotton, A. and Wilkinson, G.; John Wiley and Sons: New York, 1980, 4th edition.

CHAPTER FOUR

THE COMPLEXATION OF FLUORINATED AMINO ACIDS BY ALPHA-CYCLODEXTRIN, BETA-CYCLODEXTRIN, GAMMA-CYCLODEXTRIN AND DERIVATIVES

4.1 Introduction

The complexes formed between amino acids and cyclodextrins are often of low stability, and the discrimination observed for racemic amino acids is often small.[1,2] It is thus of interest to investigate the inclusion of simple aromatic amino acids by cyclodextrins to further understand the factors that influence the complexation of these guests. It is also of interest to use modified cyclodextrins to attempt to improve the stability of amino acid complexes and the discrimination shown for amino acid enantiomers over that of the complexes of the natural cyclodextrins. A convenient method to study the inclusion of an amino acid by a cyclodextrin is to replace a hydrogen of the amino acid by a fluorine atom and use 1D ^{19}F NMR spectroscopy to monitor the inclusion.

The three fluorinated amino acids *RS*-α-(4-fluorophenyl)glycine (GH_2^+, G^-), *RS*-*N*-acetyl-α-(4-fluorophenyl)glycine (A-GH, A-G^-) and *RS*-*N*-(4-fluorobenzoyl)valine (VH, V^-) were chosen to investigate the influence of several factors on the inclusion process. The structures of the fluorinated amino acids are shown in Figure 4.1. These guests all have the same 4-fluorophenyl moiety, but have different functional groups on the chiral carbon. The distance of the chiral centre of the guest from the aromatic portion of the molecule also varies, from adjacent to the aromatic ring for the glycine derivatives to three bond lengths removed from the aromatic ring for the valine derivatives. The different structures of the guests allow investigation of the effect of the size, charge and position of the chiral centre on the inclusion of the amino acids.

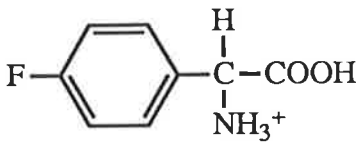

RS-α-(4-fluorophenyl)glycine (GH_2^+)

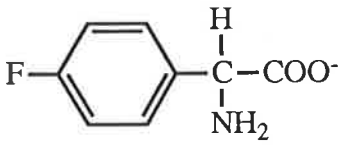

RS-α-(4-fluorophenyl)glycine (G^-)

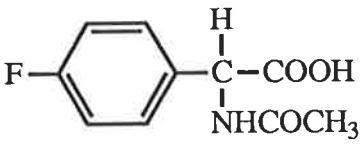

RS-*N*-acetyl-α-(4-fluorophenyl)-glycine (A-GH)

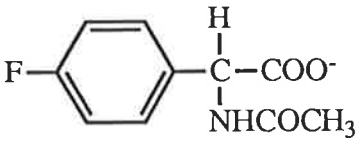

RS-*N*-acetyl-α-(4-fluorophenyl)-glycine ($A\text{-}G^-$)

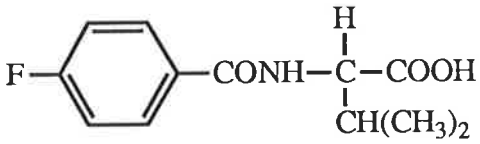

RS-*N*-(4-fluorobenzoyl)valine (VH)

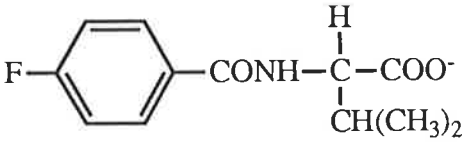

RS-*N*-(4-fluorobenzoyl)valine (V^-)

Figure 4.1 Chemical structures of the fluorinated amino acid guests studied.

The natural cyclodextrins αCD, βCD and γCD were chosen to investigate the effect of the cyclodextrin cavity size on the inclusion of the amino acids. Several modified cyclodextrins were subsequently chosen to investigate the effect of specific substitutions on the stability of the amino acid complexes and the observed chiral discrimination. The modified cyclodextrins PMαCD and PMβCD, which have all primary and secondary hydroxyl groups replaced by methyl groups, allow investigation of the effect of the increased hydrophobicity and reduced hydrogen bonding capability of the host as compared with the natural cyclodextrins. The monosubstituted cyclodextrins $\alpha CDNH_2$ and $\beta CDNH_2$, which have a primary hydroxyl replaced by an amine group, allow investigation of the effect of the increased asymmetry and possible positive charge of the host as compared with the natural cyclodextrins. The structure of $\beta CDNH_2$ is shown in Figure 2.1, and $\alpha CDNH_2$ has an analogous structure.

1D ^{19}F NMR spectroscopy is a convenient method to study the formation of the complexes of the fluorinated amino acids with the cyclodextrins. The small size of the fluorine atom, being approximately equal to that of hydrogen, means that its substitution at the 4-position of the aromatic ring does not significantly affect the molecular structure of the amino acid. Ignoring coupling effects, the 1D ^{19}F NMR spectrum of each amino acid is expected to be a singlet, as the single fluorine atom experiences a uniform magnetic environment. Coupling of the fluorine with neighbouring protons on the aromatic ring causes its resonance to be a multiplet, but ^{1}H-broad-band decoupling removes the coupling so that the observed ^{19}F spectrum of the amino acid is a singlet. As ^{19}F chemical shifts are extremely sensitive to the environment of the fluorine atom, complexation of the amino acid by a cyclodextrin is likely to result in significant changes in the chemical shift of the ^{19}F signal. The shift changes observed upon addition of a cyclodextrin to the amino acid may then be used to determine apparent stability constants. The simplicity of the 1D ^{19}F NMR spectra of the cyclodextrin complexed amino acids allows easy analysis, unlike the many overlapping signals that often occur in the ^{1}H and ^{13}C NMR spectra of cyclodextrin systems.

The formation of 1:1 inclusion complexes between a cyclodextrin, CD, and the enantiomers, *R*-F and *S*-F, of a racemic amino acid occurs as shown in Equations 4.1 - 4.2,

$$\text{CD} + R\text{-F} \underset{}{\overset{K_R}{\rightleftharpoons}} \text{CD}.R\text{-F} \qquad (4.1)$$

$$\text{CD} + S\text{-F} \underset{}{\overset{K_S}{\rightleftharpoons}} \text{CD}.S\text{-F} \qquad (4.2)$$

where K_R and K_S are the apparent stability constants for the formation of the diastereomeric cyclodextrin complexes. It is possible that the cyclodextrin will interact differently with the enantiomers of the amino acid, resulting in separate ^{19}F NMR signals for the *R* and *S* enantiomers of the included amino acid. The interactions between the cyclodextrin and the guest are quite weak (see Section 1.4), so the exchange equilibria between the free and complexed amino acids are in the fast exchange limit on the NMR timescale. This causes any ^{19}F signals to occur at the environmentally averaged shift of the free and complexed amino acid. The chemical shift of the amino acid at a particular cyclodextrin concentration may be represented as shown in Equations 4.3 - 4.4,

$$\delta_{OR} = \frac{\delta_F [R\text{-F}] + \delta_R [R\text{-F.CD}]}{[R\text{-F}] + [R\text{-F.CD}]} \qquad (4.3)$$

$$\delta_{OS} = \frac{\delta_F [S\text{-F}] + \delta_S [S\text{-F.CD}]}{[S\text{-F}] + [S\text{-F.CD}]} \qquad (4.4)$$

where δ_{OR} and δ_{OS} are the observed chemical shifts for the *R* and *S* amino acids, respectively, δ_F is the shift of the free amino acid, and δ_R and δ_S are the calculated shifts for the complexes of the *R* and *S* amino acids, respectively. Measuring the chemical shift of the amino acid at different cyclodextrin concentrations allows determination of apparent stability constants. The experimental data may be fitted to the above equations using a weighted non-linear regression analysis (see Section 6.4.3) to calculate the apparent stability constants and the chemical shifts of the complexes. If necessary, the above model may be extended to allow for other stoichiometries of complex formation.

A chiral interaction between an amino acid and a cyclodextrin may be reflected in either the apparent stability constants or the chemical shifts of the complexes of the amino acids, or both. If a chiral interaction is occurring, either K_R and K_S are different, or δ_R and δ_S are different, or both. It is obvious that if δ_R and δ_S are different, separate signals will be seen for the included *R* and *S* enantiomers. If δ_R and δ_S are different, K_R and K_S may or may not be different. Different values for δ_R and δ_S indicate that the fluorine atoms of the *R* and *S* enantiomers are in different magnetic environments in the cyclodextrin complexes. As the energy required to cause the difference in magnetic environments is substantially lower than that required to cause a detectable difference in thermodynamic values, K_R and K_S may be indistinguishable despite the difference in δ_R and δ_S. Alternatively, even if δ_R and δ_S are equal, it is possible to see separate ^{19}F signals for the *R* and *S* amino acids provided K_R and K_S are different. Equal values of δ_R and δ_S indicate that the fluorine atom is situated in a similar magnetic environment in the complexes of the *R* and *S* enantiomers. It is possible that other groups on the amino acid, such as the chiral centre, may interact differently with the cyclodextrin, which may result in different values for K_R and K_S. A difference in K_R and K_S results in the formation of different amounts of the *R* and *S* complexes, affecting the chemical shift of the time-averaged ^{19}F signal which is dependent on the concentrations of the free and bound amino acid. So even if δ_R and δ_S are equal, it is possible to see separate ^{19}F signals for the *R* and *S* amino acids provided K_R and K_S are different. In some systems separate signals may be seen for the *R* and *S* enantiomers, but neither K_R and K_S nor δ_R and δ_S are distinguishable within experimental error. This is simply a limitation in the precision of the experimental method. If separate values of K_R and K_S and δ_R and δ_S cannot be measured, K_{RS} and δ_{RS} values for the inclusion of the racemate may be able to be determined (see Section 6.4.3).

In summary, monitoring the ^{19}F chemical shift variation for a fluorinated amino acid with varying cyclodextrin concentration allows determination of apparent stability constants for the cyclodextrin-amino acid complex.

4.2 Results and Discussion

4.2.1 General

The complexation of the three fluorinated amino acids by αCD, βCD, γCD, PMαCD, PMβCD, $\alpha CDNH_3^+$, $\alpha CDNH_2$, $\beta CDNH_3^+$ and $\beta CDNH_2$ is studied using 1D ^{19}F NMR spectroscopy. Figure 4.2 shows typical experimental 1D ^{19}F NMR spectra for the addition of $\beta CDNH_3^+$ to a solution of V^-. For all of the cyclodextrin and amino acid combinations studied, the formation of a 1:1 inclusion complex is a satisfactory model to fit the experimental data. The formation of complexes of other stoichiometries has been reported in the literature, such as the α-fluoro-*trans*-cinnamate.$(\alpha CD)_2$ complex,[3] but there is no evidence for such complexes in this study. The thermodynamic discrimination (see Section 1.5) is significant if K_R and K_S are distinguishable within experimental error, and the magnetic discrimination (see Section 1.5) is significant if δ_R and δ_S are distinguishable within experimental error. The Tables of results which follow only list calculated values of (K_R/K_S) and $(\delta_R - \delta_S)$ for systems in which the discrimination is significant.

It is possible that the ^{19}F chemical shift changes observed for the amino acids upon addition of a cyclodextrin are not due to complexation alone, but also are at least partly due to the changes that occur in the solvent because of the presence of the cyclodextrin (see Section 6.4.3). To understand the possible magnitude of this medium effect, the change in ^{19}F chemical shift of an amino acid for a given concentration of glucose units is estimated using the straight chain glucose derivative maltotriose. ^{19}F chemical shifts due to complexation alone may be calculated by subtracting the estimated medium correction from the observed chemical shifts. The significance of the apparent stability constants calculated from these estimated ^{19}F chemical shifts will be discussed later. However, it is important to note that the apparent stability constants discussed in the following sections do not incorporate the estimated corrections for medium effects of the ^{19}F shifts unless this is specifically stated.

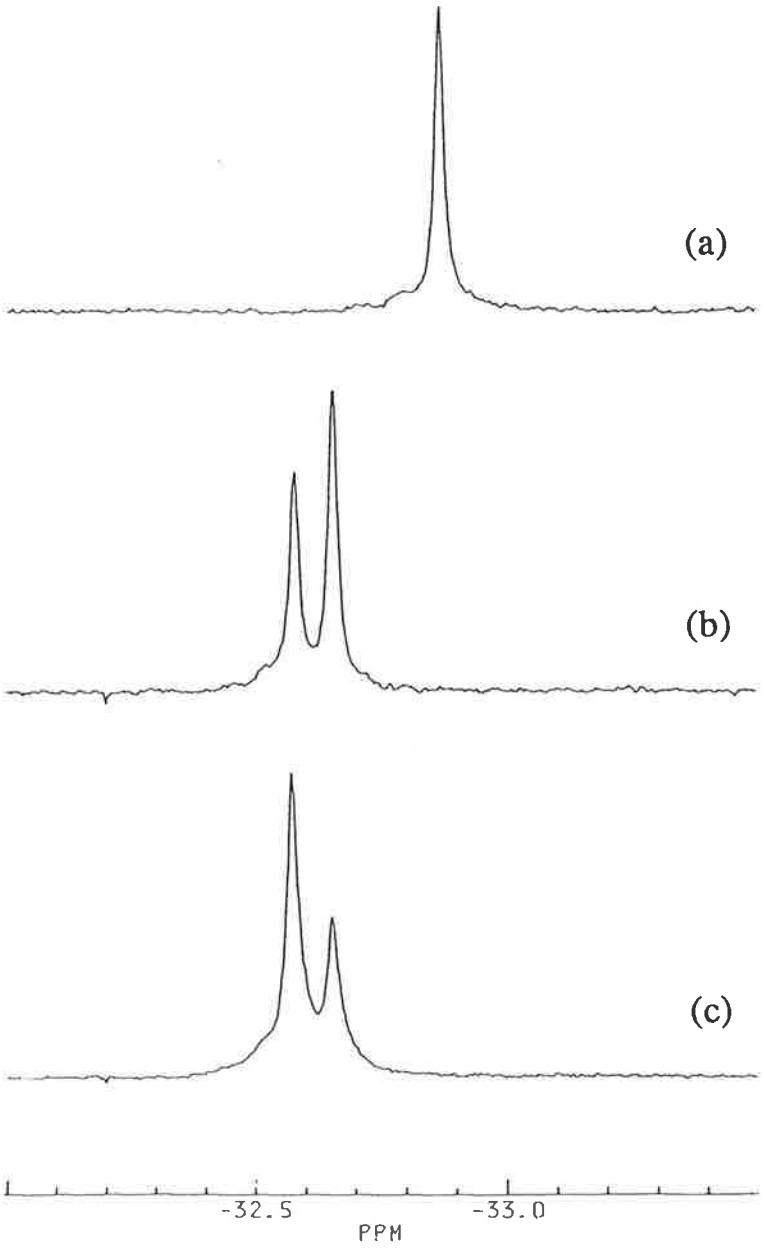

Figure 4.2 The ^{19}F NMR spectra of: (a) *RS*-V^- (1.04×10^{-3} mol dm^{-3}); (b) *RS*-V^- (1.03×10^{-3} mol dm^{-3}) and $\beta CDNH_3^+$ (1.03×10^{-2} mol dm^{-3}), and (c) *RS*-V^- (4.2×10^{-4} mol dm^{-3}), *S*-V^- (5.0×10^{-4} mol dm^{-3}) and $\beta CDNH_3^+$ (1.1×10^{-2} mol dm^{-3}), in phosphate buffer at pH 6.9, $I = 0.10$ and 295.5 K.

4.2.2 Complexation by Alpha-Cyclodextrin

The apparent stability constants derived from the best fit of the experimental data (see Section 6.4.3) to Equations 4.3 and 4.4 for the inclusion of the fluorinated amino acids by αCD are listed in Table 4.1. Figure 4.3 shows typical experimental data and best fit curves for the interaction of G^- with αCD and γCD.

The low values of the apparent stability constants in Table 4.1 indicate that the amino acids are weakly complexed by αCD. The magnitudes of the apparent stability constants are consistent with values typically reported for the interaction of aromatic guests, such as *N*-trifluoroacetyl-*DL*-4-fluorophenylalanine, *N*-trifluoroacetyl-*DL*-phenylalanine and diflunisal, with αCD.[4,5] A range of studies on cyclodextrin systems show that it is likely that the phenyl ring of a given amino acid is situated in the cavity, and that it can only be included partly within the αCD annulus (see Section 1.3). An inspection of CPK models shows that such shallow inclusion only allows the guest to have poor contact with the cyclodextrin cavity, and that there is limited opportunity for a significant interaction between the functional groups of the guest and the cyclodextrin, resulting in complexes of low stability. The shallow inclusion also means that the guests are positioned similarly in the cyclodextrin cavity, regardless of size and charge, resulting in the narrow range of apparent stability constants seen in Table 4.1. The most stable αCD complex is formed with the smallest guest, G^-.

The ^{19}F shift changes observed for the fluorine atom result from the change in environment experienced by the amino acid upon complexation by the cyclodextrin. This environmental change is likely to result from the change in solvation of the fluorine atom, and the overall environmental change experienced by the amino acid upon inclusion in the cyclodextrin cavity. It is expected that the direction of the observed ^{19}F shift change may be used to gain specific information about the environment of the fluorine in the complex, as may be done with ^1H and ^{13}C NMR spectra. However, interpretation of the direction of observed shift changes for ^{19}F NMR spectra is difficult, as the effect of factors such as solvent, hydrogen bonding or ring currents on ^{19}F chemical shifts are still not well understood.

Table 4.1 Apparent stability constants and ^{19}F chemical shifts for the complexes of αCD and the fluorinated amino acids in various buffers with 10% aqueous D_2O at $I = 0.10$ and 295.5 K.

amino acid derivative	K ($dm^3\ mol^{-1}$)	δ (ppm)	Δδ (ppm)
GH_2^+ [a]	K_R = 8.3 ± 0.4	δ_R = -37.04 ± 0.04	$\delta_R-\delta_F$ = -1.29 ± 0.04
	K_S = 8.7 ± 0.4	δ_S = -37.10 ± 0.04	$\delta_S-\delta_F$ = -1.35 ± 0.04
		δ_F = -35.752 ± 0.004	
G^- [b]	K_R = 21.8 ± 0.5	δ_R = -41.21 ± 0.01	$\delta_R-\delta_F$ = -1.09 ± 0.01
	K_S = 22.9 ± 0.5	δ_S = -41.12 ± 0.01	$\delta_S-\delta_F$ = -1.00 ± 0.01
	K_R/K_S = 0.95 ± 0.03	δ_F = -40.123 ± 0.004	$\delta_R-\delta_S$ = -0.09 ± 0.01
A-GH [a]	K_R = 14.6 ± 0.1	δ_R = -39.235 ± 0.007	$\delta_R-\delta_F$ = -1.456 ± 0.008
	K_S = 14.8 ± 0.1	δ_S = -39.325 ± 0.007	$\delta_S-\delta_F$ = -1.546 ± 0.008
		δ_F = -37.779 ± 0.004	$\delta_R-\delta_S$ = 0.09 ± 0.01
A-G^- [c]	K_R = 13.0 ± 0.3	δ_R = -40.99 ± 0.02	$\delta_R-\delta_F$ = -1.64 ± 0.02
	K_S = 14.1 ± 0.3	δ_S = -40.83 ± 0.02	$\delta_S-\delta_F$ = -1.48 ± 0.02
	K_R/K_S = 0.92 ± 0.03	δ_F = -39.355 ± 0.004	$\delta_R-\delta_S$ = -0.16 ± 0.03
VH [a]	K_{RS} = 8.5 ± 0.3	δ_{RS} = -32.99 ± 0.02	$\delta_{RS}-\delta_F$ = -0.68 ± 0.02
		δ_F = -32.308 ± 0.004	
V^- [c]	K_R = 11.9 ± 0.3	δ_R = -33.69 ± 0.01	$\delta_R-\delta_F$ = -0.87 ± 0.01
	K_S = 10.0 ± 0.3	δ_S = -33.53 ± 0.01	$\delta_S-\delta_F$ = -0.71 ± 0.01
	K_R/K_S = 1.19 ± 0.05	δ_F = -32.823 ± 0.004	$\delta_R-\delta_S$ = -0.16 ± 0.01

[a] pH 1.3
[b] pH 10.8
[c] pH 6.9

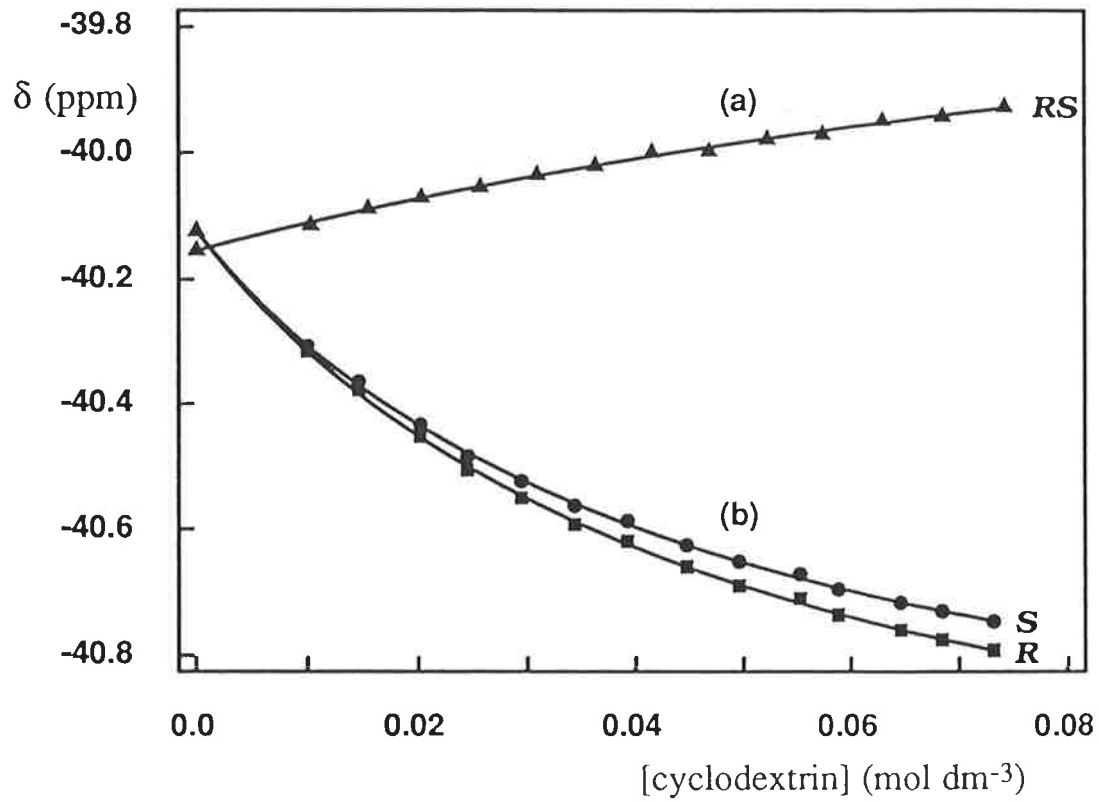

Figure 4.3 Variation of ^{19}F chemical shift (δ) for: (a) *RS*-G$^-$ (1.02 - 1.06 x 10^{-3} mol dm^{-3}) and γCD (10.3 - 74.3 x 10^{-3} mol dm^{-3}) and (b) *R*- and *S*-G$^-$ (0.958 - 0.999 x 10^{-3} mol dm^{-3}) and αCD (0.998 - 73.2 x 10^{-3} mol dm^{-3}), in NaOH/glycine buffer at pH 10.8, I = 0.10 and 295.5 K. The curves through the data points represent the best fit of the data to Equations 4.3 - 4.4 using DATAFIT (see Section 6.4.3). The difference in δ_F values for the αCD and γCD systems is thought to be due to slight CO_2 contamination of the buffer in the γCD study (see Section 6.4.1).

Generally, it is thought that the ^{19}F signal is shifted downfield if the fluorine is transferred to a polar environment or if the fluorine undergoes hydrogen bonding, and that it is shifted upfield if the fluorine is transferred to a less polar environment.[6] Thus, an upfield shift upon formation of a cyclodextrin complex is most likely to indicate that the fluorine atom is situated in the hydrophobic part of the cyclodextrin cavity, corresponding to the movement of the fluorine atom from the polar aqueous solution to the apolar cavity environment. A downfield shift upon formation of a cyclodextrin complex may indicate either that the fluorine is situated in a hydrophilic part of the cavity, such as near the hydroxyl groups, or that the fluorine is hydrogen bonded to the cyclodextrin. As several different factors may be operating, the interpretation of the chemical shift changes in this way is not conclusive, but may give some interesting information about the orientation of the different guests in the cyclodextrin cavity.

As seen in Table 4.1, all amino acids studied experience upfield ^{19}F shifts when complexed by αCD, indicating that it is probable that the fluorine atom is situated in the hydrophobic part of the cyclodextrin cavity. The glycine derivatives experience a greater ^{19}F shift change upon inclusion than the valine derivatives. The larger size of the valine derivatives, VH and V^-, means that greater portions of these guests will protrude from the αCD cavity upon complexation. This makes it likely that the overall environmental changes experienced by the valine derivatives are less than the changes experienced by the glycine derivatives, resulting in smaller shift changes for the valine derivatives.

Results in Table 4.1 show that αCD exhibits significant thermodynamic discrimination for G^-, A-G^- and V^-, and significant magnetic discrimination for G^-, A-GH, A-G^- and V^-. The discrimination shown by αCD for G^- may be seen in the clear resolution of the ^{19}F signals of the *R* and *S* enantiomers of G^- in Figure 4.3. No significant thermodynamic discrimination is observed for the neutral and cationic guests, indicating that αCD shows higher discrimination for the anionic guests. The *S* enantiomers are included more strongly than the *R* enantiomers of G^- and A-G^-, whereas the *R* enantiomer is included more strongly than the *S* enantiomer of V^-. αCD shows the greatest thermodynamic discrimination for V^-. At high cyclodextrin concentration, separate ^{19}F signals are observed for the *R* and *S* enantiomers of VH,

indicating that αCD does show slight discrimination for this guest although it is only possible to determine a K_{RS} value.

The large negative values of (δ_R - δ_S) for the anionic guests G^-, A-G^- and V^- in Table 4.1 indicate that the *S* enantiomers experience a greater environmental change upon complexation than the *R* enantiomers, and that the difference in the magnetic environments of the complexed enantiomers is quite large. This may be compared with the values of (δ_R - δ_S) for the neutral and cationic guests, where (δ_R - δ_S) is either close to or equal to zero for GH_2^+ and VH, and positive, but small, for A-GH. This indicates that the *R* and *S* enantiomers have quite similar magnetic environments in the αCD complexes of GH_2^+, A-GH and VH. These observations again suggest that the extent of the chiral interaction depends strongly on the charge of the guest, with αCD showing higher magnetic discrimination for the anionic guests. The change in sign and the substantial changes in the magnitude of (δ_R - δ_S) of the differently charged guests suggests very different orientations of the amino acids in the complexes.

The following structures proposed for the αCD complexes are known to be feasible from CPK models, and offer a possible explanation for the behaviour of the differently charged guests. As outlined previously, it is highly likely that the aromatic group of the amino acid is situated in the cavity, which is consistent with the upfield ^{19}F shifts observed for each guest. An inspection of CPK models shows that it is possible for the aromatic ring of the amino acids to be inserted from either the primary or secondary end of the cyclodextrin. It is likely that the dipole moment of αCD, directed from the primary to the secondary end of the cyclodextrin, will affect the orientation of the differently charged guests in the cavity (see Section 1.4). The anionic guests G^-, A-G^- and V^- have dipole moments directed towards the negatively charged carboxylate group, and are likely to insert the aromatic ring from the primary end of the cyclodextrin so that the dipole moments of the amino acid and cyclodextrin are antiparallel. The cationic guest GH_2^+ has a dipole moment directed towards the fluorine atom on the aromatic ring, and is likely to insert the aromatic ring from the secondary end of the cyclodextrin so that the dipole moments of the amino acid and cyclodextrin are antiparallel. The neutral guests A-GH and VH have a less defined dipole moment, and are likely to have

weaker electrostatic interactions with the cyclodextrin. These guests can have their aromatic ring inserted from either the primary or the secondary end of the cyclodextrin, although they are more likely to enter from the secondary end for steric reasons. Such opposite directions of insertion may account for the differences in the observed (δ_R - δ_S) values depending on the charge of the guest.

The effect of the medium (see Section 4.2.1) in the αCD systems may be quite significant, because a high concentration range is used for αCD (see Section 6.4.1). Applying the estimated medium correction decreases the apparent stability constants for αCD by up to 40%. However, this correction does not significantly change the observed chiral discrimination, and does not affect any of the trends discussed above.

4.2.3 Complexation by Beta-Cyclodextrin

The apparent stability constants derived from the best fit of the experimental data (see Section 6.4.3) to Equations 4.3 and 4.4 for the inclusion of the fluorinated amino acids by βCD are listed in Table 4.2. Figure 4.4 shows typical experimental data and best fit curves for the interaction of A-GH with βCD and PMαCD.

Results in Table 4.2 show that the complexes formed between the amino acids and βCD have a much greater range of apparent stability constants than the complexes formed with αCD. This indicates that the larger βCD annulus is more guest selective, probably because the guests can be included more deeply in the cavity, and specific interactions can occur between the functional groups of the guest and the hydroxyl groups of the cyclodextrin. The βCD complexes of A-GH and VH are about 2.5 and 10 times more stable, respectively, than their analogous αCD complexes, whereas the βCD complexes of G^- and $A\text{-}G^-$ are slightly less stable than their analogous αCD complexes. No apparent stability constants can be determined for the interaction of GH_2^+ and V^- with βCD. It is clear that the uncharged guests form complexes of higher stability with βCD than do the anionic guests, with the greatest stability occurring for the guest VH. The larger cavity size of βCD allows more extensive interactions between the aromatic ring of the amino acid and the hydrophobic cyclodextrin cavity. The higher stability of the complexes of the neutral guests suggests that such hydrophobic

Table 4.2 Apparent stability constants and ^{19}F chemical shifts for the complexes of βCD and the fluorinated amino acids in various buffers with 10% aqueous D_2O at $I = 0.10$ and 295.5 K.

amino acid derivative	K ($dm^3\ mol^{-1}$)		δ (ppm)		Δδ (ppm)	
G$^-$ [a]	K_R = 13	± 2	δ_R = -41.5	± 0.2	δ_R-δ_F = -1.3	± 0.2
	K_S = 21	± 3	δ_S = -41.0	± 0.1	δ_S-δ_F = -0.8	± 0.1
	K_R/K_S = 0.6	± 0.1	δ_F = -40.151	± 0.004	δ_R-δ_S = -0.5	± 0.2
A-GH [b]	K_R = 34	± 1	δ_R = -38.80	± 0.02	δ_R-δ_F = -1.06	± 0.02
	K_S = 35	± 2	δ_S = -38.83	± 0.04	δ_S-δ_F = -1.09	± 0.04
			δ_F = -37.741	± 0.004		
A-G$^-$ [c]	K_R = 12	± 1	δ_R = -40.9	± 0.1	δ_R-δ_F = -1.5	± 0.1
	K_S = 12	± 1	δ_S = -40.7	± 0.1	δ_S-δ_F = -1.3	± 0.1
			δ_F = -39.358	± 0.004		
VH [b]	K_R = 84	± 2	δ_R = -31.56	± 0.01	δ_R-δ_F = 0.79	± 0.01
	K_S = 93	± 2	δ_S = -31.55	± 0.01	δ_S-δ_F = 0.80	± 0.01
	K_R/K_S = 0.90	± 0.03	δ_F = -32.345	± 0.004		

[a] pH 10.8
[b] pH 1.3
[c] pH 6.9

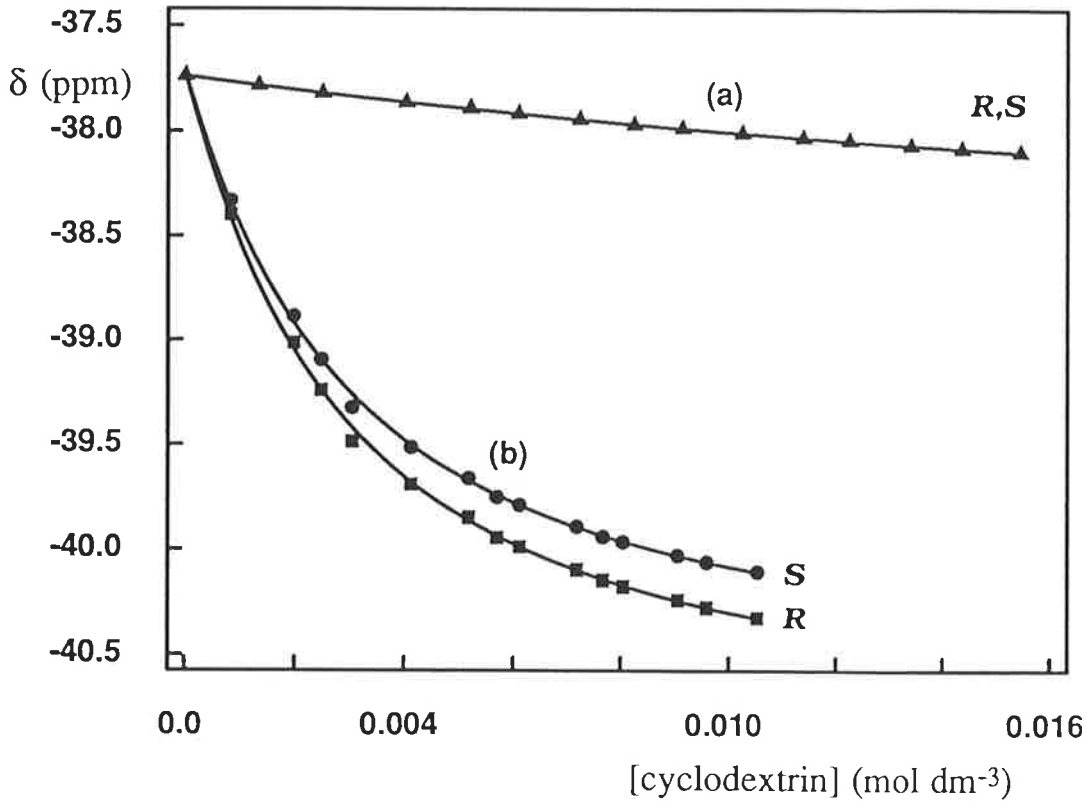

Figure 4.4 Variation of ^{19}F chemical shift (δ) for: (a) *R*- and *S*-A-GH (1.04×10^{-3} mol dm^{-3}) and βCD ($1.34 - 15.5 \times 10^{-3}$ mol dm^{-3}) in HCl/KCl buffer at pH 1.3, and (b) *R*- and *S*-A-GH ($1.06 - 1.07 \times 10^{-3}$ mol dm^{-3}) and PMαCD ($0.828 - 10.5 \times 10^{-3}$ mol dm^{-3}) in HCl at pH 1.0, at $I = 0.10$ and 295.5 K. The curves through the data points represent the best fit of the data to Equations 4.3 - 4.4 using DATAFIT (see Section 6.4.3).

interactions are more important in the complexation of the amino acids by βCD than by αCD.

As seen in Table 4.2, the ^{19}F signal for VH is shifted downfield upon complexation, and the ^{19}F signals for G^-, A-GH and $A\text{-}G^-$ are shifted upfield upon complexation. These results suggest a trend in which the ^{19}F signals of the glycine and valine derivatives are shifted upfield and downfield, respectively, by βCD. Consistent with this trend is the observation that the guest GH_2^+ shows a small but significant upfield ^{19}F shift upon addition of βCD, although an apparent stability constant cannot be determined for this guest. The ^{19}F shift change observed for the guest V^- upon addition of βCD is in a downfield direction, also consistent with the observed trend, but this small shift may be due to medium effects only and is thus not significant. As observed for αCD, the magnitude of the ^{19}F shift change experienced by the valine derivative is less than that experienced by the glycine derivatives.

The different directions and magnitudes of the ^{19}F shift changes observed for the glycine and valine derivatives indicate that the position of the fluorine in the valine complexes is quite different from the glycine complexes, and a possible explanation for these observations arises from a study of CPK models. The valine derivatives have a relatively long link between the aromatic moiety and the chiral centre of the guest. This link allows the valine guest to be deeply inserted into the βCD cavity, for complexation from either the primary or secondary end of the cyclodextrin. The steric and electrostatic interaction of the chiral centre of the valine guest with the cyclodextrin hydroxyl groups positions the fluorine substituent either in the solvent or adjacent to the cyclodextrin hydroxyl groups. The hydrophilic environment of the fluorine atom accounts for the observed downfield ^{19}F shift for VH. Conversely, the short link between the aromatic ring and the chiral centre in the glycine derivatives causes steric hindrance between the amino acid functional groups and the cyclodextrin. This steric hindrance means that the aromatic ring cannot be as deeply inserted into the cyclodextrin cavity, and the fluorine atom of the glycine derivatives is situated in the vicinity of the hydrophobic cavity wall, accounting for the upfield ^{19}F shift observed for these guests. The difference in insertion depth of these guests also accounts for the different magnitude of the observed ^{19}F shift changes. As the fluorine atom of the valine derivative is situated in a hydrophilic environment it does not experience as great an environmental change

as the fluorine of the glycine derivatives. Also, the larger valine guest is likely to be less completely encapsulated by the βCD annulus. These two factors result in a smaller overall environmental change for the valine guest, and a consequently smaller overall ^{19}F shift change.

The apparent stability constants in Table 4.2 show that βCD shows significant thermodynamic discrimination for VH and G^-, with the *S* enantiomers being included more strongly than the *R* enantiomers. The greatest thermodynamic discrimination is seen for G^-, which has the *S* enantiomer included nearly twice as strongly as the *R* enantiomer. Significant magnetic discrimination is seen for G^-, but not for A-GH, A-G^- and VH. The lack of significant thermodynamic and magnetic discrimination shown for A-GH by βCD may be seen in Figure 4.4, which shows no separation of the ^{19}F signals of the *R* and *S* enantiomers of this guest. At high cyclodextrin concentration, separate ^{19}F signals are observed for the *R* and *S* enantiomers of V^-, indicating that βCD does show slight discrimination for this guest although it is not possible to determine apparent stability constants. Conversely, βCD shows no discrimination for GH_2^+, as separate ^{19}F signals for the *R* and *S* enantiomers are not observed even at high βCD concentration. For the anionic guest G^- (δ_R - δ_S) is large and negative, as found for the interaction of anionic guests with αCD. The magnitude of (δ_R - δ_S) is insignificant for the guests A-GH, A-G^- and VH. This indicates that βCD shows reasonably low magnetic discrimination for the amino acids. Generally, the trends in (δ_R - δ_S) are similar to the trends observed with αCD, suggesting that the differently charged guests have opposing orientations in the βCD cavity, as outlined for αCD in Section 4.2.2.

It is interesting to compare the discrimination shown by βCD for the two different glycine guests. Thermodynamic and magnetic discrimination is not observed for the interaction of A-GH and A-G^- with βCD, indicating that βCD does not have strong chiral interactions with this derivative. Conversely, βCD does show a significant chiral interaction with G^-. As A-G^- and G^- differ only by the functional groups on the chiral centre, this indicates that the nature of the chiral centre is very important in determining the extent of the chiral interaction. The *N*-acetyl group of A-GH and A-G^- is more bulky and less able to form hydrogen bonds than the free amine group of G^-, and this appears to weaken the chiral

interaction. It is also interesting to compare the complexation of VH and V^- by αCD and βCD. With βCD, significant discrimination is seen for VH, but not for V^-, whereas with αCD significant discrimination is seen for V^-, but not for VH. Furthermore, for αCD the *R* enantiomer of V^- is included more strongly, whereas for βCD the *S* enantiomer of VH is included more strongly. Clearly the cavity size of the cyclodextrin and the charge on the amino acid substantially influence the inclusion of the valine derivative by αCD and βCD.

The effect of the medium in the βCD systems may be quite significant, because of the small observed ^{19}F shift changes which result from the low concentration range used for βCD (see Section 6.4.1). Applying the estimated medium correction changes the apparent stability constants for βCD by up to 30%, increasing the values for the valine derivative and decreasing the values for the glycine derivatives. As found for αCD, this correction does not significantly affect the observed discrimination and the trends discussed above.

4.2.4 Complexation by Gamma-Cyclodextrin

The apparent stability constants derived from the best fit of the experimental data (see Section 6.4.3) to Equations 4.3 and 4.4 for the inclusion of the fluorinated amino acids by γCD are listed in Table 4.3. Curve (b) in Figure 4.3 shows experimental data and a best fit curve for the interaction of G^- with γCD.

Results in Table 4.3 show that the complexes formed between γCD and the amino acids are generally of low stability. No apparent stability constants can be determined for the interaction of GH_2^+ and $A\text{-}G^-$ with γCD. The apparent stability constants for the γCD complexes are lower than those determined for βCD in all cases where comparison is possible, and lower than those determined for αCD for all guests except VH. The apparent stability constants are all similar to each other, indicating that γCD does not significantly differentiate between guests. Thermodynamic discrimination is observed only for the complexation of VH by γCD, and no separation of the signals for the *R* and *S* enantiomers is seen at high cyclodextrin concentration for any of the other guests. Figure 4.3 shows the lack of discrimination observed for the interaction of G^- with γCD, especially when compared with the discrimination seen for the interaction of this guest with αCD. As found for βCD, γCD

Table 4.3 Apparent stability constants and ^{19}F chemical shifts for the complexes of γCD and the fluorinated amino acids in various buffers with 10% aqueous D_2O at $I = 0.10$ and 295.5 K.

amino acid derivative	K ($dm^3\ mol^{-1}$)	δ (ppm)	Δδ (ppm)
G- [a]	K_{RS} = 7.4 ± 0.4	δ_{RS} = -39.52 ± 0.03 δ_F = -40.154 ± 0.004	δ_{RS}-δ_F = 0.63 ± 0.03
A-GH [b]	K_{RS} = 7.1 ± 0.1	δ_{RS} = -36.66 ± 0.01 δ_F = -37.764 ± 0.004	δ_{RS}-δ_F = 1.10 ± 0.01
VH [c]	K_R = 13.1 ± 0.1 K_S = 14.0 ± 0.1 K_R/K_S = 0.94 ± 0.01	δ_R = -31.458 ± 0.005 δ_S = -31.454 ± 0.004 δ_F = -32.299 ± 0.004	δ_R-δ_F = 0.841 ± 0.006 δ_S-δ_F = 0.845 ± 0.006
V- [d]	K_{RS} = 5.39 ± 0.09	δ_{RS} = -31.92 ± 0.01 δ_F = -32.830 ± 0.004	δ_{RS}-δ_F = 0.91 ± 0.01

[a] pH 10.8
[b] pH 1.0
[c] pH 1.3
[d] pH 6.9

includes the *S* enantiomer of VH more strongly than the *R* enantiomer, but the magnitude of the thermodynamic discrimination is lower for γCD than for βCD. The value of (δ_R - δ_S) for VH is not significant within experimental error, indicating that γCD shows no magnetic discrimination for this guest. It appears that for these amino acids the large cavity size of γCD does not favour complex formation and chiral discrimination, probably because the relatively small guests cannot interact strongly with the large γCD cavity. This is consistent with the fact that the guest which has the highest stability and shows the only discrimination with γCD is VH, the largest guest.

The results in Table 4.3 show that the ^{19}F signals of all of the guests experience a downfield shift upon complexation, which is the opposite direction to that observed with αCD. Figure 4.3 shows the different directions of the ^{19}F shift changes observed for αCD and γCD. As outlined previously, the downfield ^{19}F shift observed for the γCD systems is most likely to result from a hydrophilic interaction between the amino acid and the cyclodextrin. Interactions which may result in a downfield ^{19}F shift include the simultaneous inclusion of water molecules with the amino acid, or the interaction of the amino acid with the γCD hydroxyl groups, perhaps by hydrogen bonding. Unlike the ^{19}F shift changes observed for αCD and βCD, where the glycine derivatives are shifted more than the valine derivatives, the glycine and valine derivatives experience similar shift changes with γCD. The larger cavity of γCD allows complete encapsulation of all three guests, causing each guest to experience similar overall environmental changes, resulting in similar observed shift changes.

The effect of the medium may be very significant in the γCD systems, because a high concentration range is used for γCD (see Section 6.4.1). Applying the estimated medium correction increases the apparent stability constants by a factor of 2 - 4. The uncertainty of the magnitude of the medium effect in these systems makes the comparison of apparent stability constants and ^{19}F shift changes with other cyclodextrin systems very difficult. The increase in apparent stability constants means that the trends described previously, such as the apparent stability constants for γCD generally being lower than those determined for αCD and βCD, may no longer be valid. However, even with the applied medium correction the apparent stability constants for γCD are all still similar and low, and the observed

discrimination is small. This indicates that the basic concept of the γCD annulus being too large for these guests to form complexes of significant stability and discrimination is still valid, regardless of the medium effects that may be operating in these systems.

4.2.5 Complexation by Permethylated Cyclodextrins

The apparent stability constants derived from the best fit of the experimental data (see Section 6.4.3) to Equations 4.3 and 4.4 for the inclusion of the fluorinated amino acids by PMαCD are listed in Table 4.4. It is not possible to determine apparent stability constants for the interaction of any of the amino acids with PMβCD. Curve (b) in Figure 4.4 shows experimental data and best fit curves for the interaction of A-GH with PMαCD.

The structures of the permethylated cyclodextrins and their complexes are quite different from those of the natural cyclodextrins.[7] The replacement of the hydroxyl groups of the cyclodextrin by methyl groups increases the hydrophobicity of the cyclodextrin by extending the length of the hydrophobic cavity. The presence of the comparatively bulky methyl groups causes a narrowing of the primary end and a widening of the secondary end of the cyclodextrin. A consequence of the narrowing of the primary end of the cyclodextrin is that guests are usually included from the secondary end. Permethylation interrupts the intramolecular hydrogen bonding network which holds the natural cyclodextrins in a rigid symmetrical arrangement (see Section 1.2). This allows the permethylated cyclodextrins to be more flexible hosts capable of adjusting their conformations to fit an included guest. There is also steric hindrance between the methyl groups on the secondary end which may cause a conformational change in the macrocyclic ring, resulting in the cavity being quite distorted from the symmetrical structure of the natural cyclodextrins. The solvation of the more hydrophobic permethylated cyclodextrins is very different from that of the natural cyclodextrins, which will affect the complexation of guests. The dipole moment of the permethylated cyclodextrins will be lower than the natural cyclodextrins, and is thus likely to play a less significant role in the inclusion of guests.[8] The many differences between the permethylated and natural cyclodextrins are highlighted by X-ray crystallographic studies which show that the αCD and PMαCD complexes of a particular guest are often very different. A guest may have a different depth of inclusion, a different orientation in the cavity,

Table 4.4 Apparent stability constants and ^{19}F chemical shifts for the complexes of PMαCD and the fluorinated amino acids in various buffers with 10% aqueous D_2O at $I = 0.10$ and 295.5 K.

amino acid derivative	K ($dm^3\ mol^{-1}$)	δ (ppm)	Δδ (ppm)
GH_2^+ [a]	K_R = 54 ± 3	δ_R = -38.1 ± 0.1	δ_R-δ_F = -2.4 ± 0.1
	K_S = 59 ± 4	δ_S = -38.1 ± 0.1	δ_S-δ_F = -2.4 ± 0.1
		δ_F = -35.708 ± 0.004	
G^- [b]	K_R = 49 ± 3	δ_R = -43.0 ± 0.1	δ_R-δ_F = -2.8 ± 0.1
	K_S = 55 ± 3	δ_S = -43.0 ± 0.1	δ_S-δ_F = -2.8 ± 0.1
		δ_F = -40.207 ± 0.004	
A-GH [a]	K_R = 451 ± 7	δ_R = -40.92 ± 0.01	δ_R-δ_F = -3.19 ± 0.01
	K_S = 434 ± 7	δ_S = -40.68 ± 0.01	δ_S-δ_F = -2.95 ± 0.01
	K_R/K_S = 1.04 ± 0.02	δ_F = -37.733 ± 0.004	δ_R-δ_S = -0.24 ± 0.01
A-G^- [c]	K_R = 80 ± 3	δ_R = -43.02 ± 0.09	δ_R-δ_F = -3.64 ± 0.09
	K_S = 77 ± 3	δ_S = -42.67 ± 0.08	δ_S-δ_F = -3.29 ± 0.08
		δ_F = -39.384 ± 0.004	δ_R-δ_S = -0.4 ± 0.1
VH [a]	K_R = 142 ± 6	δ_R = -34.09 ± 0.04	δ_R-δ_F = -1.78 ± 0.04
	K_S = 155 ± 6	δ_S = -34.12 ± 0.03	δ_S-δ_F = -1.81 ± 0.03
	K_R/K_S = 0.92 ± 0.05	δ_F = -32.315 ± 0.004	
V- [c]	K_R = 143 ± 6	δ_R = -34.47 ± 0.04	δ_R-δ_F = -1.69 ± 0.04
	K_S = 153 ± 6	δ_S = -34.51 ± 0.04	δ_S-δ_F = -1.73 ± 0.04
		δ_F = -32.778 ± 0.004	

[a] pH 1.0
[b] pH 10.8
[c] pH 6.9

or even an opposite direction of inclusion with a permethylated cyclodextrin as compared with a natural cyclodextrin.[7]

Results in Table 4.4 indicate that the amino acids form complexes of reasonable stability with PMαCD. However, it is not possible to determine apparent stability constants for the interaction of any of the amino acids with PMβCD. This is because the ^{19}F shift changes caused by PMβCD are too small, only -0.08 - 0.04 ppm at 0.01 mol dm^{-3} PMβCD. This may be compared with the ^{19}F shift changes of about 0.9 - 2.5 ppm caused by PMαCD at the same concentration. Separate signals are not detected for the *R* and *S* enantiomers of any guest except A-G$^-$, indicating that the discrimination shown by PMβCD for the amino acids is very low. The lack of significant ^{19}F shift changes and discrimination observed with PMβCD may indicate either that a complex is not forming, or that the magnetic environment of the fluorine is not changed by complex formation. The latter explanation seems unlikely, as significant environmental changes have been observed for all other cyclodextrins studied, and thus are expected with PMβCD. The former explanation, a lack of complex formation with PMβCD, seems more reasonable. The hydrophobic cavity of the cyclodextrin is extended and widened by methylation, resulting in the cavity size of PMαCD resembling that of βCD, and the cavity size of PMβCD resembling that of γCD. This suggests that the complexation behaviour of PMβCD may be similar to the behaviour of γCD, as found for the guest diflunisal which has similar apparent stability constants with PMβCD and γCD.[9] The larger cavity size of γCD results in complexes of low stability and discrimination, as it is difficult for the amino acids to have significant contact with the cyclodextrin cavity, and there is little possibility of interactions between the functional groups of the amino acid and the hydroxyl groups of the cyclodextrin. Similarly, the quite large cavity of PMβCD may only allow weak interactions between the amino acids and PMβCD, resulting in complexes with low apparent stability constants. Such low apparent stability constants cannot be determined at the low cyclodextrin concentration range studied in the permethylated systems (see Section 6.4.1).

The apparent stability constants in Table 4.4 for the complexation of the amino acids by PMαCD are higher than their analogous values with αCD and βCD. The increase in

stability relative to αCD ranges from a factor of 2 for G^- up to a factor of 30 for A-GH. The range of values for the apparent stability constants indicates that PMαCD is guest selective, strongly preferring the guest A-GH to the other guests. The high stability of the A-GH and PMαCD complex is obvious from Figure 4.4, where the very steep experimental curve observed for PMαCD is a direct result of the high stability of the complex. The guests GH_2^+ and G^- form complexes of similar stability with PMαCD, as do the guests VH and V^-, indicating that the charge on the guest is not important in the complexation of these amino acid pairs. Conversely, the complex of PMαCD with A-GH is about 5.6 times more stable than the complex with $A\text{-}G^-$, indicating that the charge on the amino acid is important for this particular guest.

Results in Table 4.4 show that the interaction of all of the guests with PMαCD results in large upfield shifts of their ^{19}F signals. As the cavity of PMαCD is a strongly hydrophobic environment, the observed upfield ^{19}F shift is consistent with the positioning of the fluorine atom of the guests in the apolar cavity environment. The magnitude of the ^{19}F shift changes caused by PMαCD is at least double that caused by αCD and βCD. This is probably because the replacement of the hydroxyl groups by methyl groups makes the PMαCD cavity considerably more hydrophobic than that of the natural cyclodextrins. The amino acids thus experience a greater overall environmental change upon complexation by PMαCD than upon complexation by either αCD or βCD. As observed for αCD and βCD, the ^{19}F shift change experienced upon complexation is greater for the glycine derivatives than for the valine derivatives. An inspection of CPK models shows that the valine guest is less completely encapsulated by PMαCD, and is thus likely to experience a smaller overall environmental change, resulting in smaller overall ^{19}F shift changes.

Results in Table 4.4 indicate that significant thermodynamic discrimination is observed for the guests A-GH and VH, indicating that PMαCD only shows thermodynamic discrimination for the neutral guests. The *R* enantiomer of A-GH is included more strongly than the *S* enantiomer, an opposite trend to that observed for the interaction of this guest with αCD and βCD. The *S* enantiomer of VH is included more strongly than the *R* enantiomer, as found with βCD. The thermodynamic discrimination shown by PMαCD for the neutral guests

is approximately equal to or slightly greater than that shown by αCD and βCD, whereas the thermodynamic discrimination shown by PMαCD for the anionic guests is generally lower than that shown by αCD and βCD. This indicates that methylation does not significantly increase the thermodynamic discrimination despite the increase in complex stability.

Results in Table 4.4 indicate that within experimental error magnetic discrimination is observed for the guests A-GH and A-G$^-$ upon complexation by PMαCD. For A-GH and A-G$^-$ the value of (δ_R - δ_S) is large and negative, whereas for all other guests the (δ_R - δ_S) values are insignificant within experimental error. These values show that the *S* enantiomer experiences a greater environmental change than the *R* enantiomer of both A-GH and A-G$^-$, and that there is a significant difference in the environments of the *R* and *S* enantiomers in the complexes of these guests. Conversely, in the PMαCD complexes of GH_2^+, G$^-$, VH and V$^-$ the environment of the fluorine must be similar for the *R* and *S* enantiomers. These results do not fit the general trends observed for αCD and βCD, where (δ_R - δ_S) is large and negative for the anionic guests, and small and positive for the neutral guests, regardless of the particular guest being studied. The magnetic discrimination shown by PMαCD for the guests A-GH and A-G$^-$ is greater than that shown by αCD and βCD in all cases, and the magnetic discrimination shown by PMαCD for the anionic guests A-G$^-$ and V$^-$ is generally lower than that shown by αCD and βCD.

All amino acids form complexes of higher stability with PMαCD than with αCD. The upfield direction of the ^{19}F shift changes suggests that the fluorine atom is situated in the PMαCD cavity. The following structures proposed for the PMαCD complexes are known to be feasible from CPK models, and offer a possible explanation for the behaviour of the different guests. An inspection of CPK models shows that the primary end of PMαCD is so narrow that the guests are most likely to have their aromatic ring situated in the cavity with their chiral centre in the vicinity of the secondary ring of methyl groups. As the cavity of PMαCD is longer than that of αCD, the guests are able to have greater contact with the cyclodextrin cavity, resulting in complexes of higher stability. All amino acids experience a similar depth of inclusion of the aromatic moiety in the PMαCD cavity, so the difference in the apparent stability constants must be related to the charge and size of the chiral centre of the

guest. The guests GH_2^+ and G^- have similar apparent stability constants with PMαCD. The chiral centre of both GH_2^+ and G^- is highly charged and quite small, and the proximity of this polar group to the hydrophobic methyl rim of PMαCD results in complexes of quite low stability. The guests VH and V^- also have similar apparent stability constants with PMαCD, which are a factor of 3 higher than the values for GH_2^+ and G^-. The chiral centre of VH and V^- is quite large but reasonably linear, and its polarity varies with the charge on the guest. An inspection of CPK models shows that upon inclusion the chiral centre of VH and V^- is likely to project into the solvent, and not interact very significantly with the methyl rim of the cyclodextrin. The lack of contact of the hydrated chiral centre with the hydrophobic methyl groups results in complexes that are more stable than the GH_2^+ and G^- complexes, and also makes the inclusion independent of the charge on the valine guest. The guests A-GH and $A\text{-}G^-$ have very different apparent stability constants with PMαCD. Models show that upon inclusion the hydrated and highly charged chiral centre of $A\text{-}G^-$ is situated close to the hydrophobic methyl rim of the cyclodextrin, and this unfavourable contact results in a complex of quite low stability, comparable with GH_2^+ and G^-. The lack of charge and the presumed lower degree of solvation of the chiral centre of the neutral guest A-GH, as compared with $A\text{-}G^-$, allows favourable interactions with the cyclodextrin which result in a complex of high stability and significant discrimination. The discrimination shown for the guests A-GH and $A\text{-}G^-$ seems to result from the contact of the bulky chiral centre of these guests with the cyclodextrin methyl rim, which places constraints on the orientation of the aromatic ring in the cavity. The chiral centres of GH_2^+, G^-, VH and V^- cannot contact as strongly with the cyclodextrin methyl rim, accounting for the lower discrimination shown by PMαCD for these guests.

These results show that the complexation of the amino acids by PMαCD is very different from their complexation by αCD and βCD, as observed in the literature.[7] As expected from the hydrophobic nature of PMαCD, the guests that show the highest stability and discrimination are the most hydrophobic guests, the neutral amino acids. The generally lower discrimination shown by PMαCD for the anionic guests, as compared with αCD and βCD, suggests that the decreased possibility of favourable electrostatic interactions between the charged amino acids and the cyclodextrin lowers the discrimination. This suggests that

hydrogen bonds or dipolar interactions are important for a host cyclodextrin to show discrimination for anionic guests. However, the fact that PMαCD basically shows very similar discrimination to that shown by αCD and βCD is interesting considering the many differences between the host cyclodextrins. This observation suggests that the fundamental interactions between the guest and the cyclodextrin that are common to both the permethylated and natural cyclodextrins, such as hydrophobic interactions and London dispersion forces (see Section 1.4), are the basis of the small chiral discrimination observed in these systems. Specific interactions such as hydrogen bonding and dipolar interactions are then responsible for either increasing or decreasing the discrimination depending on the guest being studied.

The effect of the medium in the PMαCD systems is insignificant, because large ^{19}F shift changes are observed and a low concentration range is used for the cyclodextrin (see Section 6.4.1). Applying the estimated medium correction decreases the apparent stability constants for PMαCD by up to only 4%, and does not significantly affect the observed discrimination.

4.2.6 Complexation by Amino Cyclodextrins

The apparent stability constants derived from the best fit of the experimental data (see Section 6.4.3) to Equations 4.3 and 4.4 for the inclusion of the amino acids by $\alpha CDNH_3^+$ and $\alpha CDNH_2$, and $\beta CDNH_3^+$ and $\beta CDNH_2$, are listed in Tables 4.4 and 4.5, respectively. Figure 4.5 shows experimental data and best fit curves for the interaction of VH and V^- with $\beta CDNH_3^+$. Apparent stability constants for the complexation of many of the amino acids by the amino cyclodextrins cannot be accurately determined, simply because the ^{19}F shift changes caused by the cyclodextrin are too small. However, it is possible to estimate apparent stability constants of around 10 $dm^3\ mol^{-1}$ for many of the systems for which values cannot be accurately determined. As these apparent stability constants are of a similar magnitude to those determined for αCD, the fact that they are more difficult to determine for the amino cyclodextrins is probably due to the lower cyclodextrin concentration range necessitated by the buffering and ionic strength requirements (see Section 6.4.1). This difference in experimental conditions needs to be considered when comparing the results obtained with the amino cyclodextrins with those obtained with αCD, and to a lesser extent with βCD.

Table 4.5 Apparent stability constants and ^{19}F chemical shifts for the complexes of $\alpha CDNH_3^+$ and $\alpha CDNH_2$ with the fluorinated amino acids in various buffers with 10% aqueous D_2O at $I = 0.10$ and 295.5 K.

amino acid derivative/ cyclodextrin	K ($dm^3\ mol^{-1}$)	δ (ppm)	Δδ (ppm)
G$^-$	K_{RS} = 61 ± 9	δ_{RS} = -40.64 ± 0.05	δ_{RS}-δ_F = -0.53 ± 0.05
$\alpha CDNH_2$ [a]		δ_F = -40.111 ± 0.004	
A-G$^-$	K_{RS} = 16 ± 2	δ_{RS} = -40.4 ± 0.1	δ_{RS}-δ_F = -1.1 ± 0.1
$\alpha CDNH_3^+$ [b]		δ_F = -39.329 ± 0.004	
V$^-$	K_R = 12 ± 3	δ_R = -33.4 ± 0.2	δ_R-δ_F = -0.6 ± 0.2
$\alpha CDNH_3^+$ [b]	K_S = 18 ± 4	δ_S = -33.08 ± 0.06	δ_S-δ_F = -0.28 ± 0.06
		δ_F = -32.796 ± 0.004	δ_R-δ_S = -0.3 ± 0.2

[a] pH 10.8
[b] pH 6.9

Table 4.6 Apparent stability constants and ^{19}F chemical shifts for the complexes of $\beta CDNH_3^+$ and $\beta CDNH_2$ with the fluorinated amino acids in various buffers with 10% aqueous D_2O at $I = 0.10$ and 295.5 K.

amino acid derivative/ cyclodextrin	K ($dm^3\ mol^{-1}$)	δ (ppm)	$\Delta\delta$ (ppm)
A-G$^-$	K_{RS} = 17 ± 2	δ_{RS} = -40.26 ± 0.09	$\delta_{RS}-\delta_F$ = -0.88 ± 0.09
$\beta CDNH_3^+$ [a]		δ_F = -39.380 ± 0.004	
VH	K_R = 40 ± 2	δ_R = -31.28 ± 0.04	$\delta_R-\delta_F$ = 0.98 ± 0.04
$\beta CDNH_3^+$ [b]	K_S = 45 ± 1	δ_S = -31.32 ± 0.02	$\delta_S-\delta_F$ = 0.94 ± 0.02
	K_R/K_S = 0.89 ± 0.05	δ_F = -32.262 ± 0.004	
V$^-$	K_R = 46 ± 2	δ_R = -32.21 ± 0.02	$\delta_R-\delta_F$ = 0.63 ± 0.02
$\beta CDNH_3^+$ [a]	K_S = 53 ± 2	δ_S = -32.05 ± 0.02	$\delta_S-\delta_F$ = 0.79 ± 0.02
	K_R/K_S = 0.87 ± 0.05	δ_F = -32.839 ± 0.004	$\delta_R-\delta_S$ = -0.16 ± 0.03

[a] pH 6.9
[b] pH 1.0

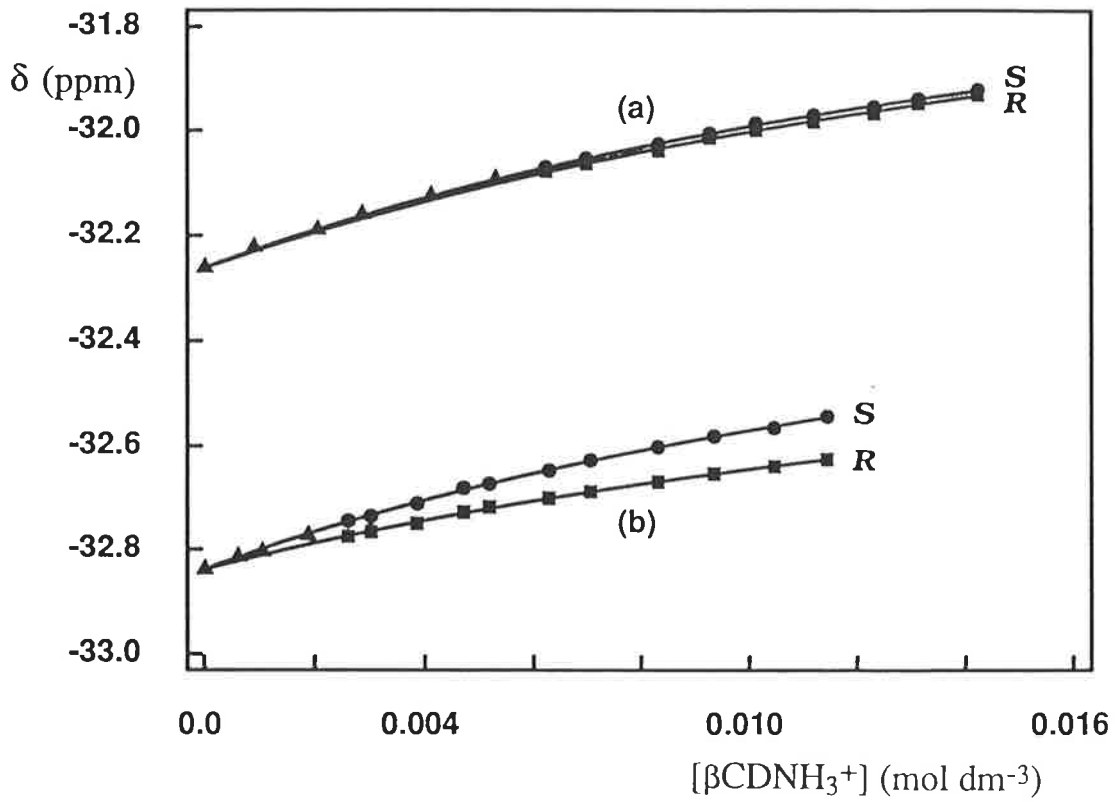

Figure 4.5 Variation of ^{19}F chemical shift (δ) for: (a) *R*- and *S*-VH (1.05 x 10^{-3} mol dm^{-3}) and $\beta CDNH_3^+$ (0.894 - 14.3 x 10^{-3} mol dm^{-3}) in HCl at pH 1.0, and (b) *R*- and *S*-V^- (1.02 - 1.03 x 10^{-3} mol dm^{-3}) and $\beta CDNH_3^+$ (0.600 - 11.5 x 10^{-3} mol dm^{-3}) in phosphate buffer at pH 6.9, at I = 0.10 and 295.5 K. The filled triangles correspond to experimental points where the *R* and *S* enantiomers have identical ^{19}F chemical shifts. The curves through the data points represent the best fit of the data to Equations 4.3 - 4.4 using DATAFIT (see Section 6.4.3).

For the complexation of the amino acids by $\alpha CDNH_3^+$ and $\alpha CDNH_2$, Table 4.5 shows that apparent stability constants can only be determined for the interaction of G^- with $\alpha CDNH_2$, and A-G^- and V^- with $\alpha CDNH_3^+$. Clearly $\alpha CDNH_3^+$ and $\alpha CDNH_2$ favour the inclusion of anionic guests. No apparent stability constants can be determined for the interaction of GH_2^+, A-GH and VH with $\alpha CDNH_3^+$, and A-G^- and V^- with $\alpha CDNH_2$. In comparison with αCD, the apparent stability constants determined for $\alpha CDNH_3^+$ and $\alpha CDNH_2$ are similar for A-G^- and V^-, and increased by a factor of about 3 for G^-. The observations that the complex stability is only increased for G^-, and that many apparent stability constants are close to 10 $dm^3\ mol^{-1}$, suggest that the substitution of an amine group on αCD does not significantly increase the stability of the amino acid complexes over those formed by αCD.

As shown in Table 4.5, the ^{19}F signals of all of the guests experience an upfield shift upon complexation by either $\alpha CDNH_3^+$ or $\alpha CDNH_2$. A ^{19}F shift change in the upfield direction is also observed for all of the guests for which apparent stability constants cannot be determined. As outlined previously, this probably indicates that the fluorine is situated in the hydrophobic part of the cyclodextrin cavity. Upfield ^{19}F shifts are also detected for the interaction of all guests with αCD and PMαCD, indicating that the inclusion of an amino acid in a cyclodextrin with an αCD annulus results in an upfield shift for the fluorine atom. The consistency of these ^{19}F shift changes indicates that there are similarities in the position of the fluorine atom in the complexes of the amino acids with αCD, PMαCD, $\alpha CDNH_3^+$ and $\alpha CDNH_2$. The ^{19}F shift changes observed with $\alpha CDNH_3^+$ and $\alpha CDNH_2$ are 0.3 - 0.6 ppm less than the shift changes observed for the analogous αCD complexes.

Results in Table 4.5 indicate that $\alpha CDNH_3^+$ and $\alpha CDNH_2$ show no thermodynamic discrimination for any of the guests, and that magnetic discrimination is only observed for the interaction of $\alpha CDNH_3^+$ with V^-. Although no discrimination is observed for the interaction of G^- with $\alpha CDNH_2$ and A-G^- with $\alpha CDNH_3^+$, separate signals are observed for the *R* and *S* enantiomers of these guests at high cyclodextrin concentration. Separate signals for the *R* and *S* enantiomers are also observed at high cyclodextrin concentration for all guests for which apparent stability constants cannot be determined, except for the A-G^- and $\alpha CDNH_2$ system.

The observed peak separation for these guests indicates that although apparent stability constants cannot be determined, complexation and discrimination is occurring in these systems. The value of (δ_R - δ_S) is negative for the interaction of VH and $\alpha CDNH_3^+$, as observed for αCD, and the magnitude of (δ_R - δ_S) is nearly twice as large as that observed with αCD. However, care should be taken when comparing the magnetic discrimination shown by αCD and $\alpha CDNH_3^+$, as the errors on (δ_R - δ_S) for $\alpha CDNH_3^+$ are quite high. In summary, the discrimination shown by $\alpha CDNH_3^+$ and $\alpha CDNH_2$ appears to be lower than that shown by αCD, but this conclusion should be treated with caution because of the less favourable experimental conditions under which the $\alpha CDNH_3^+$ and $\alpha CDNH_2$ studies are necessarily conducted.

For the complexation of the amino acids by $\beta CDNH_3^+$ and $\beta CDNH_2$, Table 4.6 shows that apparent stability constants can only be determined for the interaction of $\beta CDNH_3^+$ with $A\text{-}G^-$, VH and V^-. No apparent stability constants can be determined for the interaction of GH_2^+ and A-GH with $\beta CDNH_3^+$, and G^-, $A\text{-}G^-$ and V^- with $\beta CDNH_2$. The apparent stability constants determined with $\beta CDNH_3^+$ are higher than the values determined with βCD for the anionic guests, and lower for the neutral guest. The stability of the $A\text{-}G^-$ complex has increased by a factor of about 1.5, the stability of the VH complex has decreased by a factor of about 2, and the stability of the V^- complex has increased immeasurably, as no apparent stability constant can be determined with βCD. It is also significant that apparent stability constants can be determined for the interaction of $A\text{-}G^-$ and $\beta CDNH_3^+$, but not for the interaction of A-GH and $\beta CDNH_3^+$, and $A\text{-}G^-$ and $\beta CDNH_2$. This confirms that the guests A-GH and $A\text{-}G^-$ form their most stable complex when the guest and host are oppositely charged. This is also observed for the interaction of A-GH and $A\text{-}G^-$ with $\alpha CDNH_3^+$ and $\alpha CDNH_2$, where the only apparent stability constant that can be determined is also for the interaction of the oppositely charged $A\text{-}G^-$ and $\alpha CDNH_3^+$. This confirms that the positive charge on $\beta CDNH_3^+$ and $\alpha CDNH_3^+$ enhances the inclusion of $A\text{-}G^-$. The increased stability of the complexes of V^- with $\beta CDNH_3^+$, and $A\text{-}G^-$ with $\beta CDNH_3^+$ and $\alpha CDNH_3^+$, as compared with αCD and βCD, indicates that there is a small, but significant, increase in amino acid complex stability when the host and guest are oppositely charged. This increase in stability seems most likely to result from a direct charge-charge interaction between the

oppositely charged host and guest. These results are consistent with the observations made for the interaction of carboxylic acid and carboxylate guests with βCD, $\beta CDNH_3^+$ and $\beta CDNH_2$ (see Section 2.2.2), where the positive charge on the cyclodextrin is found to increase the stability of carboxylate guests by a factor of about 2 - 3, and decrease the stability of neutral carboxylic acid guests by a factor of about 1.5 - 2.

Results in Table 4.6 show that the magnitude of the ^{19}F shift changes seen for $\beta CDNH_3^+$ and $\beta CDNH_2$ are fairly similar to those seen for βCD. Including those guests for which apparent stability constants cannot be determined, all of the glycine guests showed an upfield shift of their ^{19}F signals upon complexation, and all of the valine guests showed a downfield shift upon complexation, except for the V^- and $\beta CDNH_2$ system. These changes are generally consistent with the changes observed for βCD indicating that there are similarities in the complexation occurring with βCD, $\beta CDNH_3^+$ and $\beta CDNH_2$.

Results in Table 4.6 show that within experimental error $\beta CDNH_3^+$ shows thermodynamic discrimination for VH and V^-, and magnetic discrimination for V^-. Figure 4.5 shows the effect of the extent of the thermodynamic and magnetic discrimination on the experimental data. The clear separation of the experimental data for the *R* and *S* enantiomers of V^- results from the significant thermodynamic and magnetic discrimination shown by $\beta CDNH_3^+$ for this guest, and the only slight separation of the experimental data for the *R* and *S* enantiomers of VH results from the low magnetic discrimination shown by $\beta CDNH_3^+$ for this guest. Although a K_{RS} value is determined for the interaction of $A\text{-}G^-$ with $\beta CDNH_3^+$, separate ^{19}F signals for the *R* and *S* enantiomers are observed at high cyclodextrin concentration. For guests for which apparent stability constants cannot be determined, separate signals for the *R* and *S* enantiomers are observed at high cyclodextrin concentration for the interaction of G^- and $A\text{-}G^-$ with $\beta CDNH_2$, indicating that some complexation and discrimination is occurring in these systems. No discrimination is observed for the interaction of GH_2^+ and A-GH with $\beta CDNH_3^+$, and V^- with $\beta CDNH_2$. The thermodynamic discrimination shown by $\beta CDNH_3^+$ is slightly higher than that shown by βCD for the guest VH, and immeasurably higher for the guest V^-, as no apparent stability constants can be determined for the interaction of βCD and V^-. $\beta CDNH_3^+$ includes the *S* enantiomer of VH

more strongly than the *R* enantiomer, as is observed for the interaction of βCD and VH. For the interaction of V^- and $\beta CDNH_3^+$, (δ_R - δ_S) is negative and of a similar magnitude to that found with αCD, whereas for the interaction of VH and $\beta CDNH_3^+$, (δ_R - δ_S) is insignificant within experimental error. These results are consistent with the trends observed in the αCD and βCD systems, where (δ_R - δ_S) is large and negative for anionic guests and insignificant within experimental error for neutral guests. As outlined for αCD in Section 4.2.2, the large difference in the behaviour of the anionic and neutral guests may be explained by an opposite direction of inclusion for the differently charged guests.

The effect of the medium in the amino cyclodextrin systems may be quite significant, because of the small observed ^{19}F shift changes which result from the low concentration range used for the amino cyclodextrins (see Section 6.4.1). Applying the estimated medium correction increases the apparent stability constants for $\alpha CDNH_3^+$ and $\alpha CDNH_2$ by up to 30%, and changes the apparent stability constants for $\beta CDNH_3^+$ by up to 20%, decreasing the values for the glycine derivative, and increasing the values for the valine derivatives. The application of the medium correction slightly decreases the observed discrimination, but does not change any of the trends discussed above.

4.2.7 Summary and General Discussion

It is interesting to compare the cyclodextrin inclusion of the three different guests in their different ionic forms. The charge on the glycine derivatives GH_2^+ and G^- strongly affects the inclusion of these guests by the cyclodextrins studied. Apparent stability constants can only be determined for the interaction of GH_2^+ with αCD and PMαCD, indicating that the cyclodextrins studied include GH_2^+ very weakly and thus show insignificant discrimination for this guest. This is consistent with many studies which show that cations are included only weakly by cyclodextrins.[7] Conversely, G^- forms complexes with a range of cyclodextrins, showing its highest stability with PMαCD and $\alpha CDNH_2$. αCD and βCD show significant thermodynamic discrimination for G^-, with the K_R/K_S value of 0.6 determined for the G^- and βCD complex being the highest discrimination observed for any of the amino acids and cyclodextrins studied. Magnetic discrimination is observed for the complexation of G^- by αCD and βCD, with high discrimination for βCD and low discrimination for αCD.

The guests A-GH and A-G$^-$ form complexes of low stability with all cyclodextrins studied except PMαCD. With the exception of the PMαCD complexes, the inclusion of A-GH and A-G$^-$ generally does not show much dependence on either the size or substitution of the cyclodextrin, or on the charge of the guest. The complex formed between A-GH and PMαCD is the most stable complex studied. The thermodynamic discrimination observed for A-GH and A-G$^-$ is very low, with slight discrimination occurring only for the complex formed between A-GH and PMαCD, and A-G$^-$ and αCD. Significant magnetic discrimination is observed for the complexes of A-GH and A-G$^-$ with αCD and PMαCD.

The valine guests VH and V$^-$ show the greatest variation in apparent stability constants and chiral discrimination, varying with the charge on the guest and the nature of the cyclodextrin. The apparent stability constants range from 5 - 150 dm^3 mol^{-1}, with the PMαCD complexes having the highest stability. Thermodynamic discrimination is observed for the interaction of VH with βCD, γCD, PMαCD and βCDNH$_3^+$, with all cyclodextrins having similar K_R/K_S values. Thermodynamic discrimination is observed for the interaction of V$^-$ with αCD and βCDNH$_3^+$, with the higher discrimination shown by αCD. Significant magnetic discrimination is seen for the interaction of V$^-$ with αCD, αCDNH$_3^+$ and βCDNH$_3^+$, but no magnetic discrimination is seen for VH. The charge on the guest significantly affects the magnitude of the thermodynamic and magnetic discrimination that is occurring.

It is clear that for the three guests studied, the valine guests VH and V$^-$ generally show the most significant complexation and discrimination. This is shown by the observation that the valine guests account for about half of the systems where the apparent stability constants are greater than or equal to 30 dm^3 mol^{-1}, and about half of the systems which show significant discrimination. The valine guests have the amino acid chiral centre about three bond lengths removed from the aromatic ring, as compared with the glycine guests which have the chiral centre directly bonded to the aromatic ring. The arrangement with the chiral centre removed from the aromatic ring seems to slightly favour cyclodextrin complexation and discrimination.

It is also interesting to compare the different cyclodextrin hosts. αCD generally forms complexes of low stability, and does not show particular preference for guests of a certain size

or charge. Thermodynamic and magnetic discrimination is seen with αCD, with the largest discrimination being shown for the anionic guests. βCD forms complexes with a wide range of apparent stability constants and shows a preference for neutral guests. Some thermodynamic and magnetic discrimination is seen with βCD, with the highest discrimination being observed for G^-. γCD forms complexes of very low stability with all of the guests studied, showing no preference for the charge and size of the guest. γCD shows virtually no discrimination for the amino acids, only showing slight thermodynamic discrimination for the largest guest, VH. Comparing the natural cyclodextrins leads to the conclusion that βCD has the most suitable cavity size to form complexes of reasonable stability. αCD appears to show the highest discrimination, although it is hard to compare results obtained with αCD and βCD due to the different concentration ranges used for these cyclodextrins (see Section 6.4.1).

PMαCD forms complexes with a wide range of apparent stability constants and shows preferential inclusion and discrimination for the guest A-GH. Although the complexes formed by the amino acids and PMαCD are more stable than the complexes formed with the natural cyclodextrins, there is no significant increase in the observed discrimination. There is no evidence for any significant complex formation between the amino acids and PMβCD.

$\alpha CDNH_3^+$ and $\alpha CDNH_2$ show preferential inclusion of anionic guests, and show no significant thermodynamic discrimination for any of the guests studied. $\beta CDNH_3^+$ shows preferential inclusion of the larger valine guests, and is not very sensitive to the charge of the valine guest as the $\beta CDNH_3^+$ complexes of VH and V^- exhibit similar stability and thermodynamic discrimination. In comparison with αCD and βCD, the protonated amino cyclodextrins show enhanced inclusion of the anionic amino acids, probably due to favourable electrostatic interactions between the oppositely charged host and guest. Although the increase in complex stability is interesting, it must be noted that the magnitude of the increase is fairly small. In comparison with αCD and βCD, the protonated amino cyclodextrins do not show any great enhancements in thermodynamic and magnetic discrimination.

In summary, significant thermodynamic discrimination is observed in ten of the systems studied, and the discrimination favours the *S* enantiomer of the amino acid in eight of these systems. Although equal numbers of anionic and neutral species show significant

thermodynamic discrimination, the magnitude of the thermodynamic discrimination is generally greater for the anions. Significant magnetic discrimination is observed in nine of the systems studied, and the discrimination favours anionic guests for seven of these systems. For all anionic guests which show magnetic discrimination the ^{19}F signal of the *S* enantiomer is shifted more than the *R* enantiomer. These results indicate that the *S* enantiomer of the anionic form of the amino acids experiences the strongest chiral interaction with the cyclodextrins studied.

BIBLIOGRAPHY

(1) Tabushi, I.; Kuroda, Y.; Mizutani, T. *J. Am. Chem. Soc.* **1986**, *108*, 4514.

(2) Barra, M.; de Rossi, R. H. *J. Org. Chem.* **1989**, *54*, 5020.

(3) Brereton, I. M.; Spotswood, T. M.; Lincoln, S. F.; Williams, E. H. *J. Chem. Soc., Faraday Trans. 1* **1984**, *80*, 3147.

(4) Smith, N. J.; Spotswood, T. M.; Lincoln, S. F. *Carbohydr. Res.* **1989**, *192*, 9.

(5) Lincoln, S. F.; Hounslow, A. M.; Coates, J. H.; Doddridge, B. G. *J. Chem. Soc., Faraday Trans. 1* **1987**, *83*, 2697.

(6) Hansen, P. E.; Dettman, H. D.; Sykes, B. D. *J. Magn. Reson.* **1985**, *62*, 487.

(7) Harata, K. *Inclusion Compounds*; Atwood, J. L., Davies, J. E., MacNicol, D. D., Eds; Oxford University Press: Oxford, **1991**, Vol. 5, pp 311-344.

(8) Sakurai, M.; Kitagawa, M.; Hoshi, H.; Inoue, Y.; Chûjô, R. *Carbohydr. Res.* **1990**, *198*, 181.

(9) Lincoln, S. F.; Hounslow, A. M.; Coates, J. H.; Villani, R. P.; Schiller, R. L. *J. Inclusion Phenom.* **1988**, *6*, 183.

CHAPTER FIVE

SUMMARY AND CONCLUSIONS

The focus of this research is the investigation of the recognition of a variety of polar molecules by a range of natural and modified cyclodextrins, with a particular interest in the recognition of enantiomers of racemic guests. This study involved the measurement of apparent stability constants to determine the relative importance of steric and electrostatic interactions, solvation, and metal ion coordination in controlling the cyclodextrin complex formation and enantiomer recognition.

Using various methods, several different cyclodextrins and guests were studied, and it is possible to make comparisons between them. The guests studied all have a single phenyl ring as the only aromatic unit, with the exception of the amino acid *RS*-tryptophan, which has indole as the aromatic unit. The guests are all polar, being either amino or carboxylic acids, and their aromatic rings are either mono- or 1,4-substituted. The modified cyclodextrins studied are either fully substituted with methyl groups or singly substituted with an amino group.

Apparent stability constants for a variety of cyclodextrin complexes were determined using different methods appropriate to the guest being studied. For the systems studied, apparent stability constants are in the range 5 - 1700 $dm^3\ mol^{-1}$ for the natural cyclodextrins, and 12 - 2600 $dm^3\ mol^{-1}$ for the modified cyclodextrins. The *RS*-tryptophan and βCDpn complex is the most stable cyclodextrin complex studied. For the complexation of amino acids, it is generally found that βCD forms the most stable complexes, and αCD and γCD form complexes of low stability regardless of either the charge or size of the guest. The positively charged amino acid, protonated *RS*-α-(4-fluorophenyl)glycine, is included only weakly by all cyclodextrins studied. The hydrophobicity of the cyclodextrin is confirmed as being an important factor in the inclusion of amino acids, as the stability of the PMαCD complexes is higher than that of any of the natural cyclodextrins.

In metallocyclodextrin systems, the presence of a metal ion, such as Co^{2+}, Ni^{2+}, Cu^{2+} or Zn^{2+}, is found to increase the stability of the complexes of *RS*-tryptophan and *RS*-phenylalanine by a factor of 4 - 57000, as compared with the stability of the complexes formed with either βCD or βCDpn in the absence of a metal ion . The ternary complex formed between *RS*-tryptophan and the Cu^{2+} complex of βCDpn shows the greatest stability enhancement.

The study of the complexation of anionic guests by positively charged cyclodextrins shows that the possibility of a direct charge-charge interaction between an oppositely charged host and guest increases the stability of the cyclodextrin complexes by a factor of up to three, as compared with the stability of the complexes of the corresponding uncharged natural cyclodextrin. The increase in complex stability is higher for carboxylate guests than for anionic amino acid guests. Convincing evidence that the increase in stability results from a direct charge-charge interaction between the oppositely charged cyclodextrin and guest comes from a 2D NMR study of the complex of 4-methylbenzoate with $\beta CDNH_3^+$.

A particular focus of this research is the investigation of the recognition of enantiomers by cyclodextrins. Although the stability of the cyclodextrin complexes is generally quite low, it is possible to detect significant chiral discrimination by the cyclodextrin for the enantiomers of a racemic guest. The chiral discrimination observed using natural cyclodextrins is small, having K_R/K_S values in the range 0.6 - 1.2 for amino and carboxylic acid guests. The largest discrimination observed using a natural cyclodextrin is for the interaction of βCD and the anionic form of *RS*-α-(4-fluorophenyl)glycine.

The two general types of modified cyclodextrins studied are the permethylated cyclodextrins, PMαCD and PMβCD, and the monosubstituted amino cyclodextrins, $\alpha CDNH_2$, $\beta CDNH_2$ and βCDpn. The complexation of amino acids by the former group of modified cyclodextrins is strongly dependent on the size of the annulus. PMβCD shows virtually no complex formation and chiral discrimination for any of the fluorinated amino acids studied, seemingly because the cavity is too large for the relatively small guests. PMαCD forms complexes that are considerably more stable than the corresponding αCD and βCD complexes, but shows similar and lower discrimination for neutral and anionic amino acids,

respectively, than that shown by αCD and βCD. This indicates that, despite the increase in complex stability which results from the increased hydrophobicity of PMαCD, the symmetry of the permethylated hosts prevents significant chiral discrimination from occurring. The fact that the observed discrimination for the amino acids is fairly similar for αCD, βCD and PMαCD is surprising considering the differences between the hosts. This suggests that the small chiral discrimination observed for the amino acids arises from the fundamental interactions between the guest and the cyclodextrin that are common to both the permethylated and natural cyclodextrins, such as hydrophobic interactions and London dispersion forces. Specific interactions such as hydrogen bonding or dipolar interactions are then responsible for either increasing or decreasing the discrimination depending on the guest being studied. Such factors are particularly important in the recognition of anions.

The second group of modified cyclodextrins studied is the monosubstituted amino cyclodextrins. Values of K_R/K_S for the inclusion of amino and carboxylic acid guests by monosubstituted cyclodextrins are in the range 0.6 - 2.8. The largest discrimination observed using a monosubstituted cyclodextrin is for the interaction of *RS*-2-phenylpropanoate and uncharged $\beta CDNH_2$. It is generally found that a monosubstituted cyclodextrin shows greater discrimination than either a natural or permethylated cyclodextrin, at least partly due to the greater asymmetry of a singly substituted cyclodextrin.

The study of the inclusion of *RS*-2-phenylpropanoic acid and the fluorinated amino acids by the natural and modified cyclodextrins indicates that the cyclodextrins generally show greater chiral discrimination for anions. This is despite the generally lower stability of the complexes of charged guests, as compared with neutral guests. Thermodynamic discrimination is found to favour either the *R* or the *S* enantiomer, depending on the system being studied, with no obvious trends being observed.

A main finding of this study is that the addition of a metal ion to the βCDpn and amino acid systems substantially increases the observed chiral discrimination. Values of K_R/K_S for the complexation of *RS*-tryptophan and *RS*-phenylalanine by the metallocyclodextrins are in the range 0.1 - 2.0, higher than the values observed in the other systems studied. The highest chiral discrimination observed is for the complexation of *RS*-tryptophan by the Ni^{2+}

complex of βCDpn, where the apparent stability constant for the *S* enantiomer is ten times larger than that for the *R* enantiomer. This chiral discrimination appears to be the highest reported thus far in the literature for a metallocyclodextrin. The conditions necessary for high chiral discrimination are the simultaneous presence of the cyclodextrin and the metal ion, and geometric constraints on the metal ion from ligand field effects. These conditions seem to be important in causing the large discrimination because they increase the asymmetry of the host cyclodextrin, and the metal ion provides an extra recognition point for the guest. The magnitude of the observed chiral discrimination is determined primarily by the nature of the metal ion, with the smallest metal ion, Ni^{2+}, showing the highest discrimination.

The study of these cyclodextrin systems leads to a better understanding of the non-covalent interactions, particularly those contributing to chiral recognition, that occur in cyclodextrin systems. The results contribute to the general understanding of non-covalent interactions in host-guest systems, and potentially provide new insights into biological host-guest systems.

CHAPTER SIX

EXPERIMENTAL AND COMPUTATIONAL METHODS

6.1 General

6.1.1 Materials

αCD, βCD, γCD, PMαCD and PMβCD (Sigma, Cyclolab) were used without further purification. $\alpha CDNH_2$, $\beta CDNH_2$ and βCDpn were prepared as in the literature.[1-3] All cyclodextrins were assumed to be anhydrous after being dried to constant weight and stored in the dark over P_2O_5 in a vacuum desiccator. All solutions were prepared using deionized water purified with a MilliQ-Reagent system, and for solutions to be used for titrations this water was boiled to remove CO_2. All salts were of analytical grade. The deuterated solvents DCl (Cambridge Isotope Laboratories), D_2O, NaOD and D_3PO_4 (Sigma) were used for NMR solutions.

6.1.2 Potentiometric Titrations

Titrations were performed using a Metrohm Dosimat E665 titrimator, an Orion SA 720 potentiometer, and either an Orion 8103 semi-micro or 8172 Sureflow Ross combination pH electrode. All titrations were thermostatted at 298.2 ± 0.1K in a water-jacketted titration vessel able to contain either 10 cm^3 or 2 cm^3 of solution. For titrations in the carboxylic acid systems the electrode was filled with 0.10 mol dm^{-3} KCl and calibrated before use with appropriate buffer solutions. Data was collected in pH units, and a pK_w value was determined by titration of 0.01 mol dm^{-3} HCl with standardized 0.05 mol dm^{-3} NaOH. For titrations in the metal systems the electrode was filled with 0.10 mol dm^{-3} $NaClO_4$, and was regularly calibrated by determination of E_0 and pK_w values by titration of 0.010 mol dm^{-3} $HClO_4$ with standardized 0.1 mol dm^{-3} NaOH. Data was collected in mV units. Throughout a titration a

stream of fine nitrogen bubbles saturated with either 0.10 mol dm^{-3} KCl or $NaClO_4$ as appropriate was passed through the titration solution which was magnetically stirred.

Derivations of apparent stability constants were performed on a SUN 3/60 workstation using the program SUPERQUAD,[4] which minimized an error-square sum based on the differences between the measured and calculated electrode potentials. At least three experimental runs were performed for each system, and at least two of these runs were averaged. The fit of a single run was considered to be statistically acceptable if χ^2 was less than 12.60 at the 95% confidence level. For a directly measured apparent stability constant, the error, σ, was calculated as one standard deviation from the mean,

$$\sigma = \sqrt{((\Sigma(K_i - K)^2)/(N-1))}$$

where K was the mean apparent stability constant, K_i was a best fit apparent stability constant from an accepted single run, and i = 1, 2, ..., N, for N accepted single runs. For a derived apparent stability constant, the error was calculated from the propagation of errors associated with the appropriate apparent stability constants.

6.2 The Complexation of Carboxylic Acids by Beta-Cyclodextrin and an Amino Beta-Cyclodextrin Derivative

6.2.1 Materials and Solutions

Benzoic acid, 4-methylbenzoic acid and *R*- and *S*-2-phenylpropanoic acid (Sigma) were used without further purification. The enantiomeric purities of *R*- and *S*-2-phenyl-propanoic acid were determined as > 97.5% and > 98.5%, respectively, by HPLC analysis of their diastereomers formed by reaction with *S*-1-phenylethylamine. These purity limits were used in the calculation of errors on the apparent stability constants for the cyclodextrin complexation of these enantiomers. All carboxylic acid/carboxylate and cyclodextrin solutions were 0.10 mol dm^{-3} in KCl.

6.2.2 Determination of Apparent Stability Constants

The pK_a values of the carboxylic acids and $\beta CDNH_3^+$ were determined by titration of either 0.002 or 0.005 mol dm^{-3} aqueous solutions (either 2.0 or 8.0 cm^3) with standardized 0.05 mol dm^{-3} NaOH.

To determine the apparent stability constants for the complexation of a carboxylic acid and its conjugate base by βCD, the burette contained a solution of 0.015 mol dm^{-3} βCD at pH 7. The pH of each 0.002 mol dm^{-3} carboxylic acid/carboxylate solution (2.0 cm^3) in the titration vessel was adjusted to a value near the pK_a of the carboxylic acid. Up to 3 cm^3 of βCD solution, in increments of less than 0.05 cm^3, was added to the carboxylic acid/carboxylate solutions. For each carboxylic acid system studied at least three similar titrations were performed, with starting pHs in the range 3.9 - 4.8.

To determine the apparent stability constants for the complexation of 4-methylbenzoic and *R*- and *S*-2-phenylpropanoic acids and their conjugate bases by $\beta CDNH_3^+$, the burette contained a solution of 0.016 mol dm^{-3} $\beta CDNH_3^+$ at pH 6. The pH of each 0.002 mol dm^{-3} carboxylic acid/carboxylate solution (2.0 cm^3) in the titration vessel was adjusted to a value near the pK_a of the carboxylic acid. Up to 3 cm^3 of $\beta CDNH_3^+$ solution, in increments of less than 0.05 cm^3, was added to the carboxylic acid/carboxylate solutions. For each carboxylic acid system studied at least three similar titrations were performed, with starting pHs in the range 3.9 - 4.5. To determine the apparent stability constants for the complexation of benzoic acid and benzoate by $\beta CDNH_3^+$, the burette contained a solution of 0.006 mol dm^{-3} benzoic acid/benzoate at pH 4. The pH of each 0.005 mol dm^{-3} $\beta CDNH_3^+$ solution (2.0 cm^3) in the titration vessel was adjusted to a value near pH 4. Up to 1 cm^3 of benzoic acid/benzoate solution, in increments of less than 0.03 cm^3, was added to the $\beta CDNH_3^+$ solution. At least three similar titrations were performed, with starting pHs in the range 3.5 - 4.5. The pH changes observed in this second method resulted from both the formation of a complex and the addition of an essentially buffered carboxylic acid/carboxylate solution to an unbuffered cyclodextrin solution. As the observed pH changes were not solely the result of complex formation, the determination of apparent stability constants by this method was less accurate than by the first method.

To determine the apparent stability constants for the complexation of a carboxylate by $\beta CDNH_3^+$ and $\beta CDNH_2$, the burette contained a solution of 0.01 - 0.02 mol dm^{-3} carboxylate at pH 7. The pH of each 0.002 mol dm^{-3} $\beta CDNH_3^+/\beta CDNH_2$ solution (2.0 cm^3) in the titration vessel was adjusted to a value near the pK_a of the cyclodextrin. Up to 3 cm^3 of carboxylate solution, in increments of less than 0.05 cm^3, was added to the $\beta CDNH_3^+/\beta CDNH_2$ solutions. For each carboxylate system studied at least three similar titrations were performed, with starting pHs in the range 8.2 - 8.8.

6.2.3 ^1H Nuclear Magnetic Resonance Spectroscopy

1D ^1H NMR spectra were run in 5 mm diameter NMR tubes on a Bruker ACP 300 spectrometer. In a typical experiment, 100 transients were collected at a spectral width of 4000 Hz. Chemical shifts were measured relative to an external reference solution of TPS in D_2O. Solutions of *RS*-2-phenylpropanoic acid and either βCD or $\beta CDNH_3^+$ were adjusted to pH 1 with DCl/D_2O, and solutions of *RS*-2-phenylpropanoate and $\beta CDNH_3^+$ were buffered at pH 6.4 with 0.20 mol dm^{-3} phosphate buffer[5] that was made up in D_2O. The concentration of the guest and cyclodextrin in each system was determined by solubility limits and a requirement that ≥ 90% of the guest species was complexed. The concentration range used was 0.01 - 0.09 mol dm^{-3} for either βCD or $\beta CDNH_3^+$, and 0.001 - 0.01 mol dm^{-3} for either *RS*-2-phenylpropanoic acid or *RS*-2-phenylpropanoate. When separate signals were observed for the *R* and *S* enantiomers of the guests in their complexes with either βCD or $\beta CDNH_3^+$, the signals were assigned by adding resolved *R*-2-phenylpropanoic acid to a solution of the racemate and observing which signal increased in intensity.

Dipolar interactions (NOEs) provide information about the proximity of protons in space, and so 2D NMR spectra may be used to gain information about the precise orientation of guests in the cyclodextrin cavity. ROESY was preferred to NOESY, as the NOEs in the laboratory frame of the NOESY experiment were found to be close to zero as a result of the unfavourable correlation time of a cyclodextrin host-guest system with a molecular weight of around 1000.[6] ROESY overcame this problem by the application of a spin-locking field during the NOESY mixing period. The effects detected by ROESY are weak, and to obtain an acceptable signal to noise it was necessary to have a significant concentration of the

cyclodextrin complex present. This required the guest to have a good solubility in the solvent and the complex to have a reasonably large apparent stability constant. Also, to allow conclusions to be drawn about the direction of inclusion, the guest needed ^1H NMR signals that could easily be interpreted as belonging to certain parts of the molecule. The 4-methyl-benzoate.$\beta CDNH_3^+$ complex was the only complex in this study which met all of these requirements satisfactorily.

2D NMR spectra were run at room temperature on either a Bruker ACP 300 spectrometer in Adelaide, or an AMX 400 spectrometer in Melbourne (by Peter Barron of Bruker (Australia)). To minimize the HOD signal, βCD and $\beta CDNH_2$ were rotavapped at 348 K in D_2O to replace exchangeable hydrogens with deuterium. Samples were made up in either deuterated phosphate buffer[5] (pH 6.4, 0.2 mol dm^{-3}, with added DCl to protonate all $\beta CDNH_2$) or DCl/D_2O (pH 1, 0.1 mol dm^{-3}), filtered through a 20 μm millipore filter and degassed. Guest and cyclodextrin concentrations were such that ≥ 90% of the guest existed in the complexed form. ROESY spectra were acquired at spectral widths of 3000 - 4000 Hz with a relaxation delay of 2 - 3 seconds, using either a 2048 x 512 matrix of 16 transients (AMX 400) or a 1024 x 256 matrix of either 32 or 48 transients (ACP 300). The HOD signal was suppressed by presaturation, and a spin-lock mixing pulse of 1 - 1.5 seconds with O1/O2 coherence was used. To assign the cyclodextrin peaks, standard ^1H decoupling and COSY spectra were performed on the ACP 300 spectrometer, and the HOD signal was suppressed using the WATR T2 relaxation method.

6.3 The Complexation of Amino Acids by Beta-Cyclodextrin, a Diamino Beta-Cyclodextrin Derivative and its Co^{2+}, Ni^{2+}, Cu^{2+} and Zn^{2+} Complexes

6.3.1 Materials and Solutions

R-, *S*- and *RS*-tryptophan, and *R*-, *S*- and *RS*-phenylalanine (Sigma) were used without further purification, and were dried to constant weight and stored in the dark over P_2O_5 in a vacuum dessicator prior to use. The enantiomeric purities of the amino acids were determined to be > 99% after HPLC analysis of their diastereomeric methyl esters in the case

of *R*- and *S*-tryptophan, and their diastereomeric *N*-benzoyl methyl esters in the case of *R*- and *S*-phenylalanine. These purity limits were used in the calculation of error limits on the apparent stability constants for the cyclodextrin complexation of these enantiomers. Metal perchlorates (Fluka) were twice recrystallized from water, and dried and stored over P_2O_5 under vacuum.

All titrations were performed using standardized 0.1 mol dm^{-3} NaOH. All 0.001 mol dm^{-3} tryptophan, βCDpn and βCD stock solutions were also 0.010 mol dm^{-3} in $HClO_4$ and 0.090 mol dm^{-3} in $NaClO_4$. The 0.1 mol dm^{-3} metal perchlorate stock solutions were prepared in water. The $Ni(ClO_4)_2$, $Cu(ClO_4)_2$ and $Zn(ClO_4)_2$ stock solutions were standardized by titration against disodium ethylenediaminetetraacetate in the presence of Murexide indicator in the first two cases and Eriochrome Black T in the third case.[7] The $Co(ClO_4)_2$ stock solution was standardized by back titration of the acid liberated by ion exchange of Co^{2+} on an Amberlite HRC-120 cation exchange column in the acid form.

6.3.2 Determination of Apparent Stability Constants

The pK_a values of $\beta CDpnH_2^{2+}$ and the diprotonated amino acids were determined by titration of 10.00 cm^3 aliquots of 0.001 mol dm^{-3} solutions. The apparent stability constants for the formation of the βCD-amino acid and βCDpn-amino acid complexes were determined by titration of 5.00 cm^3 each of 0.001 mol dm^{-3} solutions of either the *R* or *S* enantiomer and either βCD or $\beta CDpnH_2^{2+}$. The apparent stability constants for the formation of the various metal-amino acid and metal-βCDpn complexes were determined by titration of 10.00 cm^3 aliquots of 0.001 mol dm^{-3} either amino acid or $\beta CDpnH_2^{2+}$ with either 0.095 cm^3 or 0.045 cm^3 of metal perchlorate solution added. The apparent stability constants for the formation of the various metal-βCDpn-amino acid complexes were determined by titration of 5.00 cm^3 each of 0.001 mol dm^{-3} solutions of either the *R* or *S* enantiomer and $\beta CDpnH_2^{2+}$ with 0.045 cm^3 of metal perchlorate solution added.

6.3.3 ^{13}C Nuclear Magnetic Resonance Spectroscopy

Standard 1D ^{13}C NMR spectra were run in 5 mm diameter NMR tubes on a Bruker ACP 300 spectrometer. In a typical experiment, 2000 - 20000 transients were collected at a

spectral width of 20000 Hz. Chemical shifts were measured relative to an external reference solution of *t*-butanol. Solutions of βCDpn and βCDpn-Zn^{2+} in D_2O were adjusted to a pH close to 7.5 with either $HClO_4$ or NaOH as appropriate.

6.4 The Complexation of Fluorinated Amino Acids by Alpha-Cyclodextrin, Beta-Cyclodextrin, Gamma-Cyclodextrin and Derivatives

6.4.1 Materials and Solutions

RS-N-(4-Fluorobenzoyl)valine, *RS*-α-(4-fluorophenyl)glycine and *RS-N*-acetyl-α-(4-fluorophenyl)glycine were prepared and resolved as in the literature.[8] The pK_a values of the fluorinated amino acids[8] and the modifed cyclodextrins[2] in aqueous solution were determined by standard titrimetric methods at $I = 0.10$ (KCl) and 298.2 K. The aqueous solubility of the zwitterionic form of *RS*-α-(4-fluorophenyl)glycine was too low to allow this species to be studied by 1D ^{19}F NMR spectroscopy.

All NMR solutions were made up by weight and their concentrations calculated using densities determined by the standard method using 2 cm^3 pycnometers. Each amino acid-cyclodextrin solution contained 10% D_2O. The pH and 0.10 mol dm^{-3} ionic strength of the NMR solutions were maintained by buffers prepared as in the literature.[5] The buffers used were KCl/HCl and HCl for pH 1.3 and 1.0, respectively, KH_2PO_4/Na_2HPO_4 for pH 6.9, and glycine/NaOH for pH 10.8. To maintain a constant pH when working at pH 10.8 it was necessary to store all solutions under N_2 to minimize their exposure to CO_2.

The amino acid concentration in each solution was 0.001 mol dm^{-3}, and was kept constant within 1 - 6% for each system. The natural cyclodextrins were studied over concentration ranges determined by their aqueous solubility (see Section 1.2). The permethylated cyclodextrins, PMαCD and PMβCD, were studied at concentrations up to a maximum of 0.01 mol dm^{-3}. The amino cyclodextrins, $\alpha CDNH_2$ and $\beta CDNH_2$, which could become positively charged, had to be studied at concentrations below 0.015 mol dm^{-3}, to ensure that the buffer would maintain the pH and ionic strength. At pH 6.9 it was also

necessary for the amino cyclodextrin stock solution to contain enough 0.1 mol dm^{-3} HCl to fully protonate the cyclodextrin.

For systems where a high concentration of cyclodextrin was used to check for chiral discrimination, solutions of an ionic strength of approximately 1 mol dm^{-3} were made. For pH 0, 1 mol dm^{-3} HCl was used; for pH 11, 0.1 mol dm^{-3} NaOH/glycine buffer with 1 mol dm^{-3} KCl was used; and for pH 7, 0.1 mol dm^{-3} phosphate buffer with 1 mol dm^{-3} KCl was used, with added 0.1 mol dm^{-3} HCl, if necessary, to protonate the cyclodextrin.

6.4.2 ^{19}F Nuclear Magnetic Resonance Spectroscopy

The ^{1}H-broad-band decoupled 1D ^{19}F NMR spectra were recorded on a Bruker CXP 300 spectrometer at 282.35 MHz locked on the deuterium frequency of D_2O. The amino acid-cyclodextrin solutions were contained in 5 mm precision NMR tubes. In a typical experiment, an average of 1500 scans at a spectral width of 2000 - 5000 Hz were accumulated into an 8192 point database. The solution temperature was controlled at 295.5 ± 0.5 K. Chemical shifts were referenced to an external reference solution of 2% sodium trifluoroacetate in D_2O, an external reference being necessary because of the known ability of cyclodextrins to include sodium trifluoroacetate. The errors introduced into the determination of the ^{19}F chemical shifts by the use of an external reference had previously been shown to be negligible.[9]

6.4.3 Determination of Apparent Stability Constants

To determine whether it was feasible to measure an apparent stability constant for a particular amino acid-cyclodextrin system, the ^{19}F chemical shift of a solution of cyclodextrin and guest at the maximum reasonable concentration of cyclodextrin was compared with the ^{19}F chemical shift of the free amino acid. An apparent stability constant could not be determined if the addition of the cyclodextrin did not induce a significant ^{19}F chemical shift change. In systems where a cyclodextrin induced shift change was observed, this shift change was compared with the shift change caused by solutions of a straight chain glucose derivative, either maltotriose (three glucose units) or stachyose (four glucose units). If a system had cyclodextrin induced shifts of a similar magnitude to the straight chain glucose derivative

induced shifts, then no apparent stability constants for that system could be determined. For systems where the cyclodextrin induced shifts were substantially larger than the straight chain glucose derivative induced shifts, at least fourteen solutions were studied, with the cyclodextrin concentration varying between 5 x 10^{-4} mol dm^{-3} and 0.14 mol dm^{-3}, depending on the particular cyclodextrin being studied (see Section 6.4.1). In systems where separate signals were observed for the cyclodextrin complexes of the *R* and *S* enantiomers of the amino acid, the signals were assigned by adding resolved *S* enantiomer to a solution of the racemate and observing which signal increased in intensity. In systems where either separate signals could not be detected, or the difference between separate signals was small at the highest possible concentration of the cyclodextrin, an apparent stability constant for the racemate was determined. In systems where no *R* and *S* peak separation was observed, one solution close to the solubility limit of the cyclodextrin was used to determine if any chiral discrimination was occurring. Such samples were prepared at an ionic strength of 1 mol dm^{-3}, and care taken to maintain the pH as described in Section 6.4.1.

Derivations of apparent stability constants were performed on a SUN 3/60 workstation using the non-linear regression analysis program DATAFIT,[10] which minimized the residuals between the experimental and calculated surfaces until convergence within specified limits was obtained. Experimental data points were weighted inversely according to the error in the cyclodextrin concentration, as this was determined to be the most significant error. In systems where separate apparent stability constants could be determined for the complexes of the *R* and *S* enantiomers it was necessary to fit the data for the enantiomers simultaneously. Initially the data for the *R* enantiomer was fitted with fixed estimated values for the *S* enantiomer, then the data for the *S* enantiomer was fitted with the newly determined values for the *R* enantiomer as fixed parameters. This process was continued until convergence was obtained for the fitted parameters of both of the enantiomers. If there was no resolution of the *R* and *S* enantiomers at low cyclodextrin concentration, these points were given less weighting than those points at which satisfactory resolution was obtained. Occasionally obvious outliers were given less weight to obtain the best fit.

The sensitivity of ^{19}F chemical shifts to the solvent led to concerns about the effect of a bulky cyclodextrin on the solvent medium. It was possible that the ^{19}F chemical shift changes observed for the amino acids upon addition of a cyclodextrin were not due to complexation alone, but were also at least partly due to the changes that occur in the solvent because of the presence of the cyclodextrin. To investigate the possible magnitude of this medium effect, solutions of maltotriose were used to estimate the change in ^{19}F chemical shift experienced by an amino acid upon addition of a certain concentration of glucose units to the medium. Maltotriose caused a small downfield shift in the 1D ^{19}F NMR signals of the amino acids studied. The ^{19}F shift changes for each of a neutral, cationic and anionic amino acid were measured at four different concentrations of maltotriose, which allowed estimation of the magnitude of the medium effect. This estimated medium correction could then be subtracted from the ^{19}F chemical shifts observed for the interaction of each amino acid with the cyclodextrins. The resultant shift changes due to complexation alone could then be used to estimate an apparent stability constant free of medium effects.

BIBLIOGRAPHY

(1) Lincoln, S. F.; Coates, J. H.; Easton, C. J.; van Eyk, S. J.; May, B. L.; Singh, P.; Stile, M. A.; Williams, M. L. Internat Pat Appl., WO 90/02141.

(2) Brown, S. E.; Coates, J. H.; Coghlan, D. R.; Easton, C. J.; van Eyk, S. J.; Janowski, W.; Lepore, A.; Lincoln, S. F.; Luo, Y.; May, B. L.; Schiesser, D. S.; Wang, P.; Williams, M. L. *Aust. J. Chem.* **1993**, *46*, 953

(3) Brown, S. E.; Coates, J. H.; Easton, C. J.; van Eyk, S. J.; Lincoln, S. F.; May, B. L.; Stile, M. A.; Whalland, C. B.; Williams, M. L. *J. Chem. Soc., Chem. Commun.* **1994**, 47.

(4) Gans, P.; Sabatini A.; Vacca, A. *J. Chem. Soc., Dalton Trans.*, **1985**, 1195.

(5) *Biochemists' Handbook*; Long, C., Ed.; Spon: London, **1961**.

(6) Bothner-By, A. A.; Stephens, R. L.; Lee, J.; Warren, C. D.; Jeanloz, R. W. *J. Am. Chem. Soc.* **1984**, *106*, 811.

(7) *Quantitative Inorganic Anaylsis*, Vogel, A. I., Ed; Longmans: London; **1961**, 3rd edition.

(8) Brown, S. E.; Coates, J. H.; Coghlan, D. R.; Easton, C. J.; Lincoln, S. F. *J. Chem. Soc., Faraday Trans.* **1991**, *87*, 1195.

(9) Brereton, I. M.; Spotswood, T. M.; Lincoln, S. F.; Williams, E. H. *J. Chem. Soc., Faraday Trans.* **1984**, *80*, 3147.

(10) Gal, M. E.; Kelly, G. R.; Kurucsev, T. *J. Chem. Soc., Faraday Trans. 1* **1973**, *69*, 395.

APPENDICES

EXPERIMENTAL DATA

A.1 The Complexation of Carboxylic Acids by Beta-Cyclodextrin and an Amino Beta-Cyclodextrin Derivative

The experimental titration curves used to calculate the apparent stability constants for the complexation of the carboxylic acid and carboxylate guests by βCD, $\beta CDNH_3^+$ and $\beta CDNH_2$ are shown in Figures A.1.1 - A.1.12. Each point on a graph represents an experimental pH reading, and the three curves for each system correspond to similar experiments conducted at different starting pHs. All titrations were performed at $I = 0.10$ (KCl) and 298.2 K, as outlined in Section 6.2.

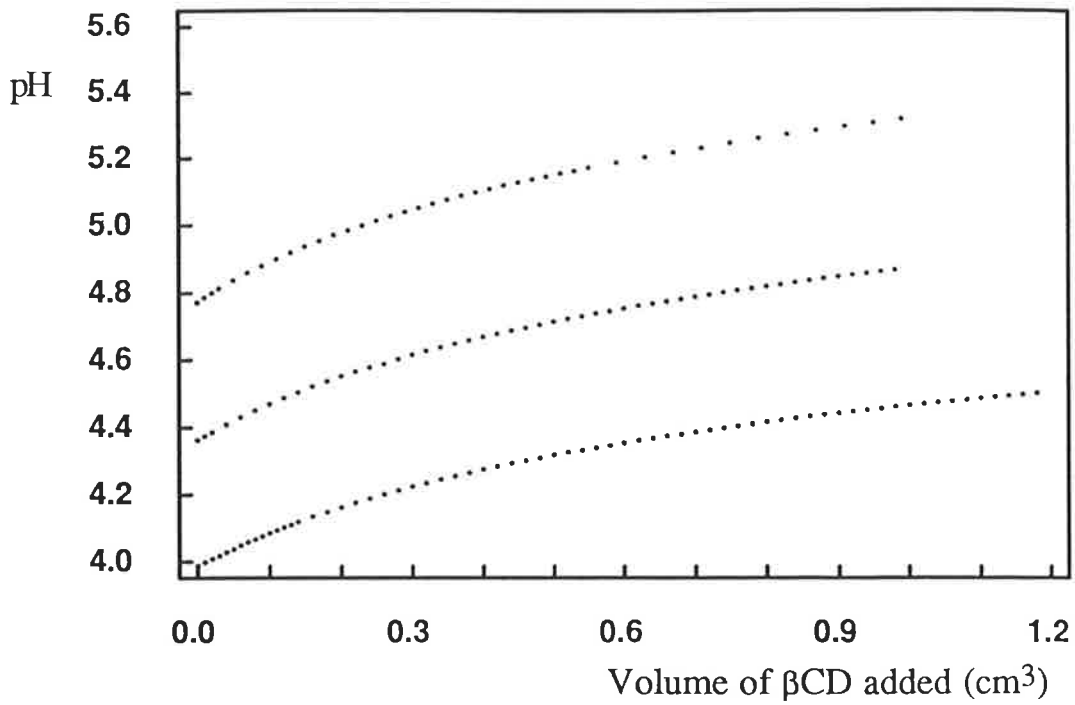

Figure A.1.1 Variation of the pH of three 2.0 cm^3 solutions of benzoic acid/benzoate (1.04×10^{-3} mol dm^{-3}) with volume of added βCD (1.51×10^{-2} mol dm^{-3}).

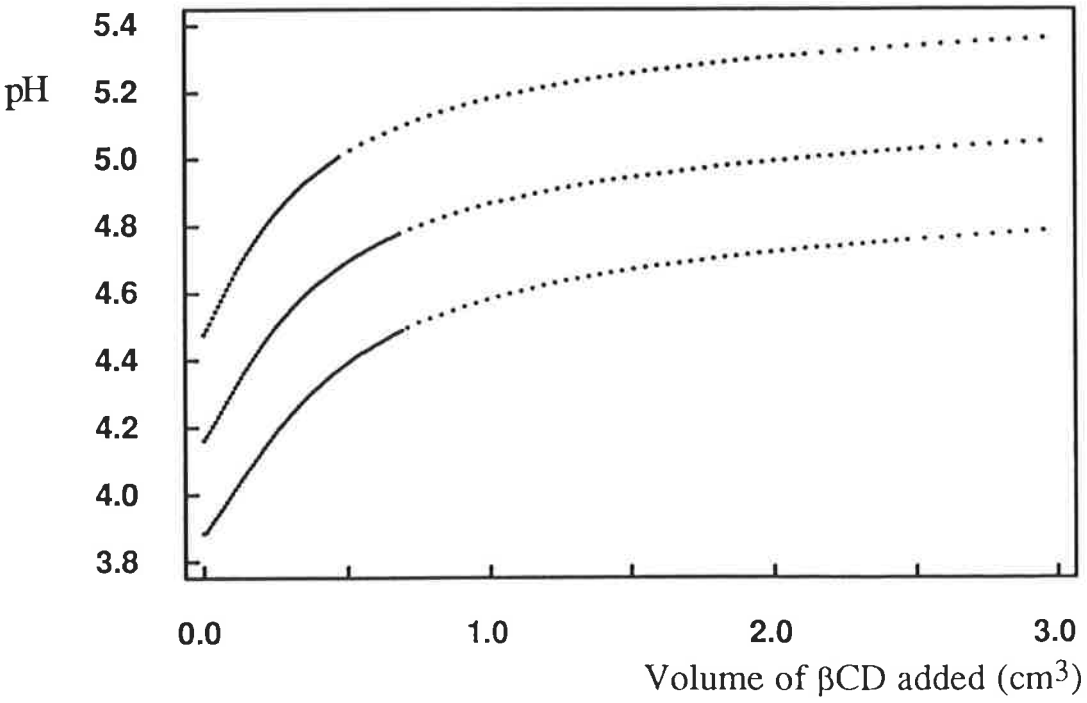

Figure A.1.2 Variation of the pH of three 2.0 cm^3 solutions of 4-methylbenzoic acid/4-methylbenzoate (2.14×10^{-3} mol dm^{-3}) with volume of added βCD (1.49×10^{-2} mol dm^{-3}).

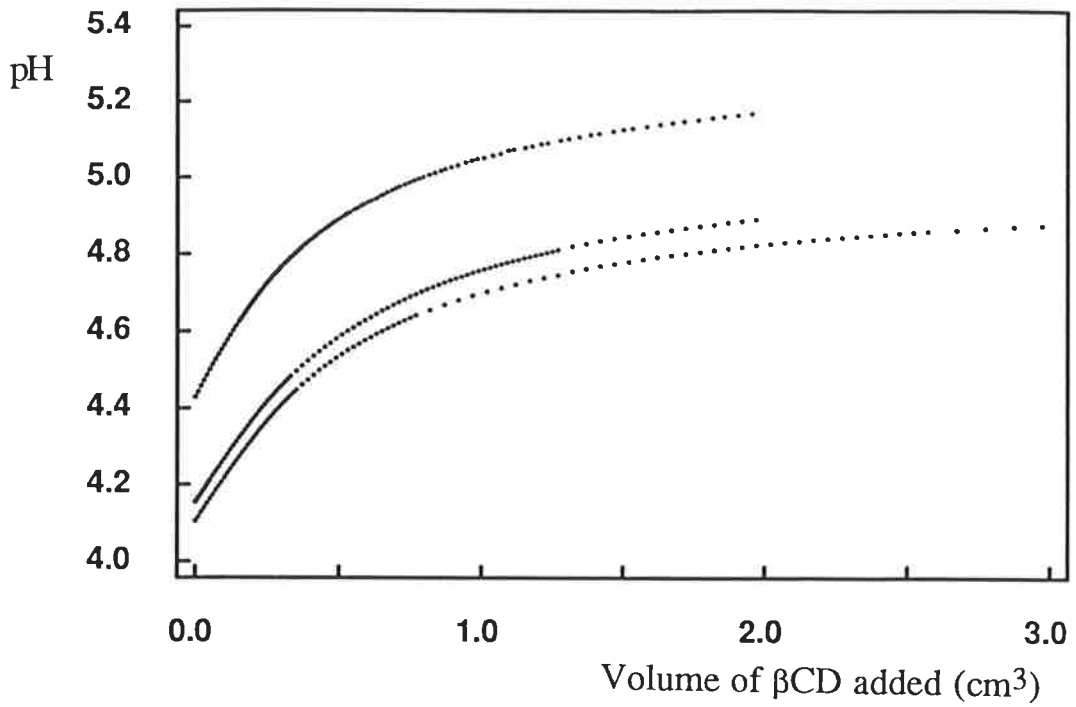

Figure A.1.3 Variation of the pH of three 2.0 cm^3 solutions of *R*-2-phenylpropanoic acid/phenylpropanoate (2.28 x 10^{-3} mol dm^{-3}) with volume of added βCD (1.51 x 10^{-2} mol dm^{-3}).

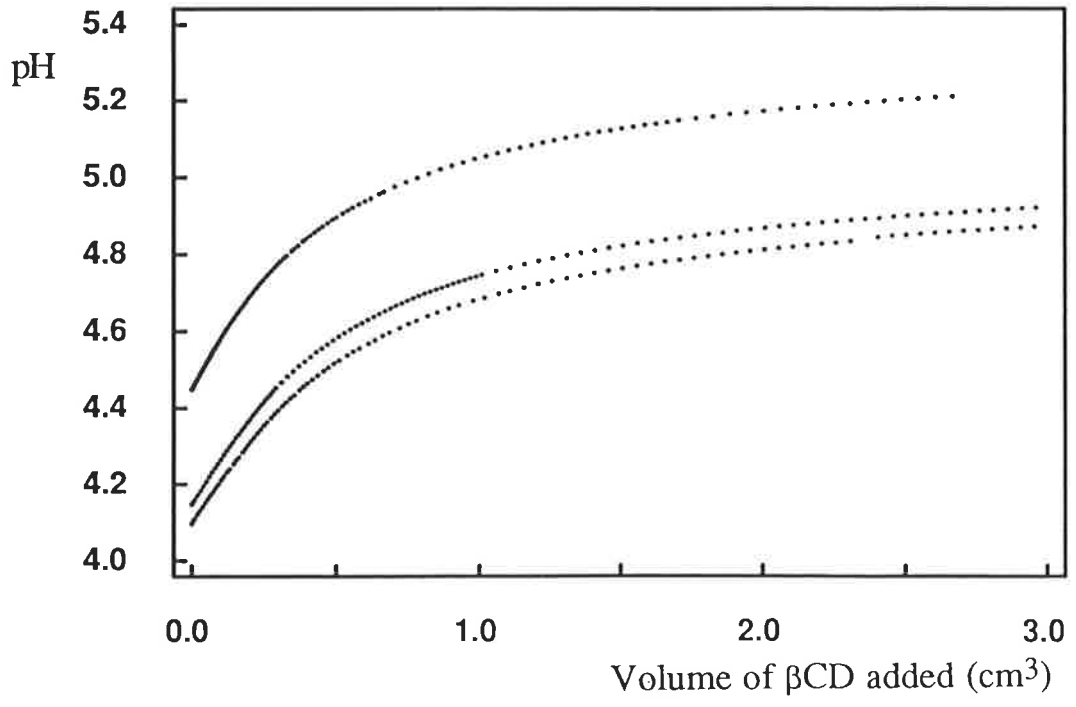

Figure A.1.4 Variation of the pH of three 2.0 cm^3 solutions of *S*-2-phenylpropanoic acid/phenylpropanoate (2.10 x 10^{-3} mol dm^{-3}) with volume of added βCD (1.51 x 10^{-2} mol dm^{-3}).

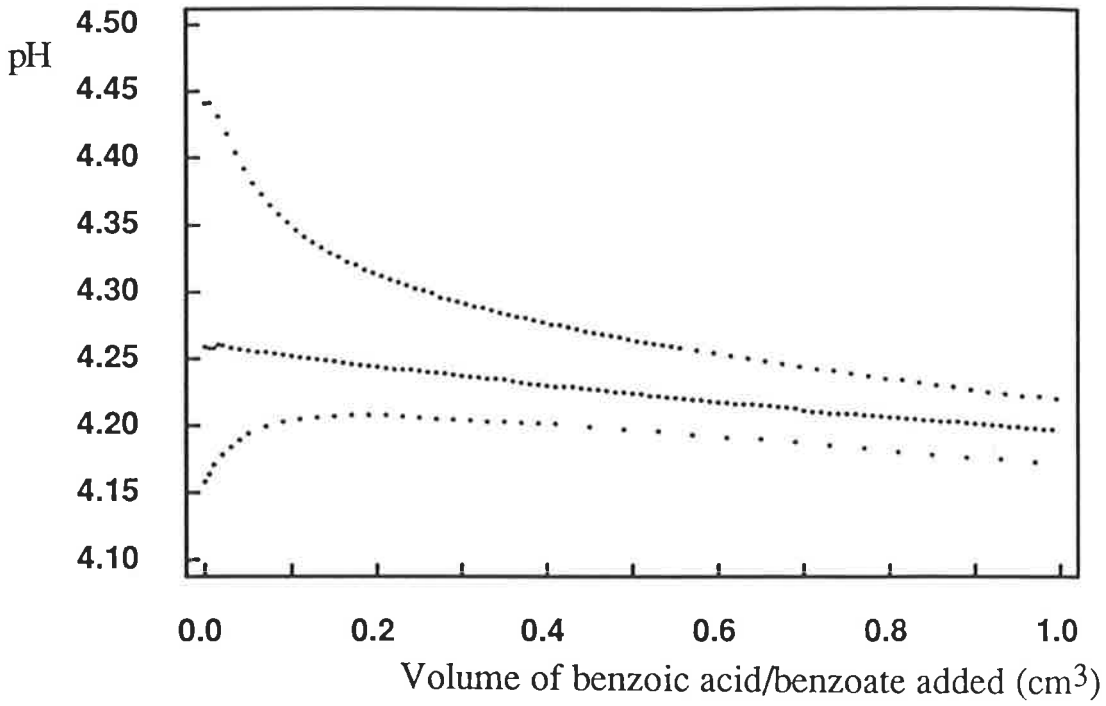

Figure A.1.5 Variation of the pH of three 2.0 cm^3 solutions of $\beta CDNH_3^+$ (4.55 x 10^{-3} mol dm^{-3}) with volume of added benzoic acid/benzoate (2.01 x 10^{-2} mol dm^{-3}).

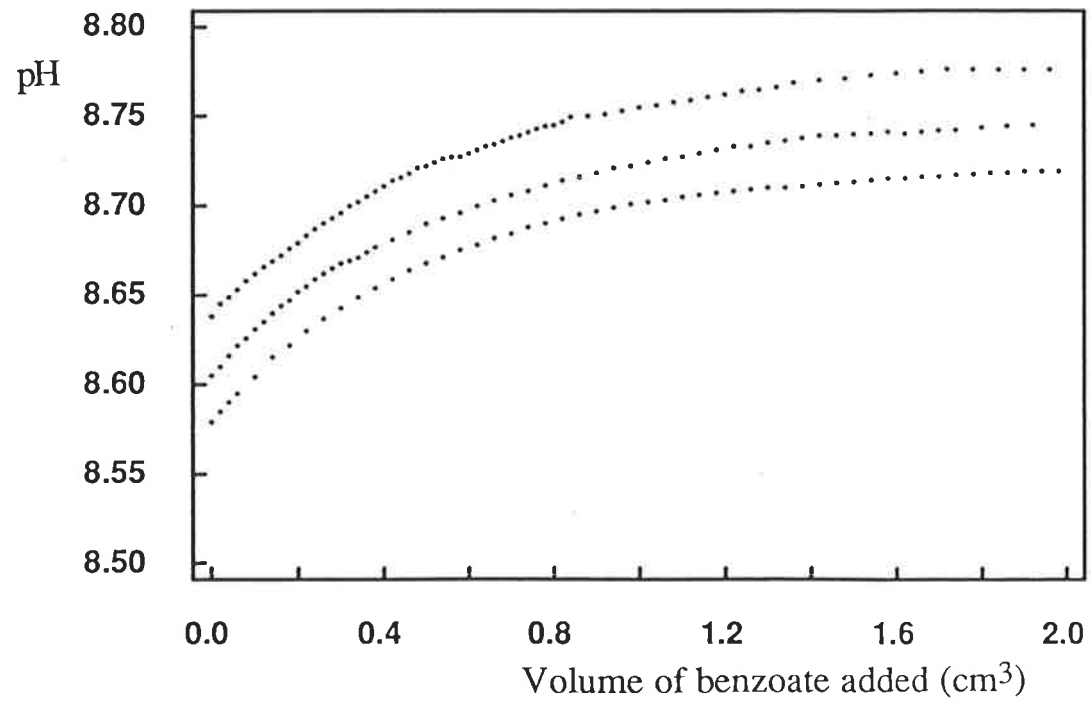

Figure A.1.6 Variation of the pH of three 2.0 cm^3 solutions of $\beta CDNH_3^+/\beta CDNH_2$ (1.26 x 10^{-3} mol dm^{-3}) with volume of added benzoate (2.03 x 10^{-2} mol dm^{-3}).

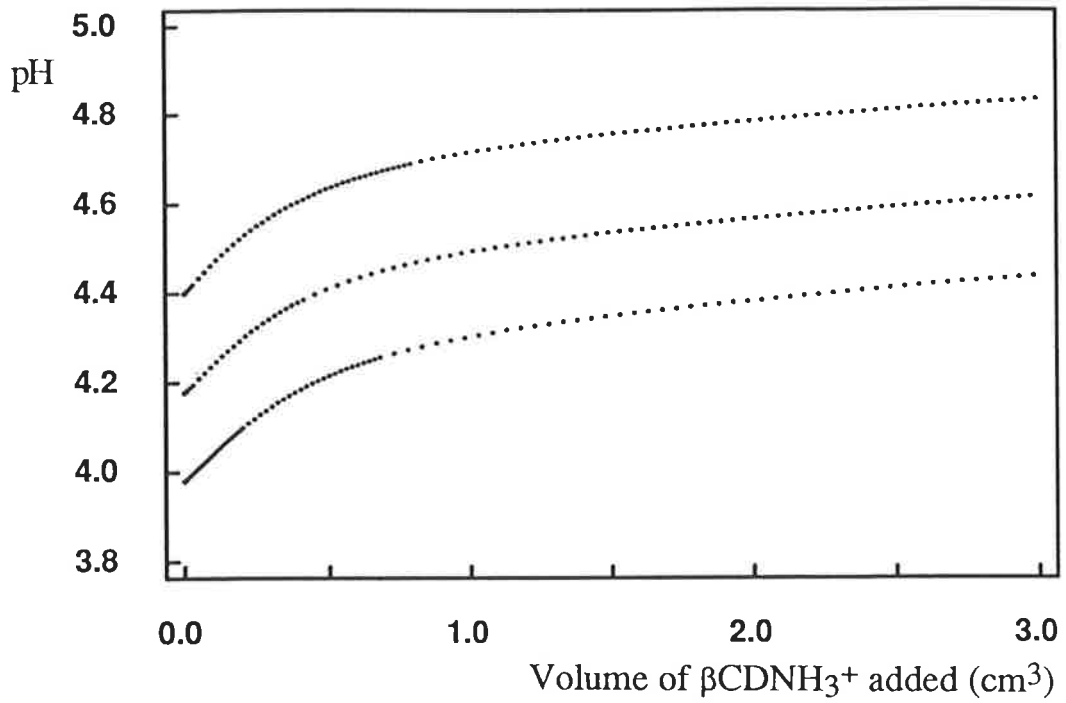

Figure A.1.7 Variation of the pH of three 2.0 cm^3 solutions of 4-methylbenzoic acid/4-methylbenzoate (2.14 x 10^{-3} mol dm^{-3}) with volume of added $\beta CDNH_3^+$ (1.58 x 10^{-2} mol dm^{-3}).

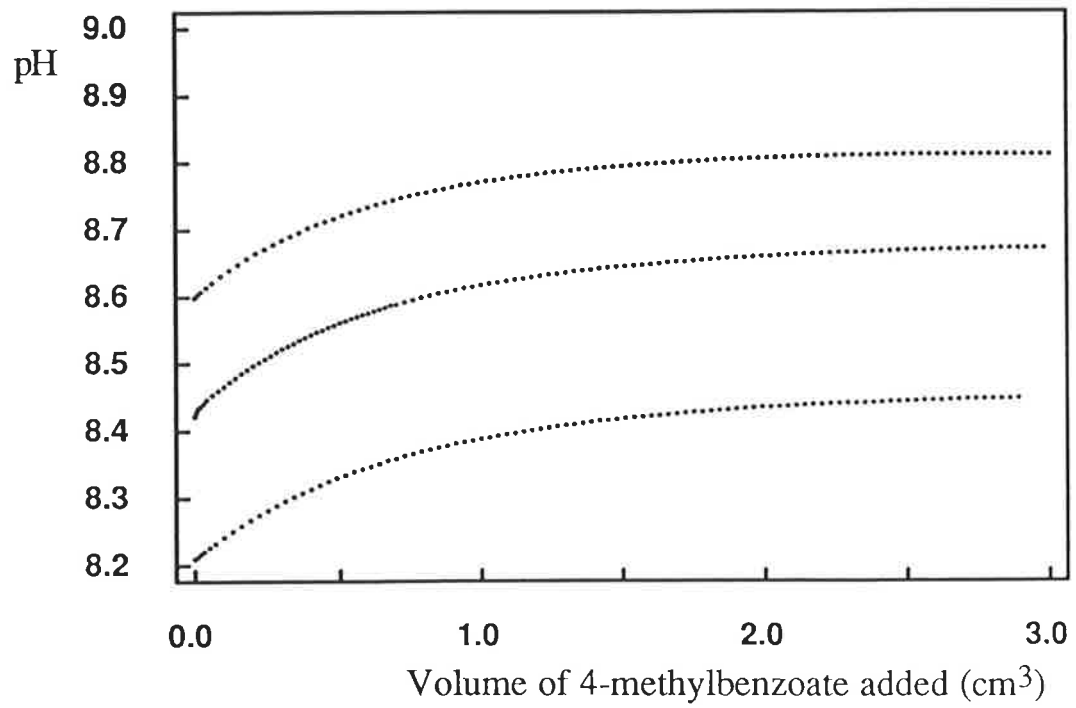

Figure A.1.8 Variation of the pH of three 2.0 cm^3 solutions of $\beta CDNH_3^+/\beta CDNH_2$ (2.21 x 10^{-3} mol dm^{-3}) with volume of added 4-methylbenzoate (1.11 x 10^{-2} mol dm^{-3}).

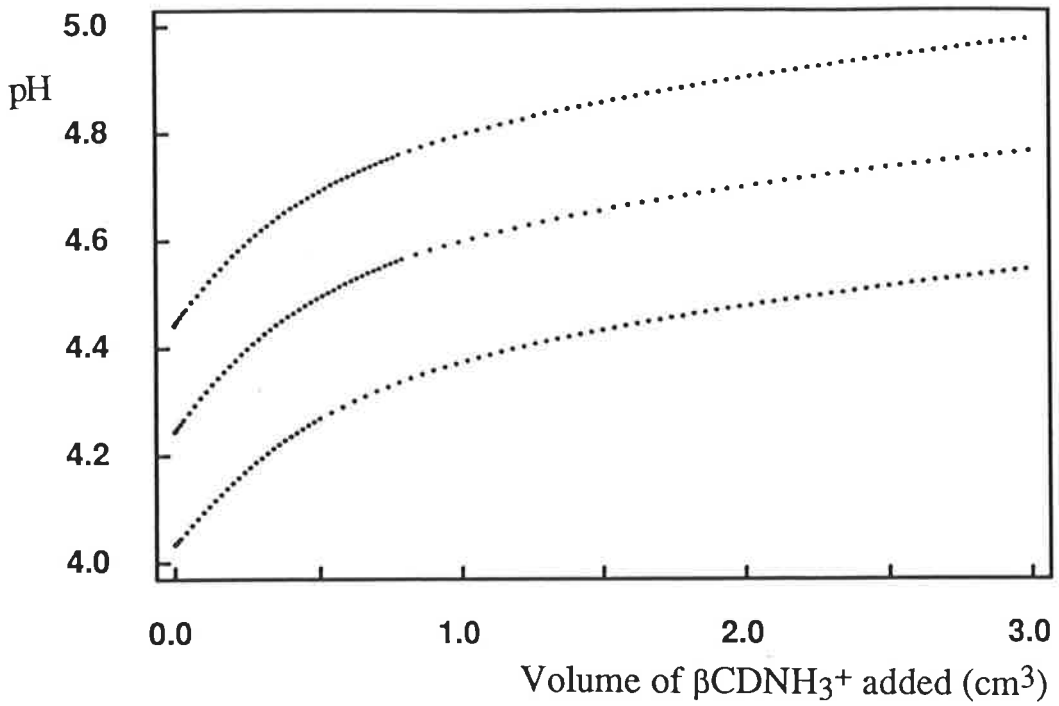

Figure A.1.9 Variation of the pH of three 2.0 cm^3 solutions of *R*-2-phenylpropanoic acid/phenylpropanoate (2.28 x 10^{-3} mol dm^{-3}) with volume of added $\beta CDNH_3^+$ (1.58 x 10^{-2} mol dm^{-3}).

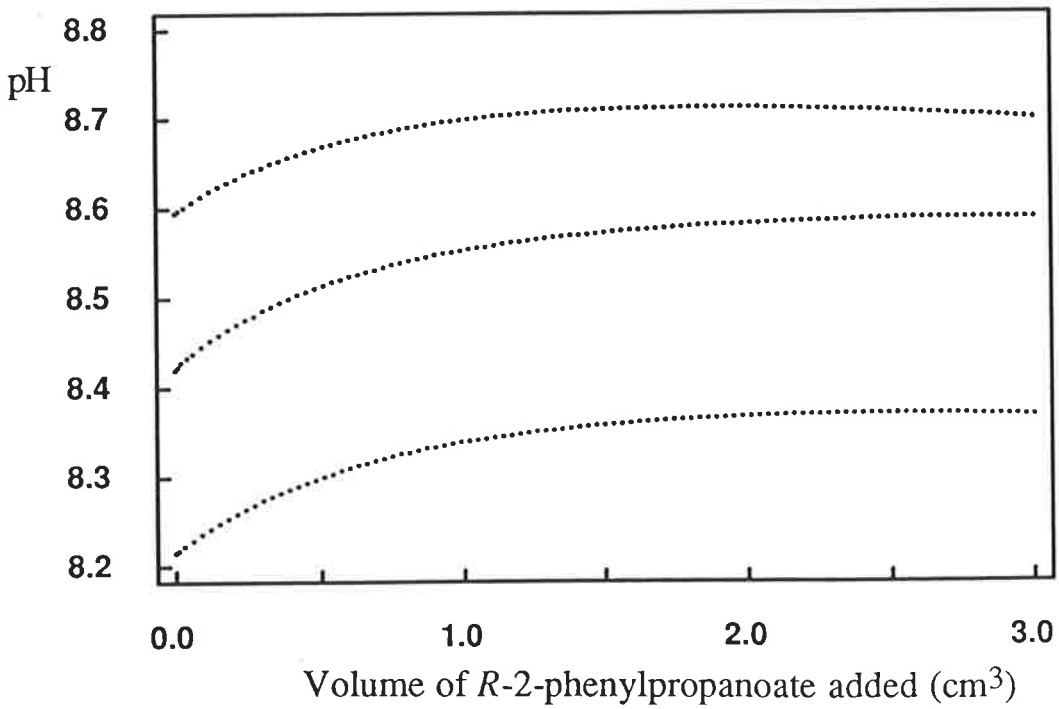

Figure A.1.10 Variation of the pH of three 2.0 cm^3 solutions of $\beta CDNH_3^+/\beta CDNH_2$ (2.21 x 10^{-3} mol dm^{-3}) with volume of added *R*-2-phenylpropanoate (1.40 x 10^{-2} mol dm^{-3}).

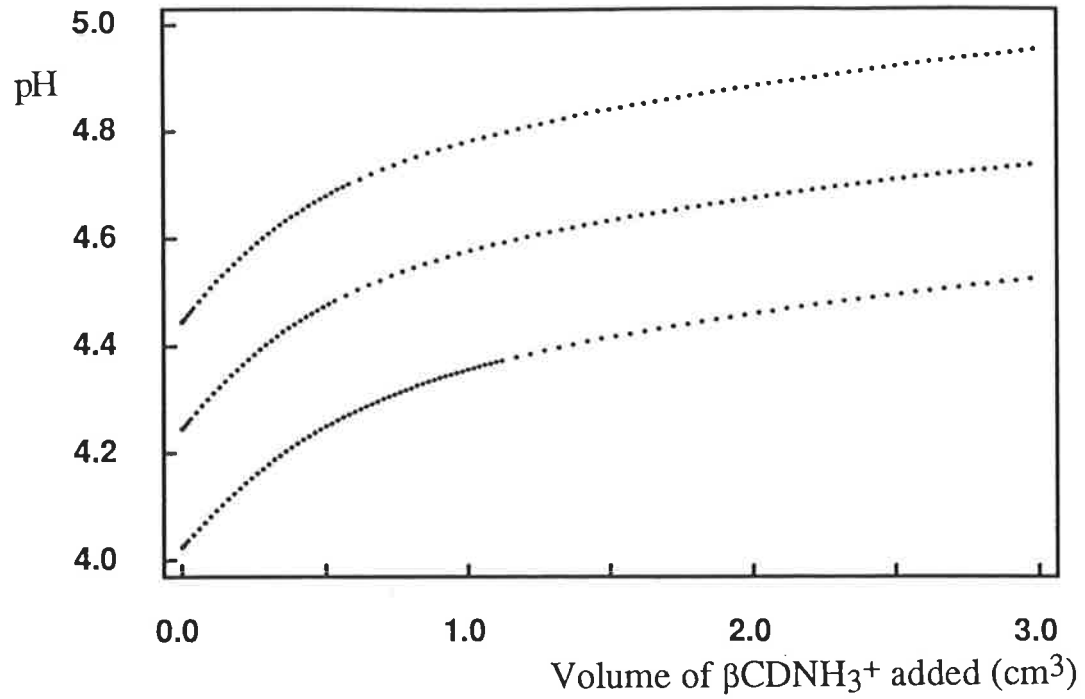

Figure A.1.11 Variation of the pH of three 2.0 cm^3 solutions of *S*-2-phenylpropanoic acid/phenylpropanoate (2.10 x 10^{-3} mol dm^{-3}) with volume of added $\beta CDNH_3^+$ (1.58 x 10^{-2} mol dm^{-3}).

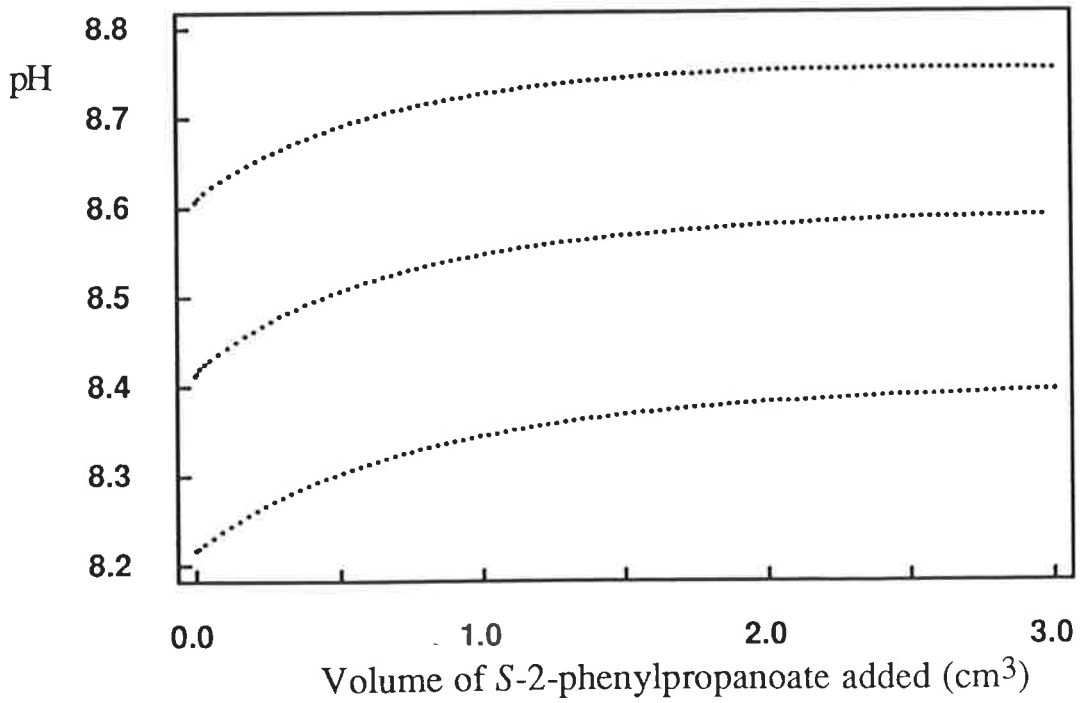

Figure A.1.12 Variation of the pH of three 2.0 cm^3 solutions of $\beta CDNH_3^+/\beta CDNH_2$ (2.21 x 10^{-3} mol dm^{-3}) with volume of added *S*-2-phenylpropanoate (1.50 x 10^{-2} mol dm^{-3}).

A.2 The Complexation of Amino Acids by Beta-Cyclodextrin, a Diamino Beta-Cyclodextrin Derivative and its Co^{2+}, Ni^{2+}, Cu^{2+}, and Zn^{2+} Complexes

Titration curves representative of the experimental data used to calculate the apparent stability constants for the metal, βCDpn and amino acid systems are shown in Figures A.2.1 - A.2.12. All titrations were performed in aqueous 0.010 mol dm^{-3} $HClO_4$ and 0.090 mol dm^{-3} $NaClO_4$ at 298.2 K, as outlined in Section 6.3. Each point on a graph represents an experimental pH reading. Points are omitted in the regions where precipitation occurs, and below an added NaOH volume of 1.2 cm^3, where only the excess acid is being titrated. At least three similar titrations were performed for each system, including titrations at some different cyclodextrin and amino acid to metal ratios, but only one representative titration is shown for each system. For systems where there is a possibility of chiral discrimination, a titration curve for only one of the enantiomers is shown.

In most systems, interesting comparisons may be made by plotting the titration curve of a system relative to a titration curve for either one or two of the components alone. However, it is not possible to make such graphical comparisons for all systems studied. In the βCD- and βCDpn-amino acid systems, it is not meaningful to compare the titration curves to either the amino acid or βCDpn pK_a curves, due to a difference in the starting concentrations in these systems. For the interaction of *RS*-phenylalanine with Co^{2+} and Ni^{2+}, and *RS*-phenylalanine with βCDpn and Co^{2+} and Ni^{2+}, it is not meaningful to compare the curves to *RS*-phenylalanine in the first case or *RS*-phenylalanine-βCDpn in the second case, due to a small difference in the excess acid concentrations in these systems.

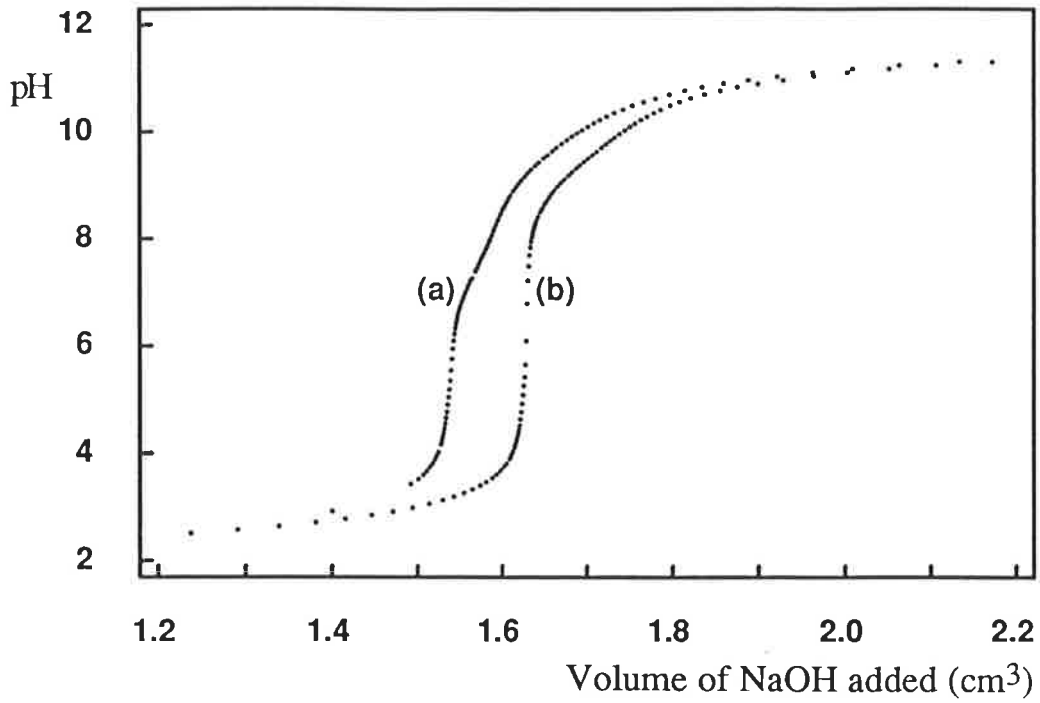

Figure A.2.1 Titration profiles of: (a) $\beta CDpnH_2^{2+}$ (5.02×10^{-4} mol dm^{-3}) and *R*-tryptophan (5.08×10^{-4} mol dm^{-3}) and (b) βCD (9.19×10^{-4} mol dm^{-3}) and *R*-tryptophan (9.14×10^{-4} mol dm^{-3}), against 0.101 mol dm^{-3} NaOH.

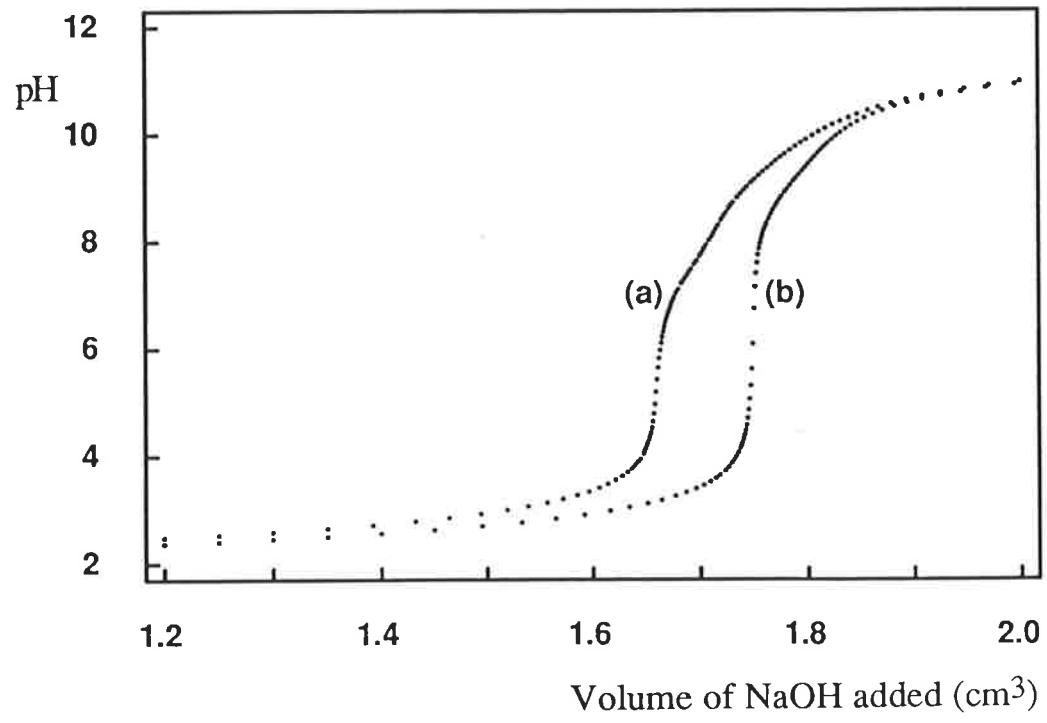

Figure A.2.2 Titration profiles of: (a) $\beta CDpnH_2^{2+}$ (5.01×10^{-4} mol dm^{-3}) and *R*-phenylalanine (5.08×10^{-4} mol dm^{-3}) and (b) βCD (5.08×10^{-4} mol dm^{-3}) and *R*-phenylalanine (4.98×10^{-4} mol dm^{-3}), against 0.0962 mol dm^{-3} NaOH.

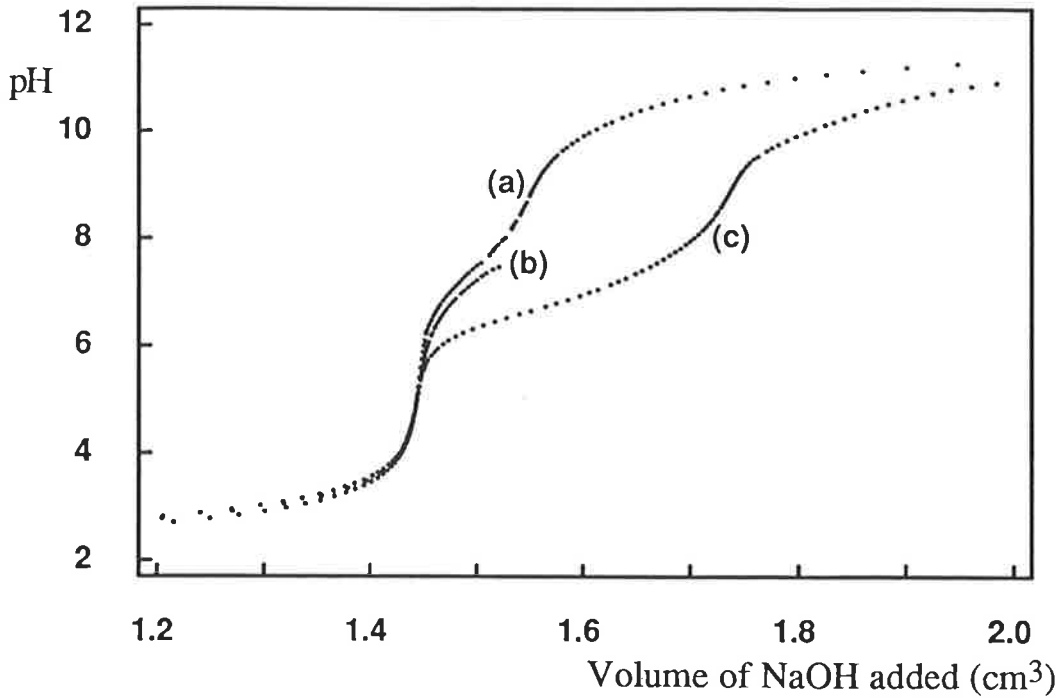

Figure A.2.3 Titration profiles of: (a) $\beta CDpnH_2^{2+}$ (1.01×10^{-3} mol dm^{-3}); (b) $\beta CDpnH_2^{2+}$ (9.99×10^{-4} mol dm^{-3}) and Zn^{2+} (9.41×10^{-4} mol dm^{-3}) and (c) $\beta CDpnH_2^{2+}$ (1.00×10^{-3} mol dm^{-3}) and Cu^{2+} (9.80×10^{-4} mol dm^{-3}), against 0.101 mol dm^{-3} NaOH.

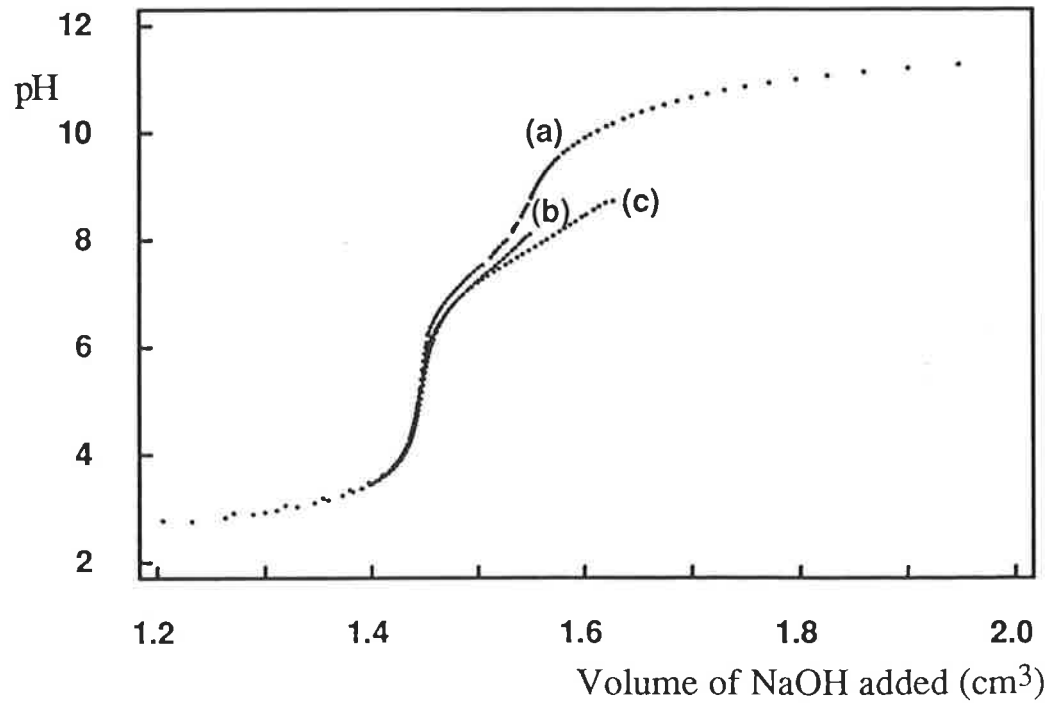

Figure A.2.4 Titration profiles of: (a) $\beta CDpnH_2^{2+}$ (1.01×10^{-3} mol dm^{-3}); (b) $\beta CDpnH_2^{2+}$ (1.01×10^{-3} mol dm^{-3}) and Co^{2+} (9.45×10^{-4} mol dm^{-3}) and (c) $\beta CDpnH_2^{2+}$ (9.99×10^{-4} mol dm^{-3}) and Ni^{2+} (9.45×10^{-4} mol dm^{-3}), against 0.101 mol dm^{-3} NaOH.

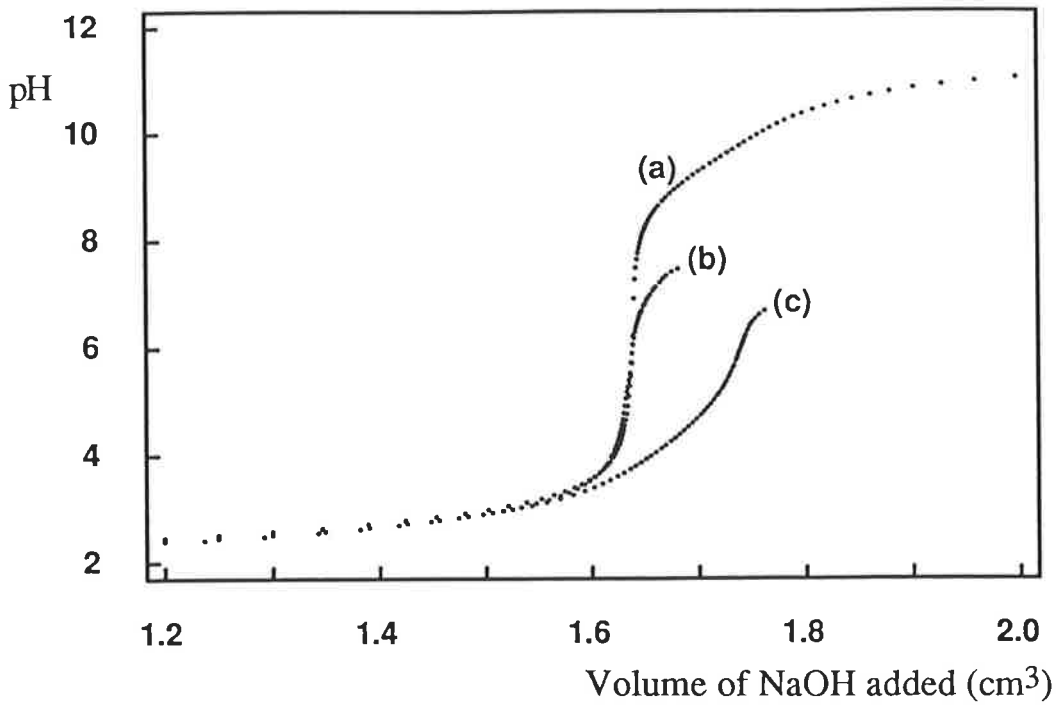

Figure A.2.5 Titration profiles of: (a) *S*-tryptophan (1.01×10^{-3} mol dm^{-3}); (b) *R*-tryptophan (1.00×10^{-3} mol dm^{-3}) and Zn^{2+} (9.42×10^{-4} mol dm^{-3}) and (c) *S*-tryptophan (1.00×10^{-3} mol dm^{-3}) and Cu^{2+} (9.47×10^{-4} mol dm^{-3}), against 0.101 mol dm^{-3} NaOH.

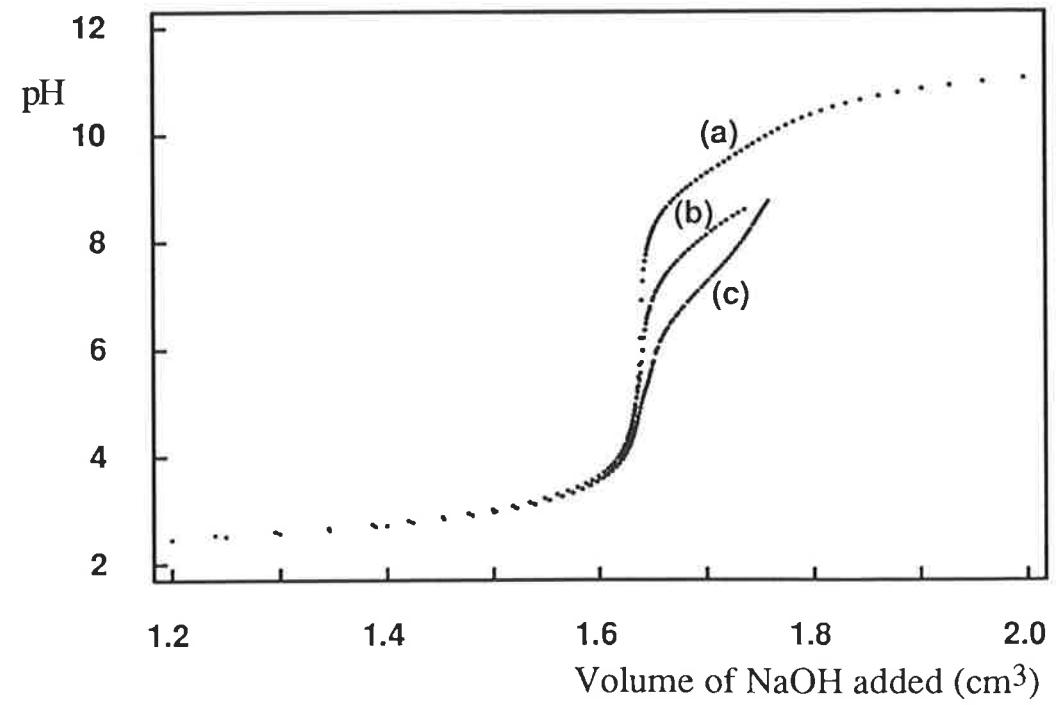

Figure A.2.6 Titration profiles of: (a) *S*-tryptophan (1.01×10^{-3} mol dm^{-3}); (b) *S*-tryptophan (1.00×10^{-3} mol dm^{-3}) and Co^{2+} (9.46×10^{-4} mol dm^{-3}) and (c) *R*-tryptophan (1.00×10^{-3} mol dm^{-3}) and Ni^{2+} (9.38×10^{-4} mol dm^{-3}), against 0.101 mol dm^{-3} NaOH.

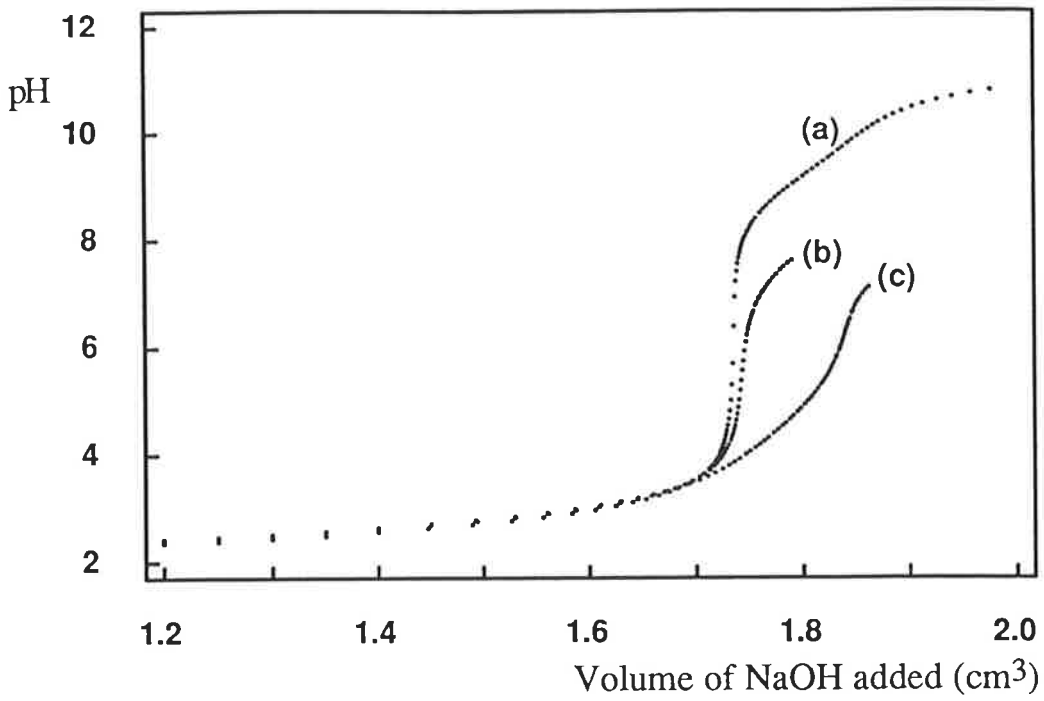

Figure A.2.7 Titration profiles of: (a) *S*-phenylalanine (1.00×10^{-3} mol dm^{-3}); (b) *R*-phenylalanine (9.93×10^{-4} mol dm^{-3}) and Zn^{2+} (9.41×10^{-4} mol dm^{-3}) and (c) *R*-phenylalanine (9.93×10^{-4} mol dm^{-3}) and Cu^{2+} (9.58×10^{-4} mol dm^{-3}), against 0.0962 mol dm^{-3} NaOH.

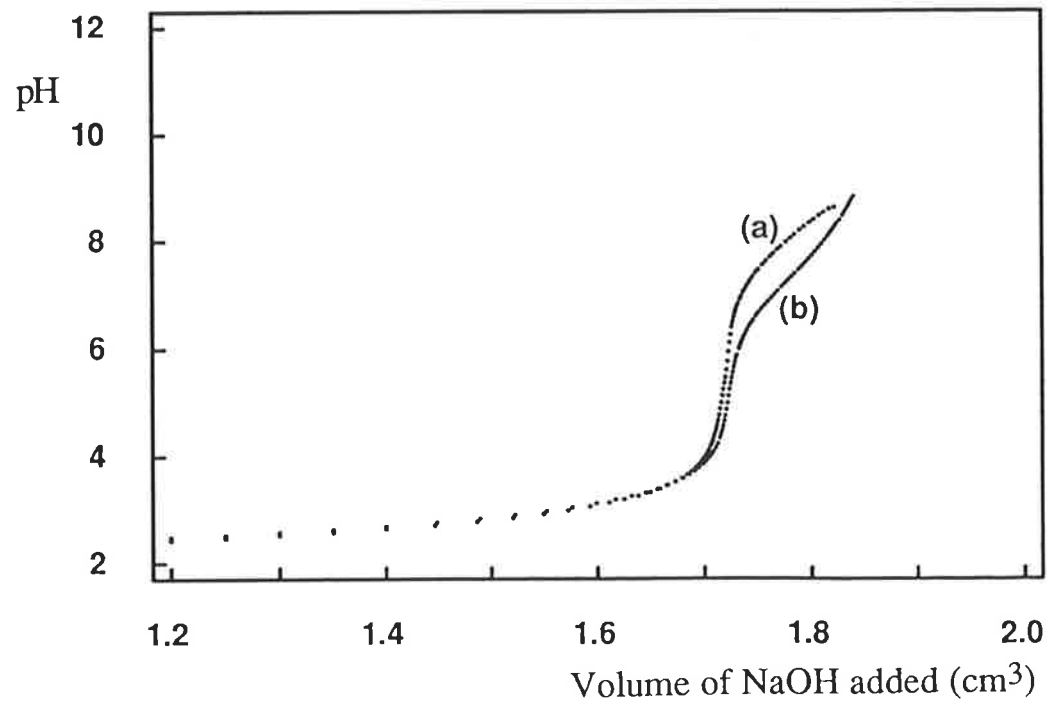

Figure A.2.8 Titration profiles of: (a) *R*-phenylalanine (9.93×10^{-4} mol dm^{-3}) and Co^{2+} (9.48×10^{-4} mol dm^{-3}) and (b) *S*-phenylalanine (9.96×10^{-4} mol dm^{-3}) and Ni^{2+} (9.25×10^{-4} mol dm^{-3}), against 0.0962 mol dm^{-3} NaOH.

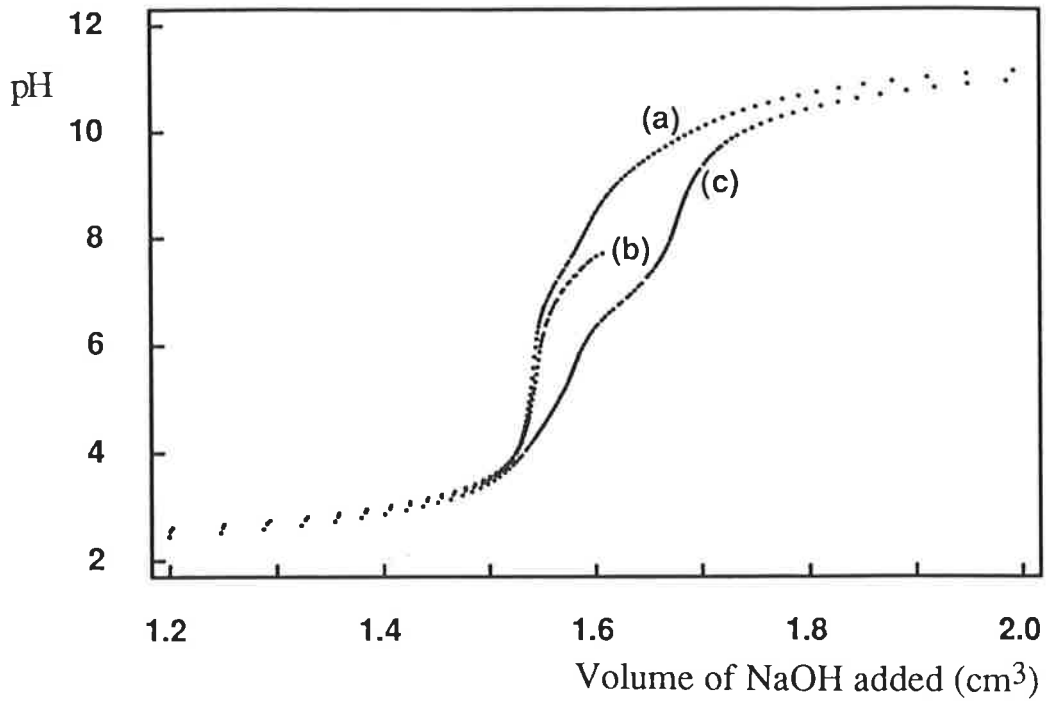

Figure A.2.9 Titration profiles of: (a) $\beta CDpnH_2^{2+}$ (5.04×10^{-4} mol dm^{-3}) and *S*-tryptophan (5.08×10^{-4} mol dm^{-3}); (b) $\beta CDpnH_2^{2+}$ (5.02×10^{-4} mol dm^{-3}), *S*-tryptophan (5.05×10^{-4} mol dm^{-3}) and Zn^{2+} (4.40×10^{-4} mol dm^{-3}) and (c) $\beta CDpnH_2^{2+}$ (5.02×10^{-4} mol dm^{-3}), *S*-tryptophan (5.07×10^{-4} mol dm^{-3}) and Cu^{2+} (4.60×10^{-4} mol dm^{-3}), against 0.101 mol dm^{-3} NaOH.

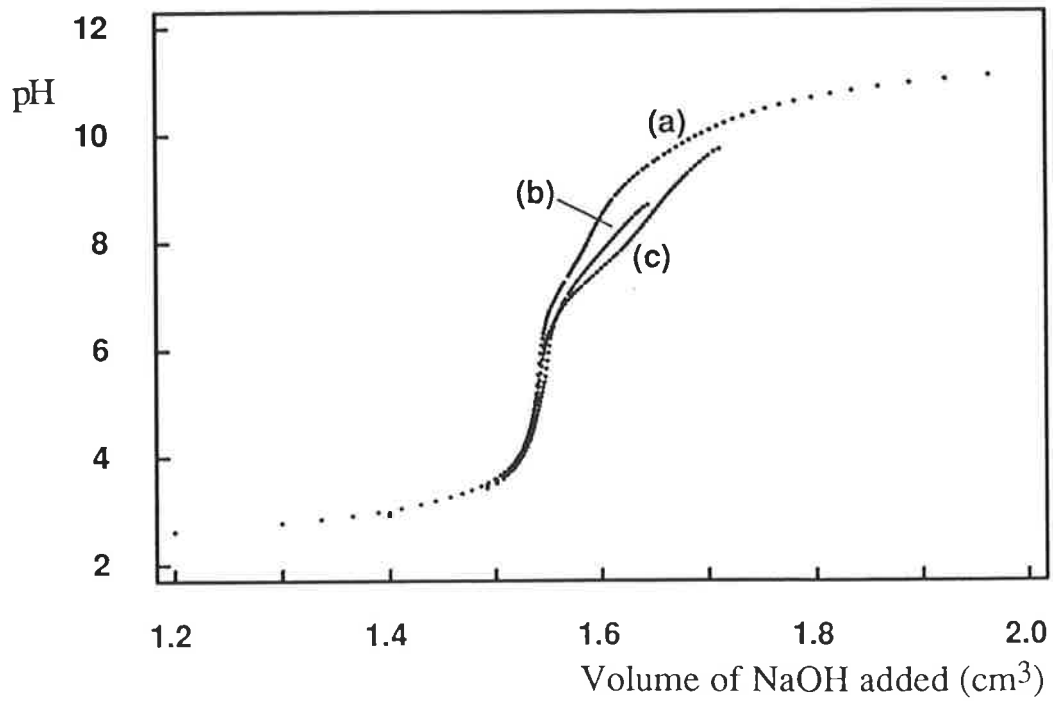

Figure A.2.10 Titration profiles of: (a) $\beta CDpnH_2^{2+}$ (5.02×10^{-4} mol dm^{-3}) and *R*-tryptophan (5.08×10^{-4} mol dm^{-3}); (b) $\beta CDpnH_2^{2+}$ (5.08×10^{-4} mol dm^{-3}), *R*-tryptophan (5.03×10^{-4} mol dm^{-3}) and Co^{2+} (4.44×10^{-4} mol dm^{-3}) and (c) $\beta CDpnH_2^{2+}$ (5.08×10^{-4} mol dm^{-3}), *R*-tryptophan (5.04×10^{-4} mol dm^{-3}) and Ni^{2+} (4.47×10^{-4} mol dm^{-3}), against 0.101 mol dm^{-3} NaOH.

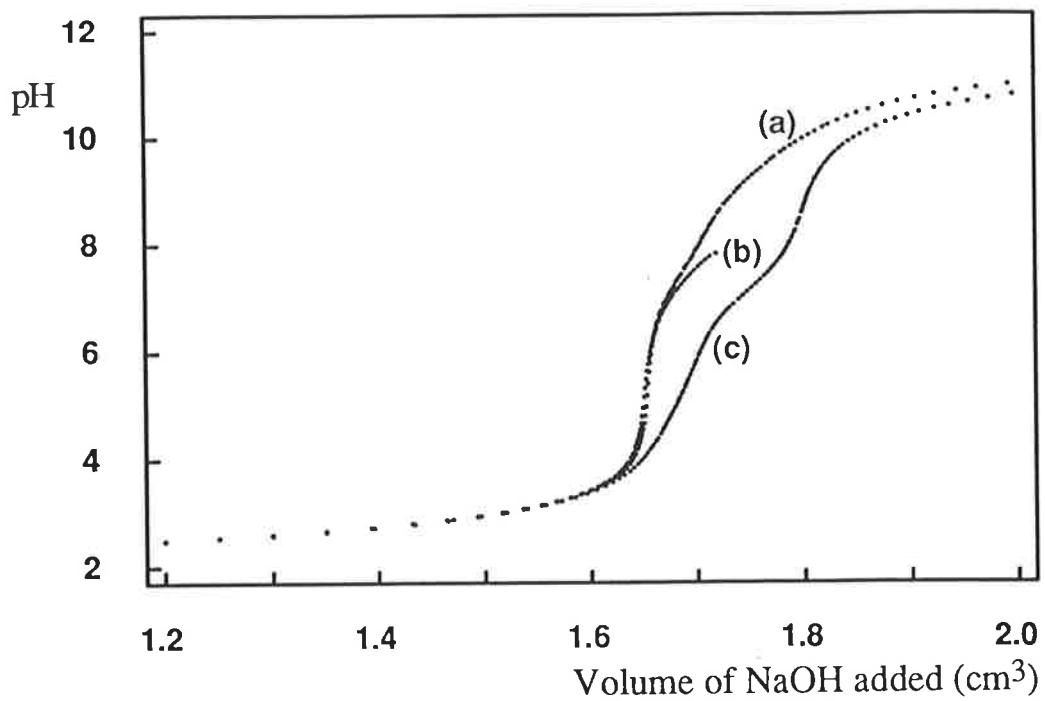

Figure A.2.11 Titration profiles of: (a) $\beta CDpnH_2^{2+}$ (5.01 x 10^{-4} mol dm^{-3}) and *S*-phenylalanine (5.02 x 10^{-4} mol dm^{-3}); (b) $\beta CDpnH_2^{2+}$ (4.98 x 10^{-4} mol dm^{-3}), *S*-phenylalanine (5.00 x 10^{-4} mol dm^{-3}) and Zn^{2+} (4.27 x 10^{-4} mol dm^{-3}) and (c) $\beta CDpnH_2^{2+}$ (4.99 x 10^{-4} mol dm^{-3}), *S*-phenylalanine (4.99 x 10^{-4} mol dm^{-3}) and Cu^{2+} (4.48 x 10^{-4} mol dm^{-3}), against 0.0962 mol dm^{-3} NaOH.

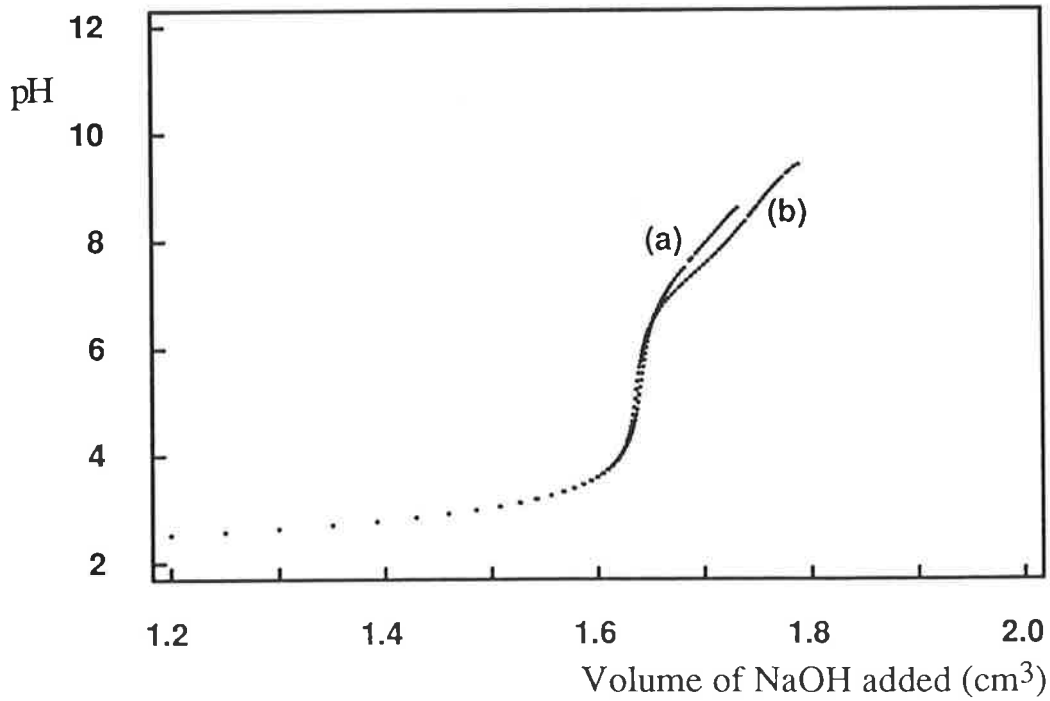

Figure A.2.12 Titration profiles of: (a) $\beta CDpnH_2^{2+}$ (4.99 x 10^{-4} mol dm^{-3}), *R*-phenylalanine (5.03 x 10^{-4} mol dm^{-3}) and Co^{2+} (4.46 x 10^{-4} mol dm^{-3}) and (b) $\beta CDpnH_2^{2+}$ (5.02 x 10^{-4} mol dm^{-3}), *R*-phenylalanine (4.95 x 10^{-4} mol dm^{-3}) and Ni^{2+} (4.42 x 10^{-4} mol dm^{-3}), against 0.0962 mol dm^{-3} NaOH.

A.3 The Complexation of Fluorinated Amino Acids by Alpha-Cyclodextrin, Beta-Cyclodextrin, Gamma-Cyclodextrin and Derivatives

The experimental concentrations and 1D ^{19}F NMR chemical shifts for the complexation of the fluorinated amino acids by αCD, βCD, γCD, PMαCD, PMβCD, $\alpha CDNH_3^+$, $\alpha CDNH_2$, $\beta CDNH_3^+$ and $\beta CDNH_2$ are shown in Tables A.3.1 - A.3.6. All 1D ^{19}F NMR spectra were recorded at $I = 0.10$ (various buffers) and 295.5 K, as outlined in Section 6.4. The symbols δ_{OR} and δ_{OS} that are used in the Tables are defined in Section 4.1. The symbol δ_{ORS} represents either the ^{19}F chemical shift of the amino acid (equivalent to δ_F in Section 4.1), or the ^{19}F chemical shift of an amino acid-cyclodextrin solution in a system in which no significant chiral discrimination is observed. In the latter systems, footnotes indicate whether any resolution of the cyclodextrin complexed *R* and *S* enantiomers is observed.

Table A.3.1 Concentration and ^{19}F NMR chemical shift data for the guest GH_2^+ with different cyclodextrins, CD, at pH 1.3 or 1.0.

CD	[CD] (mol dm^{-3}) x10^3	[GH_2^+] (mol dm^{-3}) x10^3	δ_{ORS} (ppm)	δ_{OR} (ppm)	δ_{OS} (ppm)
αCD [a]	0	0.998	-35.752		
	9.91	0.987		-35.852	-35.860
	19.8	0.980		-35.932	-35.945
	24.6	0.978		-35.969	-35.992
	30.0	0.986		-36.003	-36.027
	34.5	0.971		-36.027	-36.052
	39.0	0.956		-36.061	-36.090
	45.1	0.990		-36.101	-36.134
	49.5	0.975		-36.124	-36.158
	52.7	0.945		-36.139	-36.174
	59.7	0.979		-36.180	-36.218
	63.7	0.968		-36.197	-36.234
	68.6	0.957		-36.214	-36.253
	72.7	0.959		-36.233	-36.273
	79.5	0.984		-36.253	-36.294
βCD [a]	0	1.19	-35.752		
	15.7	1.20	-35.774		
γCD [b]	0	1.01	-35.690		
	106	1.07	-35.509		
PMαCD [b]	0	1.09	-35.708		
	0.906	1.09		-35.825	-35.834
	2.13	1.09		-35.953	-35.974
	2.56	1.09		-35.973	-35.996
	3.06	1.09		-36.038	-36.066
	3.86	1.09		-36.105	-36.138
	4.53	1.09		-36.166	-36.204
	5.19	1.09		-36.195	-36.235
	5.90	1.09		-36.263	-36.306
	6.50	1.09		-36.330	-36.377
	7.15	1.08		-36.360	-36.406
	7.95	1.08		-36.418	-36.467
	8.60	1.08		-36.458	-36.509
	9.10	1.08		-36.461	-36.513
	10.4	1.08		-36.554	-36.606
PMβCD [b]	0	1.00	-35.690		
	9.97	0.999	-35.688		

Table A.3.1, continued

CD	[CD] (mol dm^{-3}) x10^3	[GH_2^+] (mol dm^{-3}) x10^3	δ_{ORS} (ppm)	δ_{OR} (ppm)	δ_{OS} (ppm)
$\alpha CDNH_3^+$ [a,c]	0	1.05	-35.758		
	14.4	1.06	-35.895		
$\beta CDNH_3^+$ [a,d]	0	1.01	-35.690		
	10.0	1.02	-35.718		

[a]pH 1.3, HCl/KCl buffer.

[b]pH 1.0, HCl.

[c]At an $\alpha CDNH_3^+$ concentration of ≈77 x 10^{-3} mol dm^{-3} the observed *R* and *S* peak separation is 0.031 ppm ($I \approx 1$).

[d]At a $\beta CDNH_3^+$ concentration of ≈31 x 10^{-3} mol dm^{-3} no peak separation is observed ($I \approx 1$).

Table A.3.2 Concentration and ^{19}F NMR chemical shift data for the guest G^- with different cyclodextrins, CD, at pH 10.8 (NaOH/glycine buffer).

CD	[CD] (mol dm^{-3}) x10^3	[G$^-$] (mol dm^{-3}) x10^3	δ_{ORS} (ppm)	δ_{OR} (ppm)	δ_{OS} (ppm)
αCD	0	0.977	-40.123		
	9.98	0.979		-40.315	-40.307
	14.6	0.958		-40.377	-40.364
	20.2	0.999		-40.452	-40.433
	24.5	0.978		-40.506	-40.484
	29.5	0.970		-40.550	-40.524
	34.4	0.983		-40.592	-40.563
	39.3	0.976		-40.619	-40.587
	44.7	0.981		-40.659	-40.625
	49.6	0.983		-40.689	-40.651
	55.3	0.991		-40.710	-40.671
	58.8	0.972		-40.736	-40.695
	64.6	0.986		-40.760	-40.716
	68.5	0.977		-40.775	-40.730
	73.2	0.972		-40.792	-40.746
βCD	0	1.02	-40.151		
	0.976	1.03		-40.161	-40.161
	2.95	1.03		-40.197	-40.197
	5.27	1.03		-40.232	-40.232
	7.34	1.03		-40.265	-40.256
	9.30	1.03		-40.294	-40.284
	10.3	1.03		-40.303	-40.292
	11.2	1.03		-40.316	-40.304
	12.6	1.03		-40.334	-40.316
	12.8	1.03		-40.337	-40.322
	13.3	1.03		-40.348	-40.332
	13.8	1.03		-40.348	-40.332
	14.3	1.03		-40.354	-40.335
	15.1	1.03		-40.367	-40.348
	15.5	1.03		-40.370	-40.350
γCD	0	1.02	-40.154		
	10.3	1.03	-40.114		
	15.5	1.03	-40.088		
	20.3	1.03	-40.070		
	25.7	1.04	-40.054		
	31.0	1.04	-40.034		
	36.4	1.04	-40.020		
	41.6	1.04	-39.999		
	46.9	1.05	-39.997		
	52.3	1.05	-39.978		
	57.5	1.05	-39.970		
	63.0	1.06	-39.949		
	68.6	1.06	-39.942		
	74.3	1.06	-39.927		

Table A.3.2, continued

CD	[CD] (mol dm^{-3}) x10^3	[G^-] (mol dm^{-3}) x10^3	δ_{ORS} (ppm)	δ_{OR} (ppm)	δ_{OS} (ppm)
PMαCD	0	1.04	-40.207		
	0.966	1.04		-40.342	-40.352
	2.26	1.04		-40.466	-40.488
	3.06	1.04		-40.545	-40.573
	4.09	1.04		-40.655	-40.690
	4.91	1.04		-40.740	-40.780
	5.57	1.04		-40.797	-40.839
	5.97	1.04		-40.821	-40.864
	7.11	1.04		-40.896	-40.943
	7.58	1.04		-40.943	-40.992
	7.93	1.04		-40.965	-41.014
	8.24	1.04		-40.949	-40.998
	8.89	1.04		-41.033	-41.085
	9.53	1.04		-41.070	-41.123
	10.0	1.04		-41.109	-41.161
PMβCD	0	1.01	-40.154		
	10.6	0.986	-40.128		
$\alpha CDNH_2$ [a]	0	1.01	-40.111		
	1.03	1.03	-40.149		
	1.88	1.02	-40.171		
	2.98	1.03	-40.191		
	4.01	1.02	-40.217		
	5.03	1.02	-40.243		
	5.95	1.02	-40.250		
	6.38	1.01	-40.264		
	6.98	1.02	-40.271		
	7.53	1.03	-40.290		
	7.98	1.01	-40.288		
	8.60	1.02	-40.302		
	8.69	0.995	-40.303		
	9.47	1.02	-40.316		
	10.0	1.02	-40.331		
$\beta CDNH_2$ [b]	0	1.03	-40.149		
	10.1	1.03	-40.267		

[a]At an $\alpha CDNH_2$ concentration of ≈33 x 10^{-3} mol dm^{-3} the observed *R* and *S* peak separation is 0.020 ppm ($I \approx 1$).

[b]At a $\beta CDNH_2$ concentration of ≈32 x 10^{-3} mol dm^{-3} the observed *R* and *S* peak separation is 0.029 ppm ($I \approx 1$).

Table A.3.3 Concentration and ^{19}F NMR chemical shift data for the guest A-GH with different cyclodextrins, CD, at pH 1.3 or 1.0.

CD	[CD] (mol dm^{-3}) x10^3	[A-GH] (mol dm^{-3}) x10^3	δ_{ORS} (ppm)	δ_{OR} (ppm)	δ_{OS} (ppm)
αCD [a]	0	1.00	-37.779		
	10.0	1.01		-37.964	-37.977
	15.8	1.01		-38.046	-38.065
	20.5	1.01		-38.113	-38.137
	25.9	1.01		-38.176	-38.205
	31.0	1.01		-38.227	-38.260
	36.8	1.02		-38.285	-38.322
	41.0	1.02		-38.318	-38.356
	47.8	1.02		-38.372	-38.415
	51.8	1.02		-38.401	-38.446
	58.2	1.02		-38.445	-38.492
	62.4	1.03		-38.467	-38.515
	69.0	1.03		-38.507	-38.557
	74.1	1.03		-38.532	-38.583
	79.4	1.03		-38.558	-38.612
βCD [a]	0	1.04	-37.741		
	1.34	1.04		-37.788	-37.788
	2.51	1.04		-37.823	-37.823
	4.04	1.04		-37.866	-37.866
	5.21	1.04		-37.892	-37.892
	6.10	1.04		-37.918	-37.927
	7.24	1.04		-37.944	-37.953
	8.25	1.04		-37.970	-37.983
	9.15	1.04		-37.987	-37.996
	10.3	1.04		-38.009	-38.022
	11.4	1.04		-38.031	-38.044
	12.3	1.04		-38.044	-38.056
	13.4	1.04		-38.069	-38.082
	14.4	1.05		-38.082	-38.095
	15.5	1.04		-38.100	-38.117
γCD [b]	0	1.04	-37.764		
	5.18	1.05	-37.723		
	10.2	1.05	-37.688		
	15.4	1.05	-37.655		
	20.3	1.06	-37.624		
	25.6	1.06	-37.594		
	31.1	1.06	-37.566		
	36.0	1.06	-37.542		
	41.5	1.07	-37.515		
	51.8	1.07	-37.471		
	62.8	1.08	-37.428		
	73.6	1.08	-37.384		
	84.6	1.09	-37.353		
	95.6	1.09	-37.320		
	108	1.10	-37.286		

Table A.3.3, continued

CD	[CD] (mol dm^{-3}) x10^3	[A-GH] (mol dm^{-3}) x10^3	δ_{ORS} (ppm)	δ_{OR} (ppm)	δ_{OS} (ppm)
PMαCD [b]	0	1.07	-37.733		
	0.827	1.06		-38.399	-38.332
	1.99	1.06		-39.014	-38.886
	2.49	1.06		-39.241	-39.096
	3.05	1.07		-39.487	-39.325
	4.13	1.07		-39.693	-39.515
	5.18	1.07		-39.851	-39.663
	5.70	1.07		-39.948	-39.753
	6.12	1.07		-39.990	-39.791
	7.18	1.07		-40.099	-39.893
	7.67	1.07		-40.148	-39.942
	8.04	1.07		-40.179	-39.966
	9.05	1.07		-40.241	-40.030
	9.59	1.07		-40.277	-40.062
	10.5	1.07		-40.325	-40.107
PMβCD [b]	0	1.08	-37.742		
	10.2	1.08	-37.823		
αCDNH$_3^+$ [b]	0	1.09	-37.784		
	14.5[c]	1.10	-37.953		
βCDNH$_3^+$ [b,d]	0	1.04	-37.727		
	14.2	1.05	-37.947		

[a]pH 1.3, HCl/KCl buffer.

[b]pH 1.0, HCl.

[c]At an αCDNH$_3^+$ concentration of 14.5 x 10^{-3} mol dm^{-3} the observed *R* and *S* peak separation is 0.013 ppm.

[d]At a βCDNH$_3^+$ concentration of ≈30 x 10^{-3} mol dm^{-3} no peak separation is observed ($I \approx 1$).

Table A.3.4 Concentration and ^{19}F NMR chemical shift data for the guest A-G$^-$ with different cyclodextrins, CD, at pH 6.9 or 10.8.

CD	[CD] (mol dm^{-3}) x10^3	[A-G$^-$] (mol dm^{-3}) x10^3	δ_{ORS} (ppm)	δ_{OR} (ppm)	δ_{OS} (ppm)
αCD [a]	0	1.02	-39.355		
	15.0	1.02		-39.637	-39.630
	19.7	1.01		-39.711	-39.697
	24.4	0.996		-39.769	-39.752
	29.4	1.00		-39.821	-39.800
	34.5	1.01		-39.894	-39.870
	39.4	1.01		-39.970	-39.941
	45.6	1.03		-40.022	-39.988
	49.0	0.999		-40.047	-40.013
	54.8	1.02		-40.092	-40.054
	59.2	0.996		-40.139	-40.097
	64.6	1.00		-40.177	-40.132
	69.6	1.02		-40.216	-40.169
	75.1	1.02		-40.249	-40.201
	78.6	1.00		-40.266	-40.215
βCD [a]	0	1.13	-39.358		
	0.892	1.14		-39.373	-39.373
	2.51	1.14		-39.399	-39.399
	4.20	1.14		-39.437	-39.424
	5.18	1.14		-39.454	-39.442
	6.20	1.14		-39.467	-39.454
	7.17	1.14		-39.485	-39.470
	8.07	1.14		-39.498	-39.481
	9.29	1.14		-39.518	-39.501
	10.4	1.14		-39.532	-39.513
	11.4	1.14		-39.550	-39.527
	12.2	1.14		-39.561	-39.537
	13.5	1.14		-39.580	-39.553
	14.2	1.14		-39.591	-39.563
	15.2	1.14		-39.605	-39.575
PMαCD [a]	0	1.07	-39.384		
	0.916	1.07		-39.636	-39.602
	1.82	1.07		-39.823	-39.764
	2.54	1.07		-39.974	-39.898
	3.08	1.07		-40.037	-39.952
	3.98	1.07		-40.219	-40.113
	4.46	1.07		-40.304	-40.188
	5.10	1.07		-40.397	-40.270
	6.13	1.07		-40.553	-40.408
	6.48	1.07		-40.538	-40.395
	7.10	1.07		-40.657	-40.501
	8.12	1.07		-40.768	-40.600
	8.68	1.07		-40.822	-40.648
	9.09	1.07		-40.880	-40.700
	10.2	1.06		-40.982	-40.792

Table A.3.4, continued

CD	[CD] (mol dm^{-3}) x10^3	[A-G$^-$] (mol dm^{-3}) x10^3	δ_{ORS} (ppm)	δ_{OR} (ppm)	δ_{OS} (ppm)
γCD [a]	0	1.03	-39.353		
	109	1.09	-39.189		
PMβCD [a]	0	1.01	-39.344		
	10.3 [c]	1.01	-39.367		
αCDNH$_3^+$ [a,d]	0	1.03	-39.329		
	0.674	1.03	-39.341		
	1.07	1.03	-39.347		
	1.55	1.03	-39.358		
	1.99	1.03	-39.365		
	2.62	1.03	-39.375		
	3.02	1.03	-39.381		
	3.63	1.03	-39.390		
	4.24	1.03	-39.401		
	5.10	1.03	-39.415		
	6.21	1.03	-39.431		
	7.11	1.03	-39.444		
	8.28	1.03	-39.465		
	9.44	1.03	-39.479		
	10.7	1.03	-39.496		
αCDNH$_2$ [b,e]	0	1.04	-39.319		
	10.4	1.05	-39.496		
βCDNH$_3^+$ [a,f]	0	1.03	-39.380		
	0.541	1.03	-39.388		
	1.14	1.03	-39.398		
	1.57	1.03	-39.404		
	2.04	1.03	-39.411		
	2.62	1.03	-39.420		
	3.08	1.03	-39.427		
	3.55	1.03	-39.434		
	4.17	1.03	-39.441		
	5.13	1.03	-39.453		
	6.01	1.03	-39.466		
	7.08	1.03	-39.481		
	8.23	1.03	-39.494		
	9.23	1.04	-39.508		
	10.3	1.04	-39.523		
βCDNH$_2$ [b]	0	1.07	-39.328		
	10.2 [g]	1.07	-39.466		

Table A.3.4, continued

[a]pH 6.9, phosphate buffer.
[b]pH 10.8, NaOH/glycine buffer.
[c]At a PMβCD concentration of 10.3 x 10^{-3} mol dm^{-3} the observed *R* and *S* peak separation is 0.026 ppm.
[d]At an $\alpha CDNH_3^+$ concentration of ≈82 x 10^{-3} mol dm^{-3} the observed *R* and *S* peak separation is 0.026 ppm ($I \approx 1$).
[e]At an $\alpha CDNH_2$ concentration of ≈32 x 10^{-3} mol dm^{-3} no peak separation is observed ($I \approx 1$).
[f]At a $\beta CDNH_3^+$ concentration of ≈32 x 10^{-3} mol dm^{-3} the observed *R* and *S* peak separation is 0.026 ppm ($I \approx 1$).
[g]At a $\beta CDNH_2$ concentration of 10.2 x 10^{-3} mol dm^{-3} the observed *R* and *S* peak separation is 0.016 ppm.

Table A.3.5 Concentration and ^{19}F NMR chemical shift data for the guest VH with different cyclodextrins, CD, at pH 1.3 or 1.0.

CD	[CD] (mol dm^{-3}) x10^3	[VH] (mol dm^{-3}) x10^3	δ_{ORS} (ppm)	δ_{OR} (ppm)	δ_{OS} (ppm)
αCD [a]	0	1.04	-32.308		
	5.39	1.04	-32.337		
	10.4	1.04	-32.362		
	14.8	1.04	-32.383		
	20.2	1.05	-32.409		
	26.2	1.05	-32.432		
	30.8	1.05	-32.451		
	37.7	1.05	-32.474		
	41.0	1.05	-32.487		
	46.3	1.06	-32.500		
	52.8	1.06	-32.520		
	57.6	1.06	-32.531		
	61.8	1.06	-32.543		
	68.3	1.07	-32.557		
	74.5 [c]	1.07	-32.576		
βCD [a]	0	1.06	-32.345		
	1.16	1.06		-32.274	-32.274
	2.50	1.06		-32.214	-32.201
	4.02	1.06		-32.161	-32.142
	5.01	1.06		-32.118	-32.098
	6.35	1.06		-32.083	-32.061
	7.14	1.06		-32.063	-32.041
	8.16	1.06		-32.036	-32.011
	9.08	1.06		-32.016	-31.991
	10.2	1.06		-31.993	-31.968
	11.1	1.06		-31.978	-31.952
	12.4	1.07		-31.954	-31.928
	13.4	1.07		-31.939	-31.913
	14.4	1.07		-31.924	-31.898
	15.8	1.07		-31.904	-31.878
γCD [a]	0	1.06	-32.299		
	3.21	1.06		-32.265	-32.265
	5.11	1.06		-32.243	-32.243
	10.2	1.07		-32.192	-32.192
	15.2	1.07		-32.152	-32.152
	20.4	1.07		-32.123	-32.113
	25.5	1.07		-32.088	-32.076
	31.0	1.08		-32.057	-32.044
	41.6	1.08		-32.004	-31.989
	52.0	1.09		-31.961	-31.945
	62.8	1.09		-31.921	-31.906
	73.5	1.10		-31.889	-31.872
	84.1	1.10		-31.860	-31.845
	95.4	1.11		-31.834	-31.817
	106	1.12		-31.808	-31.792

Table A.3.5, continued

CD	[CD] (mol dm^{-3}) x10^3	[VH] (mol dm^{-3}) x10^3	δ_{ORS} (ppm)	δ_{OR} (ppm)	δ_{OS} (ppm)
PMαCD [b]	0	1.04	-32.315		
	1.07	1.03		-32.518	-32.537
	1.98	1.03		-32.672	-32.703
	2.48	1.03		-32.746	-32.782
	3.05	1.03		-32.826	-32.870
	3.87	1.03		-32.889	-32.934
	4.42	1.03		-32.957	-33.005
	5.03	1.03		-33.023	-33.073
	5.99	1.03		-33.092	-33.145
	6.40	1.03		-33.146	-33.197
	6.96	1.03		-33.159	-33.213
	7.96	1.03		-33.227	-33.281
	8.45	1.03		-33.253	-33.307
	8.98	1.03		-33.277	-33.332
	10.2	1.03		-33.344	-33.400
PMβCD [b]	0	1.04	-32.307		
	10.6	1.04	-32.360		
αCDNH$_3^+$ [b,d]	0	1.05	-32.318		
	10.5	1.05	-32.348		
βCDNH$_3^+$ [b]	0	1.05	-32.262		
	0.894	1.05		-32.222	-32.222
	2.05	1.05		-32.189	-32.189
	2.86	1.05		-32.160	-32.160
	4.12	1.05		-32.124	-32.124
	5.32	1.05		-32.092	-32.092
	6.23	1.05		-32.078	-32.070
	6.98	1.05		-32.063	-32.054
	8.34	1.05		-32.039	-32.026
	9.29	1.05		-32.015	-32.006
	10.1	1.05		-31.999	-31.986
	11.2	1.05		-31.984	-31.971
	12.3	1.05		-31.968	-31.955
	13.2	1.05		-31.948	-31.939
	14.3	1.05		-31.932	-31.922

[a]pH 1.3, HCl/KCl buffer.

[b]pH 1.0, HCl.

[c]At an αCD concentration of 74.5 x 10^{-3} mol dm^{-3} the observed *R* and *S* peak separation is 0.014 ppm.

[d]At an αCDNH$_3^+$ concentration of ≈72 x 10^{-3} mol dm^{-3} the observed *R* and *S* peak separation is 0.010 ppm ($I \approx 1$).

Table A.3.6 Concentration and ^{19}F NMR chemical shift data for the guest V^- with different cyclodextrins, CD, at pH 6.9 or 10.8.

CD	[CD] (mol dm^{-3}) x10^3	[V^-] (mol dm^{-3}) x10^3	δ_{ORS} (ppm)	δ_{OR} (ppm)	δ_{OS} (ppm)
αCD [a]	0	0.990	-32.823		
	4.87	0.990		-32.869	-32.856
	9.95	0.990		-32.913	-32.887
	15.1	0.990		-32.952	-32.914
	20.1	0.990		-32.988	-32.940
	24.9	0.990		-33.020	-32.963
	30.1	0.990		-33.052	-32.987
	34.9	0.990		-33.074	-33.003
	39.9	0.990		-33.102	-33.025
	44.9	0.990		-33.120	-33.039
	50.1	0.990		-33.152	-33.064
	53.9	0.990		-33.157	-33.067
	59.9	0.990		-33.180	-33.085
	70.0	0.990		-33.216	-33.115
γCD [a]	0	1.02	-32.830		
	2.99	1.03	-32.815		
	5.41	1.03	-32.803		
	10.3	1.03	-32.781		
	15.3	1.03	-32.760		
	20.3	1.03	-32.740		
	30.8	1.04	-32.700		
	41.3	1.05	-32.664		
	52.5	1.05	-32.630		
	63.1	1.06	-32.601		
	74.0	1.06	-32.571		
	84.4	1.07	-32.547		
	99.9	1.07	-32.511		
	107	1.08	-32.498		
	118	1.08	-32.477		
	129	1.09	-32.455		
PMαCD [a]	0	1.04	-32.778		
	0.331	1.04		-32.849	-32.849
	0.581	1.04		-32.909	-32.909
	0.994	1.04		-32.971	-32.971
	1.57	1.04		-33.065	-33.083
	2.17	1.04		-33.137	-33.165
	2.57	1.04		-33.198	-33.230
	2.99	1.04		-33.248	-33.284
	4.14	1.04		-33.373	-33.417
	5.01	1.04		-33.429	-33.474
	5.98	1.04		-33.524	-33.574
	7.15	1.04		-33.610	-33.662
	8.14	1.04		-33.655	-33.706
	9.15	1.04		-33.700	-33.751
	10.1	1.04		-33.773	-33.829

Table A.3.6, continued

CD	[CD] (mol dm^{-3}) x10^3	[V$^-$] (mol dm^{-3}) x10^3	δ_{ORS} (ppm)	δ_{OR} (ppm)	δ_{OS} (ppm)
βCD [a]	0	1.02	-32.875		
	16.3	1.03		-32.841	-32.854
PMβCD [a]	0	1.04	-32.835		
	9.96	1.04	-32.876		
αCDNH$_3^+$ [a]	0	1.09	-32.796		
	2.89	1.09		-32.816	-32.809
	3.02	1.09		-32.820	-32.812
	3.65	1.09		-32.822	-32.812
	4.87	1.09		-32.832	-32.818
	5.72	1.09		-32.840	-32.822
	6.26	1.09		-32.842	-32.823
	7.11	1.09		-32.847	-32.826
	8.06	1.10		-32.855	-32.831
	8.70	1.09		-32.858	-32.833
	9.46	1.10		-32.865	-32.837
	9.99	1.10		-32.866	-32.837
	10.7	1.10		-32.871	-32.840
	12.0	1.10		-32.878	-32.845
αCDNH$_2$ [b]	0	1.00	-32.824		
	9.99	1.00		-32.902	-32.878
βCDNH$_3^+$ [a]	0	1.02	-32.839		
	0.600	1.02		-32.815	-32.815
	1.04	1.02		-32.805	-32.805
	1.88	1.02		-32.773	-32.773
	2.61	1.03		-32.775	-32.745
	3.01	1.03		-32.766	-32.736
	3.86	1.03		-32.750	-32.711
	4.72	1.03		-32.728	-32.681
	5.19	1.03		-32.718	-32.673
	6.29	1.03		-32.701	-32.647
	7.05	1.03		-32.688	-32.627
	8.31	1.03		-32.669	-32.602
	9.36	1.03		-32.653	-32.581
	10.5	1.03		-32.639	-32.565
	11.5	1.03		-32.625	-32.543
βCDNH$_2$ [b,c]	0	1.01	-32.824		
	10.2	1.01	-32.832		

[a]pH 6.9, phosphate buffer.

[b]pH 10.8, NaOH/glycine buffer.

[c]At a βCDNH$_2$ concentration of ≈31 x 10^{-3} mol dm^{-3} no peak separation is observed ($I \approx 1$).

PUBLICATIONS LIST

Some of the work in this thesis appears in the following publications.

"Metallocyclodextrins of 6^A-(3-Aminopropylamino)-6^A-deoxy-β-cyclodextrin; their Formation and Enantioselective Complexation of *R*- and *S*-Tryptophan Anions in Aqueous Solution"
Brown, S. E.; Coates, J. H.; Easton, C. J.; Lincoln, S. F.
J. Chem. Soc., Faraday. Trans. accepted for publication.

"Tryptophan Anion Complexes of β-Cyclodextrin (Cyclomaltaheptaose), an Aminopropyl-amino-β-cyclodextrin and its Enantioselective Nickel(II) Complex"
Brown, S. E.; Coates, J. H.; Easton, C. J.; van Eyk, S. J.; Lincoln, S. F.; May, B. L.; Stile, M. A.; Whalland, C. B.; Williams, M. L.
J. Chem. Soc., Chem. Commun. **1994**, 47.

"Substituent Effects and Chiral Discrimination in the Complexation of Benzoic, 4-Methylbenzoic, and (*RS*)-2-Phenylpropanoic Acids and their Conjugate Bases by β-Cyclodextrin and 6^A-Amino-6^A-deoxy-β-cyclodextrin in Aqueous Solution: Potentiometric Titration and ^{1}H Nuclear Magnetic Resonance Spectroscopic Study"
Brown, S. E.; Coates, J. H.; Duckworth, P. A.; Lincoln, S. F.; Easton, C. J.; May, B. L.
J. Chem. Soc., Faraday Trans. **1993**, *89*, 1035.

"Chiral Molecular Recognition: A ^{19}F Nuclear Magnetic Resonance Study of the Diastereomer Inclusion Complexes formed between Fluorinated Amino Acid Derivatives and α-Cyclodextrin in Aqueous Solution"
Brown, S. E.; Coates, J. H.; Lincoln, S. F.; Coghlan, D. R.; Easton, C. J.
J. Chem. Soc., Faraday Trans. **1991**, *87*, 2699.

Tryptophan Anion Complexes of β-Cyclodextrin (Cyclomaltaheptaose), an Aminopropylamino-β-cyclodextrin and its Enantioselective Nickel(II) Complex

Susan E. Brown, John H. Coates, Christopher J. Easton*, Steven J. van Eyk, Stephen F. Lincoln,* Bruce L. May, Martyn A. Stile, Craig B. Whalland and Michael L. Williams

Department of Chemistry, University of Adelaide, South Australia 5005, Australia

6^{I}-(3-Aminopropylamino)-6^{I}-deoxy-cyclomaltaheptaose (βCDpn) exhibits enhanced complexation of tryptophan anion, by comparison with βCD, while the nickel(II) complex of βCDpn complexes tryptophan anion even more strongly and exhibits a tenfold enantioselectivity in favour of the (*S*)-tryptophan anion.

As part of a study of the complexation characteristics of modified cyclodextrins we have prepared 6^{I}-(3-aminopropylamino)-6^{I}-deoxy-cyclomaltaheptaose (βCDpn) and its nickel(II) complex {[Ni(βCDpn)]$^{2+}$} and investigated the complexation of tryptophan anion (trp^{-}) by these species. The complexation characteristics of unmodified cyclodextrins and their ability to discriminate between enantiomers are well documented.[1–5] Substituents on a cyclodextrin are known to affect the extent of complexation and chiral discrimination. Thus, by comparison with βCD, 6^{I}-amino-6^{I}-deoxy-cyclomaltaheptaose shows greater enantioselectivity in its complexation of sodium 2-phenylpropanoate, although the complexes with βCD are more stable.[4] The aminopropylamino substituent of βCDpn offers greater structural flexibility for interaction with guests, and provides an opportunity for chelation of metal ions. Such metal complexes, or metallocyclodextrins, have been studied as metalloprotein models[6] and recently their enantiomeric complexation characteristics have attracted attention.[7,8] We now report that βCDpn, by comparison with βCD, exhibits enhanced complexation of trp^{-}, while [Ni(βCDpn)]$^{2+}$ exhibits a further enhancement in complexation and also a tenfold enantioselectivity between (*R*)-trp^{-} and (*S*)-trp^{-}, which is much higher than reported previously for a metallocyclodextrin.[7,8]

βCDpn [^{13}C NMR (D_2O): 32.5 (C2′), 39.6 (C3′), 47.4 (C1′) and 50.4 (C6^{I})] was prepared by treatment of 6^{I}-*O*-(4-methylphenylsulfonyl)-cyclomaltaheptaose[9] with 1,3-diaminopropane (1.5 equiv.) in *N*,*N*-dimethylformamide at 313 K for 24 h, and isolated in 93% yield after recrystallization from water–acetone of the precipitate obtained by diluting the cooled reaction mixture with acetone.

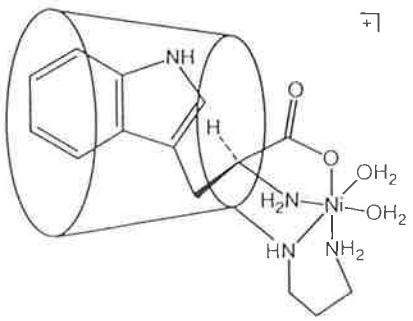

Fig. 1 A possible structure for [Ni(βCDpn)(*S*)-trp]$^{+}$, where the cyclodextrin annulus is shown as a truncated cone with the narrow and wide ends representing the circles delineated by the primary and secondary hydroxy groups, respectively

Table 1 Stability constants (*K*) for cyclodextrin and tryptophan anion complexes in aqueous solution at 298.2 K and I = 0.10 ($NaClO_4$)

Complexation	log (*K*/dm^3 mol^{-1})
βCD + (*R*)-trp^{-} ⇌ βCD(*R*)-trp^{-}	2.33 ± 0.06
βCD + (*S*)-trp^{-} ⇌ βCD(*S*)-trp^{-}	2.33 ± 0.08
βCDpn + (*R*)-trp^{-} ⇌ βCDpn(*R*)-trp^{-}	3.41 ± 0.05
βCDpn + (*S*)-trp^{-} ⇌ βCDpn(*S*)-trp^{-}	3.40 ± 0.07
βCDpn + Ni^{2+} ⇌ [Ni(βCDpn)]$^{2+}$	5.2 ± 0.1
[Ni(βCDpn)]$^{2+}$ + (*R*)-trp^{-} ⇌ [Ni(βCDpn)(*R*)-trp]$^{+}$	4.1 ± 0.2
[Ni(βCDpn)]$^{2+}$ + (*S*)-trp^{-} ⇌ [Ni(βCDpn)(*S*)-trp]$^{+}$	5.1 ± 0.2
Ni^{2+} + trp^{-} ⇌ [Ni(trp)]$^{+}$	5.42 ± 0.03

The stability constants for complexation of Ni^{2+} by βCDpn, and (*R*)-trp^{-} and (*S*)-trp^{-} by Ni^{2+}, βCD, βCDpn and [Ni(βCDpn)]$^{2+}$, determined using standard automated pH titration procedures,[4] are presented in Table 1. Neither βCDpn nor βCD discriminate between the enantiomers of trp^{-}, whereas the metallocyclodextrin [Ni(βCDpn)]$^{2+}$ complexes (*S*)-trp^{-} enantioselectively. It appears that the metal is important for chiral discrimination and, since the chirality of βCDpn is essential to the enantioselectivity displayed by [Ni(βCDpn)]$^{2+}$, it seems likely that [Ni(βCDpn)(*S*)-trp]$^{+}$ has both (*S*)-trp^{-} and βCDpn coordinated to Ni^{2+} as shown in Fig. 1. A similar structure is anticipated for [Ni(βCDpn)(*R*)-trp]$^{+}$. It has been suggested that discrimination between the enantiomers of trp^{-} by metallocyclodextrins requires the indole moiety of the more strongly bound enantiomer to be inside the cyclodextrin annulus while that of the other enantiomer is excluded from it.[7,8] We have no evidence for such a major structural difference in our system.

The stronger complexation of trp^{-} by the metallocyclodextrin [Ni(βCDpn)]$^{2+}$, relative to that by βCDpn and βCD, is consistent with bidentate coordination of trp^{-} stabilizing its complexation. However, this stronger complexation does not result from a simple combination of the effects of the cyclodextrin annulus and Ni^{2+}, as is apparent from the observation that the stability constant for [Ni(trp)]$^{+}$ is greater than that for either [Ni(βCDpn)(*R*)-trp]$^{+}$ or [Ni(βCDpn)(*S*)-trp]$^{+}$.

The award of an Australian Postgraduate Priority Research Award to S. E. B., and research funding from the Australian Research Council, Australian Commercial Research and Development Ltd. and the University of Adelaide are gratefully acknowledged.

Received, 28th June 1993; Com. 3/03662F

References

1 R. J. Clarke, J. H. Coates and S. F. Lincoln, *Adv. Carbohydr. Chem. Biochem.*, 1989, **46**, 205.
2 J. Szejtli, *Cyclodextrin Technology*, Kluwer, Dordrecht, 1988.
3 S. E. Brown, J. H. Coates, S. F. Lincoln, D. R. Coghlan and C. J. Easton, *J. Chem. Soc., Faraday Trans.*, 1991, **87**, 2699.
4 S. E. Brown, J. H. Coates, P. A. Duckworth, S. F. Lincoln, C. J. Easton and B. L. May, *J. Chem. Soc., Faraday Trans.*, 1993, **89**, 1035.
5 K. B. Lipkowitz, S. Raghothama and J. Yang, *J. Am. Chem. Soc.*, 1992, **114**, 1554.
6 I. Tabushi, *Coord. Chem. Rev.*, 1988, **86**, 1.
7 G. Impellizzeri, G. Maccarrone, E. Rizzarelli, G. Vecchio, R. Corradini and R. Marchelli, *Angew. Chem., Int. Ed. Engl.*, 1991, **30**, 1348.
8 V. Cucinotta, F. D'Alessandro, G. Impellizzeri, G. Maccarrone and G. Vecchio, *J. Chem. Soc., Chem. Commun.*, 1992, 1743.
9 Y. Chao, PhD Thesis, Columbia University, 1972; M. Shiono, T. Shibanuma and T. Mukaiyama, *Chem. Lett.*, 1976, 1041.

Substituent Effects and Chiral Discrimination in the Complexation of Benzoic, 4-Methylbenzoic and (*RS*)-2-Phenylpropanoic Acids and their Conjugate Bases by β-Cyclodextrin† and 6^A-Amino-6^A-deoxy-β-cyclodextrin in Aqueous Solution: Potentiometric Titration and ^1H Nuclear Magnetic Resonance Spectroscopic Study

Susan E. Brown, John H. Coates, Paul A. Duckworth and Stephen F. Lincoln*
Department of Physical and Inorganic Chemistry, University of Adelaide, South Australia 5001, Australia
Christopher J. Easton and Bruce L. May
Department of Organic Chemistry, University of Adelaide, South Australia 5001, Australia

A potentiometric titration study in aqueous solution ($I = 0.10$ mol dm^{-3}, KCl) of the complexation of benzoic, 4-methylbenzoic and (*RS*)-2-phenylpropanoic acids (HA) and their conjugate bases (A^-) with β-cyclodextrin, βCD, and its substituted analogue, 6^A-amino-6^A-deoxy-β-cyclodextrin, $\beta CDNH_2$, in which a primary hydroxy group is replaced by an amino group which may be protonated to produce a singly charged species, $\beta CDNH_3^+$, is reported. At 298.2 K the stability constants for the complexes have the values (in dm^3 mol^{-1}) shown in parentheses: benzoic acid · βCD ($K_{1HA} = 590 \pm 60$); benzoate · βCD ($K_{1A} = 60 \pm 10$); benzoic acid · $\beta CDNH_3^+$ ($K_{2HA} = 340 \pm 30$); benzoate · $\beta CDNH_3^+$ ($K_{2A} = 120 \pm 20$); benzoate · $\beta CDNH_2$ ($K_{3A} = 50 \pm 20$); 4-methylbenzoic acid · βCD ($K_{1HA} = 1680 \pm 90$); 4-methylbenzoate · βCD ($K_{1A} = 110 \pm 1$); 4-methylbenzoic acid · $\beta CDNH_3^+$ ($K_{2HA} = 910 \pm 20$); 4-methylbenzoate · $\beta CDNH_3^+$ ($K_{2A} = 330 \pm 20$); and 4-methylbenzoate · $\beta CDNH_2$ ($K_{3A} = 100 \pm 20$). These data indicate that for a given cyclodextrin the guest carboxylic acids form complexes of higher stability than do their conjugate base analogues, and that $\beta CDNH_3^+$ forms more stable complexes with the conjugate bases than do βCD and $\beta CDNH_2$. These trends are also observed for the complexation of (*RS*)-2-phenylpropanoic acid and (*RS*)-2-phenylpropanoate where the complexes indicated are characterised by the stability constants (in dm^3 mol^{-1}) shown in parentheses: (*RS*)-2-phenylpropanoic acid · βCD ($K_{1RHA} = 1090 \pm 30$, $K_{1SHA} = 1010 \pm 40$); (*RS*)-2-phenylpropanoate · βCD ($K_{1RA} = 63 \pm 8$, $K_{1SA} = 52 \pm 5$); (*RS*)-2-phenylpropanoic acid · $\beta CDNH_3^+$ ($K_{2RHA} = 580 \pm 20$, $K_{2SHA} = 480 \pm 10$); (*RS*)-2-phenylpropanoate · $\beta CDNH_3^+$ ($K_{2RA} = 150 \pm 8$, $K_{2SA} = 110 \pm 10$); and (*RS*)-2-phenylpropanoate · $\beta CDNH_2$ ($K_{3RA} = 36 \pm 6$, $K_{3SA} = 13 \pm 7$). These data also show that while K_{1RHA} and K_{1SHA}, and K_{1RA} and K_{1SA} are indistinguishable for (*RS*)-2-phenylpropanoic acid · βCD and (*RS*)-2-phenylpropanoate · βCD, chiral discrimination is indicated by $K_{2RHA} > K_{2SHA}$ for (*RS*)-2-phenylpropanoic acid · $\beta CDNH_3^+$, $K_{2RA} > K_{2SA}$ for (*RS*)-2-phenylpropanoate · $\beta CDNH_3^+$, and $K_{3RA} > K_{3SA}$ for (*RS*)-2-phenylpropanoate · $\beta CDNH_2$. The ^1H NMR spectra of the methyl groups of the enantiomers of (*RS*)-2-phenylpropanoic acid appear as two separate doublets, indicating chiral discrimination when complexed by βCD or $\beta CDNH_3^+$, but such chiral discrimination is not observed for (*RS*)-2-phenylpropanoate when complexed by $\beta CDNH_3^+$. The implications of these observations are discussed.

The ability of the chiral α-1,4-linked cyclic oligomers of D-glucopyranose, or cyclodextrins (CDs), to act as host species in the formation of inclusion complexes with a wide range of guest species is well established.[1–9] Because CDs exist only as D enantiomers, two diastereomeric complexes are formed with racemic guest species, which may result in distinct NMR spectra being observed for each of the (*R*) and (*S*) guest enantiomers in solution,[10–12] partial resolution of racemic guests through preferential precipitation of one diastereomeric complex[13–15] and the chromatographic separation of enantiomers on columns where the stationary phase consists of CDs bonded to silica.[16–18] More recently the effect of substitution of CD hydroxy groups by other moieties on the complexation characteristics of CDs has become an area of active study as a consequence of the modification of complexation characteristics and solubilities of CDs which can result from such substitution.[19–24] We are particularly interested in the influence of such substitution, and the effect of substituent charge, on the complexation process and chiral discrimination between enantiomeric guests; an area which has not previously been subjected to systematic study. Accordingly we have selected β-cyclodextrin, βCD, and 6^A-amino-6^A-deoxy-β-cyclodextrin, $\beta CDNH_2$, in which a primary hydroxy group of βCD is replaced by an amino group which may be protonated to produce a positively charged species, $\beta CDNH_3^+$,[20,21] to examine the effect of substitution and charge on the complexation and chiral discrimination characteristics of βCD. The guest species, benzoic acid, 4-methylbenzoic acid, (*RS*)-2-phenylpropanoic acid, and their conjugate bases provide convenient conjugate acid–base pairs to test the effect of changing the guest charge from neutral to negative on complexation by these three CD hosts.

† Cycloheptamaltaose.

Experimental

βCD (Sigma) and $\beta CDNH_2$, prepared as in the literature,[20,21] were dried to constant weight and stored over P_2O_5 in a vacuum desiccator prior to use. The carboxylic acids (Sigma) were used as received. The enantiomeric purities of (*R*)- and (*S*)-2-phenylpropanoic acid were determined to be >97.5% and >98.5%, respectively, after HPLC analysis of their diastereomeric amides formed with (*S*)-1-phenylethylamine. These purity limits were used in calculations of error limits of the stability constants characterising the complexation of these enantiomers by CDs. Deionised

water was purified with a MilliQ-Reagent system to produce water with a specific resistance of >15 MΩ cm, which was then boiled to remove CO_2. All solutions were prepared from this water, and were 0.10 mol dm^{-3} in KCl which acted as the supporting electrolyte. Titrations were performed using a Metrohm Dosimat E665 titrimator, an Orion SA 720 potentiometer and an Orion 8103 Ross combination pH electrode which was filled with 0.10 mol dm^{-3} KCl and calibrated before use with appropriate buffer solutions. Throughout a titration a stream of fine nitrogen bubbles (previously passed through aqueous 0.10 mol dm^{-3} KCl) was passed through the titration solution which was magnetically stirred and thermostatted at 298.2 ± 0.1 K in a water-jacketted titration vessel which was closed to the atmosphere with the exception of a vent which permitted egress of the nitrogen stream. A pK_w value was determined by titration of 1.0×10^{-2} mol dm^{-3} HCl (8.0 or 2.0 cm^3) with standardised 5.0×10^{-2} mol dm^{-3} NaOH. The pK_a values of the carboxylic acids and $\beta CDNH_3^+$ were determined by titration of 2×10^{-3} mol dm^{-3} aqueous solutions (8.0 or 2.0 cm^3) with standardised 5.0×10^{-2} mol dm^{-3} NaOH.

To determine the stability constants for the complexation of a guest carboxylic acid and its conjugate base by βCD, the burette contained a solution of 1.5×10^{-2} mol dm^{-3} βCD at pH 7. The pH of each 2×10^{-3} mol dm^{-3} carboxylic acid–carboxylate solution (2.0 cm^3) in the titration vessel was adjusted to a value near the pK_a of the carboxylic acid. Up to 3 cm^3 of βCD solution were titrated into the carboxylic acid–carboxylate solutions in increments not greater than 0.05 cm^3, and the observed pH increased by 0.4–0.9 pH units in total, depending on the carboxylic acid being studied. At least three similar titrations, with starting pHs in the range 3.9–4.8, were performed for each carboxylic acid system studied.

To determine the stability constants for the complexation of 4-methylbenzoic and (*R*)- and (*S*)-2-phenylpropanoic acids and their conjugate bases by $\beta CDNH_3^+$, the burette contained a solution of 1.6×10^{-2} mol dm^{-3} $\beta CDNH_3^+$ at pH 6. The pH of each 2×10^{-3} mol dm^{-3} carboxylic acid–carboxylate solution (2.0 cm^3) in the titration vessel was adjusted to a value near the pK_a of the carboxylic acid. Up to 3 cm^3 of $\beta CDNH_3^+$ solution were titrated into the carboxylic acid–carboxylate solutions in increments not greater than 0.05 cm^3, and the pH increased by *ca.* 0.4 pH units in total. At least three similar titrations, with starting pHs in the range 3.9–4.5, were performed for each carboxylic acid system studied. To determine the stability constants for the complexation of benzoic acid and benzoate by $\beta CDNH_3^+$, the burette contained a solution of 6.0×10^{-3} mol dm^{-3} benzoic acid–benzoate at pH 4. The pH of each 5×10^{-3} mol dm^{-3} $\beta CDNH_3^+$ solution (2.0 cm^3) in the titration vessel was adjusted to a value near pH 4. Up to 1 cm^3 of benzoic acid–benzoate solution was titrated into the $\beta CDNH_3^+$ solution in increments of 0.01 cm^3, and the observed pH increased by *ca.* 0.3 pH units in total. At least three similar titrations, with starting pHs in the range 3.5–4.5, were performed.

To determine the stability constants for the complexation of a guest carboxylate with $\beta CDNH_3^+$ and its conjugate base $\beta CDNH_2$, the burette contained a solution of 0.01–0.02 mol dm^{-3} carboxylate at pH 7. The pH of each 2×10^{-3} mol dm^{-3} $\beta CDNH_2$ solution (2.0 cm^3) in the titration vessel was adjusted to a value near the pK_a of $\beta CDNH_3^+$. Up to 3 cm^3 of carboxylate solution were added to the $\beta CDNH_3^+$–$\beta CDNH_2$ solutions in increments not greater than 0.05 cm^3, and the pH increased by 0.1–0.3 pH units, depending on the carboxylate being studied. At least three similar titrations, with starting pHs in the range 8.2–8.8, were performed for each carboxylate system studied.

^1H NMR spectra were run in D_2O solution in 5 mm diameter NMR tubes on a Bruker ACP 300 spectrometer. The sweep width was 4000 Hz and typically 100 transients were collected prior to Fourier transformation. Chemical shifts were measured from external sodium 3-trimethylsilylpropane-1-sulfonate (TPS) in D_2O. Solutions of βCD or $\beta CDNH_3^+$ and (*RS*)-2-phenylpropanoic acid were adjusted to pH 1 with DCl–D_2O, and solutions of $\beta CDNH_3^+$ and (*RS*)-2-phenylpropanoate were buffered at pH 6.4 with phosphate buffer (0.20 mol dm^{-3}) made up in D_2O. The concentration of βCD or $\beta CDNH_3^+$ was in the range $(1.0–9.0) \times 10^{-2}$ mol dm^{-3}, and that of (*RS*)-2-phenylpropanoic acid or (*RS*)-2-phenylpropanoate was in the range 1.0×10^{-3}–1.0×10^{-2} mol dm^{-3} so that ≥90% of the guest species was complexed. When separate resonances were observed in the (*RS*)-2-phenylpropanoic acid systems for the guest enantiomers in the two diastereomers, the resonances were assigned by adding resolved (*R*)-2-phenylpropanoic acid to the solution and observing which resonance increased in intensity. The $\beta CDNH_3^+$ and (*RS*)-2-phenylpropanoate solutions were prepared at the higher end of the concentration scales indicated above, which together with the high phosphate buffer concentration, may result in an increased solution viscosity which may explain the broader ^1H resonances observed in these solutions.

Results and Discussion

The complexation of a carboxylic acid, HA, and its conjugate base, A^-, by βCD may be expressed as in Scheme 1, where the acidity constant, K_a, characterises the carboxylic acid, K_{1HA} and K_{1A} are the stability constants for the complexation of HA and A^-, respectively, by βCD, and K_a' characterises HA in the HA · βCD complex.

The variation of the pH of a benzoic acid–benzoate solution in the vicinity of the pK_a ($\equiv -\log K_a$) of benzoic acid as it was titrated with βCD solution (Fig. 1), arises because

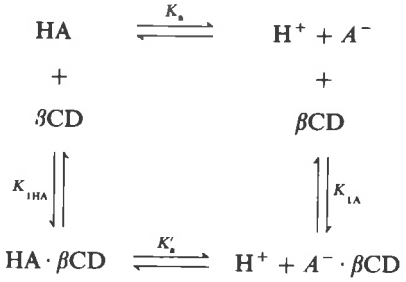

Scheme 1

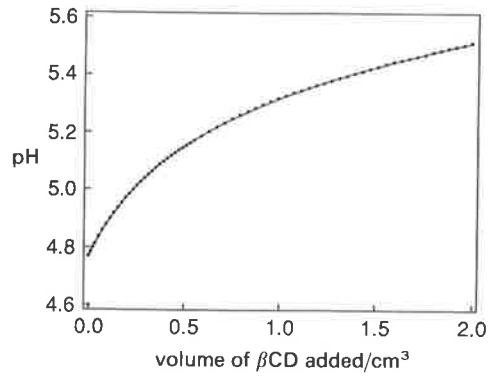

Fig. 1 Variation of the pH of a solution (2.0 cm^3) of benzoic acid–benzoate (1.04×10^{-3} mol dm^{-3}) with volume of added βCD (1.51×10^{-2} mol dm^{-3}) at 298.2 K and $I = 0.10$ mol dm^{-3} (KCl). The curve through the data points represents the best fit of the data to the equilibria shown in Scheme 1 using SUPERQUAD.

$pK_a \neq pK'_a$ or $K_{1HA} \neq K_{1A}$ (and analogous inequalities hold for the other titrations discussed herein). The best fit of the data to the expressions for K_{1HA} and K_{1A}, employing the independently determined value of K_a, using program SUPERQUAD[25] yields the curve through the data points in Fig. 1. (The value of K'_a was subsequently calculated from these three values.) Similar curves were obtained for the titration of 4-methylbenzoic acid–4-methylbenzoate and (*R*)- and (*S*)-2-phenylpropanoic acid–phenylpropanoate by βCD, and the data were fitted in a similar manner. The pK_a and pK'_a values for benzoic, 4-methylbenzoic and (*R*)- and (*S*)-2-phenylpropanoic acid appear in Table 1, as do the K_{1HA} and K_{1A} values for the complexation of these carboxylic acids and their conjugate bases by βCD.

The complexation of a guest carboxylate (A^-) by $\beta CDNH_3^+$ and its conjugate base, $\beta CDNH_2$, may be expressed as in Scheme 2, where K_a is the acidity constant of $\beta CDNH_3^+$, K_{2A} and K_{3A} are the stability constants for the complexation of A^- by $\beta CDNH_3^+$ and $\beta CDNH_2$, respectively, and pK'_a characterises $\beta CDNH_3^+$ in the $A^- \cdot \beta CDNH_3^+$ complex.

The variations of the pH of solutions of $\beta CDNH_3^+$–$\beta CDNH_2$ in the vicinity of the pK_a of $\beta CDNH_3^+$ as they were titrated with a solution of either (*R*)- or (*S*)-2-phenylpropanoate are shown in Fig. 2. The best fit of the data to the expressions for K_{2A} and K_{3A}, employing the independently determined value of K_a, using program SUPERQUAD[25] yields the curve through the data points in Fig. 2. (The value of K'_a was subsequently calculated from these three values.) Similar curves were obtained for the titration of $\beta CDNH_3^+$–$\beta CDNH_2$ by benzoate and 4-methylbenzoate, and the data were similarly fitted. The pK_a and pK'_a values for $\beta CDNH_3^+$ appear in Table 1, and the K_{2A} and K_{3A} values for the complexation of benzoate, 4-methylbenzoate, and (*R*)- and (*S*)-2-phenylpropanoate by $\beta CDNH_3^+$ and $\beta CDNH_2$ also appear in Table 1.

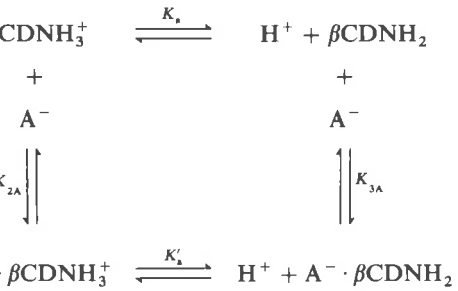

Scheme 2

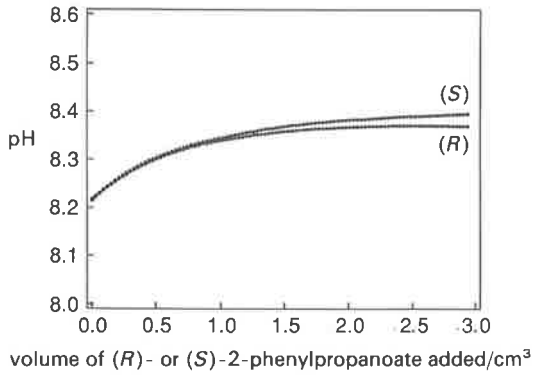

Fig. 2 Variation of the pH of a solution (2.0 cm^3) of $\beta CDNH_3^+$–$\beta CDNH_2$ (2.21×10^{-3} mol dm^{-3}) with volume of added (*R*)- or (*S*)-2-phenylpropanoate (1.40×10^{-2} and 1.50×10^{-2} mol dm^{-3}, respectively) at 298.2 K and $I = 0.10$ mol dm^{-3} (KCl). The upper and lower data sets refer to (*S*)- and (*R*)-2-phenylpropanoate, respectively. The curves through the data points represent the best fits of the data to the equilibria shown in Scheme 2 using SUPERQUAD.

Table 1 *K*, pK_a and pK'_a values for cyclodextrin complexes, cyclodextrins and guest species at $I = 0.10$ mol dm^{-3} (KCl) and 298.2 K

species	K^a/dm^3 mol^{-1}	$pK_a{}^b$	$pK'_a{}^c$
benzoic acid		4.06 ± 0.04	
benzoic acid · βCD	$K_{1HA} = 590 \pm 60$		5.1 ± 0.1
benzoate · βCD	$K_{1A} = 60 \pm 10$		
$\beta CDNH_3^+$		8.49 ± 0.01[d]	
benzoic acid · $\beta CDNH_3^+$	$K_{2HA} = 340 \pm 30$		4.5 ± 0.1
benzoate · $\beta CDNH_3^+$	$K_{2A} = 120 \pm 20$		8.9 ± 0.2
benzoate · $\beta CDNH_2$	$K_{3A} = 50 \pm 20$		
4-methylbenzoic acid		4.20 ± 0.08	
4-methylbenzoic acid · βCD	$K_{1HA} = 1680 \pm 90$		5.39 ± 0.09
4-methylbenzoate · βCD	$K_{1A} = 110 \pm 1$		
4-methylbenzoic acid · $\beta CDNH_3^+$	$K_{2HA} = 910 \pm 20$		4.6 ± 0.1
4-methylbenzoate · $\beta CDNH_3^+$	$K_{2A} = 330 \pm 20$		9.0 ± 0.1
4-methylbenzoate · $\beta CDNH_2$	$K_{3A} = 100 \pm 20$		
(*R*)-2-phenylpropanoic acid		4.23 ± 0.05	
(*R*)-2-phenylpropanoic acid · βCD	$K_{1RHA} = 1090 \pm 30$		5.47 ± 0.08
(*R*)-2-phenylpropanoate · βCD	$K_{1RA} = 63 \pm 8$		
(*R*)-2-phenylpropanoic acid · $\beta CDNH_3^+$	$K_{2RHA} = 580 \pm 20$		4.82 ± 0.06
(*R*)-2-phenylpropanoate · $\beta CDNH_3^+$	$K_{2RA} = 150 \pm 8$		9.11 ± 0.08
(*R*)-2-phenylpropanoate · $\beta CDNH_2$	$K_{3RA} = 36 \pm 6$		
(*S*)-2-phenylpropanoic acid		4.23 ± 0.05	
(*S*)-2-phenylpropanoic acid · βCD	$K_{1SHA} = 1010 \pm 40$		5.52 ± 0.07
(*S*)-2-phenylpropanoate · βCD	$K_{1SA} = 52 \pm 5$		
(*S*)-2-phenylpropanoic acid · $\beta CDNH_3^+$	$K_{2SHA} = 480 \pm 10$		4.87 ± 0.07
(*S*)-2-phenylpropanoate · $\beta CDNH_3^+$	$K_{2SA} = 110 \pm 10$		9.4 ± 0.4
(*S*)-2-phenylpropanoate · $\beta CDNH_2$	$K_{3SA} = 13 \pm 7$		

[a] Errors quoted for *K* (the mean of *N* runs) represent the standard deviation, $\sigma = \sqrt{\{[\Sigma(K_i - K)^2]/(N-1)\}}$, where K_i is a value from a single run for the best fit of the variation of pH with added volume of cyclodextrin or carboxylic acid–carboxylate titrant obtained through SUPERQUAD, and $i = 1, 2, \ldots, N$. [b] Errors quoted for pK_a are similarly calculated for the best fit of the variation of pH with added volume of NaOH titrant obtained through SUPERQUAD. [c] Errors quoted for pK'_a represent those calculated from the propagation of errors associated with pK_a and *K*. [d] This pK_a observed for $\beta CDNH_3^+$ is lower than that reported in ref. 21 (8.72 ± 0.02) at a higher *I* (0.5 mol dm^{-3}).

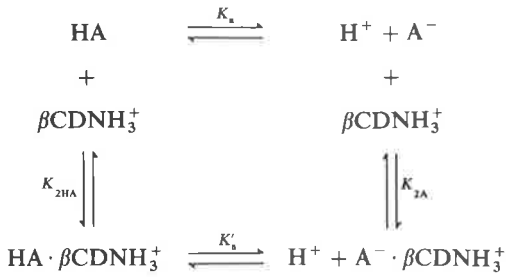

Scheme 3

The complexation of HA and A^- by $\beta CDNH_3^+$ may be expressed as in Scheme 3, where K_a, K'_a, K_{2HA} and K_{2A} are constants characterising the equilibria, and whose values appear in Table 1. The variations of the pH of (*R*)- and (*S*)-2-phenylpropanoic acid–phenylpropanoate solutions in the vicinity of the pK_a of (*RS*)-2-phenylpropanoic acid as they were titrated with $\beta CDNH_3^+$ solutions are shown in Fig. 3. The best fit of the data to the expressions for K_{2HA} and K_{2A}, employing the independently determined value of K_a, using program SUPERQUAD[25] yields the curve through the data points in Fig. 3. (The value of K'_a was subsequently calculated from these three values.) Similar curves were obtained for the titration of 4-methylbenzoic acid–4-methylbenzoate by $\beta CDNH_3^+$, and for the titration of $\beta CDNH_3^+$ by benzoic acid–benzoate, and the data were similarly fitted. The pK_a and pK'_a values for benzoic, 4-methylbenzoic and (*RS*)-2-phenylpropanoic acid appear in Table 1, and the K_{2HA} and K_{2A} values for the complexation of these carboxylic acids and their conjugate bases by $\beta CDNH_3^+$ also appear in Table 1. A typical plot of the variation of species concentration with pH, calculated from data in Table 1, is shown in Fig. 4.

The formation of a CD inclusion complex involves dipolar, hydrogen bonding and van der Waals interactions to varying degrees depending on the nature of the CD and the guest species, and also solvent interactions with the CD and the guest species.[1–4,26] The general structure of the inclusion complex usually shows the aromatic moiety of the guest species to be in the annulus in the vicinity of the hydrophobic ring delineated by the ether oxygens,[27–30] with the dipole moment of the guest species aligned antiparallel to that of the CD.[31–33] The CD dipole moment is in the range 10–20 D†

† 1 D ≈ 3.335 64 × 10^{-30} C m.

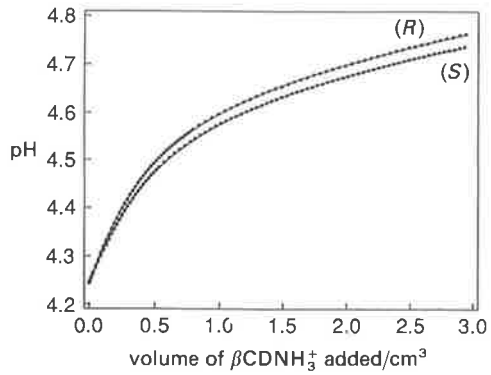

Fig. 3 Variation of the pH of a solution (2.0 cm^3) of (*R*)- or (*S*)-2-phenylpropanoic acid–phenylpropanoate (2.28×10^{-3} and 2.10×10^{-3} mol dm^{-3}, respectively) with volume of added $\beta CDNH_3^+$ (1.58×10^{-2} mol dm^{-3}) at 298.2 K and $I = 0.10$ mol dm^{-3} (KCl). The upper and lower data sets refer to (*R*)- and (*S*)-2-phenylpropanoic acid–phenylpropanoate, respectively. The curves through the data points represent the best fits of the data to the equilibria shown in Scheme 3 using SUPERQUAD.

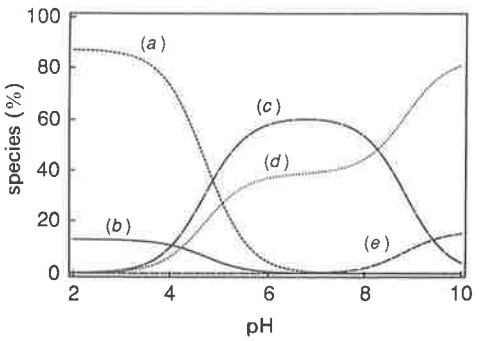

Fig. 4 Speciation plot for the $\beta CDNH_2$–$\beta CDNH_3^+$–(*S*)-2-phenylpropanoic acid–(*S*)-2-phenylpropanoate system calculated from pK_a, K_{2SHA}, K_{2SA} and K_{3SA} (Table 1). The total concentration of (*S*)-2-phenylpropanoic acid–(*S*)-2-phenylpropanoate is 10^{-3} mol dm^{-3} and the total concentration of $\beta CDNH_2$–$\beta CDNH_3^+$ is 1.5×10^{-2} mol dm^{-3}. The total concentration of (*S*)-2-phenylpropanoic acid–(*S*)-2-phenylpropanoate is defined as 100% and the free $\beta CDNH_2$–$\beta CDNH_3^+$ concentration is not shown. The curves represent: (*a*) (*S*)-2-phenylpropanoic acid · $\beta CDNH_3^+$, (*b*) (*S*)-2-phenylpropanoic acid, (*c*) (*S*)-2-phenylpropanoate · $\beta CDNH_3^+$, (*d*) (*S*)-2-phenylpropanoate and (*e*) (*S*)-2-phenylpropanoate · $\beta CDNH_2$.

with the positive and negative poles adjacent to the primary and secondary hydroxy groups delineating the narrow and wide ends of the CD annulus, respectively.[31–33] It has been observed that the carboxylic acid group of benzoic acid is in the vicinity of the primary hydroxy groups of αCD in the benzoic acid · αCD complex consistent with an antiparallel alignment of the αCD and benzoic acid dipole moments,[30] and similar antiparallel dipolar orientations are assumed in the complexes appearing in Table 1.

The magnitude of the CD inclusion complex stability constant reflects the competitive abilities of the CD to complex the guest species and water to solvate it, and accordingly the data in Table 1 indicate the changes in these abilities as both the natures of the host CD and the guest species are varied. Six distinct trends emerge from the data in Table 1 and are now discussed.

(i) For all systems the carboxylic acid complex is of higher stability than the analogous carboxylate complex. This suggests that the negative charge of the carboxylates causes a stronger solvation than in the case of the uncharged conjugate carboxylic acids with the consequence that, although the van der Waals interactions between the aromatic moieties of the guests and the hydrophobic interior of the CD annulus still result in complexation, the stronger solvation of the carboxylates results in a lower stability for their inclusion complexes.

(ii) The stabilities of the carboxylate complexes increase in the sequence $A^- \cdot \beta CDNH_2 \leqslant A^- \cdot \beta CD < A^- \cdot \beta CDNH_3^+$. This trend may be rationalised on the basis that the positive charge on $\beta CDNH_3^+$ increases its dipole moment and provides an increased electrostatic interaction with the carboxylate with a consequent increase in stability of the inclusion complex.

(iii) For a given CD complex, stability increases with the nature of the carboxylic acid in the sequence benzoic acid < (*S*)-2-phenylpropanoic acid ⩽ (*R*)-2-phenylpropanoic acid < 4-methylbenzoic acid. The areas of the hydrophobic surfaces of (*RS*)-2-phenylpropanoic acid and 4-methylbenzoic acid are greater than that of benzoic acid and they probably have more extensive van der Waals interactions with the CD as a consequence. In addition the carboxylic acid group, at which significant solvation may occur, represents a proportionately smaller part of their total surface area than is the case for benzoic acid. It is also possible that the fit of the guest species

to the CD cavity improves in the sequence benzoic acid < (*RS*)-2-phenylpropanoic acid < 4-methylbenzoic acid. The combination of these effects produces a lower stability constant characterising the benzoic acid complex.

(iv) For a given CD complex stability increases with the nature of the carboxylate in the sequence (*S*)-2-phenylpropanoate ⩽ benzoate ⩽ (*R*)-2-phenylpropanoate < 4-methylbenzoate. Clearly the factors discussed under (iii) apply here also, but it is evident that the increase in solvation arising from the negative carboxylate charge causes this factor to become more important, with the consequence that the stabilities of the benzoate and (*RS*)-2-phenylpropanoate complexes become comparable.

(v) Significant chiral discrimination in favour of complexation of (*R*)-2-phenylpropanoic acid and (*R*)-2-phenylpropanoate over the (*S*)-enantiomers is observed for βCDNH$_3^+$ and βCDNH$_2$, but not for βCD. The replacement of a primary hydroxy group by NH_3^+ or NH_2 increases the asymmetry of the CD annulus and accordingly βCDNH$_3^+$ and βCDNH$_2$ are more likely to discriminate between guest enantiomers through the formation of diastereomeric complexes than is βCD.

(vi) For the guest carboxylic acids and for βCDNH$_3^+$, $pK_a < pK_a'$, which indicates that in the inclusion complex the conjugate base is destabilised relative to the conjugate acid, by comparison with the situation in the uncomplexed state. Because of its charge the carboxylate will be more strongly solvated than the carboxylic acid, and evidently the decreased solvation resulting from inclusion in the CD annulus has a greater effect on the carboxylate with the consequence that it is destabilised by comparison to the included carboxylic acid. This has the overall effect of decreasing the acidity of the carboxylic acid. In the case of βCDNH$_3^+$ the decrease in acidity occurring on formation of the inclusion complex may be a consequence of disruption of the interactions between the NH_3^+ substituent and adjacent hydroxy residues and the ether linkages which are thought to confer the rather low pK_a value on βCDNH$_3^+$.[21] In addition, the cancellation of the βCDNH$_3^+$ charge by that of the included carboxylate may decrease the acidity of βCDNH$_3^+$.

In the presence of βCD in D_2O–DCl at pH 1, the methyl group of (*RS*)-2-phenylpropanoic acid is characterised by two ^{1}H NMR doublet resonances arising from the (*R*)-enantiomer ($\delta = 1.409$, $J_{H-H} = 6.6$ Hz) and the (*S*)-enantiomer ($\delta = 1.421$, $J_{H-H} = 6.9$ Hz), which compares with the doublet observed for (*RS*)-2-phenylpropanoic acid ($\delta = 1.289$, $J_{H-H} = 7.2$ Hz) in the absence of βCD, as seen in Fig. 5. The identification of the enantiomer resonances was made by adding (*R*)-2-phenylpropanoic acid to (*RS*)-2-phenylpropanoic acid in the presence of βCD and noting the relative increase in amplitude of the upfield doublet. In the presence of βCDNH$_3^+$ in D_2O–DCl at pH 1, the methyl group of (*RS*)-2-phenylpropanoic acid is characterised by two doublet resonances arising from the (*R*)-enantiomer ($\delta = 1.428$, $J_{H-H} = 6.9$ Hz) and the (*S*)-enantiomer ($\delta = 1.440$, $J_{H-H} = 6.9$ Hz) and the enantiomer resonances were identified as for the previous system. In contrast, in the presence of βCDNH$_3^+$ in D_2O–phosphate buffer at pH 6.4 the resonance of the methyl group of (*RS*)-2-phenylpropanoate appears as a doublet ($\delta = 1.315$, $J_{H-H} = 6.9$ Hz), which compares with the doublet observed for (*RS*)-2-phenylpropanoate ($\delta = 1.357$, $J_{H-H} = 7.2$ Hz) in the absence of βCDNH$_3^+$. (It was not possible to carry out similar experiments with (*RS*)-2-phenylpropanoate in the presence of βCD or βCDNH$_2$ as K_{1RA}, K_{1SA}, K_{3RA} and K_{3SA} are too small to give sufficient concentrations of the inclusion complexes within the solubility limits of the systems.) The observation of separate resonances for (*RS*)-2-phenylpropanoic acid in the presence of βCD and βCDNH$_3^+$ indicates that the magnetic environment of the methyl protons in the diastereomeric complexes is different, while the absence of separate resonances for (*RS*)-2-phenylpropanoate in the presence of βCDNH$_3^+$ indicates that the magnetic environment of the methyl protons in the diastereomeric complexes is not significantly different. Thus, a spectroscopic chiral discrimination occurs when (*RS*)-2-phenylpropanoic acid is complexed by either βCD or βCDNH$_3^+$, but not when (*RS*)-2-phenylpropanoate is complexed by βCDNH$_3^+$. In contrast, a significant thermodynamic chiral discrimination occurs in the complexation of both (*RS*)-2-phenylpropanoic acid and (*RS*)-2-phenylpropanoate by βCDNH$_3^+$, but no significant thermodynamic chiral discrimination occurs in the complexation of these guests by βCD. This demonstrates that although the titrimetric method may detect a significant thermodynamic chiral discrimination, such discrimination does not necessarily induce sufficient magnetic inequivalence in the diastereomeric complexes to be detectable by ^{1}H NMR spectroscopy. Conversely, although different diastereomeric complexes may be identified by ^{1}H NMR spectroscopy, this does not necessarily imply the existence of a significant thermodynamic chiral discrimination as the energy differences involved in the spectroscopic distinction are small.

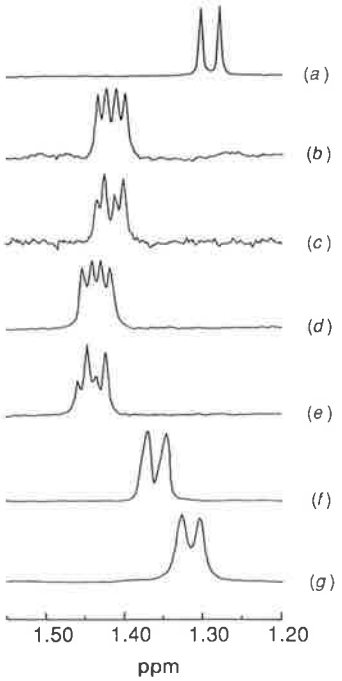

Fig. 5 ^{1}H NMR (300 M Hz) spectra of the methyl groups of: (*a*) (*RS*)-2-phenylpropanoic acid (0.005 mol dm^{-3}) at pH 1, (*b*) (*RS*)-2-phenylpropanoic acid (0.003 mol dm^{-3}) in the presence of βCD (0.011 mol dm^{-3}) at pH 1, (*c*) (*RS*)-2-phenylpropanoic acid (0.001 mol dm^{-3}) with added (*R*)-2-phenylpropanoic aicd (0.0003 mol dm^{-3}) in the presence of βCD (0.011 mol dm^{-3}) at pH 1, (*d*) (*RS*)-2-phenylpropanoic acid (0.005 mol dm^{-3}) in the presence of βCDNH$_3^+$ (0.03 mol dm^{-3}) at pH 1, (*e*) (*RS*)-2-phenylpropanoic acid (0.002 mol dm^{-3}) with added (*R*)-2-phenylpropanoic acid (0.002 mol dm^{-3}) in the presence of βCDNH$_3^+$ (0.03 mol dm^{-3}) at pH 1, (*f*) (*RS*)-2-phenylpropanoate (0.01 mol dm^{-3}) at pH 6.4, (*g*) (*RS*)-2-phenylpropanoate (0.01 mol dm^{-3}) in the presence of βCDNH$_3^+$ (0.09 mol dm^{-3}) at pH 6.4. The chemical shifts are downfield from TPS. The broader resonances observed in (*f*) and (*g*) are thought to be due to the higher viscosity of these solutions.

We are grateful to the Australian Research Council, Australian Commercial Research and Development Limited and the University of Adelaide for supporting this research. The award of an Australian Postgraduate Research Award to S.E.B. is gratefully acknowledged.

References

1 M. L. Bender and M. Komiyama, *Cyclodextrin Chemistry*, Springer, New York, 1977.
2 J. Szejtli, *Cyclodextrins and their Inclusion Complexes*, Akademiai Kiado, Budapest, 1982.
3 W. Saenger, *Inclusion Compounds*, 1984, **2**, 231.
4 R. J. Clarke, J. H. Coates and S. F. Lincoln, *Adv. Carbohyd. Chem. Biochem.*, 1989, **46**, 205.
5 I. M. Brereton, T. M. Spotswood, S. F. Lincoln and E. H. Williams, *J. Chem. Soc., Faraday Trans. 1*, 1984, **80**, 3147.
6 D. L. Pisaniello, S. F. Lincoln and J. H. Coates, *J. Chem. Soc., Faraday Trans. 1*, 1985, **81**, 1247.
7 S. F. Lincoln, A. M. Hounslow, J. H. Coates and B. G. Doddridge, *J. Chem. Soc., Faraday Trans. 1*, 1987, **83**, 2697.
8 S. F. Lincoln, A. M. Hounslow, J. H. Coates, R. P. Villani and R. L. Schiller, *J. Inclusion Phenom.*, 1988, **6**, 183.
9 S. E. Brown, J. H. Coates, C. J. Easton, S. F. Lincoln, Y. Luo and A. K. W. Stephens, *Aust. J. Chem.*, 1991, **44**, 855.
10 D. Greatbanks and R. Pickford, *Magn. Reson. Chem.*, 1987, **25**, 208.
11 N. J. Smith, T. M. Spotswood and S. F. Lincoln, *Carbohydr. Res.*, 1989, **192**, 9.
12 S. E. Brown, J. H. Coates, S. F. Lincoln, D. R. Coghlan and C. J. Easton, *J. Chem. Soc., Faraday Trans.*, 1991, **87**, 2699.
13 F. Cramer and W. Dietsche, *Chem. Ber.*, 1959, **92**, 378.
14 M. Mikolajczyk, J. Drabowicz and F. Cramer, *J. Chem. Soc., Chem. Commun.*, 1971, 317.
15 M. Mikolajczyk and J. Drabowicz, *J. Am. Chem. Soc.*, 1978, **100**, 2510.
16 W. L. Hinze, T. E. Rieh, D. W. Armstrong, W. DeMond, A. Alak and T. Ward, *Anal. Chem.*, 1985, **57**, 237.
17 D. W. Armstrong, T. Ward, R. D. Armstrong and T. E. Beesley, *Science*, 1986, **232**, 1132.
18 N. A. Karnik, R. J. Prankerd and J. H. Perrin, *Chirality*, 1991, **3**, 124.
19 R. P. Villani, S. F. Lincoln and J. H. Coates, *J. Chem. Soc., Faraday Trans. 1*, 1987, **83**, 2751.
20 S. F. Lincoln, J. H. Coates, C. J. Easton, S. J. van Eyk, B. L. May, P. Singh, M. A. Stile and M. L. Williams, *Int. Pat. Appl.*, WO 90/02141.
21 S. E. Brown, J. H. Coates, D. R. Coghlan, C. J. Easton, S. J. van Eyk, W. Janowski, A. Lepore, S. F. Lincoln, Y. Luo, B. L. May, D. S. Schiesser, P. Wang and M. L. Williams, *Aust. J. Chem.*, in the press.
22 J. Pitha, J. Milecki, H. Fales, L. Pennell and K. Uekama, *Int. J. Pharm.*, 1986, **29**, 73.
23 D. Duchêne, *New Trends in Cyclodextrins and Derivatives*, Editions de Santé, Paris, 1991.
24 A. K. Yatsimirsky and A. V. Eliseev, *J. Chem. Soc., Perkin Trans. 2*, 1991, 1769.
25 P. Gans, A. Sabatini and A. Vacca, *J. Chem. Soc., Dalton Trans.*, 1985, 1195.
26 R. I. Gelb, L. M. Schwartz, B. Cardelino, H. S. Fuhrman, R. F. Johnson and D. A. Laufer, *J. Am. Chem. Soc.*, 1981, **103**, 1750.
27 K. Harata, *Bull. Chem. Soc. Jpn.*, 1975, **48**, 2409.
28 K. Harata, *Bull. Chem. Soc. Jpn.*, 1976, **49**, 1493.
29 K. Harata, *Bull. Chem. Soc. Jpn.*, 1976, **49**, 2066.
30 K. Harata, *Bull. Chem. Soc. Jpn.*, 1977, **50**, 1416.
31 M. Kitagawa, H. Hoshi, M. Sakurai, Y. Inoue and R. Chûjô, *Carbohyd. Res.*, 1987, **163**, c1.
32 M. Sakurai, M. Kitagawa, H. Hoshi, Y. Inoue and R. Chûjô, *Chem. Lett.*, 1988, 895.
33 M. Sakurai, M. Kitigawa, H. Hoshi, Y. Inoue and R. Chûjô, *Carbohydr. Res.*, 1990, **198**, 181.

Paper 2/06389A; *Received* 30*th November*, 1992

Chiral Molecular Recognition: A ^{19}F Nuclear Magnetic Resonance Study of the Diastereoisomer Inclusion Complexes formed between Fluorinated Amino Acid Derivatives and α-Cyclodextrin in Aqueous Solution

Susan E. Brown, John H. Coates and Stephen F. Lincoln*
Department of Physical and Inorganic Chemistry, University of Adelaide, South Australia 5001, Australia
Daniel R. Coghlan and Christopher J. Easton
Department of Organic Chemistry, University of Adelaide, South Australia 5001, Australia

A ^{19}F NMR spectroscopic study (282.35 MHz) of the formation of diastereoisomeric inclusion complexes by fluorinated amino acid derivatives and α-cyclodextrin (αCD) in 10% aqueous D_2O solution yields the apparent stability constants K_R and K_S/dm^3 mol^{-1} = 7.7 ± 0.3 and 8.2 ± 0.3 for protonated α-(*p*-fluorophenyl)glycine (**1** + H), 21.5 ± 0.4 and 22.5 ± 0.4 for deprotonated α − (*p*-fluorophenyl)glycine (**1** − H), 14.4 ± 0.1 and 14.6 ± 0.1 for *N*-acetyl-α-(*p*-fluorophenyl)glycine (**2**), 13.1 ± 0.5 and 14.1 ± 0.5 for deprotonated *N*-acetyl-α-(*p*-fluorophenyl)-glycine (**2** − H), and 12.4 ± 0.3 and 10.6 ± 0.4 for deprotonated *N*-(*p*-fluorobenzoyl)valine (**3** − H), where the first and second of each pair of values refers to the diastereoisomer formed between αCD and the *R* and *S* enantiomer, respectively. The chemical shifts of the *R*-amino acid derivative · αCD inclusion complexes are upfield from those of their *S* analogues for deprotonated *N*-(*p*-fluorobenzoyl)valine (**3** − H), deprotonated α-(*p*-fluorophenyl) glycine (**1** − H), and deprotonated *N*-acetyl-α-(*p*-fluorophenyl)glycine (**2** − H), but this relationship is reversed for protonated α-(*p*-fluorophenyl)glycine (**1** + H) and *N*-acetyl-α-(*p*-fluorophenyl)glycine (**2** + H). In the case of the *N*-(*p*-fluorobenzoyl)valine · αCD inclusion complex (**3** · αCD) the chemical shift difference between the diastereoisomers formed with the *R* and *S* enantiomers is too small for quantitative analysis and accordingly a composite $K_{R,S}$/dm^3 mol^{-1} = 8.3 ± 0.3 was determined. The factors causing the variations in apparent stability constants and chemical shifts are discussed.

Chiral molecular recognitition is a well established feature of biological chemistry, and is currently the subject of increasing attention in areas as diverse as electronic energy-transfer processes,[1] chromatography[2,3] and drug interaction studies.[4,5] The ability of the chiral α-1,4-linked cyclic oligomers of D-glucopyranose, or cyclodextrins (CDs), to act as host molecules in the formation of inclusion complexes with a wide range of guest molecules is well established,[6–14] and renders them very suitable for chiral recognition studies. As CDs only exist as D enantiomers, two diastereoisomeric inclusion complexes may be formed with a racemic guest molecule. In some cases the formation of such diastereoisomers leads to a physical discrimination between the guest enantiomers based on their chirality as indicated by the partial resolution of racemic guests by the preferential precipitation of one diastereoisomer inclusion complex,[15–17] and also by the chromatographic separation of enantiomers on columns in which the stationary phase consists of CDs bonded to silica.[2,3] Chiral discrimination by CDs has also been directly observed in solution for propranolol where the formation of diastereoisomeric inclusion complexes with βCD and γCD results in separate ^1H NMR spectra for the propranolol enantiomers.[18] However, the quantitative aspects of such chiral discrimination in solution have been little studied.[12] Accordingly we have investigated the chiral discrimination exhibited by αCD† in its complexation of the chiral guest species *N*-(*p*-fluorobenzoyl)valine (**3**), α-(*p*-fluorophenyl)glycine (**1**), and *N*-acetyl-α-(*p*-fluorophenyl)glycine (**2**) which offer an opportunity to test the effects of (*a*), the proximity of the chiral centre to the *p*-fluorophenyl moiety; (*b*), the size of the chiral centre; and (*c*), the variation in charge of the guest species resulting from changes in the position of protonic equilibria, through observation of the variation of the ^{19}F chemical shift of the guest F substituent which other studies[10–12] have shown to be particularly sensitive to changes in environment.

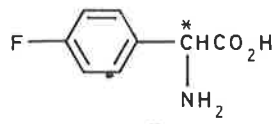

1

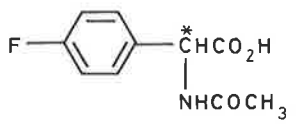

2

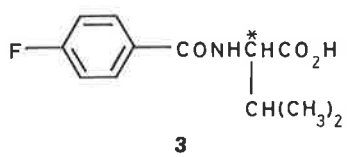

3

* indicates chiral centre

Experimental

αCD (Sigma) was dried to constant weight and stored over P_2O_5 in a vacuum desiccator prior to use. All other reagents

† αCD was chosen because of its high solubility in water (145 g dm^{-3}) by comparison to βCD (18.5 g dm^{-3}), and because its small annular diameter (470–520 pm) substantially decreases the possibility of the inclusion of guest species as dimers which occurs with γCD (diameter = 750–830 pm) and which might obscure observation of chiral interactions.

were of analytical grade. (2*RS*)-*N*-(*p*-Fluorobenzoyl)valine and the corresponding (2*S*)- and (2*R*)-valine derivatives were prepared by reaction of the corresponding free amino acids with *p*-fluorobenzoyl chloride.[19,20] (2*RS*)-α-(*p*-Fluorophenyl)-glycine was prepared by condensation of *p*-fluorobenzaldehyde with chloroform and ammonia[21,22] and resolved by treatment of the corresponding *N*-acetyl derivative with hog renal acylase 1.[23] The *N*-acetyl derivatives of (2*RS*)- and (2*S*)-α-(*p*-fluorophenyl)glycine were prepared through reaction with acetic anhydride.[24]

The pK_a values of the amino acid derivatives were determined by standard titrimetric methods in aqueous solutions of the amino acid derivative (10^{-3} mol dm^{-3}) and KCl (10^{-1} mol dm^{-3}) thermostatted at 298.2 K, using a Metrohm Dosimat E665 titrimator and an Orion SA 720 potentiometer. Appropriate water titration corrections were made. Buffer solutions (KCl–HCl, KH_2PO_4–Na_2HPO_4, and glycine–NaOH) used to buffer the amino acid derivative–αCD solutions used in the ^{19}F NMR studies were prepared as in the literature.[25]

The ^1H-broad-band decoupled ^{19}F NMR spectra were recorded on a Bruker CXP 300 spectrometer at 282.35 MHz locked on the deuterium frequency of D_2O. The fluorinated amino acid derivative and αCD in 10% aqueous D_2O solutions were contained in 5 mm NMR tubes. Chemical shifts were measured from a 2% CF_3CO_2Na–D_2O external reference solution. An average of 2000 transients were accumulated in a 8192 point data base for each solution, and the solution temperature (295.5 K) was controlled by a Bruker B-VT1000 variable temperature unit to within ±0.3 K.

Results

The singlet ^{19}F resonances of the protonated glycine (**1** + H) (pK_a 2.3), *N*-acetylglycine (**2**) (pK_a 2.8) and valine (**3**) (pK_a 3.4), and their deprotonated analogues exhibit substantial upfield shifts and split into symmetrical doublets with increasing concentration of αCD, as shown in Fig. 1–3, consistent with the formation of two diastereoisomers (in the case of the valine **3**, the splitting was insufficient for separate analysis of the data from the *R* and *S* enantiomers). The glycine **1** (pK_a 8.8) was insufficiently soluble to study by ^{19}F NMR spectroscopy. Identification of the diastereoisomers was made both by the measurement of the ^{19}F chemical shift for the pure *S*-amino acid derivative in the presence of αCD, and by the addition of pure *S*-amino acid derivative to a solution of the racemic amino acid derivative in the presence of αCD and observing which component of the ^{19}F doublet

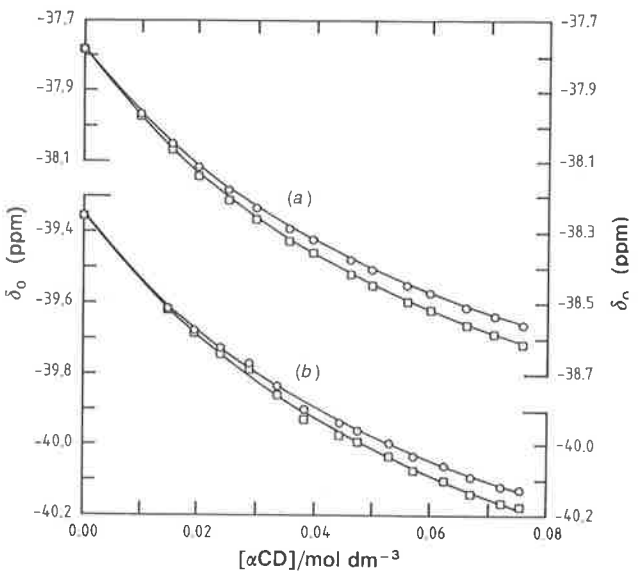

Fig. 2 The variation of ^{19}F δ_{obs} for (*a*), the racemic *N*-acetylglycine **2** (0.982×10^{-3} mol dm^{-3}, pH 1.3) ○, *R*; □, *S*; and (*b*), the racemic deprotonated *N*-acetylglycine (**2** − H) (1.01×10^{-3} mol dm^{-3}, pH 6.9) ○, *S*; □, *R*; in the presence of αCD at $I = 0.100$ and 295.5 K. The amino acid derivative enantiomer in the diastereoisomer formed with αCD is identified by *R* or *S*. The solid curves represent the least squares best fit of the δ_{obs} data to eqn. (2)

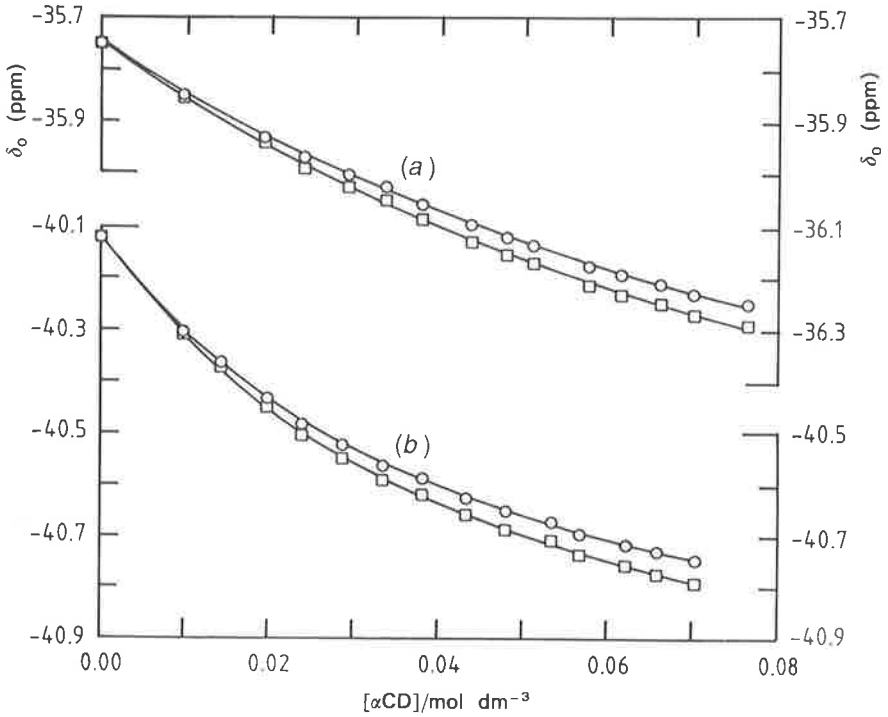

Fig. 1 The variation of ^{19}F δ_{obs} for (*a*), the racemic protonated glycine (**1** + H) (1.00×10^{-3} mol dm^{-3}, pH 1.3) ○, *R*; □, *S*; and (*b*), the racemic deprotonated glycine (**1** − H) (1.02×10^{-3} mol dm^{-3}, pH 10.8) ○, *S*; □, *R*; in the presence of αCD at $I = 0.100$ and 295.5 K. The amino acid derivative enantiomer in the diastereoisomer formed with αCD is identified by *R* or *S*. The solid curves represent the least-squares best fit of the δ_{obs} data to eqn. (2)

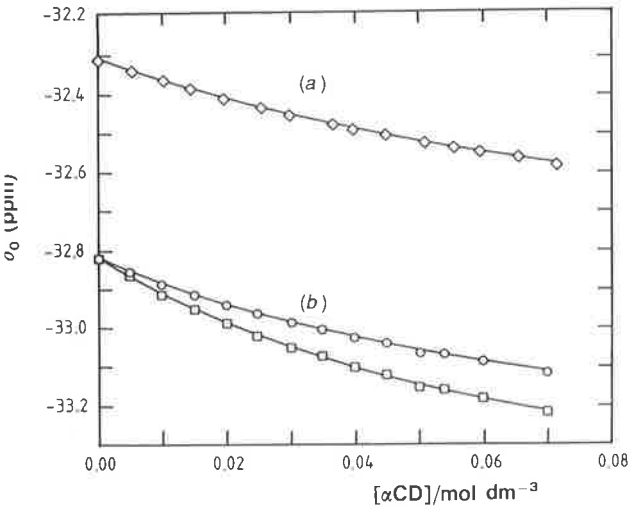

ig. 3 The variation of ^{19}F δ_{obs} for (*a*), the racemic valine 3 .02 × 10^{-3} mol dm^{-3}, pH 1.3) ◇, *R*, *S*; and (*b*), the racemic depro-)nated valine (3 − H) (0.990 × 10^{-3} mol dm^{-3}, pH 6.9) ○, *S*; □, *R*; ı the presence of αCD at $I = 0.100$ and 295.5 K. The amino acid erivative enantiomer in the diastereoisomer formed with αCD is lentified by *R* or *S*. The solid curves represent the least-squares best t of the δ_{obs} data to eqn. (2)

ncreased in intensity. The variation of the ^{19}F chemical shift vith αCD concentration for each enantiomer (E) is consistent vith the formation of a 1 : 1 diastereoisomeric inclusion :omplex (E · αCD) according to eqn. (1) and is given by eqn. 2), where δ_{obs} is the environmentally averaged shift of E and E · αCD under the fast exchange conditions applying to these ;ystems, and δ_F and δ_R or δ_S (depending on which enantio-ner is complexed) are the chemical shifts of E and E · αCD, espectively.[10–12] The δ_{obs} data for the *R* enantiomer (*RE*) vere fitted to eqn. (2) (an equivalent equation was used for SE) using a non-linear regression analysis, and the derived ıpparent stability constants, K_R and K_S, {where for the *RE*, $K_R = [RE \cdot \alpha CD][RE]^{-1}[\alpha CD]^{-1}$, and an equivalent expression holds for *SE*} and δ_F, δ_R and δ_S, appear in Table 1.

$$E + \alpha CD \underset{}{\overset{K_R \text{ or } K_S}{\rightleftharpoons}} E \cdot \alpha CD \quad (1)$$

$$\delta_{obs} = (\delta_F[RE] + \delta_R[RE \cdot \alpha CD])/([RE] + [RE \cdot \alpha CD]) \quad (2)$$

The formation of guest · $(\alpha CD)_2$ complexes has been reported for other guests in some cases, as indicated by a biphasic variation of the substrate chemical shift.[10,11] No evidence for such a stoichiometry was obtained in this study.

Discussion

The thermodynamic discrimination between the enantiomers of a given amino acid derivative is small, and in some cases is insignificant within experimental error (Table 1). Nevertheless, the separate resonances observed for the diastereoisomers (Fig. 1–3) indicate a significant difference in the magnetic environment of the ^{19}F nuclei of the diastereoisomers formed with a given amino acid derivative, and thereby a difference in the interaction between αCD and the *R* and *S* enantiomers, arising from their opposite chiralities. The difference in the chemical shift of the F substituent of the amino acid derivative in the solvated state, δ_F, and the complexed state, δ_R and δ_S, arises from a combination of the change in the local environment of the F substituent and the overall environmental change of the amino acid derivative on complexation. Corey–Pauling–Koltun (CPK) models show that the *p*-fluorophenyl moieties of the amino acid derivatives can enter the αCD annulus from either end, but that steric constraints position the F substituent in the hydrophobic section of the annulus in the vicinity of the ether linkages. This also results in the inclusion of a substantial portion of the phenyl ring in the annulus with the amino acid substituent in the vicinity of the hydroxy groups of αCD. (CPK models also show that, should the amino acid substituent reside wholly within the αCD annulus, steric interactions are likely to minimise the entry of the phenyl ring into the annulus, but this orientation seems less likely as crystallographic X-ray studies of αCD inclusion complexes with a range of aromatic guests show a substantial portion of the aromatic moiety to be within the αCD annulus.[26–29]) The resulting solvation change of the F substituent is probably a

Table 1 Apparent stability constants and ^{19}F chemical shifts of α-cyclodextrin–amino acid derivative diastereomers in 10% aqueous D_2O at $I = 0.100$ and 295.5 K

amino acid derivative (charge)	pH	buffer or electrolyte	K_R and K_S [a] /dm^3 mol^{-1}	δ_R and δ_S [a,b] (ppm)	$\Delta\delta$ (ppm)
1 + H (+1)	1.3	KCl–HCl	K_R, 7.7 ± 0.3	δ_R, −37.13 ± 0.03	$\delta_R - \delta_F$, −1.38 ± 0.03
			K_S, 8.2 ± 0.3	δ_S, −37.19 ± 0.04	$\delta_S - \delta_F$, −1.44 ± 0.04
				δ_F, −35.75 ± 0.004	$\delta_R - \delta_S$, 0.06 ± 0.04
1 − H (−1)	10.8	glycine–NaOH	K_R, 21.5 ± 0.4	δ_R, −41.24 ± 0.01	$\delta_R - \delta_F$, −1.12 ± 0.01
			K_S, 22.5 ± 0.4	δ_S, −41.14 ± 0.01	$\delta_S - \delta_F$, −1.02 ± 0.01
				δ_F, −40.12 ± 0.004	$\delta_R - \delta_S$, −0.10 ± 0.01
2 (0)	1.3	KCl–HCl	K_R, 14.4 ± 0.1	δ_R, −39.28 ± 0.01	$\delta_R - \delta_F$, −1.50 ± 0.01
			K_S, 14.6 ± 0.1	δ_S, −39.37 ± 0.01	$\delta_S - \delta_F$, −1.59 ± 0.01
				δ_F, −37.78 ± 0.004	$\delta_R - \delta_S$, 0.09 ± 0.01
2 − H (−1)	6.9	KH_2PO_4–Na_2HPO_4	K_R, 13.1 ± 0.5	δ_R, −41.02 ± 0.04	$\delta_R - \delta_F$, −1.66 ± 0.04
			K_S, 14.1 ± 0.5	δ_S, −40.85 ± 0.03	$\delta_S - \delta_F$, −1.49 ± 0.03
				δ_F, −39.36 ± 0.004	$\delta_R - \delta_S$, −0.17 ± 0.04
3 (0)[c]	1.3	KCl–HCl	$K_{R,S}$, 8.3 ± 0.3	$\delta_{R,S}$, −33.03 ± 0.02	$\delta_{R,S} - \delta_F$, −0.72 ± 0.02
				δ_F, −32.31 ± 0.004	
3 − H (−1)	6.9	KH_2PO_4–Na_2HPO_4	K_R, 12.4 ± 0.3	δ_R, −33.67 ± 0.01	$\delta_R - \delta_F$, −0.85 ± 0.01
			K_S, 10.6 ± 0.4	δ_S, −33.51 ± 0.02	$\delta_S - \delta_F$, −0.69 ± 0.02
				δ_F, −32.82 ± 0.004	$\delta_R - \delta_S$, −0.16 ± 0.02

[a] Errors represent one standard deviation derived from a least-squares fit of the data to eqn. (2), except for δ_F where the error represents the digital resolution of the spectrum. [b] Chemical shifts referenced to external 2% CF_3CO_2Na in D_2O which was assigned a shift of zero. Thus the more negative the value the further is δ upfield from the reference. [c] At the highest αCD concentration studied (0.065 mol dm^{-3}) the observed $\delta_R - \delta_S = 0.021 \pm 0.004$ ppm, which is insufficient for a reliable derivation of K_R and K_S and as a consequence a composite $K_{R,S}$ is derived.

major cause of the variation in chemical shift resulting from formation of the diastereoisomers. However, the overall environmental changes of the amino acid derivatives vary as a consequence of the different sizes of the amino acid substituents. Thus the amino acid substituents of the glycine **1** and the *N*-acetylglycine **2** are in close proximity to either the primary or secondary hydroxy groups of αCD, depending on the orientation of the amino acid derivative in the αCD annulus (see below). By comparison, the amino acid and propyl substituents of the valine **3** protrude further from the αCD complex, and the overall environmental changes experienced by both the valine **3** and its deprotonated analogue (**3** − H) are proportionately less, which is consistent with the smaller change in chemical shift characterizing these species on complexation.

For the diastereoisomers formed with the three negatively charged deprotonated amino acid derivatives $|\delta_R| > |\delta_S|$, whereas for those formed with the positively charged protonated glycine (**1** + H) and the zero charged *N*-acetylglycine **2**, $|\delta_R| < |\delta_S|$ (Table 1). This suggests that the change in charge produces a reorientation of the enantiomers inside the αCD annulus. The dipole moment of αCD is estimated to be 13.5 D,† with the positive and negative ends of the dipole adjacent to the rings of primary and secondary hydroxy groups, respectively, delineating the narrow and wide ends of the αCD annulus.[30,31] It has been observed that the dipole moments of *p*-nitrophenol, *p*-hydroxybenzoic acid, and benzoic acid are antiparallel to the direction of the dipole moment of αCD in their inclusion complexes such that the nitro and carboxylic acid substituents of the guests are in the vicinity of the αCD primary hydroxy groups.[30] As the localised charge of the carboxylate group of a negatively charged amino acid derivative enantiomer dominates the orientation of its dipole moment, is is probable that the enantiomer will be oriented with its F substituent near the hydrophobic region of the annulus and its carboxylate group hydrogen-bonded to a primary hydroxy group of αCD in the diastereoisomer. Thus the interaction between the negatively charged enantiomers and αCD may be subdivided into: (*a*) the interaction of the *p*-fluorophenyl moiety and αCD; (*b*) hydrogen bonding between the carboxylate group at the chiral centre and the primary hydroxy groups of αCD; and (*c*) the interaction of the other groups at the chiral centre with the primary hydroxy groups of αCD. For a given deprotonated amino acid derivative it is the arrangement of the groups involved in interaction (*c*) which determines the enantiomer discrimination resulting in the observation that $|\delta_R| > |\delta_S|$.

In addition to the reversal of the relative chemical shifts alluded to above, the modulus $|\delta_R - \delta_S|$ is greater for the diastereoisomers formed by the deprotonated amino acids ($|\delta_R| > |\delta_S|$) than for those formed by the protonated glycine (**1** + H) and the *N*-acetylglycine (**2**) ($|\delta_R| < |\delta_S|$). This suggests a change in effectiveness of the chiral interactions with change in enantiomer charge. The localised positive charge on the amine function of the protonated glycine (**1** + H) will probably reverse the direction of its dipole moment and its orientation in the αCD annulus, by comparison with that of its negatively charged analogue. On this basis, the interaction between the protonated glycine (**1** + H) and αCD may be subdivided into: (*a*) the inclusion of the *p*-fluorophenyl moiety in the hydrophobic region of the annulus of αCD; (*b*) hydrogen bonding between the ammonium group at the chiral centre and the secondary hydroxy groups of αCD; and (*c*) the interaction of the other groups at the chiral centre with the secondary hydroxy groups of αCD, resulting in $|\delta_R| < |\delta_S|$.

† 1 D = 3.335 64 × 10^{-30} C m.

The direction of the dipole moment of the *N*-acetylglycin **2** is uncertain and thus the deduction of the orientation of th diastereoisomers formed with αCD on this basis is als uncertain. Nevertheless, it is likely that chiral discriminatio results from (*a*) the inclusion of the *p*-fluorophenyl moiety i the annulus of αCD; and (*b*) interaction of the two pola groups at the chiral centre with hydroxy groups of αCD. I the case of the valine **3**, inclusion of the *p*-fluorobenzoy moiety in the αCD annulus leaves only one other polar grou at the chiral centre to interact with the hydroxy groups o αCD, with the result that there is less chiral discriminatio than is the case for the *N*-acetylglycine **2**.

The driving force for the complexation of an aromatic sub strate by a CD arises from a combination of changes in sol vation of the substrate and the CD resulting fron complexation, and hydrophobic, van der Waals, hydroge bonding and dipolar interactions between the substrate an the CD in varying degrees. The interplay of these factors ha been adequately discussed elsewhere,[6–9] and only thos aspects which may explain the variations observed in thi study are considered here. Despite the small, and in som cases insignificant, thermodynamic discrimination betwee the amino acid derivative enantiomers by αCD, the variatio of K_R and K_S can be interpreted in terms of interaction within the diastereoisomers for amino acid derivatives o similar charge. Hence, as the interaction of the *p*-fluoropheny moiety and αCD, and hydrogen bonding between the carbox ylate group at the chiral centre and the primary hydrox groups of αCD probably make similar contributions to th stability in complexes of all three deprotonated amino aci derivatives, the diminution of K_R and K_S for these substrate in the sequence: glycine (**1** − H) ≫ *N*-acetylglycin (**2** − H) > valine (**3** − H) is largely attributable to the differ ing characteristics of the other groups at the chiral centre Thus, the dipolar interaction of the amino group of glycine **1** with primary hydroxy groups of αCD is greater than th interaction of the acetamido group of *N*-acetylglycine **2** which is in turn greater than that of the propyl group o valine **3**.

This conclusion, that dipolar interactions constitute a significant component of the binding force in the complexes studied here, in addition to their importance in complex orientation, is similar to that reached on the basis of data for the inclusion of *p*-hydroxybenzoate, *p*-nitrobenzoate and *m*-hydroxybenzoate by αCD.[32] The K_R and K_S values for complexation of the deprotonated amino acid derivative enantiomers are comparable to the *K* values obtained for the complexation by αCD of *p*-hydroxybenzoate (11.5, 298.2 K), *p*-nitrobenzoate (27.4, 303.2 K), and *m*-hydroxybenzoate (6.8, 293.2 K).

We are grateful to the Australian Research Council and the University of Adelaide for supporting this research.

References

1 D. H. Metcalf, W. S. Snyder, J. N. Demas and F. S. Richardson, *J. Am. Chem. Soc.*, 1990, **112**, 5681.
2 W. L. Hinze, T. E. Rieh, D. W. Armstrong, W. DeMond, A. Alak and T. Ward, *Anal. Chem.*, 1985, **57**, 237.
3 D. W. Armstrong, T. Ward, R. D. Armstrong and T. E. Beesley, *Science*, 1986, **232**, 1132.
4 A. Rubin, M. P. Knadler, P. P. Ho, L. D. Bechtol and R. L. Wole, *J. Pharm. Sci.*, 1985, **74**, 82.
5 J. A. Hamilton and L. Chen, *J. Am. Chem. Soc.*, 1988, **110**, 4379.
6 J. Szejtli, *Cyclodextrins and Their Inclusion Complexes*, Akademiai Kiado, Budapest, 1982.
7 M. L. Bender and M. Komiyama, *Cyclodextrin Chemistry*, Springer, New York, 1977.

8 R. J. Clarke, J. H. Coates and S. F. Lincoln, *Adv. Carbohyd. Chem. Biochem.*, 1989, **46**, 205.
9 W. Saenger, *Inclusion Compounds*, 1984, **2**, 231.
10 I. M. Brereton and T. M. Spotswood, S. F. Lincoln and E. H. Williams, *J. Chem. Soc., Faraday Trans. 1*, 1984, **80**, 3147.
11 D. L. Pisaniello, S. F. Lincoln and J. H. Coates, *J. Chem. Soc., Faraday Trans. 1*, 1985, **81**, 1247.
12 N. J. Smith, T. M. Spotswood and S. F. Lincoln, *Carbohydr. Res.*, 1989, **192**, 9.
13 S. F. Lincoln, A. M. Hounslow, J. H. Coates and B. G. Doddridge, *J. Chem. Soc., Faraday Trans. 1*, 1987, **83**, 2697.
14 S. F. Lincoln, A. M. Hounslow, J. H. Coates, R. P. Villani and R. L. Schiller, *J. Inclusion Phenom.*, 1988, **6**, 183.
15 F. Cramer and W. Dietsche, *Chem. Ber.*, 1959, **92**, 378.
16 M. Mikolajczyk, J. Drabowicz and F. Cramer, *J. Chem. Soc., Chem. Commun.*, 1971, 317.
17 M. Mikolajczyk and J. Drabowicz, *J. Am. Chem. Soc.*, 1978, **100**, 2510.
18 D. Greatbanks and R. Pickford, *Magn. Reson. Chem.*, 1987, **25**, 208.
19 M. P. Spratt, Y. Meng and H. C. Dorn, *Anal. Chem.*, 1985, **57**, 76.
20 J. H. Coates, D. R. Coghlan, C. J. Easton, B. F. Hoskins, S. F. Lincoln and E. R. T. Tiekink, *Z. Krist.*, 1989, **188**, 131.
21 E. L. Compere and D. A. Weinstein, *Synthesis*, 1977, 852.
22 D. Landini, F. Montanari and F. Rolla, *Synthesis*, 1979, 26.
23 J. E. Baldwin and T. S. Wan, *Tetrahedron*, 1981, **37**, 1589.
24 A. Schouteen, Y. Christidis and G. Mattioda, *Bull. Soc. Chim. Fr.*, 1978, 248.
25 *Biochemists' Handbook*, ed. C. Long, Spon, London, 1961, p. 30, 32, 36.
26 K. Harata, *Bull. Chem. Soc. Jpn.*, 1975, **48**, 2409.
27 K. Harata, *Bull. Chem. Soc. Jpn.*, 1976, **49**, 1493.
28 K. Harata, *Bull. Chem. Soc. Jpn.*, 1976, **49**, 2066.
29 K. Harata, *Bull. Chem. Soc. Jpn.*, 1977, **50**, 1416.
30 M. Kitagawa, H. Hoshi, M. Sakurai, Y. Inoue and R. Chujo, *Carbohydr. Res.*, 1987, **163**, c1.
31 M. Sakurai, M. Kitagawa, H. Hoshi, Y. Inoue and R. Chujo, *Chem. Lett.*, 1988, 895.
32 R. I. Gelb, L. M. Schwartz, B. Cardelino, H. S. Fuhrman, R. F. Johnson and D. A. Laufer, *J. Am. Chem. Soc.*, 1981, **103**, 1750.

Paper 1/00963J; *Received* 1st *March*, 1991